Conjugate Effects of Stress Work and Conduction on Magnetohydrodynamic Natural Convection Flows

by

Md. Mahmud Alam

A THESIS SUBMITTED TO THE DEPARTMENT OF MATHEMATICS IN PARTIAL FULFILLMENT OF THE REQUIREMENT FOR THE DEGREE OF DOCTOR OF PHILOSOPY IN MATHEMATICS
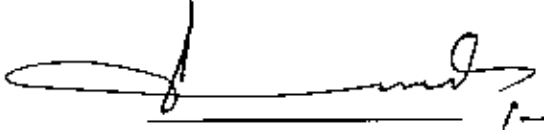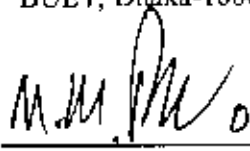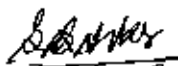
Department of Mathematics

BANGLADESH UNIVERSITY OF ENGINEERING AND TECHNOLOGY,

DHAKA-1000

August- 2007

RECOMMENDATION OF THE BOARD OF EXAMINERS

The thesis titled, "Conjugate Effects of Stress Work and Conduction on Magneto-hydrodynamic Natural Convection Flows", submitted by Md. Mahmud Alam, Roll no: P04020901F, session: April 2002, has been accepted as satisfactory in partial fulfillment of the requirements for the degree of DOCTOR OF PHILOSOPHY on 1st August, 2007.

BOARD OF EXAMINERS

_01.08.07_

1. **Dr. Md. Mustafa Kamal Chowdhury**
    Professor
    Department of Mathematics
    BUET, Dhaka-1000

Chairman
(Supervisor)

_01.08.07_

2. **Head**
    Department of Mathematics
    BUET, Dhaka-1000

Member
(Ex-officio)

_01.8.07_

3. **Dr. Md. Abdul Maleque**
    Professor
    Department of Mathematics
    BUET, Dhaka-1000

Member

4. **Dr. Md. Abdul Hakim Khan**
    Professor
    Department of Mathematics
    BUET, Dhaka-1000

Member

iii

A. Alim
01.8.07

Member

5   **Dr. Md. Abdul Alim**
Assistant Professor
Department of Mathematics
BUET, Dhaka-1000

1-8-07

Member

6.   **Dr. Gazi Md. Khalil**
Professor
Department of Naval Architecture and Marine Engineering,
BUET, Dhaka-1000

01.08.07

Member

7.   **Dr. M. Mahabubur Razzaque**
Associate Professor
Department of Mechanical Engineering
BUET, Dhaka-1000

01.08.07

Member
(External)

8   **Dr. M. Shamsul Alam Sarker**
Professor
Department of Applied Mathematics
University of Rajshahi, Rajshahi - 6205

ACKNOWLEDGEMENTS

CANDIDATE'S DECLARATION

It is hereby declared that this thesis or any part of it has not been submitted elsewhere for the award of any degree or diploma.

Mahmud 01.08.07

Md. Mahmud Alam   August, 2007

NOMENCLATURE

a : Radius of the sphere [m]

a_r : Rosseland mean absorption coefficient [-]

$\vec{B}$: Magnetic field [A/m]

B_0 : Magnetic field strength [-]

b : Plate thickness [m]

Cf_x : Local skin friction coefficient, $Cf_x = x(\partial^2 f/\partial y^2)_{y=0}$ [-]

C_p : Specific heat at constant pressure kJ/(kg.°C)

$\vec{D}$: The electron displacement [m]

d : $(T_b - T_\infty)/T_\infty$

$\vec{E}$: Electric field [-]

$\vec{F}$: The body force per unit volume [kg.m/s^2]

f : Dimensionless stream function [$f(x,\eta)$]

Ge : Pressure work parameter [kg.m/s^2]

Gr : Grashof Number [$g\beta(T_b-T_\infty)a^3/\nu^2$]

g : Acceleration due to gravity [m/s^2]

h : Dimensionless temperature function [$h(x,\eta)$]

$\vec{J}$: Current density [kg/m^3]

Jul : Joule heating parameter [$\sigma B_0^2 \nu d^{1/2}/\rho C_p(T_b-T_\infty)$]

L : Reference length. $(\nu^{2/3}/g^{1/3})$ = Length scale

l : Length of the plate [m]

M : Magnetic parameter / Hartmann Number [$\sigma B_0^2 L^2/\mu d^{1/2}$][-]

N : Viscous dissipation parameter [$\nu^2 d/L^2 c_p(T_b-T_\infty)$][-]

Nu_x : Nusselt number. $Nu_x = -(\partial\theta/\partial y)_{y=0}$ [-]

P : Pressure [m/s^2]

p : Coupling parameter, $p = (\kappa_f/\kappa_s)(b/L) d^{1/4}$[-]

Pr : Prandtl Number [$\mu C_p / \kappa_f$][-]

Q : Heat generation parameter [$Q_0 L^2 / \mu C_p d^{1/2}$][-]

Q_0 : Heat generation coefficient [-]

q_r : Radiative heat flux [w/m^2]

$\vec{q}$: Velocity vector field [m/s]

r : Radial axis [m]

R_e : Reynolds number [UL / ν][-]

Rd : Radiation parameter [$Rd = 4\sigma T_\infty^3 / k(a_r + \sigma_r)$][-]

T : Temperature [$^\circ$K or $^\circ$C]

T_b : Temperature at outside surface of the plate [$^\circ$K or $^\circ$C]

T_f : Temperature of the fluid [$^\circ$K or $^\circ$C]

T_s : Temperature of the solid [$^\circ$K or $^\circ$C]

T_w : Temperature at the wall [$^\circ$K or $^\circ$C]

T_∞ : Fluid asymptotic temperature, Ambient fluid temperature   [$^\circ$K or $^\circ$C]

U, U_∞ : Reference velocity [m/s]

V : The transpiration velocity [m/s]

U, V : Velocity components [m/s]

u, v : Dimensionless velocity components [-]

X, Y : Cartesian coordinates [m]

x, y : Dimensionless Cartesian coordinates [-]

GREEK SYMBOLS

α : Thermal diffusivity $[m^2/s]$

β : Co-efficient of thermal expansion [1/K]

β_0 : Magnetic field strength [-]

γ : Cone apex half-angle[^{0}]

$\dot{V}$: Vector differential operator [-]

ε : Electric permeability of the medium [-]

η : Dimensionless similarity variable $[yx^{-1/5}(1+x)^{-1/20}][-]$

κ : Thermal conductivity $[W/(m.^\circ C)]$

κ_f, κ_s : Fluid and solid thermal conductivities [-]

μ : Dynamic viscosity [kg/(ms)]

μ_e : The magnetic permeability of the medium [-]

ν : Kinematic of viscosity $[m^2/s]$

π : Angle of the sphere[^{o}]

θ : Dimensionless temperature, Surface temperature [-]

ρ : Density of the fluid $[kg/m^3]$

ρ_e : Charge density $[kg/m^3]$

ρ_∞ : Density of the ambient fluid $[kg/m^3]$

σ : Electric conductivity, Stephman-Boltzman constant $[W/(m^2.K^4)]$

σ_0 : Electric conduction [-]

σ_s : Scattering co-efficient [-]

τ_w : Shear stress [-]

Ω : Angular velocity [-]

φ : The viscous energy dissipation term [-]

Ψ : Stream function $[m^2/s]$

CONTENTS

CHAPTER 1   1–14

CHAPTER 2   15–41

CHAPTER 3   42–57

Conjugate effects of viscous dissipation and pressure work on MHD natural convection flow along a vertical flat plate with heat conduction

CHAPTER 4   58–75

Viscous dissipation and pressure work effects on Magnetohydrodynamic free convection flow along a vertical flat plate with Joule heating and heat conduction

CHAPTER 5

Conjugate Effect of Stress Work and Heat Generation on Magneto-
hydrodynamic Free Convection Flow along a Vertical flat plate with Joule
heating and heat Conduction

CHAPTER 6

Viscous dissipation and Pressure work effects on magnetohydrodynamic
natural convection flow over a sphere in the presence of heat generation

CHAPTER 7

Conjugate effects of stress work and magnetohydrodynamic natural convection
flow over a sphere in the presence of heat generation and radiation

CHAPTER 8

List of Tables

xv

List of Figures

Abstract

Numerical investigations on the steady of two-dimensional magnetohydrodynamic (MHD) natural convection flow of an electrically conducting fluid such as (i) along a vertical flat plate and (ii) on a sphere are made with various flow conditions. Implicit finite difference method is used as numerical tools. The governing equations are made dimensionless by using a new class of transformations. The dimensionless equations are then solved numerically in the entire region starting from the lower part of the plate to the downstream by means of the implicit finite difference method with the Keller box scheme. Introducing the suitable transformations, similarity equations of the momentum and energy equations are derived. The works depending on various flow conditions are abstracted below.

First, the effects of viscous dissipation and pressure stress work on magneto-hydrodynamic free convection flow along a vertical flat plate has been investigated. Magnetohydrodynamic free convection flow and heat conduction due to wall thickness b are considered in the investigation. Numerical results for the velocity profiles, temperature profiles, skin friction coefficient and the surface temperature distributions are shown both on graphs and in tabular form for different values of the parameters such as the Prandtl number Pr, the magnetic parameter M, the viscous dissipation parameter N and the pressure work parameter Ge entering into the problem.

Second, the effects of viscous dissipation and pressure work on the magneto-hydrodynamic free convection flow from the vertical flat plate with heat conduction and Joule-heating effect have been analyzed. The dimensionless skin friction co-efficient, the surface temperature distribution, the velocity distribution and the temperature profile over the whole boundary layer are shown graphically for different values of the parameters such as the Prandtl number Pr, the magnetic parameter M, the viscous dissipation parameter N, the Joule-heating parameter Jul and the pressure work parameter Ge.

Third, the effect of conduction and convection on magnetohydrodynamic boundary layer flow has been studied numerically. The dimensionless skin friction co-efficient, the surface temperature distribution; the velocity and temperature profiles over the

whole boundary layer are displayed graphically for different values of the parameters. The skin-friction and surface temperature distributions are also obtained and presented in tabular forms.

Fourth, we describe the pressure work and viscous dissipation effects with magnetohydrodynamic natural convection flow over a sphere in presence of heat generation. The natural convection laminar flow from a sphere immersed in a viscous incompressible optically thin fluid in the presence of heat generation effect has been investigated. Here, the attention is focused on the evolution of the shear stress in terms of local skin friction and the rate of heat transfer in terms of local Nusselt number, velocity profiles as well as temperature profiles for some selected values of parameters set consisting of heat generation parameter Q, magnetic parameter M, pressure work parameter Ge, viscous dissipation parameter N and the Prandlt number Pr.

Lastly, the conjugate stress work and magnetohydrodynamic effects on natural convection flow over a sphere in presence of heat generation and radiation are studied. Here the evolution of the surface shear stress in terms of local skin friction and the rate of heat transfer in terms of local Nusselt number, velocity distribution as well as temperature distribution for a selection of parameters set consisting of heat generation parameter, magnetic parameter, the viscous dissipation parameter, the pressure work parameter, the radiation parameter, the surface temperature parameter and also the Prandlt number Pr are focused.
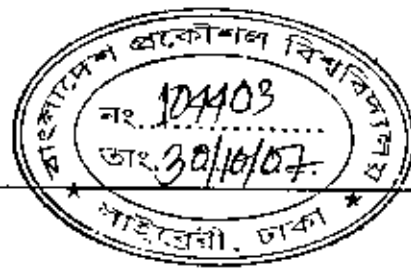
1.1 Introduction

The problems of free convection boundary layer flow over or on bodies of various shapes have been discussed by many researchers. Natural convection heat transfer gained considerable attention because of its numerous applications in the areas of energy conservations cooling of electrical and electronic components, design of solar collectors, heat exchangers and many others. The main difficulty in solving natural convection problems lies in the determination of the velocity field, which greatly influences the heat transfer process. Gebhart (1962) shown that the viscous dissipation effect plays an important role in natural convection flow. With this understanding Takhar and Soundalgekar(1980a) studied the effects of viscous and Joule heating on the problem posed by Sparrow and Cess [(1961a), (1961b)], using the series expansion method of Gebhart (1962).

The study of the flow of electrically conducting fluid in presence of magnetic field is important from the technical point of view and such types of problems have received much attention of many researches. The terms magnetohydrodynamics, hydromagnetics, magnetogasdynamics and magneto-aerodynamics, all refer to the branch of fluid dynamics that deals with the motion of electrically conducting fluids in presence of electric and magnetic fields. The interaction of a magnetic field and the moving electric charge carried by a flowing fluid induces a force, which tends to oppose the fluid velocity which is very small so that the magnetic force proportional to the magnitude of the longitudinal velocity and acting in the opposite direction is also very small. Consequently, the influence of the magnetic field on the boundary layer is exerted only through induced forces within the boundary layer itself, with no additional effects arising from the free stream pressure gradient. In this work, implicit finite difference method has been adapted to obtain the solution for the transient MHD incompressible flow along a vertical flat plate with heat conduction and MHD natural convection flow over a sphere.

1.2 Present problems

There are many natural convection problems in the branches of MHD fields such as vertical flat plate, inclined flat plate, porous flat plate, cylindrical cross section, circular cone, permeable circular cone and over a sphere. The followings two basic problems for different configuration are considered.

1. Conjugate effects of stress work and heat generation on Magnetohydrodynamic free convection flow along a vertical flat plate with Joule heating and heat conduction. The flow configuration and the coordinates system are shown in Figure 1.1
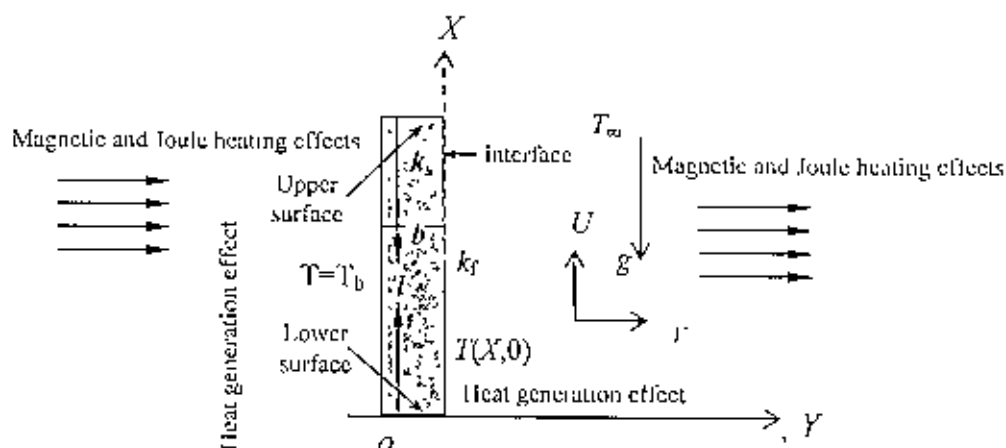
Figure1.1: Physical configuration and coordinate system

Steady two dimensional laminar free convection boundary layer flow of a viscous incompressible fluid along one side of a semi-infinite vertical flat plate of thickness 'b' insulated on the edges with temperature T_b, where U and V are the velocity components along the X and Y axis respectively, T is the temperature of the fluid in the boundary layer, T_b is the temperature of the plate in the boundary layer, g is the acceleration due to gravity, b is vertical flat plate of thickness, k_1 is the thermal conductivity of fluid, k_s is the thermal conductivity of the solid body. $T(X,0)$ is the unknown temperature.

2. Conjugate effects of stress work and magnetohydrodynamic natural convection flow over a sphere in the presence of heat generation and radiation
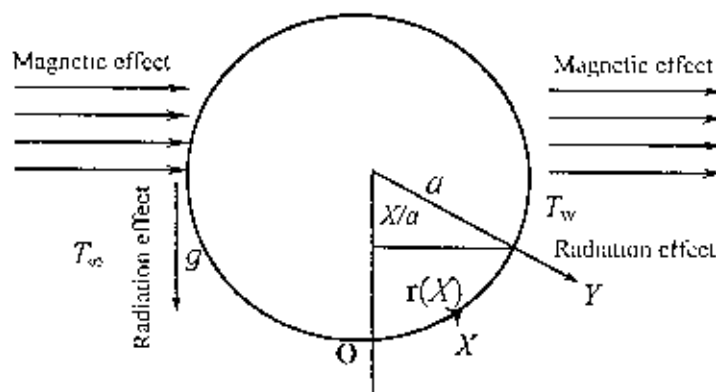
Figure1.2: Physical model and coordinate system

Natural convection boundary layer flow over a sphere of an electrically conducting and steady two-dimensional viscous incompressible fluid in presence of strong magnetic field and heat generation is considered. It is assumed that the surface temperature of the sphere is T_w. Where $T_w > T_\infty$, T_∞ is the ambient temperature of the fluid. Here a is the radius of sphere, r is the radial distance from the symmetrical axis to the surface of the sphere, g is the acceleration due to gravity, T is the local temperature, X/a is the angle of the sphere.

1.3 Literature review with MHD flows

Free convection flow is often encountered in cooling of nuclear reactors or in the study of the structure of stars and planets. Along with the free convection flow the phenomenon of the boundary layer flow of an electrically conducting fluid to a vertically flat plate in the presence of Joule-heating, magnetic field and heat generation are also very common, because of their applications in nuclear engineering in connection with the cooling of reactors.

Magnetohydrodynamics is that branch of continuum mechanics that deals with the flow of electrically conducting fluids in electric and magnetic fields. Probably the largest advance towards such phenomena comes from the field of astrophysics. It has long been suspected that most of the matter in the universe is in the plasma or highly

ionized gaseous state, and much of the basic knowledge in the area of electromagnetic fluid dynamics evolved from these studies. Many natural phenomena and engineering problems are susceptible to MHD analysis. It is useful in astrophysics. Geophysicists encounter MHD phenomena in the interactions of conducting fluid and magnetic fields that are present in and around heavenly bodies. Engineers employ MHD principles in the design of heat exchangers, pumps and flow meters, in space vehicle propulsion, control and re-entry, in creating novel power generating systems, and in developing confinement schemes for controlled fusion.

The most important application of MHD is in the generation of electrical power with the flow of an electrically conducting fluid through a transverse magnetic field. Recently, experiments with ionized gases have been performed with the hope of producing power of a large scale in stationary plants with large magnetic fields. Cryogenic and superconducting magnets are required to produce these very large magnetic fields. Generation of MHD power on a smaller scale is of interest for space applications.

To convert the heat energy into electricity, several intermediate transformations are necessary. Each of these steps means a loss of energy. This naturally limits the overall efficiency, reliability and compactness of the conversion process. Methods of direct conversion to energy are now increasingly receiving attention. Of these, the fuel cell converts the chemical energy of fuel directly into electrical energy, fusion energy utilizes the energy released when two hydrogen nuclei fuse into a heavier one, and thermo-electrical power generation uses a thermocouple. Magnetohydrodynamic power generation is another important new process that is receiving worldwide attention.

Hall current problems

The principles of magnetohydrodynamics could be utilized in a practical way to pump liquid metals in pipes. The imminence of hypersonic and space flight to stimulate great interest in this field was pointed out by Hartmann (1937). The current trend for the application of magnetofluiddynamics is towards a strong magnetic field (so that the influence of electromagnetic force is noticeable) and towards a low density of gas (such as in space flight and in nuclear fusion research). Under this condition the Hall current and ion slip become important. The history of Hall effect begins in 1879 when Edwin

H. Hall discovered that a small transverse voltage appeared across a current-carrying thin metal strip in an applied magnetic field. Until that time, electrical measurements provided only the carrier density-mobility product and the separation of these two important physical quantities had to rely on other difficult measurements. The discovery of the Hall effect removed this difficulty. Development of the technique has since led to a mature and practical tool, which today is used routinely for testing the electrical properties and quality of almost all of the semiconductor materials used by industry

The importance of the Hall effects is underscored by the need to determine accurately carrier density, electrical resistivity, and the mobility of carries in semiconductors. The Hall effect provides a relatively simple method for doing this. Because of its simplicity, low cost, and fast turnaround time, it is an indispensable characterization technique in the semiconductor industry and in research laboratories. In a recent industrial survey, it is listed as one of the most-commonly used characterization tools. Furthermore, two recent Nobel prizes (1985, 1998) are based upon the Hall effect. Effect of Hall current on the hydromagnetic free convection flow for various shape have been investigated by Pop (1971), Hossain *et al.* [(1987), (1988)] and Jha (1991).

The equation of electric current density may be derived from the diffusion velocities of the charge particles [Hughes & Young (1966), Cramer & Pai (1974), Pai (1962) and Sherchff (1965)]. The major forces on the charged particles are electromagnetic forces. If we consider only the electromegnetic forces, we may obtain the generalized Ohm's law. However, the deduction from the diffusion velocities of charged particles is more complicated than the generalized Ohm's law. When we apply electric field $\vec{E}$, there will be an electric current in the direction of $\vec{E}$. If the magnetic field $\vec{B}$ is perpendicular to $\vec{E}$, there will be an electromagnetic force $\vec{J} \wedge \vec{B}$ which is perpendicular to both $\vec{B}$ and $\vec{E}$. We have a new component of electric current density in the direction perpendicular to both $\vec{E}$ and $\vec{B}$ which are known as Hall current, discovered by Hall Furthermore, the masses of ions and electrons are different For the same electromagnetic force, the motion of ions is different from that of the electrons. Usually the diffusion velocity of electrons is much larger than that of ions From the magneto fluid dynamics approximations, we may consider that the electron current density is determined mainly by the diffusion velocity of the electrons in plasma. However, when

the electromagnetic force is very large (such as in a very strong magnetic field), the diffusion velocity of ions may not be negligible. A steady two- dimensional MHD free convection and mass transfer flow with Hall current, viscous dissipation and Joule heating of an electrically conducting viscous incompressible fluid past an infinite vertical porous plate with wall temperature and concentration was studied numerically by Sattar and Maleque (2000).

Vertical flat Plate problems

The problem of free convection with variable properties about an isothermal vertical plate was analysized independently by Van Driest (1951), Sparrow (1956) and Sparrow and Gregg [(1956), (1958)]. The effects of magnetic field on the free convection heat transfer have been studied by Sparrow and Cess (1961a). Pools (1961) investigated the laminar natural convection flow in magnetohydrodynamics. The laminar natural convection boundary layer on a horizontal circular disk was analyzed by Zakerullah and Ackroyd (1979) taking account of property variation in the fluid. Alam (1995) in his Ph.D. thesis studied the effects of Joule heating on the unsteady MHD free convection and mass transfer flow with Hall current of an electrically conducting viscous incompressible fluid past in accelerated infinite vertical porous plate with time dependent wall temperature and concentration. Unsteady free convection interaction with thermal radiation in a boundary layer flow past a vertical porous plate has been studied by Sattar *et al.* (1996). Zakerullah and Maleque (1996) investigated the laminar combined convective flow about a vertical inclined surface. The steady magneto-hydrodynamic boundary layer flow due to an infinite disk rotating with a uniform angular velocity in the presence of an axial magnetic field was investigated by Hassan and Hazem (1997). They neglected the induced magnetic field but considered the Hall current and accordingly solved the steady state equations numerically using the finite difference approximation

On studying the literature of laminar boundary layer natural convection flows, it is observed that a little attention has been paid to include both viscous dissipation and pressure work effects in energy equation. In conventional analysis both effects are generally ignored. In view of the above points, it appears to be inevitable that we consider the fluid to be of variable properties and that the necessary state and transport properties be examined with some care. In the present investigation the fluids studied

are taken to be either a thermally and calorically perfect gas undergoing small changes in temperature and pressure. Steady and transient free convection of an electrically conducting fluid from a vertical plate in the presence of magnetic field has been studied by Gupta (1961). Braun *et al* (1961) investigated the free convection similarity flows about two-dimensional and axisymmetric with closed lower ends Usually in the discussion and analysis of natural convection flows, pressure and viscous stress work effects are generally ignored. However, the influence and importance of viscous stress work effects in laminar flows have been examined by Gebhart (1962) and Gebhart and Mollendorf (1969). In both of the investigations, special flows over semi-infinite flat surfaces parallel to the direction of body force were considered. Gebhart (1962) considered flows generated by the plate surface temperatures, which vary as powers of ξ (the distance along the plate surface from the leading edge). Cramer (1963) investigated the several magnetohydrodynamic free convection solutions. Thermal convection in magnetohydrodynamics has been studied by Sing *et al*. (1963). Gebhart and Mollendorf (1969) considered flows generated by plate surface temperatures, which vary exponentially in ξ. Here the effects of pressure and viscous stress work are retained in the energy equation. Lock *et al*. (1968) investigated the laminar free convection from a downward projecting fin. Nanda *et al*. (1970) studied the hydromagnetic free convection for high and low Prandtl numbers. Kuiken (1970) studied the problem of magnetohydrodynamic free convection in a strong crossflow. Zakerullah (1972) considered the pressure work and viscous work terms for the axi-symmetric natural convection flows. Compressible and incompressible flows of various shapes have been studied by [Chen et al. (1956), Hansen (1964), Loyd *et al*. (1970), Clarke (1973), Chao *et al*. (1983), Nicolas *et al*. (1993) and Ganzarlli *et al*. (1995)]. Ackroyd (1974) discussed the effects of both viscous and pressure stress work in natural convection flow on flat plate surface. Magneto-hydrodynamic free convection about a semi-infinite vertical plate in a strong cross-field has been studied by Wilks (1976) Chida et al. (1976) investigated the effect on conjugate heat transfer by vectorial dimensional analysis. Many experimental and theoretical works on combined effects of magneto-hydrodynamic (MHD) free and forced convection boundary layer flow are done but only a few works considered the conjugate problem Miyamoto *et al* (1980) studied the effect of axial heat conduction in a vertical flat plate on free convection heat transfer. Takhar and Soundalgekar (1980a) studied the effects of viscous and Joule

heating on the problem posed by Sparrow and Cess (1961), using the series expansion method of Gebhart (1962). Momentum Transfer in Boundary Layers has been discussed by Cebeci & Bradshow (1977). Chen *et al.* (1977) studied the effect of mixed convection in the boundary layer flow on a horizontal plate. Takhar and Soundalgekar (1980b) studied the dissipation effects on MHD free convection flow past a semi-infinite vertical plate. A transformation of the boundary layer equations for free convection past a vertical flat plate with arbitrary blowing and wall temperature variations has been discussed by Vedhanayagam *et al.* (1980). Joshi and Gebhart (1981) shown that the effect of pressure stress work and viscous dissipation in some natural convection flows Curle (1981) investigated the development and separation of a laminar boundary layer flow with an exponentially increasing pressure gradient. Vafai (1981) studied the boundary and inertia effects on flow and heat transfer in porous media. Raptis and Kafoussias (1982) have investigated the problem of magnetohydrodynamic free convection flow and mass transfer through a porous medium bounded by an infinite vertical porous plate with constant heat flux. Heat and mass transfer for natural convection in a porous medium studied by Bejan *et al.* (1985). November *et al.* (1987) studied the natural convection in a rectangular enclosure heated from below and cooled along one surface. Pozzi and Lupo (1988) investigated the coupling of conduction with laminar convection along a flat plate. Kumari *et al.* (1990) studied the effect of natural convection in porous media above a near horizontal uniform heat flux surface. Moreover, Hossain *et al.* [(1990), (1997), (1998)] discussed the both forced and free convection boundary layer flow of an electrically conducting fluid in presence of magnetic field. Hossain (1992) analyzed the viscous and Joule heating effects on MHD free convection flow with variable plate temperature. Vajravelu and Hadjinolauo (1993) studied the heat transfer characteristics in the laminar boundary layer of a viscous fluid over a stretching sheet with viscous dissipation or frictional heating and internal heat generation. Unsteady hydromagnetic free convection flow with Hall current mass transfer and variable suction through a porous medium near an infinite vertical porous plate with constant heat flux has been studied by Sattar (1994). Pop *et al.* (1995) investigated the conjugate free convection on a vertical surface in porous medium. The effect of temperature dependent viscosity on the free convective laminar boundary layer past a vertical isothermal flat plate has been discussed by Kafoussius *et al.* (1995). Heat and mass transfer flow with thermal diffusion has been discussed by Alam (1995). Numerical studied of various flows have been investigated

by [Nachhtsheim and Swigert, (1965), Keller *et al.* {(1971), (1972)}, Keller (1978). Soundalgekar *et al.* {(1980), (1981)}, Shiralkar (1982), Cebeci and Bradshow (1984), Kafoussius *et al.* (1988), Chiam (1998) and Al-Khawaja *et al.* (1999)]. Moreover, Hossain *et al.* [(1990), (1994), (1996), (1997b), (1998b), (1999)] discussed both forced and free convection boundary layer flow of an electrically conducting fluid in presence of magnetic field. Velusamy *et al.* (1998) investigated the laminar natural convection in an enclosure formed by non-isotherm walls. MHD free convection flow of visco-elastic fluid past an infinite porous plate was investigated by Chowdhury and Islam (2000). Numerical solution of MHD free convection and mass transfer flow with Hall current, viscous dissipation and Joule heating have been investigated by Sattar *et al* (2000). Also the effects of the conjugate conduction-natural convection heat transfer along a thin vertical plate with non-uniform heat generation have been studied by Mendez and Trevino (2000). Elbashbeshy (2000) also discussed the effect of free convection flow with variable viscosity and thermal diffusivity along a vertical plate in the presence of magnetic field. Alam *et al.* (2001) studied the analytical solution of the free convection and mass transfer flow with thermal diffusion. Khan (2002) investigated the conjugate effect of conduction and convection with natural convection flow from a vertical flat plate and in an inclined square cavity. Ramadan et al. (2003) studied the effect of hydromagnetic free convection of a particulate suspension from a permeable inclined plate with heat absorption for non-uniform particle-phase density. El-Amin (2003) studied combined effect of viscous dissipation and Joule heating on MHD forced convection over a non isothermal horizontal cylinder embedded in a fluid saturated porous medium. Finite difference analysis of unsteady natural convection MHD flow past an inclined plate with variable surface heat and mass flux has been investigated by Gansan *et al.* (2004). Molla *et al.* (2004) also discussed the problem of natural convection flow along a vertical wavy surface with uniform surface temperature in presence of heat generation / absorption. Shariful (2004) in his M. Phil. thesis investigated the Thermal-Diffusion and diffusion thermo effects on magnetohydrodynamics heat and mass transfer. Effects of viscous dissipation and Joule heating on magnetohydrodynamic hiemenz flow of micropolar fluid have been investigated by El-Amin *et al.* (2005). Umavathi *et al.* (2005) studied magneto-hydrodynamic mixed convection in a vertical channel. Alam *et al.* (2006) investigated the effect of pressure stress work and viscous dissipation in natural convection flow along a vertical flat plate with heat conduction. Combined effect of viscous dissipation

and Joule heating on the coupling of conduction and free convection along a vertical flat plate have been studied by Alim *et al.* (2007).

Over a sphere, cylinder and cone problems

Theoretical studies on laminar free convection flow on axisymmetric bodies have received wider attention, especially in case of non-uniform surface temperature and surface heat flux distributions. Merk and Prins (1954) developed the general relations for similar solutions on isothermal axisymmetric forms and showed that for the flow past a vertical cone has such a solution. Braun *et al.* (1961) contributed free convection similarity flows about two-dimensional and axisymmetric bodies with closed lower end for which similar solutions exist, and used an integral method to provide heat transfer results for these and the cone over a wide range of Prandtl number. In the above investigation, the authors obtained the results by numerical integration of the differential equations for fluid having Prandtl number 0.72. The similarity solutions for free convection from the vertical cone have been exhausted by Hering and Grosh (1962). They showed that the similarity solutions to the boundary layer equations for a cone exist when the wall temperature distribution is a power function of distance along a cone ray. In their paper they presented results for an isothermal surface as well as for a surface maintained at a temperature varying linearly with the distance measured from the apex of the cone for Prandtl number 0.7. Hering and Grosh (1962) studied the effect of laminar free convection from a non-isothermal cone. Hering (1965) also investigated the laminar free convection from a non-isothermal cone at low Prandtl numbers. Roy (1974) has investigated the free convection over a slender vertical cone at high Prandtl numbers. Laminar free convection from a vertical cone with uniform surface heat flux and blowing and suction have been studied by Lin [(1976), (1988)] and Merkin [(1972), (1975)]. Steady state heat transfer within porous medium with temperature-dependent heat generation has been investigated by Moalem (1976). On the other hand, the analysis of mixed forced and free convection around a sphere was discussed by Chen and Mucoglu (1977). Na and Chiou (1979a) studied the effect of slenderness on the natural convection flow over a slender frustum of a cone. The problem of natural convection flow over a frustum of a cone without transverse curvature effect (i.e., large cone angles when the boundary layer thickness is small compared with the local radius of the cone) has been treated in the literature, even though the problem for a full cone has been considered quite extensively by Sparrow and Guinle (1968), Lin (1976),

Kuiken (1968) and Oosthuizen and Donaldson (1972). Cheng (1982) studied the effects of mixed convection about a horizontal cylinder and a sphere in a fluid-saturated porous medium. Latter, Na and Chiou (1979b) studied the laminar natural convection flow over a frustum of a cone. In the above investigations the wall temperature as well as the wall heat flux were considered constant. On the other hand, Alamgir (1979) investigated the overall heat transfer in laminar natural convection flow from vertical cones by using the integral method. Natural convection from a semi infinite plate inclined at a small angle at the horizontal in saturated porous medium has been studied by Ingham *et al.* (1985). Huang and Chen (1987) investigated the laminar free convection from a sphere with blowing and suction. Moreover, Hossain *et al.* [(1997a), (1998a)] discussed both forced and free convection boundary layer flow of an electrically conducting fluid in presence of magnetic field. Jha (1991) investigated MHD unsteady mixed convection flow through a porous medium. Maleque (1996) studied the similarity solutions of combined forced and free convection laminar boundary layer flows in curvilinear co-ordinates. Natural convection flow of a viscous fluid about a truncated cone with temperature dependent viscosity and thermal conductivity have been investigated by Hossain *et al.* (2000). Amongst them are Huang and Chen (1987), Nazar *et al.* [(2002a), (2002b)], considered the free convection boundary layer on an isothermal sphere and on an isothermal horizontal circular cylinder in a micropolar fluid. The non-uniform surface temperature and non-uniform surface heat flux over a free convection from a vertical permeable circular cone have been investigated by Hossain and Paul [(2001a), (2001b)] Natural convection flow of a viscous incompressible fluid in a rectangular porous medium cavity heated from below has been studied by Hossain *et al.* (2003). Hossain *et al.* (2004) investigated conjugate effect of heat and mass transfer in natural convection flows from an isothermal sphere with chemical reaction. Very recently, Hossain *et al.* (2004) studied the conjugate effect of heat and mass transfer in natural convection flow from an isothermal sphere for temperature dependent thermal conductivity and radiation effect respectively. Molla *et al.* (2005) studied the effects of magnetohydrodynamic natural convection flow on a sphere in presence of heat generation. Magnetohydrodynamic natural convection flow on a sphere with uniform heat flux in presence of heat generation has been investigated by Molla *et al.* (2006). Pressure work effect on natural convection flow from a vertical circular cone with suction and non-uniform surface temperature have been discussed by Alim *et al.* (2006). Viscous dissipation effects on MHD natural convection flow along a sphere has been

investigated by Alam *et al.* (2006) Alam *et al.* (2007) studied the free convection from a vertical permeable circular cone with pressure work and non-uniform surface temperature. Alam *et al.* (2007) studied the viscous dissipation effects on MHD natural convection flow over a sphere in the presence of heat generation.

From above discussions, it is found that various magnetohydrodynamics problems of vertical flat plate, cylinder, sphere and circular cone have been investigated for velocity and temperature distribution, skin friction coefficient as well as local heat transfer coefficient.

1.4 Objective of the present work

A steady two dimensional MHD laminar free convection flow with viscous dissipation and Joule heating together with the boundary conditions based on conduction and convection from a vertical flat plate will be investigated. In addition to that the stress work effects on MHD steady natural convection flow in the presence of heat generation and radiation over a sphere will be considered. Solutions will be obtained and analyzed in terms of skin-friction coefficients and the local rate of heat transfer, the surface temperature distribution, velocity and temperature profiles for different values of relevant physical parameters like the magnetic parameter or Hartmann Number M, the Joule heating parameter Jul, the dissipation parameter N, the pressure work parameter Ge, and also the heat generation parameter Q will be discussed including the radiation parameter Rd.

1.5 Importance of the present study
The problems of free convection boundary layer flow over or on bodies of various shapes have been discussed by many mathematicians, versed engineers and researchers. Natural convection heat transfer gained considerable attention because of its numerous applications in the areas of energy conservations cooling of electrical and electronic components, design of solar collectors, heat exchangers and many others. Many natural phenomena and engineering problems are susceptible to MHD analysis. It is useful in astrophysics. Geophysicists encounter MHD phenomena in the interactions of conducting fluid and magnetic fields that are present in and around heavenly bodies. The most important application of MHD is in the generation of electrical power with the flow of an electrically conducting fluid through a transverse magnetic field. Recently,

experiments with ionized gases have been performed with the hope of producing power of a large scale in stationary plants with large magnetic fields. Cryogenic and superconducting magnets are required to produce these very large magnetic fields. Generation of MHD power on a smaller scale is of interest for space applications.

1.6 Outline of the thesis

In Chapter one, published works regarding heat conduction, MHD flow, viscous dissipation, pressure work, heat generation and radiation are summarized.

In chapter two governing equations of the flows are included and also the implicit finite difference with Keller-Box scheme is discussed elaborately.

In chapter three, locally similar solution of the steady stress work effects on natural convection flow along a vertical flat plate in presence of magnetic field with heat conduction is discussed. The results of the numerical solution are then presented graphically in the form of velocity and temperature profiles, as well as skin friction coefficient and surface temperature. The skin friction coefficient and surface temperature are also displayed in tables showing the effects of various parameters on them.

In chapter four, the viscous dissipation and the pressure effects on two dimensional viscous incompressible and electrically conducting fluids from a vertical flat plate in presence of transverse magnetic field and Joule heating with heat conduction have been discussed. The effects of various parameters on the velocity and temperature fields as well as on the skin friction coefficient and surface temperature have been investigated. The skin friction coefficient and the surface temperature are also displayed in tables whose are depicted in Appendix C.

In chapter five, the investigations concerned with the conjugate effects of stress work and heat generation on magnetohydrodynamics free convection flow along a vertical flat plate with Joule heating and heat conduction are carried out. The results of the numerical solution are then presented graphically in the form of velocity and temperature profiles, as well as skin friction and surface temperature. The skin friction and surface temperature are displayed in tables showing the effects of various

parameters such as the magnetic parameter M, the Joule heating parameter *Jul*, the Prandtl number Pr, the viscous dissipation parameter N, the pressure work parameter Ge and the heat generation parameter Q on them. The numerical tables are also displayed in Appendix C.

In chapter six, the description of the pressure work and viscous dissipation effects with magnetohydrodynamic natural convection flow on a sphere in presence of heat generation has been presented. The evolution of the shear stress in terms of local skin friction and the rate of heat transfer in terms of local Nusselt number, velocity profiles as well as temperature profiles for some set of parameter consisting of heat generation parameter Q, magnetic parameter or Hartmann Number M, pressure work parameter Ge, viscous dissipation parameter N and the Prandtl number Pr are explained.

The conjugate effects of stress work and magneto- hydrodynamic natural convection flow on a sphere in presence of heat generation and radiation has been described in chapter seven. Here, attention is focused on the evolution of the surface shear stress in terms of local skin friction and the rate of heat transfer in terms of local Nusselt number, velocity distribution as well as temperature distribution for a set of parameters consisting of heat generation parameter, magnetic parameter or Hartmann Number, pressure work parameter, dissipation parameter, radiation parameter, surface temperature parameter and the Prandtl number.

Finally, a general discussion on all problems dealt with is presented in chapter eight with some concluding remarks. References and Tables relating to all chapters are displayed here.

2.1 The Fundamental Electromagnetic Equations

Magnetohydrodynamic equations are the ordinary electromagnetic and hydrodynamic equations modified to take account of the interaction between the motion of the fluid and electromagnetic field. Formulation of electromagnetic theory in mathematical form is known as Maxwell's equations. Maxwell's basic equations show the relation of basic field quantities and their products. But here we will always assume that all velocities are small in comparison with the speed of light. Before writing down the MHD equations we should first of all know the ordinary electromagnetic equations and hydromagnetic equations Cramer & Pai, (1974).

First we give the electromagnetic equations.

Charge Continuity:	$\nabla . \vec{D} = \rho_e$	(2.1)
Current Continuity:	$\nabla . \vec{J} = -\dfrac{\partial \rho_e}{\partial t}$	(2.2)
Magnetic field continuity:	$\nabla . \vec{B} = 0$	(2.3)
Ampere's Law:	$\nabla \wedge B_0 = \vec{J} + \dfrac{\partial \vec{D}}{\partial t}$	(2.4)
Faraday's Law:	$\nabla \wedge \vec{E} = -\dfrac{\partial \vec{B}}{\partial t}$	(2.5)
Constitutive equations for D and B:	$\vec{D} = \varepsilon \vec{E}$ and $\vec{B} = \mu_e B_0$	(2.6)
Total current density flow:	$\vec{J} = \sigma\left(\vec{E} + \vec{q} \wedge \vec{B}\right) + \rho_e \vec{q}$	(2.7)

The above equations (2.1) to (2.7) are Maxwell's equations where $\vec{D}$ is the electron displacement, ρ_e is the charge density, $\vec{E}$ is the electric field, $\vec{B}$ is the magnetic field, B_0 is the magnetic field strength, $\vec{J}$ is the current density, $\partial \vec{D}/\partial t$ is the displacement current density, ε is the electric permeability of the medium, μ_e is the magnetic permeability of the medium, $\vec{q}$ is the velocity field and σ is the electric conductivity.

The electromagnetic equations as shown above are not usually applied in their present form and require interpretation and several assumptions to provide the set to be used in MHD. In MHD we consider a fluid that is grossly neutral. The charge density ρ_e in Maxwell's equations must then be interpreted, as an excess charge density, which is

generally not large. If we disregard the excess charge density then we must disregard the displacement current. In most problems the displacement current, the excess charge density and the current due to convection of the excess charge are small. Considering this effect the electromagnetic equations can be reduced to the following form:

$$\nabla.\vec{D} = 0 \tag{2.8}$$

$$\nabla.\vec{J} = 0 \tag{2.9}$$

$$\nabla.\vec{B} = 0 \tag{2.10}$$

$$\nabla \wedge B_0 = \vec{J} \tag{2.11}$$

$$\nabla \wedge \vec{E} = -\frac{\partial \vec{B}}{\partial t} \tag{2.12}$$

$$\vec{D} = \varepsilon\vec{E} \text{ and } \vec{B} = \mu_e B_0 \tag{2.13}$$

$$\vec{J} = \sigma\left(\vec{E} + \vec{q} \wedge \vec{B}\right) \tag{2.14}$$

We shall now suitably represent the equations of fluid dynamics to take account of the electromagnetic phenomena.

The continuity equation

The MHD continuity equation for viscous incompressible electrically conducting fluid remains same as that of usual continuity equation

$$\nabla \cdot \vec{q} = 0 \tag{2.15}$$

The Navier-Stokes equation

The motion of the conducting fluid across the magnetic field generates electric currents, which change the magnetic field and the action of the magnetic field on these current gives rise to mechanical forces, which modify the flow of the fluid. Thus, the fundamental equation of the magneto-fluid combines the equations of the motion from fluid mechanics with Maxwell's equations from electrodynamics.

Then the Navier-stokes equation for a viscous incompressible fluid may be written in the following form:

$$\rho(\vec{q} \cdot \nabla)\vec{q} = -\nabla P + \mu\nabla^2\vec{q} + \vec{F} + \vec{J} \times \vec{B} \tag{2.16}$$

where, ρ is the fluid density μ is the viscosity and P is the pressure. The first term on the right hand side of equation (2.16) is the pressure gradient, second term is the viscous

dissipation, third term is the body force per unit volume and last term is the electromagnetic force due to motion of the fluid.

The energy equation

The energy equation for a viscous incompressible fluid is obtained by adding the electromagnetic energy term into the classic gas dynamic energy equation. This equation can be written as

$$\rho C_P \left(\vec{q} \cdot \nabla \right) T = \nabla \cdot \left(\kappa \nabla T \right) + \left(\vec{q} \cdot \nabla \right) P + \left(\vec{J} \times \vec{B} \right) \mu + \mu \phi \qquad (2.17)$$

Here, κ is the thermal conductivity, C_P is the specific heat with constant pressure. The left side of equation (2.17) represents the net energy transfer due to mass transfer, the first term on the right hand side represents conductive heat transfer, second term the pressure work term, the third term is Joule heating term due to the resistance of the fluid to the flow of current and the last term is the viscous energy dissipation in the fluid due to the internal friction.

Where $\vec{q} = (U,V)$, U and V are the velocity components along the X and Y axes respectively, $\vec{F}$ is the body force per unit volume which is defined as $-\rho g$, the terms $\vec{J}$ and $\vec{B}$ are respectively the current density and magnetic induction vector and the term $\vec{J} \times \vec{B}$ is the force on the fluid per unit volume produced by the interaction of the current and magnetic field in the absence of excess charges, T is the temperature of the fluid in the boundary layer, g is the acceleration due to gravity, κ is the thermal conductivity and C_p is the specific heat at constant pressure and μ is the viscosity of the fluid. In the energy equation the viscous dissipation, pressure work and Joule heating terms are included.

Here $\vec{B} = \mu_e B_0$, μ_e being the magnetic permeability of the fluid, B_0 is the uniformly distributed transverse magnetic field of strength and ∇ is the vector differential operator and is defined for two dimensional case as

$$\nabla = \hat{i}_x \frac{\partial}{\partial x} + \hat{i}_y \frac{\partial}{\partial y}$$

Where $\hat{i}_x$ and $\hat{i}_y$ are the unit vector along x and y axes respectively. When the external electric field is zero and the induced electric field is negligible, the current density is related to the velocity by Ohm's law as follows

$$\vec{J} = \sigma\left(\vec{q} \times \vec{B}\right) \tag{2.18}$$

Where σ denotes the electric conductivity of the fluid. Under the condition that the magnetic Reynolds number is small, the induced magnetic field is negligible compared to applied field. This condition is well satisfied in terrestrial applications, especially in (low velocity) free convection flows. So we can write

$$\vec{B} = \hat{i}_y B_0 \tag{2.19}$$

Bringing together equations (2.18) and (2.19) the force per unit volume $\vec{J} \times \vec{B}$ acting along the x-axis takes the form.

$$\vec{J} \times \vec{B} = \sigma B_0^2 u \tag{2.20}$$

Under the Boussinesq approximation, the variation of ρ is taken into account only in the term $\vec{F}$ in equation (2.16) and the variation of ρ in the inertia term is neglected. We then can write:

$$\rho = \rho_\infty \left[1 - \beta(T - T_\infty)\right] \tag{2.21}$$

Where ρ_∞ and T_∞ are the density and temperature respectively for the ambient fluid, β is the coefficient of thermal expansion.

We consider viscous dissipation, pressure work and Joule heating effects on a steady two-dimensional incompressible magnetohydrodynamic laminar free convection boundary layer flow. Using the equations (2.18) to (2.21) with respect to above considerations into the basic equations (2.15) to (2.17), the steady two-dimensional, laminar free convection boundary layer flow of viscous incompressible and conducting fluid through a uniformly distributed transverse magnetic field of strength B_0 take the following form:

$$\frac{\partial U}{\partial X} + \frac{\partial V}{\partial Y} = 0 \tag{2.22}$$

$$U\frac{\partial U}{\partial X} + V\frac{\partial U}{\partial Y} = g\beta(T - T_\infty) + \nu\frac{\partial^2 U}{\partial Y^2} - \frac{\sigma B_0^2}{\rho}U \tag{2.23}$$

$$U\frac{\partial T}{\partial X} + V\frac{\partial T}{\partial Y} = \kappa\frac{\partial^2 T}{\partial Y^2} + \frac{\sigma B_0^2}{\rho}U^2 + \frac{\nu}{C_p}\left(\frac{\partial U}{\partial Y}\right)^2 + \frac{T\beta U}{\rho C_p}\frac{\partial P}{\partial X} \tag{2.24}$$

Here U and V are the velocity components associated with the direction of increasing coordinates X and Y, measured along and normal to the vertical plate, respectively, T is the temperature of the fluid in the boundary layer, g is the acceleration due to gravity,

C_p is the specific heat at constant pressure, β is the coefficient of thermal expansion , and which is defined by $\beta = 1/T$, κ is the thermal conductivity, ρ is the density of the fluid, σ is the electric conductivity, T_∞ is the temperature of the ambient fluid.

The boundary conditions are

$$U = V = 0, \quad T = T_w \text{ as } Y = 0$$
$$U \to 0, \ T \to T_\infty \text{ at } \ Y \to \infty$$

(2.25)

2.2 General governing equations of the flow along a vertical flat plate

The steady two dimensional laminar free convection boundary layer flow of a viscous incompressible and electrically conducting fluid along a side of a vertical flat plate of thickness 'b' insulated on the edges with temperature T_b maintained on the other side in the presence of a uniformly distributed transverse magnetic field has been considered. The flow configuration and the coordinates system are shown in figure 2.1
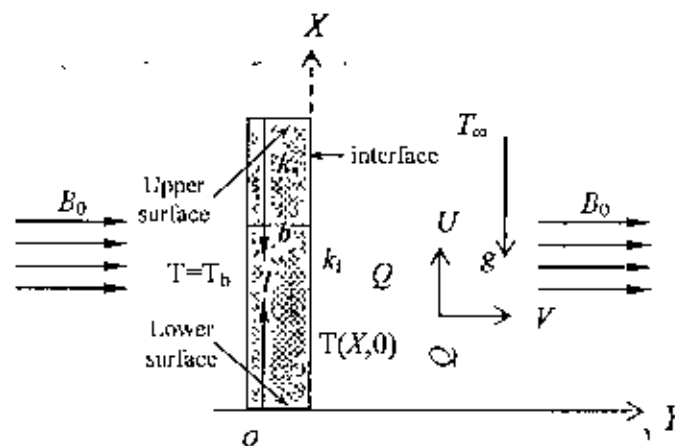
Figure 2.1: Physical configuration and coordinate system

The mathematical statement of the basic conservation laws of mass, momentum and energy for the steady viscous incompressible and electrically conducting flow are given by Crammer and Pie (1974)

$$\nabla.\vec{q} = 0$$

(2.26)

$$\rho(\vec{q}.\nabla)\vec{q} = -\nabla p + \mu\nabla^2\vec{q} + \vec{F} + \vec{J}\times\vec{B}$$

(2.27)

$$\rho C_p (\vec{q}.\nabla) T - (\vec{q}.\nabla) P = \nabla.(\kappa \nabla T) + (\vec{J} \times \vec{B}) U + \mu \phi + \frac{Q_0}{\rho C_p}(T - T_o) \qquad (2.28)$$

Where $\vec{q} = (U,V)$, U and V are the velocity components along the X and Y axis respectively, $\vec{F}$ is the body force per unit volume which is defined as $-\rho g$, the terms $\vec{J}$ and $\vec{B}$ are respectively the current density and magnetic induction vector and the term $\vec{J} \times \vec{B}$ is the force on the fluid per unit volume produced by the interaction of the current and magnetic field in the absence of excess charges, T is the temperature of the fluid in the boundary layer , g is the acceleration due to gravity, κ is the thermal conductivity, C_p is the specific heat at constant pressure and μ is the viscosity of the fluid. In the energy equation the viscous dissipation and pressure work terms are included. The amount of heat generated or absorbed per unit volume is $Q_0(T - T_\infty)$, Q_0 being a constant, which may take either positive or negative. The source term represents the heat generation when $Q_0 > 0$ and the heat absorption when $Q_0 < 0$. In the energy equation the viscous dissipation, pressure work and Joule heating terms are included.

After simplifying we have the followings

$$\frac{\partial U}{\partial X} + \frac{\partial V}{\partial Y} = 0 \qquad (2.29)$$

$$U \frac{\partial U}{\partial X} + V \frac{\partial U}{\partial Y} = v \frac{\partial^2 U}{\partial Y^2} + g \beta(T - T_\infty) - \frac{\sigma B_0^2 U}{\rho} \qquad (2.30)$$

$$U \frac{\partial T}{\partial X} + V \frac{\partial T}{\partial Y} = \frac{\kappa}{\rho c_p} \frac{\partial^2 T}{\partial Y^2} + \frac{v}{c_p}(\frac{\partial U}{\partial Y})^2 - \frac{T \beta U}{\rho C_p} \rho g + \frac{\sigma B_0^2}{\rho C_p} U^2 + \frac{Q_0}{\rho C_p}(T - T_\infty) \qquad (2.31)$$

where for exterior conditions we know, $\partial P / \partial X = -\rho_e g$ and $\rho = \rho_e$, P is the pressure. The appropriate boundary conditions to be satisfied by the above equations are

$U = 0$, $V = 0$ at $Y = 0$

$U \rightarrow 0, T \rightarrow T_\infty$ as $Y \rightarrow \infty$ $\qquad (2.32)$

The temperature and the heat flux are considered continuous at the interface for the coupled conditions and at the interface we must have

$$\frac{k_s}{k_f} \frac{\partial T_{so}}{\partial Y} = (\frac{\partial T}{\partial Y})_{1 = 0} \qquad (2.33)$$

Where k_s and k_f are the thermal conductivity of the solid and the fluid respectively. The temperature T_{so} in the solid as given by A. Pozzi and M. Lupo (1988) is

$$T_{\omega} = T(X,0) - \{T_b - T(X,0)\}\frac{Y}{b} \tag{2.34}$$

Where $T(X, 0)$ is the unknown temperature at the interface to be determined from the solutions of the equations.

We observe that the equations (2.29) - (2.31) together with the boundary conditions (2.32) - (2.33) are non-linear partial differential equations. In this chapter the solution of finite difference method of these equations are discussed in details.

Transformation of the governing equations

Equations (2.29) – (2.31) may now be non-dimensionalized by using the following dimensionless dependent and independent variables:

$$x = \frac{X}{L}, \quad y = \frac{Y}{L}d^{1/4}, \quad U = \frac{v}{L}d^{1/2}u, \quad V = \frac{v}{L}d^{1/4}v, \quad \theta = \frac{T - T_\infty}{T_b - T_\infty}$$
$$L = \frac{v^{2/3}}{g^{1/3}}, \quad d = \beta(T_b - T_\infty) \tag{2.35}$$

As the problem of natural convection, its parabolic character, has no characteristic length, L has been defined in terms of v and g, which are the intrinsic properties of the system. The reference length along the 'y' direction has been modified by a factor $d^{-1/4}$ in order to eliminate this quantity from the dimensionless equations and the boundary conditions

The magnetohydrodynamic field in the fluid is governed by the boundary layer equations, which in the non-dimensional form obtained by introducing the dimensionless variables described in (2.35) may be written as

$$\frac{\partial u}{\partial x} + \frac{\partial v}{\partial y} = 0 \tag{2.36}$$

$$u\frac{\partial u}{\partial x} + v\frac{\partial u}{\partial y} + Mu = \frac{\partial^2 u}{\partial y^2} + \theta \tag{2.37}$$

$$u\frac{\partial \theta}{\partial x} + v\frac{\partial \theta}{\partial y} = \frac{1}{Pr}\frac{\partial^2 \theta}{\partial y^2} + N(\frac{\partial u}{\partial y})^2 + Jul(u^2) - G_e\frac{\{T_\infty + (T_b - T_\infty)\theta\}}{(T_b - T_\infty)} + Q\theta \tag{2.38}$$

Where $M = \sigma B_0^2 L^2/\mu d^{1/2}$, the dimensionless magnetic parameter which is Known Hartmann Number, $Pr = \mu C_p/\kappa_f$, the Prandtl number and $N = v^2 d/L^2 c_p(T_b - T_\infty)$, the dimensionless viscous dissipation parameter, $Jul = \sigma B_0^2 v d^{1/2}/\rho C_p(T_b - T_\infty)$, is the Joule heating parameter and $Q_0 L^2/\mu C_p d^{1/2} = Q$ is the heat generation parameter.

Also, the pressure work parameter $G_e = g\beta L/C_p$, which is suggested by Gebhart (1962).

At 250^oK the values of Prandtl number are $Pr = 0.722$ for air. Again for steam at 700^oK $Pr = 1.00$, for mercury at 250^oC $Pr = 0.0103$, for water at 20^oC, 60^oC, 100^oC and 300^oC the values of Prandtl number are $Pr = 7.02$, $Pr = 1.74$, $Pr = 3.02$ and $Pr = 1.019$ respectively.

Evaluation of solution for $M > 2$ becomes tedious and hence neglected for $M > 2$. With the increase of M velocity profiles decrease because of the retarding effect of the magnetic force and at some stage velocity profiles cannot be evaluated within the boundary layer. Therefore the momentum boundary layer thickness becomes larger and the separation of the boundary layer will occur earlier. In the present work the values of dimensionless parameter $M = 0.1$ to 2.0 are assumed which is comparable with Table-B_5.

If the heat generation parameter Q increases, both the velocity and temperature profiles increase. As Q increases, the velocity gradient at the surface increases which enhances the fluid velocity. Therefore the limiting values of Q between 0.00 to 0.60 are taken to compare with Table-B_9.

The values of dimensionless viscous dissipation parameter N have been taken in the range 0.1 to 0.9 in accordance with table-B_8.

The values of dimensionless pressure work parameter Ge are taken in 0.1 to 1.0 which compared with Table-B_{11}.

Joule heating occurs when an electrical current is passed through a material and the material's resistivity to the current cause's heat generation. When current flows in an electrical conductor such as wire, electrical energy is lost due to the resistance of the electrical conductor. This lost electrical energy is converted into thermal energy called Joule heating. This is because of the electrical power loss equals the thermal energy. So that for thermal energy Joule heating parameter obey the same nature of heat generation parameter i.e. for increasing values of Joule heating parameter both velocity and temperature profiles increase. The velocity gradient at the surface increases which

accelerate the fluid velocity. For this reason we cannot find the actual laminar boundary layer. Therefore we take the minimum values of Joule heating parameter that is less than one. In the present work the values of non-dimensional parameter *Jnl* are considered 0.2 to 0.9 which compared with Table-B$_{10}$.

Calculation of numerical values of magnetic and Joule heating parameters are shown in Table- B$_{12}$ for water at 20"C.

Prandtl number is the ratio of kinematics viscosity to the thermal diffusivity, $Pr = \nu / \alpha$.

The rate at which the pressure does work known as pressure work on one side of a surface in the fluid is the product of the pressure, the area of the surface and the normal component of velocity.

In order to explain the effect of viscous dissipation, we shall first take a grossly simplified view that the compressibility effect may be neglected and the properties such as viscosity, thermal conductivity and specific heat are constant.

Magnetohydrodynamic is that branch of continuum mechanics which deals with the flow of electrically conducting fluids with magnetic fields. The magnetic parameter is obtained from the ratio of the magnetic force to the inertia force.

When current flows in an electrical conductor such wire, electrical energy is lost due to the resistance of the electrical conductor, this lost electrical energy is converted into thermal energy called Joule heating.

Heat generation means heat is generated internally due to Joule heating of electrical conductor or internal heating of solid-state electronic device.

The corresponding boundary conditions (2.32) - (2.34) take the following form:

$$u=v=0 \, , \; \theta - 1 = p(\partial\theta/\partial y) \text{ at } y = 0 \tag{2.39}$$
$$u \to 0, \; \theta \to 0 \; \text{ as } y \to \infty$$

Where P is the pressure and p is the conjugate conduction parameter given by

$p = \kappa_f/\kappa_s \, (b/L) \, d^{1/4}$. Here the coupling parameter 'p' governs the described problem. The order of magnitude of 'p' depends actually on b/L and κ_f/κ_s, $d^{1/4}$ being the order of unity. The term b/L attains values much greater than one because of L being small. In case of air, κ_f/κ_s becomes very small when the vertical plate is highly conductive i e. $\kappa_s > > 1$ and for materials, such as glass O $(\kappa_f/\kappa_s) = 0.1$. Therefore, in different cases 'p'

is different but not always a small number. In the present investigation we have considered $p = 1$ which is accepted for b/L of O (κ_f/κ_s).

To solve the equations (2.37) – (2.38) subject to the boundary conditions (2.39), the following transformations were introduced for the flow region starting from upstream to downstream.

$$\psi = x^{3/5}(1+x)^{-1/20} f(x,\eta), \quad \eta = yx^{-1/5}(1+x)^{-1/20}, \quad \theta = x^{1/5}(1+x)^{-1/5} h(x,\eta) \tag{2.40}$$

Here η is the dimensionless similarity variable and ψ is the stream function which satisfies the equation of continuity and $u = \dfrac{\partial \psi}{\partial y}, v = -\dfrac{\partial \psi}{\partial x}$ and $h(x,\eta)$ is the dimensionless temperature. Therefore,

$$u = \frac{\partial \psi}{\partial y} = x^{3/5}(1+x)^{-1/10}\frac{\partial f}{\partial \eta}, \quad u^2 = x^{6/5}(1+x)^{-1/5}\left(\frac{\partial f}{\partial \eta}\right)^2$$

$$\frac{\partial u}{\partial y} = x^{2/5}(1+x)^{-3/20}\frac{\partial^2 f}{\partial \eta^2}, \quad \frac{\partial^2 u}{\partial y^2} = x^{1/5}(1+x)^{-1/5}\frac{\partial^3 f}{\partial \eta^3},$$

$$v = -\frac{\partial \psi}{\partial x} = -x^{4/5}(1+x)^{-1/20}\left\{\frac{15x+16}{20x(1+x)}f(x,\eta)\right.$$

$$\left. -\frac{\eta(4+5x)}{20x(1+x)}\frac{\partial f}{\partial \eta}+\frac{\partial f}{\partial x}\right\}, \quad \frac{\partial u}{\partial x} = x^{3/5}(1+x)^{-1/10}\left\{\frac{\partial^2 f}{\partial \eta \partial x}-\frac{\eta(4x+5)}{20x(1+x)}\frac{\partial^2 f}{\partial \eta^2}\right. \tag{2.41}$$

$$\left. +\frac{(5x+6)}{10x(1+x)}\frac{\partial f}{\partial \eta}\right\}, \quad \frac{\partial \theta}{\partial y} = (1+x)^{1/4}\frac{\partial h}{\partial \eta}, \quad \frac{\partial^2 \theta}{\partial y^2} = x^{-1/5}(1+x)^{-3/10}\frac{\partial^2 h}{\partial \eta^2},$$

$$\frac{\partial \theta}{\partial x} = x^{1/5}(1+x)^{-1/5}\left\{\frac{h(x,\eta)}{5x(1+x)}+\frac{\partial h}{\partial x}-\frac{\eta(4+5x)}{20x(1+x)}\frac{\partial h}{\partial \eta}\right\}$$

In view of equations (2.40)-(2.41), equations (2.37) and (2.38) become

$$f''' + \frac{16+15x}{20(1+x)}ff'' - \frac{6+5x}{10(1+x)}f'^2 - Mx^{2/5}(1+x)^{1/10}f' + h = x(f'\frac{\partial f'}{\partial x}-f''\frac{\partial f}{\partial x}) \tag{2.42}$$

$$\frac{1}{P_r}h'' + \frac{16+15x}{20(1+x)}fh' - \frac{1}{5(1+x)}f'h + Jul\,x^{2/5}(1+x)^{1/10}f'^2 + Qx^{2/5}(1+x)^{1/10}h(x,\eta)$$

$$+Nxf''^2 - G_e\,x\left\{\left(\frac{1+x}{x}\right)^{\frac{1}{5}}\left(\frac{T_\infty}{T_b-T_\infty}\right)\frac{\partial f}{\partial \eta}+h(x,\eta)\right\}\frac{\partial f}{\partial \eta}\right\} = x(f'\frac{\partial h}{\partial x}-h'\frac{\partial f}{\partial x}) \tag{2.43}$$

In the above equations the primes denote differentiation with respect to η.

The boundary conditions (2.39) then take the following form

2.2.1 Numerical Methods

The theoretical treatment of Magnetohydrodynamics flows or any other flows both in horizontal or incline planes have so far been made mostly analytically, applying laplace transform and perturbation methods. In some cases asymptotic method has been applied. However, our solutions would be based mainly on numerical methods. For this purpose the shooting method of Nachtshiem-swigert iteration technique and finite difference method together with Keller box Scheme will be used for problems for which similarity solutions of ordinary differential equations are sought. In order to obtain non-similar solutions to partial differential equations, an implicit finite-difference method has been applied. Since only one problem of this type has been considered the above finite-difference method will be discussed in the respective chapter.

Finite Difference Method

To get the solutions of the parabolic differential equations (2.42) and (2.43) along with the boundary condition (2.44), we shall employ the most practical, efficient and accurate solution technique, known as implicit finite difference method together with Keller-box elimination technique which is well documented and widely used by Keller (1978) and Cebeci(1984) and recently by Hossain (1992).

To apply the aforementioned method, we first convert the equations (2.42) and (2.43) and their boundary condition into the system of first order equations. For this purpose we introduce new dependent variables $u(\xi,\eta)$, $v(\xi,\eta)$ and $p(\xi,\eta)$ so that the transformed momentum and energy equations can be written as

$$f' = u \tag{2.46}$$

$$u' = v \tag{2.47}$$

$$g' = p \tag{2.48}$$

$$v' + p_1 fv - p_2 u^2 - p_3 u + g = \xi(u\frac{\partial u}{\partial \xi} - v\frac{\partial f}{\partial \xi}) \tag{2.49}$$

$$\frac{1}{P_r} p' + p_1 fp - p_4 ug + p_5 v^2 + p_6 u^2 + p_7 gu + p_8 u + p_9 g = \xi(u\frac{\partial g}{\partial \xi} - p\frac{\partial f}{\partial \xi}) \tag{2.50}$$

Where $x = \xi$, $h = g$ and $td = \dfrac{T_\infty}{T_b - T_\infty}$

$$\frac{16+5x}{20(1+x)}=p_1 , \quad \frac{6+5x}{10(1+x)}=p_2 , Mx^{2/5}(1+x)^{1/10}=p_3 , \frac{1}{5(1+x)}=p_4 , Nx=p_5 ,$$

$$Jx^{2/5}(1+x)^{-1/2}=p_6 , G_e x=p_7 , G_r x\left(\frac{1+x}{x}\right)^{1/5} td=p_8 , Qx^{1/5}(1+x)^{-1/5}=p_9 ,$$

and the boundary conditions are

$$f(\xi,0)=0, \; u(\xi,0)=0, \; p(\xi,0)=-(1+\xi)^{1/4}+\xi^{1/5}(1+\xi)^{1/20} g(\xi,0)$$
$$u(\xi,\infty)=0, g(\xi,\infty)=0$$

(2.51)

We now consider the net rectangle on the (ξ, η) plane shown in the figure 2.2 and denote the net points by

$$\xi^0=0, \; \xi^n=\xi^{n-1}+k_n , \; n=1,2,.. \; N$$
$$\eta_0=0, \; \eta_j=\eta_{j-1}+h_j , \quad j=1,2,...J$$

(2.52)
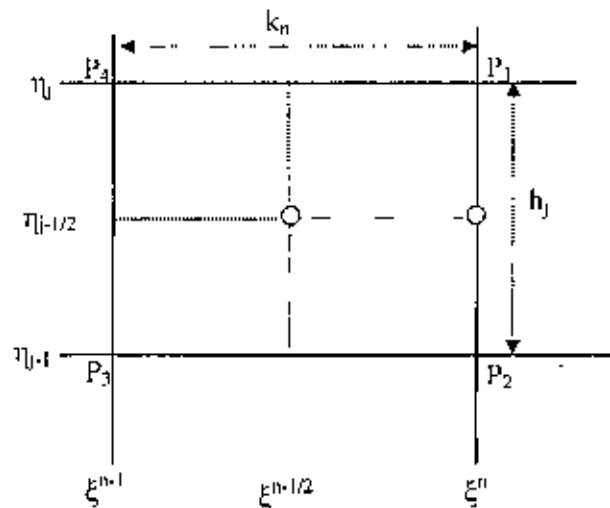
Figure 2.2. Net rectangle for difference approximations for the Box scheme.

Here 'n' and 'j' are just sequence of numbers on the (ξ, η) plane, k_n and h_j are the variable mesh widths.

We approximate the quantities f, u, v, p at the points (ξ^n, η_j) of the net by f^n_j, u^n_j, v^n_j, p^n_j which we call net function . We also employ the notation g^n_j for the quantities midway between net points shown in figure (2.2) and for any net function as

$$\xi^{n-1/2}=\frac{1}{2}(\xi^n+\xi^{n-1})$$

(2.53)

$$\eta_{i-1/2} = \frac{1}{2}(\eta_i + \eta_{i-1}) \tag{2.54}$$

$$g_i^{n-1/2} = \frac{1}{2}(g_i^{n} + g_j^{n-1}) \tag{2.55}$$

$$g_{j-1/2}^{n} = \frac{1}{2}(g_i^{n} + g_{j-1}^{n}) \tag{2.56}$$

The finite difference approximations according to Box method to the three first order ordinary differential equations (2.46)-(2 48) are written for the mid point $(\zeta^n, \eta_{j-1/2})$ of the segment P_1P_2shown in the figure (2.2) and the finite difference approximations to the two first order differential equations (2.49)-(2.50) are written for the mid point $(\zeta^{n-1/2}, \eta_{j-1/2})$ of the rectangle $P_1P_2P_3P_4$. This procedure yields,

$$h_j^{-1}(f_j^{n} - f_{j-1}^{n}) = u_{j-1/2}^{n} = \frac{u_{j-1}^{n} + u_j^{n}}{2} \tag{2.57}$$

$$h_j^{-1}(u_j^{n} - u_{j-1}^{n}) = v_{j-1/2}^{n} = \frac{v_{j-1}^{n} + v_j^{n}}{2} \tag{2.58}$$

$$h_j^{-1}(g_j^{n} - g_{j-1}^{n}) = p_{j-1/2}^{n} = \frac{p_{j-1}^{n} + p_j^{n}}{2} \tag{2.59}$$

$$\frac{1}{2}(\frac{v_j^{n} - v_{j-1}^{n}}{h_j} + \frac{v_j^{n-1} - v_{j-1}^{n-1}}{h_j}) + (p_1 fv)_{j-1/2}^{n-1/2} - (p_2 u^2)_{j-1/2}^{n-1/2} - (p_3 u)_{j-1/2}^{n-1/2}$$

$$+ g_{j-1/2}^{n-1/2} = \xi_{j-1/2}^{n-1/2}(u_{j-1/2}^{n-1/2} \frac{u_{j-1/2}^{n} - u_{j-1/2}^{n-1}}{k_n} - v_{j-1/2}^{n-1/2} \frac{f_{j-1/2}^{n} - f_{j-1/2}^{n-1}}{k_n}) \tag{2.60}$$

$$\frac{1}{2P_r}(\frac{p_j^{n} - p_{j-1}^{n}}{h_j} + \frac{p_j^{n-1} - p_{j-1}^{n-1}}{h_j}) + (p_1 fp)_{j-1/2}^{n-1/2} - (p_4 ug)_{j-1/2}^{n-1/2} + (p_5 v^2)_{j-1/2}^{n-1/2}$$

$$+ (p_6 u^2)_{j-1/2}^{n-1/2} + (p_7 gu)_{j-1/2}^{n-1/2} + (p_8 u)_{j-1/2}^{n-1/2} + (p_9 g)_{j-1/2}^{n-1/2}$$

$$= \xi_{j-1/2}^{n-1/2}(u_{j-1/2}^{n-1/2} \frac{g_{j-1/2}^{n} - g_{j-1/2}^{n-1}}{k_n} - p_{j-1/2}^{n-1/2} \frac{f_{j-1/2}^{n} - f_{j-1/2}^{n-1}}{k_n}) \tag{2.61}$$

Now from the equation (2.60) we get

$$\frac{1}{2}(\frac{v_j^{n} - v_{j-1}^{n}}{h_j}) + \frac{1}{2}(\frac{v_j^{n-1} - v_{j-1}^{n-1}}{h_j}) + \frac{1}{2}\{(p_1 fv)_{j-1/2}^{n} + (p_1 fv)_{j-1/2}^{n-1}\}$$

$$- \frac{1}{2}\{(p_2 u^2)_{j-1/2}^{n} + (p_2 u^2)_{j-1/2}^{n-1}\} - \frac{1}{2}\{(p_3 u)_{j-1/2}^{n} + (p_3 u)_{j-1/2}^{n-1}\}$$

$$+ \frac{1}{2}\{g_{j-1/2}^{n} + g_{j-1/2}^{n-1}\} = \frac{1}{2k_n}\xi_{j-1/2}^{n-1/2}(u_{j-1/2}^{n} + u_{j-1/2}^{n-1})(u_{j-1/2}^{n} - u_{j-1/2}^{n-1})$$

$$- \frac{1}{2k_n}\xi_{j-1/2}^{n-1/2}(v_{j-1/2}^{n} + v_{j-1/2}^{n-1})(f_{j-1/2}^{n} - f_{j-1/2}^{n-1})$$

$$\Rightarrow h_j^{-1}(v_j^n - v_{j-1}^n) + h_j^{-1}(v_j^{n-1} - v_{j-1}^{n-1}) + (p_1)_{j-1/2}^n (fv)_{j-1/2}^n + (p_1)_{j-1/2}^{n-1}(fv)_{j-1/2}^{n-1}$$

$$-(p_2)_{j-1/2}^n (u^2)_{j-1/2}^n - (p_2)_{j-1/2}^{n-1}(u^2)_{j-1/2}^{n-1} - (p_3)_{j-1/2}^n (u)_{j-1/2}^n$$

$$-(p_3)_{j-1/2}^{n-1}(u)_{j-1/2}^{n-1} + g_{j-1/2}^n + g_{j-1/2}^{n-1} = \alpha_n \left\{ (u^2)_{j-1/2}^n - (u)_{j-1/2}^n (u)_{j-1/2}^{n-1} \right\}$$

$$+\alpha_n \left((u)_{j-1/2}^n (u)_{j-1/2}^{n-1} - (u^2)_{j-1/2}^{n-1} - (fv)_{j-1/2}^n + v_{j-1/2}^n f_{j-1/2}^{n-1} - v_{j-1/2}^{n-1} f_{j-1/2}^n \right) + \alpha_n (fv)_{j-1/2}^{n-1}$$

$$\Rightarrow h_j^{-1}(v_j^n - v_{j-1}^n) + \left\{ (p_1)_{j-1/2}^n + \alpha_n \right\} (fv)_{j-1/2}^n - \left\{ (p_2)_{j-1/2}^n + \alpha_n \right\} (u^2)_{j-1/2}^n$$

$$-(p_3)_{j-1/2}^n (u)_{j-1/2}^n + g_{j-1/2}^n = \alpha_n \left(-(u^2)_{j-1/2}^{n-1} + v_{j-1/2}^n f_{j-1/2}^{n-1} - v_{j-1/2}^{n-1} f_{j-1/2}^n + (fv)_{j-1/2}^{n-1} \right)$$

$$-(p_1)_{j-1/2}^{n-1}(fv)_{j-1/2}^{n-1} + (p_2)_{j-1/2}^{n-1}(u^2)_{j-1/2}^{n-1} - h_j^{-1}(v_j^{n-1} - v_{j-1}^{n-1})$$

$$\Rightarrow h_j^{-1}(v_j^n - v_{j-1}^n) + \left\{ (p_1)_{j-1/2}^n + \alpha_n \right\} (fv)_{j-1/2}^n - \left\{ (p_2)_{j-1/2}^n + \alpha_n \right\} (u^2)_{j-1/2}^n$$

$$-(p_3)_{j-1/2}^n (u)_{j-1/2}^n + g_{j-1/2}^n + \alpha_n (v_{j-1/2}^{n-1} f_{j-1/2}^n - v_{j-1/2}^n f_{j-1/2}^{n-1})$$

$$= \alpha_n \left\{ (fv)_{j-1/2}^{n-1} - (u^2)_{j-1/2}^{n-1} \right\} - (p_1)_{j-1/2}^{n-1}(fv)_{j-1/2}^{n-1}$$

$$+(p_2)_{j-1/2}^{n-1}(u^2)_{j-1/2}^{n-1} - h_j^{-1}(v_j^{n-1} - v_{j-1}^{n-1}) - (p_3)_{j-1/2}^{n-1}(u)_{j-1/2}^{n-1}$$

$$-g_{j-1/2}^{n-1}$$

$$\Rightarrow h_j^{-1}(v_j^n - v_{j-1}^n) + \left\{ (p_1)_{j-1/2}^n + \alpha_n \right\} (fv)_{j-1/2}^n - \left\{ (p_2)_{j-1/2}^n + \alpha_n \right\} (u^2)_{j-1/2}^n$$

$$-(p_3)_{j-1/2}^n (u)_{j-1/2}^n + g_{j-1/2}^n + \alpha_n (v_{j-1/2}^{n-1} f_{j-1/2}^n - v_{j-1/2}^n f_{j-1/2}^{n-1})$$

$$= -L_{j-1/2}^{n-1} + \alpha_n \left\{ (fv)_{j-1/2}^{n-1} - (u^2)_{j-1/2}^{n-1} \right\}$$

$$L_{j-1/2}^{n-1} = (p_1)_{j-1/2}^{n-1}(fv)_{j-1/2}^{n-1} - (p_2)_{j-1/2}^{n-1}(u^2)_{j-1/2}^{n-1} +$$

$$h_j^{-1}(v_j^{n-1} - v_{j-1}^{n-1}) + (p_3)_{j-1/2}^{n-1}(u)_{j-1/2}^{n-1} + g_{j-1/2}^{n-1}$$

$$\Rightarrow h_j^{-1}(v_j^n - v_{j-1}^n) + \left\{ (p_1)_{j-1/2}^n + \alpha_n \right\} (fv)_{j-1/2}^n - \left\{ (p_2)_{j-1/2}^n + \alpha_n \right\} (u^2)_{j-1/2}^n$$

$$-(p_3)_{j-1/2}^n (u)_{j-1/2}^n + g_{j-1/2}^n + \alpha_n (v_{j-1/2}^{n-1} f_{j-1/2}^n - v_{j-1/2}^n f_{j-1/2}^{n-1}) = R_{j-1/2}^{n-1} \tag{2.62}$$

$$R_{j-1/2}^{n-1} = -L_{j-1/2}^n + \alpha_n \left\{ (fv)_{j-1/2}^{n-1} - (u^2)_{j-1/2}^{n-1} \right\}$$

Where $\alpha_n = \dfrac{\xi_{j-1/2}^{n-1/2}}{k_n}$

Again from the equation (2.61) we get

$$\frac{1}{2P_r}\left\{ \frac{(p_j^n - p_{j-1}^n)}{h_j} + \frac{(p_j^{n-1} - p_{j-1}^{n-1})}{h_j} \right\} + (p_3 fp)_{j-1/2}^{n-1/2} - (p_4 ug)_{j-1/2}^{n-1/2} + (p_5 v^2)_{j-1/2}^{n-1/2}$$

$$+(p_6 u^2)_{j-1/2}^{n-1/2} + (p_7 ug)_{j-1/2}^{n-1/2} + (p_8 u)_{j-1/2}^{n-1/2} + (p_9 g)_{j-1/2}^{n-1/2}$$

$$= \xi_{j-1/2}^{n-1/2} \left\{ u_{j-1/2}^{n-1/2} \frac{g_{j-1/2}^n - g_{j-1/2}^{n-1}}{k_n} - p_{j-1/2}^{n-1/2} \frac{f_{j-1/2}^n - f_{j-1/2}^{n-1/2}}{k_n} \right\}$$

$$\frac{1}{2P_r}\frac{\left(p_j^n - p_{j-1}^n\right)}{h_j} + \frac{1}{2P_r}\frac{\left(p_j^{n-1} - p_{j-1}^{n-1}\right)}{h_j} + \frac{1}{2}\left\{\left(p_1 fp\right)_{j-1/2}^n + \left(p_1 fp\right)_{j-1/2}^{n-1}\right\}$$

$$-\frac{1}{2}\left\{\left(p_4 ug\right)_{j-1/2}^n + \left(p_4 ug\right)_{j-1/2}^{n-1}\right\} - \frac{1}{2}\left\{\left(p_5 v^2\right)_{j-1/2}^n + \left(p_5 v^2\right)_{j-1/2}^{n-1}\right\}$$

$$+\frac{1}{2}\left\{\left(p_6 u^2\right)_{j-1/2}^n + \left(p_6 u^2\right)_{j-1/2}^{n-1}\right\} + \frac{1}{2}\left\{\left(p_7 ug\right)_{j-1/2}^n + \left(p_7 ug\right)_{j-1/2}^{n-1}\right\}$$

$$+\frac{1}{2}\left\{\left(p_8 u\right)_{j-1/2}^n + \left(p_8 u\right)_{j-1/2}^{n-1}\right\} + \frac{1}{2}\left\{\left(p_9 g\right)_{j-1/2}^n + \left(p_9 g\right)_{j-1/2}^{n-1}\right\}$$

$$= \xi_{j-1/2}^{n-1/2}\left\{ \begin{array}{l} \dfrac{1}{2}\left\{u_{j-1/2}^n + u_{j-1/2}^{n-1}\right\}\dfrac{g_{j-1/2}^n - g_{j-1/2}^{n-1}}{k_n} \\[2ex] -\dfrac{1}{2}\left(p_{j-1/2}^n + p_{j-1/2}^{n-1}\right)\dfrac{f_{j-1/2}^n - f_{j-1/2}^{n-1}}{k_n} \end{array} \right\}$$

$$\frac{1}{P_r}\frac{\left(p_j^n - p_{j-1}^n\right)}{h_j} + \frac{1}{P_j}\frac{\left(p_j^{n-1} - p_{j-1}^{n-1}\right)}{h_j} + \left\{\left(p_1 fp\right)_{j-1/2}^n + \left(p_1 fp\right)_{j-1/2}^{n-1}\right\}$$

$$-\left\{\left(p_4 ug\right)_{j-1/2}^n + \left(p_4 ug\right)_{j-1/2}^{n-1}\right\} + \left\{\left(p_5 v^2\right)_{j-1/2}^n + \left(p_5 v^2\right)_{j-1/2}^{n-1}\right\}$$

$$+\left\{\left(p_6 u^2\right)_{j-1/2}^n + \left(p_6 u^2\right)_{j-1/2}^{n-1}\right\} + \left\{\left(p_7 ug\right)_{j-1/2}^n + \left(p_7 ug\right)_{j-1/2}^{n-1}\right\}$$

$$+\left\{\left(p_8 u\right)_{j-1/2}^n + \left(p_8 u\right)_{j-1/2}^{n-1}\right\} + \left\{\left(p_9 g\right)_{j-1/2}^n + \left(p_9 g\right)_{j-1/2}^{n-1}\right\}$$

$$= \frac{\xi_{j-1/2}^{n-1/2}}{k_n}\left\{\left(u_{j-1/2}^n + u_{j-1/2}^{n-1}\right)\left(g_{j-1/2}^n - g_{j-1/2}^{n-1}\right) - \left(p_{j-1/2}^n + p_{j-1/2}^{n-1}\right)\left(f_{j-1/2}^n - f_{j-1/2}^{n-1}\right)\right\}$$

$$\frac{1}{P_j}\frac{\left(p_j^n - p_{j-1}^n\right)}{h_j} + \frac{1}{P_r}\frac{\left(p_j^{n-1} - p_{j-1}^{n-1}\right)}{h_j} + \left(p_1\right)_{j-1/2}^{n-1/2}\left(fp\right)_{j-1/2}^n + \left(p_1\right)_{j-1/2}^{n-1/2}\left(fp\right)_{j-1/2}^{n-1}$$

$$-\left(p_4\right)_{j-1/2}^{n-1/2}\left(ug\right)_{j-1/2}^n - \left(p_4\right)_{j-1/2}^{n-1/2}\left(ug\right)_{j-1/2}^{n-1} + \left(p_5\right)_{j-1/2}^{n-1/2}\left(v^2\right)_{j-1/2}^n + \left(p_5\right)_{j-1/2}^{n-1/2}\left(v^2\right)_{j-1/2}^{n-1}$$

$$+\left(p_6\right)_{j-1/2}^{n-1/2}\left(u^2\right)_{j-1/2}^n + \left(p_6\right)_{j-1/2}^{n-1/2}\left(u^2\right)_{j-1/2}^{n-1} + \left(p_7\right)_{j-1/2}^{n-1/2}\left(ug\right)_{j-1/2}^n + \left(p_7\right)_{j-1/2}^{n-1/2}\left(ug\right)_{j-1/2}^{n-1}$$

$$+\left(p_8\right)_{j-1/2}^{n-1/2}\left(u\right)_{j-1/2}^n + \left(p_8\right)_{j-1/2}^{n-1/2}\left(u\right)_{j-1/2}^{n-1} + \left(p_9\right)_{j-1/2}^{n-1/2}\left(g\right)_{j-1/2}^n + \left(p_9\right)_{j-1/2}^{n-1/2}\left(g\right)_{j-1/2}^{n-1}$$

$$= \frac{\xi_{j-1/2}^{n-1/2}}{k_n}\left\{\left(u_{j-1/2}^n g_{j-1/2}^n + u_{j-1/2}^{n-1} g_{j-1/2}^n - u_{j-1/2}^n g_{j-1/2}^{n-1} - u_{j-1/2}^{n-1} g_{j-1/2}^{n-1}\right)\right\}$$

$$- \frac{\xi_{j-1/2}^{n-1/2}}{k_n}\left\{\left(p_{j-1/2}^n f_{j-1/2}^n + p_{j-1/2}^{n-1} f_{j-1/2}^n - p_{j-1/2}^n f_{j-1/2}^{n-1} - f_{j-1/2}^{n-1} p_{j-1/2}^{n-1}\right)\right\}$$

$$\frac{1}{P_r} h_j^{-1}(p_j^n - p_{j-1}^n) + \left\{(p_1)_{j-1/2}^{n-1/2} + \alpha_n\right\}(fp)_{j-1/2}^n - \left\{(p_4)_{j-1/2}^{n-1/2} - (p_7)_{j-1/2}^{n-1/2} + \alpha_n\right\}(ug)_{j-1/2}^n$$

$$+ \left(p_5\right)_{j-1/2}^{n-1/2}\left(v^2\right)_{j-1/2}^n + \left(p_6\right)_{j-1/2}^{n-1/2}\left(u^2\right)_{j-1/2}^n + \left(p_8\right)_{j-1/2}^{n-1/2}\left(u\right)_{j-1/2}^n + \left(p_9\right)_{j-1/2}^{n-1/2}\left(g\right)_{j-1/2}^n$$

$$+ \alpha_n(u_{j-1/2}^n g_{j-1/2}^{n-1} - u_{j-1/2}^{n-1} g_{j-1/2}^n - p_{j-1/2}^n f_{j-1/2}^{n-1} + p_{j-1/2}^{n-1} f_{j-1/2}^n)$$

$$= -M_{j-1/2}^{n-1} + \alpha_n\left\{(fp)_{j-1/2}^{n-1} - (ug)_{j-1/2}^{n-1}\right\}$$

$$M_{j-1/2}^{n-1} = \frac{1}{P_r} h_j^{-1}(p_j^{n-1} - p_{j-1}^{n-1}) + (p_1)_{j-1/2}^{n-1/2}(fp)_{j-1/2}^{n-1} - (p_4)_{j-1/2}^{n-1/2}(ug)_{j-1/2}^{n-1}$$

$$+ \left(p_7\right)_{j-1/2}^{n-1/2}\left(ug\right)_{j-1/2}^{n-1} + \left(p_5\right)_{j-1/2}^{n-1/2}\left(v^2\right)_{j-1/2}^{n-1} + \left(p_6\right)_{j-1/2}^{n-1/2}\left(u^2\right)_{j-1/2}^{n-1}$$

$$+ \left(p_8\right)_{j-1/2}^{n-1/2}\left(u\right)_{j-1/2}^{n-1} + \left(p_9\right)_{j-1/2}^{n-1/2}\left(g\right)_{j-1/2}^{n-1}$$

$$\Rightarrow \frac{1}{P_r} h_j^{-1}(p_j^n - p_{j-1}^n) + \left\{(p_1)_{j-1/2}^{n-1/2} + \alpha_n\right\}(fp)_{j-1/2}^n - \left\{(p_4)_{j-1/2}^{n-1/2} - (p_7)_{j-1/2}^{n-1/2}\right.$$

$$\left. + \alpha_n\right\}(ug)_{j-1/2}^n + \left(p_5\right)_{j-1/2}^{n-1/2}\left(v^2\right)_{j-1/2}^n + \left(p_6\right)_{j-1/2}^{n-1/2}\left(u^2\right)_{j-1/2}^n + \left(p_8\right)_{j-1/2}^{n-1/2}\left(u\right)_{j-1/2}^n$$

$$+ \left(p_9\right)_{j-1/2}^{n-1/2}\left(g\right)_{j-1/2}^n + \alpha_n(u_{j-1/2}^n g_{j-1/2}^{n-1} - u_{j-1/2}^{n-1} g_{j-1/2}^n)$$

$$- \alpha_n\left(p_{j-1/2}^n f_{j-1/2}^{n-1} - p_{j-1/2}^{n-1} f_{j-1/2}^n\right) = T_{j-1/2}^{n-1}$$

$$= -M_{j-1/2}^{n-1} + \alpha_n\left\{(fp)_{j-1/2}^{n-1} - (ug)_{j-1/2}^{n-1}\right\}$$

$$\tag{2.63}$$

$$T_{j-1/2}^{n-1} = -M_{j-1/2}^{n-1} + \alpha_n\left\{(fp)_{j-1/2}^{n-1} - (ug)_{j-1/2}^{n-1}\right\} \tag{2.64}$$

The boundary conditions become

$$f_0^n = 0, \quad u_0^n = 0, \quad p_0^n = -(1 + \xi)^{1/4} + \xi^{1/5}(1 + \xi)^{1/20} g_0^n$$

$$u_J^n = 0, \quad g_J^n = 0 \tag{2.65}$$

If we assume $f_j^{n-1}, u_j^{n-1}, v_j^{n-1}, g_j^{n-1}, p_j^{n-1}$ to be known for $0 \le j \le J$, equations (2.57) to (2.59) and (2.62) to (2.63) form a system of $5J + 5$ nonlinear equations for the solutions of the $5J + 5$ unknowns ($f_j^n, u_j^n, v_j^n, g_j^n, p_j^n$), $j = 0, 1, 2 \ldots J$. These non-linear systems of algebric equations are to be linearized by Newton's quasi-linearization method. We define the iterates $[f_j^n, u_j^n, v_j^n, g_j^n, p_j^n]$, $i = 0, 1, 2 \ldots N$ with initial values equal to those at the previous x-station (which is usually the best initial available) . For the higher iterates we set

$$f_j^{(i+1)} = f_j^{(i)} + \delta f_j^{(i)} \tag{2.66}$$

$$u_j^{(i+1)} = u_j^{(i)} + \delta u_j^{(i)} \tag{2.67}$$

$$v_j^{(i+1)} = v_j^{(i)} + \delta v_j^{(i)} \tag{2.68}$$

$$g_j^{(i+1)} = g_j^{(i)} + \delta g_j^{(i)} \tag{2.69}$$

$$p_j^{(i+1)} = p_j^{(i)} + \delta p_j^{(i)} \tag{2.70}$$

Now by substituting the right hand sides of the above equations in place of f_j^n, u_j^n, v_j^n and g_j^n omitting the terms that are quadratic in $\delta f_j^i, \delta u_j^i, \delta v_j^i$ and δg_j^i, we get the equations (2.57) to (2.59) and (2.62) in the following form:

$$\frac{f_j^{(i)} - f_{i-1}^{(i)}}{h_j} + \frac{\delta f_j^{(i)} - \delta f_{i-1}^{(i)}}{h_j} = u_{j-\frac{1}{2}}^{(i)} + \delta u_{i-\frac{1}{2}}^{(i)}$$

$$= \frac{1}{2}\left[u_j^{(i)} + u_{j-1}^{(i)} + \delta u_j^{(i)} + \delta u_{j-1}^{(i)}\right]$$

$$f_j^{(i)} + \delta f_j^{(i)} - f_{j-1}^{(i)} - \delta f_{j-1}^{(i)} = \frac{h_j}{2}\left\{u_j^{(i)} + \delta u_j^{(i)} + u_{j-1}^{(i)} + \delta u_{j-1}^{(i)}\right\}$$

$$\delta f_j^{(i)} - \delta f_{j-1}^{(i)} - \frac{h_j}{2}\left(\delta u_j^{(i)} + \delta u_{j-1}^{(i)}\right) = (r_1)_j \tag{2.71}$$

Where $(r_1)_j = f_{j-1}^{(i)} - f_j^{(i)} + h_j u_{j-1/2}^{(i)}$ \hfill (2.72)

$$\delta u_j^{(i)} - \delta u_{j-1}^{(i)} - \frac{h_j}{2}\left(\delta v_j^{(i)} + \delta v_{j-1}^{(i)}\right) = (r_4)_j \tag{2.73}$$

$$(r_4)_j = u_{j-1}^{(i)} - u_j^{(i)} + h_j v_{j-1/2}^{(i)} \tag{2.74}$$

$$\delta g_j^{(i)} - \delta g_{j-1}^{(i)} - \frac{h_j}{2}\left(\delta p_j^{(i)} + \delta p_{j-1}^{(i)}\right) = (r_5)_j \tag{2.75}$$

$$(r_5)_j = p_{j-1}^{(i)} - p_j^{(i)} + h_j p_{j-1/2}^{(i)} \tag{2.76}$$

From figure 2.2, the following procedure yields,

$$h_j^{-1}\left(f_j^n - f_{j-1}^n\right) = u_{j-1/2}^n = \frac{u_{j-1}^n + u_j^n}{2} \tag{2.77}$$

$$h_j^{-1}\left(u_j^n - u_{j-1}^n\right) = v_{j-1/2}^n = \frac{v_{j-1}^n + v_j^n}{2} \tag{2.78}$$

$$h_j^{-1}\left(g_j^n - g_{j-1}^n\right) = p_{j-1/2}^n = \frac{p_{j-1}^n + p_j^n}{2} \tag{2.79}$$

Where $(r_4)_j = u_{j-1}^{(i)} - u_j^{(i)} + h_j v_{j-1/2}^{(i)}$ \hfill (2.80)

Now equation (2.62) can be written in the following form

$$h_j^{-1}(v_j^{(i)} + \delta v_j^{(i)} - v_{j-1}^{(i)} - \delta v_{j-1}^{(i)}) + \left\{(p_1)_{j-1/2}^n + \alpha_n\right\}\left\{(fv)_{j-1/2}^{(i)} + \delta(fv)_{j-1/2}^{(i)}\right\}$$

$$-\left\{(p_2)_{j-1/2}^n + \alpha_n\right\}\left\{(u^2)_{j-1/2}^{(i)} + \delta(u^2)_{j-1/2}^{(i)}\right\} - (p_3)_{j-1/2}^n\left\{(u)_{j-1/2}^{(i)} + \delta(u)_{j-1/2}^{(i)}\right\}$$

$$+g_{j-1/2}^{(i)} + \delta g_{j-1/2}^{(i)} + \alpha_n(f_{j-1/2}^{(i)} + \delta f_{j-1/2}^{(i)})v_{j-1/2}^{n-1}$$

$$-\alpha_n(v_{j-1/2}^{(i)} + \delta v_{j-1/2}^{(i)})f_{j-1/2}^{n-1} = R_{j-1/2}^{n-1}$$

$$\Rightarrow h_j^{-1}(v_j^{(i)} + \delta v_j^{(i)} - v_{j-1}^{(i)} - \delta v_{j-1}^{(i)}) + \{(p_1)_{j-1/2}^n + \alpha_n\}$$

$$\left\{ (fv)_{j-1/2}^{(i)} + \frac{1}{2}(f_j^{(i)}\delta(v)_j^{(i)} + v_j^{(i)}\delta(f)_j^{(i)} + f_{j-1}^{(i)}\delta(v)_{j-1}^{(i)} + v_{j-1}^{(i)}\delta(f)_{j-1}^{(i)}) \right\}$$

$$-\left\{ (p_2)_{j-1/2}^n + \alpha_n \right\}\left\{ (u^2)_{j-1/2}^{(i)} + u_j^{(i)}\delta(u)_j^{(i)} + u_{j-1}^{(i)}\delta(u)_{j-1}^{(i)} \right\}$$

$$-(p_3)_{j-1/2}^n \left\{ (u)_{j-1/2}^{(i)} + \frac{1}{2}(\delta(u)_j^{(i)} + \delta(u)_{j-1}^{(i)}) \right\} + g_{j-1/2}^{(i)} + \frac{1}{2}(\delta g_j^{(i)} + \delta g_{j-1}^{(i)})$$

$$+\alpha_n \left\{ v_{j-1/2}^{n-1}(f_{j-1/2}^{(i)} + \frac{1}{2}(\delta f_j^{(i)} + \delta f_{j-1}^{(i)})) - (v_{j-1/2}^{(i)} + \frac{1}{2}(\delta v_j^{(i)} + \delta v_{j-1}^{(i)}))f_{j-1/2}^{n-1} \right\} = R_{j-1/2}^{n-1}$$

$$\Rightarrow (s_1)_j \,\delta v_j^{(i)} + (s_2)_j \,\delta v_{j-1}^{(i)} + (s_3)_j \,\delta f_j^{(i)} + (s_4)_j \,\delta f_{j-1}^{(i)} + (s_5)_j \,\delta u_j^{(i)}$$
$$+(s_6)_j \,\delta u_{j-1}^{(i)} + (s_7)_j \,\delta g_j^{(i)} + (s_8)_j \,\delta g_{j-1}^{(i)} + (s_9)_j .0 + (s_{10})_j .0 = (r_2)_j \tag{2.81}$$

Where $(s_1)_j = (h_j^{-1} + \dfrac{(p_1)_{j-1/2}^n + \alpha_n}{2} f_j^{(i)} - \dfrac{1}{2}\alpha_n f_{j-1/2}^{n-1}$ \hfill (2.82)

$$(s_2)_j = (-h_j^{-1} + \dfrac{(p_1)_{j-1/2}^n + \alpha_n}{2} f_{j-1}^{(i)} - \dfrac{1}{2}\alpha_n f_{j-1/2}^{n-1} \tag{2.83}$$

$$(s_3)_j = (\dfrac{(p_1)_{j-1/2}^n + \alpha_n}{2} v_j^{(i)} + \dfrac{1}{2}\alpha_n v_{j-1/2}^{n-1} \tag{2.84}$$

$$(s_4)_j = (\dfrac{(p_1)_{j-1/2}^n + \alpha_n}{2} v_{j-1}^{(i)} + \dfrac{1}{2}\alpha_n v_{j-1/2}^{n-1} \tag{2.85}$$

$$(s_5)_j = (-\dfrac{(p_2)_{j-1/2}^n + \alpha_n}{2} u_j^{(i)} - \dfrac{(p_1)_{j-1/2}^n}{2} \tag{2.86}$$

$$(s_6)_j = (-\dfrac{(p_2)_{j-1/2}^n + \alpha_n}{2} u_{j-1}^{(i)} - \dfrac{(p_3)_{j-1/2}^n}{2} \tag{2.87}$$

$$(s_7)_j = 0.5 \tag{2.88}$$
$$(s_8)_j = 0.5 \tag{2.89}$$
$$(s_9)_j = 0 \tag{2.90}$$
$$(s_{10})_j = 0 \tag{2.91}$$

$$(r_2)_j = R_{j-1/2}^{n-1} - \left\{ h_j^{-1}(v_j^{(i)} - v_{j-1}^{(i)}) + ((p_1)_{j-1/2}^n + \alpha_n)(fv)_{j-1/2}^{(i)} \right\}$$
$$+((p_2)_{j-1/2}^n + \alpha_n)(u^2)_{j-1/2}^{(i)} - \alpha_n(f_{j-1/2}^{(i)} v_{j-1/2}^{n-1} - f_{j-1/2}^{n-1} v_{j-1/2}^{(i)}) \tag{2.92}$$
$$+\alpha_n \left\{ (p_3)_{j-1/2}^n u_{j-1/2}^{(i)} - g_{j-1/2}^{(i)} \right\}$$

Here the coefficients $(s_9)_j$ and $(s_{10})_j$ which are zero in this case are included

here for generalization. Similarly by using the equations (2.71) to (2.75) we get

the equation (2.64) in the following form:

$$\Rightarrow \frac{1}{P_r} h_j^{-1}(p_j^n - p_{j-1}^n) + \left\{(p_1)_{j-1/2}^{n-1/2} + \alpha_n\right\}(fp)_{j-1/2}^n - \left\{(p_4)_{j-1/2}^{n-1/2} - (p_7)_{j-1/2}^{n-1/2}\right.$$

$$\left. + \alpha_n\right\}(ug)_{j-1/2}^n + (p_5)_{j-1/2}^{n-1/2}(v^2)_{j-1/2}^n + (p_6)_{j-1/2}^{n-1/2}(u^2)_{j-1/2}^n + (p_8)_{j-1/2}^{n-1/2}(u)_{j-1/2}^n$$

$$+ (p_9)_{j-1/2}^{n-1/2}(g)_{j-1/2}^n + \alpha_n(u_{j-1/2}^n g_{j-1/2}^{n-1} - u_{j-1/2}^{n-1} g_{j-1/2}^n)$$

$$- \alpha_n(p_{j-1/2}^n f_{j-1/2}^{n-1} - p_{j-1/2}^{n-1} f_{j-1/2}^n) = T_{j-1/2}^{n-1}$$

$$= -M_{j-1/2}^{n-1} + \alpha_n\left\{(fp)_{j-1/2}^{n-1} - (ug)_{j-1/2}^{n-1}\right\}$$

$$\frac{1}{P_r} h_j^{-1}(p_j' + \delta p_j' - p_{j-1}' - \delta p_{j-1}') + \left\{(p_1)_{j-1/2}^{n-1/2} + \alpha_n\right\}\left\{(fp)_{j-1/2}' + \delta(fp)_{j-1/2}'\right\}$$

$$- \left\{(p_4)_{j-1/2}^{n-1/2} - (p_7)_{j-1/2}^{n-1/2} + \alpha_n\right\}\left\{(ug)_{j-1/2}' + \delta(ug)_{j-1/2}'\right\}$$

$$+ (p_5)_{j-1/2}^{n-1/2}\left\{(v^2)_{j-1/2}' + \delta(v^2)_{j-1/2}'\right\} + (p_6)_{j-1/2}^{n-1/2}\left\{(u^2)_{j-1/2}' + \delta(u^2)_{j-1/2}'\right\}$$

$$+ (p_8)_{j-1/2}^{n-1/2}\left\{(u)_{j-1/2}' + \delta(u)_{j-1/2}'\right\} + (p_9)_{j-1/2}^{n-1/2}\left\{(g)_{j-1/2}' + \delta(g)_{j-1/2}'\right\}$$

$$+ \alpha_n\left\{(u_{j-1/2}' + \delta u_{j-1/2}')g_{j-1/2}^{n-1} - u_{j-1/2}^{n-1}(g_{j-1/2}' + \delta g_{j-1/2}')\right\}$$

$$- \alpha_n\left\{(p_{j-1/2}' + \delta p_{j-1/2}')f_{j-1/2}^{n-1} - p_{j-1/2}^{n-1}(f_{j-1/2}' + \delta f_{j-1/2}')\right\} = T_{j-1/2}^{n-1}$$

$$\frac{1}{P_r} h_j^{-1}(p_j' + \delta p_j' - p_{j-1}' - \delta p_{j-1}') + \left\{(p_1)_{j-1/2}^{n-1/2} + \alpha_n\right\}\left\{(fp)_{j-1/2}' + \frac{1}{2}\left\{\delta(fp)_j' + \delta(fp)_{j-1}'\right\}\right\}$$

$$- \left\{(p_4)_{j-1/2}^{n-1/2} - (p_7)_{j-1/2}^{n-1/2} + \alpha_n\right\}\left\{(ug)_{j-1/2}' + \frac{1}{2}\left\{\delta(ug)_j' + \delta(ug)_{j-1}'\right\}\right\}$$

$$+ (p_5)_{j-1/2}^{n-1/2}\left\{(v^2)_{j-1/2}' + \frac{1}{2}\left\{\delta(v^2)_j' + \delta(v^2)_{j-1}'\right\}\right\} + (p_6)_{j-1/2}^{n-1/2}\left\{(u^2)_{j-1/2}' + \frac{1}{2}\left\{\delta(u^2)_j' + \delta(u^2)_{j-1}'\right\}\right\}$$

$$+ (p_8)_{j-1/2}^{n-1/2}\left\{(u)_{j-1/2}' + \frac{1}{2}\left\{\delta(u)_j' + \delta(u)_{j-1}'\right\}\right\} + (p_9)_{j-1/2}^{n-1/2}\left\{(g)_{j-1/2}' + \frac{1}{2}\left\{\delta(g)_j' + \delta(g)_{j-1}'\right\}\right\}$$

$$+ \alpha_n\left\{(u_{j-1/2}' + \frac{1}{2}(\delta u_j' + \delta u_{j-1}'))g_{j-1/2}^{n-1} - u_{j-1/2}^{n-1}(g_{j-1/2}' + \frac{1}{2}(\delta g_j' + \delta g_{j-1}'))\right\}$$

$$- \alpha_n\left\{(p_{j-1/2}' + \frac{1}{2}(\delta p_j' + \delta p_{j-1}'))f_{j-1/2}^{n-1} - p_{j-1/2}^{n-1}(f_{j-1/2}' + \frac{1}{2}(\delta f_j' + \delta f_{j-1}'))\right\} = T_{j-1/2}^{n-1}$$

$$(t_1)_j \, \delta p_j^{(i)} + (t_2)_j \, \delta p_{j-1}^{(i)} + (t_3)_j \, \delta f_j^{(i)} + (t_4)_j \, \delta f_{j-1}^{(i)} + (t_5)_j \, \delta u_j^{(i)}$$
$$+ (t_6)_j \, \delta u_{j-1}^{(i)} + (t_7)_j \, \delta g_j^{(i)} + (t_8)_j \, \delta g_{j-1}^{(i)} + (t_9)_j \, \delta v_j^{(i)} + (t_{10})_j \, \delta v_{j-1}^{(i)} = (r_3)_j \tag{2.93}$$

Where $(t_1)_j = \dfrac{1}{P_r} h_j^{-1} + \dfrac{(p_1)_{j-1/2}^{n-1/2} + \alpha_n}{2} f_j^{(i)} - \dfrac{1}{2}\alpha_n f_{j-1/2}^{n-1}$ \hfill (2.94)

$(t_2)_j = -\dfrac{1}{P_r} h_j^{-1} + \dfrac{(p_1)_{j-1/2}^{n-1/2} + \alpha_n}{2} f_{j-1}^{(i)} - \dfrac{1}{2}\alpha_n f_{j-1/2}^{n-1}$ \hfill (2.95)

$$(t_3)_j = \frac{(p_1)_{j-1/2}^{n-1/2} + \alpha_n}{2} p_j^{(i)} + \frac{1}{2}\alpha_n p_{j-1/2}^{n-1} \tag{2.96}$$

$$(t_4)_j = \frac{(p_1)_{j-1/2}^{n-1/2} + \alpha_n}{2} p_{j-1}^{(i)} + \frac{1}{2}\alpha_n p_{j-1/2}^{n-1} \tag{2.97}$$

$$(t_5)_j = -\frac{(p_1)_{j-1/2}^{n-1/2} - (p_7)_{j-1/2}^{n-1/2} + \alpha_n}{2} g_j^{(i)} + (p_6)_{j-1/2}^{n-1/2} u_j^i + \frac{1}{2}(p_8)_{j-1/2}^{n-1/2} + \frac{1}{2}\alpha_n g_{j-1/2}^{n-1} \tag{2.98}$$

$$(t_6)_j = -\frac{(p_4)_{j-1/2}^{n-1/2} - (p_7)_{j-1/2}^{n-1/2} + \alpha_n}{2} g_{j-1}^{(i)} + (p_6)_{j-1/2}^{n-1/2} u_{j-1}^i + \frac{1}{2}(p_8)_{j-1/2}^{n-1/2} + \frac{1}{2}\alpha_n g_{j-1/2}^{n-1} \tag{2.99}$$

$$(t_7)_j = -\frac{(p_4)_{j-1/2}^{n-1/2} - (p_7)_{j-1/2}^{n-1/2} + \alpha_n}{2} u_j^{(i)} + \frac{(p_9)_{j-1/2}^{n-1/2}}{2} - \frac{1}{2}\alpha_n u_{j-1/2}^{n-1} \tag{2.100}$$

$$(t_8)_j = -\frac{(p_4)_{j-1/2}^{n-1/2} - (p_7)_{j-1/2}^{n-1/2} + \alpha_n}{2} u_{j-1}^{(i)} + \frac{(p_9)_{j-1/2}^{n-1/2}}{2} - \frac{1}{2}\alpha_n u_{j-1/2}^{n-1} \tag{2.101}$$

$$(t_9)_j = (p_5)_{j-1/2}^{n-1/2} v_j^{(i)} \tag{2.102}$$

$$(t_{10})_j = = (p_5)_{j-1/2}^{n-1/2} v_{j-1}^{(i)} \tag{2.103}$$

$$(r_3)_j = T_{j-1/2}^{n-1} - \frac{1}{P_j} h_j^{-1}(p_j^n - p_{j-1}^n) + \left\{(p_1)_{j-1/2}^{n-1/2} + \alpha_n\right\}(fp)_{j-1/2}^n - \left\{(p_4)_{j-1/2}^{n-1/2} - (p_7)_{j-1}^{n-1}\right.$$
$$+ \alpha_n\right\}(ug)_{j-1/2}^n + (p_5)_{j-1/2}^{n-1/2}(v^2)_{j-1/2}^n + (p_6)_{j-1/2}^{n-1/2}(u^2)_{j-1/2}^n + (p_8)_{j-1/2}^{n-1/2}(u)_{j-1/2}^n$$
$$+ (p_9)_{j-1/2}^{n-1/2}(g)_{j-1/2}^n - \alpha_n(u_{j-1/2}^{(i)} g_{j-1/2}^{n-1} - u_{j-1/2}^{n-1} g_{j-1/2}^{(i)}) \tag{2.104}$$
$$+ \alpha_n(p_{j-1/2}^{(i)} f_{j-1/2}^{n-1} - p_{j-1/2}^{n-1} f_{j-1/2}^{(i)})$$

The boundary conditions (2.65) become
$$\delta f_0^n = 0, \ \delta u_0^n = 0, \ \delta p_0^n = \delta\left[-(1+\xi)^{1/4} + \xi^{1/5}(1+\xi)^{1/20} g_0^n\right]$$
$$\delta u_J^n = 0, \ \delta g_J^n = 0 \tag{2.105}$$

which express the requirement for the boundary conditions to remain during the iteration process. Now the system of linear equations (2.71) - (2.80), (2.92), (2.93) and (2.104) together with the boundary conditions (2.105) can be written in a block matrix form a coefficient matrix, which are solved by modified 'Keller Box' methods especially introduced by Keller (1978).

2.3 General governing equations of the flow over a sphere

Natural convection boundary layer flow on a sphere of an electrically conducting and steady two-dimensional viscous incompressible fluid in presence of strong magnetic field and heat generation is considered. It is assumed that the surface temperature of the sphere is T_w Where $T_u > T_\infty$, T_∞ is the ambient temperature of the fluid. Under the usual Boussinesq and boundary layer approximation, the basic equations are

$$\frac{\partial}{\partial X}(r\,U) + \frac{\partial}{\partial Y}(r\,V) = 0 \tag{2.106}$$

$$U\frac{\partial U}{\partial X} + V\frac{\partial U}{\partial Y} = v\frac{\partial^2 U}{\partial Y^2} + g\beta(T-T_\infty)\,\sin\!\left(\frac{X}{a}\right) - \frac{\sigma_0 \beta_0^{\,2}}{\rho}U \tag{2.107}$$

$$U\frac{\partial T}{\partial X} + V\frac{\partial T}{\partial Y} = \frac{k}{\rho c_p}\left(\frac{\partial^2 T}{\partial Y^2} - \frac{1}{k}\frac{\partial q_r}{\partial Y}\right) + \frac{v}{\rho C_p}\left(\frac{\partial U}{\partial Y}\right)^2 \tag{2.108}$$
$$+\frac{Q_0}{\rho C_p}(T-T_\infty) + \frac{T\beta}{\rho C_p}U\frac{\partial p}{\partial X}$$

The boundary conditions for the equations (2.107) to (2.108) are

$$U = V = 0, \qquad T = T_w \qquad \text{on } Y = 0$$
$$U \to 0, \qquad T \to T_\infty \quad \text{at } Y \to \infty \tag{2.109}$$

$$r(X) = a\,\sin\left(\frac{X}{a}\right), \text{ where } r = r(X). \tag{2.110}$$

where, a is the radius of sphere, r is the radial distance from the symmetrical axis to the surface of the sphere, g is the acceleration due to gravity, β is the coefficient of thermal expansion, β_0 is the magnetic field strength, C_p is the specific heat at constant pressure, T_∞ is the ambient temperature, T_w is the surface temperature, T is the local temperature and v is the kinematic viscosity.

The amount of heat generated or absorbed per unit volume is $Q_0 (T- T_w)$, Q_0 being a constant, which may take either positive or negative. The source term represents the heat generation when $Q_0 > 0$ and the heat absorption when $Q_0 < 0$, ρ is the density, σ_0 is the electrical conduction and Pr is the Prandtl number.
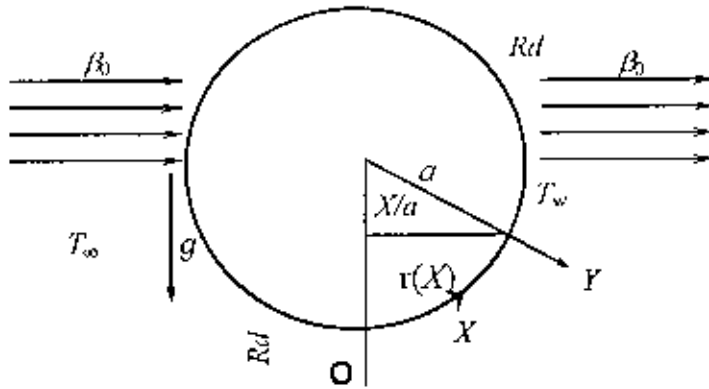
Figure 2.3: Physical model and coordinate system

Thus radiation heat flux term is simplified by the Rosseland diffusion approximation [Özisik (1973)] and is given by

$$. q_r = -\frac{4\sigma}{3(a_r + \sigma_s)}\frac{\partial T^4}{\partial Y} \tag{2.111}$$

where a_r is the Rosseland mean absorption co-efficient. σ_s is the scattering co-efficient and σ is the Stephman-Boltzman constant, q_r is the radiative heat flux in the Y direction. In order to reduce the complexity of the problem and to provide a means of comparison with future studies that will employ a more detail representation for the radiative heat flux; we will consider the optically thick radiation limit. To transform the above equations into non-dimensional form, the following dimensionless variables are introduced:

$$x = \frac{X}{a}, \ \ y = G_r^{\frac{1}{4}}\frac{Y}{a}, \ \ u = \frac{a}{v}G_r^{-\frac{1}{2}}U, \ \ v = \frac{a}{v}G_r^{-\frac{1}{4}}V, \ \ \theta = \frac{T - T_\infty}{T_w - T_\infty} \tag{2.112}$$

$$\theta_w = \frac{T_w}{T_\infty}, \ \Lambda = \theta_w - 1 = \frac{T_w}{T_\infty} - 1 = \frac{T_w - T_\infty}{T_\infty}, \ Rd = \frac{4\sigma T_\infty^3}{k(a_r + \sigma_s)} \tag{2.113}$$

Where, $G_r = g\beta(T_w - T_\infty)a^3/v^2$ is the Grashof number and θ is the non-dimensional temperature and θ_w is the surface temperature parameter.

Grashof number is a dimemsionless number in fluid dynamics, which approximates the ratio of the buoyancy force to the viscous force acting on a fluid.

Thus (2.110) becomes $r(x) = a\sin x$ (2.114)

Using the above values, the equations (2.106) to (2.108) take the following form:

$$\frac{\partial}{\partial x}(ru) + \frac{\partial}{\partial y}(rv) = 0 \tag{2.115}$$

$$u\frac{\partial u}{\partial x} + v\frac{\partial u}{\partial y} = \frac{\partial^2 u}{\partial y^2} + \theta\sin x - \frac{\sigma_0\beta_0^2 a^2}{\rho v Gr^{\frac{1}{2}}}u \tag{2.116}$$

$$u\frac{\partial\theta}{\partial x} + v\frac{\partial\theta}{\partial y} = \frac{1}{Pr}\frac{\partial}{\partial y}\left[\left\{1 + \frac{4}{3}Rd\left(1 + (\theta_w - 1)\theta\right)^3\right\}\frac{\partial\theta}{\partial y}\right]$$

$$+ \frac{Gr}{a^2 C_p (T_w - T_\infty)}\left(\frac{\partial u}{\partial y}\right)^2 - \left(\frac{T_\infty}{T_w - T_\infty} + \theta\right)\frac{g\beta a}{C_p}u + \frac{Q_0}{\rho C_P}\frac{a^2}{v Gr^{\frac{1}{2}}}\theta \tag{2.117}$$

Here, $M = \left(\sigma_0\beta_0^2 a^2/\rho v Gr^{1/2}\right)$ is the magnetic parameter or Hartmann number, $Q = \left(Q_0 a^2/v\rho C_p Gr^{1/2}\right)$ is the heat generation parameter. $N = Gr/a^2 C_p (T_w - T_\infty)$ is the viscous dissipation parameter and $g\beta a/C_p = Ge$ is pressure work parameter and $Rd = 4\sigma I_\infty^3/k(a_r + \sigma_s)$ is the radiation parameter.

The values of dimensionless parameter Rd has been taken 0.0 to 4.0 in accordance with Table-B$_7$. Also it is considered the values of surface temperature θ_w 0. to 1.2 are taken to compare with Table-B$_6$.

Therefore momentum and energy equations (2.116) and (2.117) can be written as

$$u\frac{\partial u}{\partial x} + v\frac{\partial u}{\partial y} + Mu - \theta\sin x = \frac{\partial^2 u}{\partial y^2} \tag{2.118}$$

$$u\frac{\partial\theta}{\partial x} + v\frac{\partial\theta}{\partial y} = \frac{1}{Pr}\frac{\partial}{\partial y}\left[\left\{1 + \frac{4}{3}Rd(1 + (\theta_w - 1)\theta)^3\right\}\frac{\partial\theta}{\partial y}\right]$$

$$+ Q\theta + N\left(\frac{\partial u}{\partial y}\right)^2 - Ge\left(\frac{T_\infty}{T_w - T_\infty} + \theta\right)u \tag{2.119}$$

The boundary conditions associated with equations (2.109) become

$$u = v = 0, \quad \theta = 1 \text{ at } y = 0$$
$$u \to 0, \quad \theta \to 0 \text{ as } y \to \infty \tag{2.120}$$

To solve equations (2.118) and (2.119) subject to the boundary conditions (2.120), we assume the following variables u and v where $\psi(x,y) =$

$xr(x)f(x,y)$, $\psi(x,v)$ is a non-dimensional stream function, which is related

to the velocity components in the usual way as $u = \dfrac{1}{r}\dfrac{\partial \psi}{\partial y}$ and $v = -\dfrac{1}{r}\dfrac{\partial \psi}{\partial x}$ (2.121)

$$u = x(\partial f/\partial y), \ (\partial u/\partial y) = x(\partial^2 f/\partial y^2), \ (\partial^2 u/\partial y^2) = x(\partial^3 f/\partial y^3)$$

$$v = -[(1 + x\cos x/\sin x)f(x,y) + x(\partial f/\partial x)], \ (\partial u/\partial x) = (\partial f/\partial y) + x(\partial^2 f/\partial x \partial y)$$ (2.122)

Using the above transformed values in equations (2.118) and (2.119) and simplifying, we have the following:

$$\frac{\partial^3 f}{\partial y^3} + \left(1 + \frac{x}{\sin x}\cos x\right)f\frac{\partial^2 f}{\partial y^2} - \left(\frac{\partial f}{\partial y}\right)^2 + \frac{\theta}{x}\sin x - M\frac{\partial f}{\partial y} = x\left(\frac{\partial f}{\partial y}\frac{\partial^2 f}{\partial y \partial x} - \frac{\partial f}{\partial x}\frac{\partial^2 f}{\partial y^2}\right)$$ (2.123)

$$\frac{1}{Pr}\frac{\partial}{\partial y}\left\{\left(1 + \frac{4}{3}Rd(1 + (\theta_w - 1)\theta)^3\right)\frac{\partial \theta}{\partial y}\right\} + \left(1 + \frac{x}{\sin x}\cos x\right)f\frac{\partial \theta}{\partial y} + Q\theta$$ (2.124)

$$+ Nx^2\left(\frac{\partial^2 f}{\partial y^2}\right)^2 - Ge\left(\frac{T_w}{T_w - T_\infty} + \theta\right)\frac{\partial f}{\partial y} = x\left(\frac{\partial f}{\partial y}\frac{\partial \theta}{\partial x} - \frac{\partial \theta}{\partial y}\frac{\partial f}{\partial x}\right)$$

The corresponding boundary conditions are

$$f = \frac{\partial f}{\partial y} = 0 \ , \ \theta = 1 \text{ at } y = 0$$

$$\frac{\partial f}{\partial y} \to 0, \ \theta \to 0 \quad \text{as } y \to \infty$$ (2.125)

It has been seen that for the lower stagnation point of the sphere ie $x \approx 0$, equations (2.123) and (2.124) reduce to the following ordinary differential equations:

$$\frac{d^3 f}{dy^3} + 2f\frac{d^2 f}{dy^2} - \left(\frac{df}{dy}\right)^2 + \theta - M\frac{df}{dy} = 0$$ (2.126)

$$\frac{1}{Pr}\left[\left\{1 + \frac{4}{3}Rd(1 + (\theta_w - 1)\theta)^3\right\}\theta'\right]' + 2f\theta' - Ge\left(\frac{T_w}{T_w - T_\infty} + \theta\right)\frac{\partial f}{\partial y} + Q\theta = 0$$ (2.127)

Along with the boundary conditions

$$f = \frac{\partial f}{\partial y} = 0, \ \theta = 1 \text{ at } y = 0$$

$$\frac{\partial f}{\partial y} \to 0, \ \theta \to 0 \quad \text{as } y \to \infty$$ (2.128)

In practical application, the physical quantities of principal interest are the heat transfer and the skin- friction coefficient, which can be written in non- dimensional form as

$$Nu_x = \frac{aGr^{-\frac{1}{4}}}{k\left(T_w - T_\infty\right)}q_w \quad \text{and} \quad C_{fx} = \frac{Gr^{-\frac{3}{4}}a^2}{\mu\nu}\tau_w \tag{2.129}$$

Where, $q_w = -k\left(\dfrac{\partial T}{\partial Y}\right)_{Y=0}$ and $\tau_w = \mu\left(\dfrac{\partial U}{\partial Y}\right)_{Y=0}$, k being the thermal conductivity of the fluid. Using the variables (2.112), (2.113), we have

$$q_w = -k\left(\frac{\partial(T_\infty + \theta(T_w - T_\infty))}{\partial(aGr^{-\frac{1}{4}}y)}\right)_{y=0}$$

$$= -\frac{k(T_w - T_\infty)}{aGr^{-\frac{1}{4}}}\left(\frac{\partial\theta}{\partial y}\right)_{y=0}$$

And $\tau_w = \mu\left(\dfrac{\partial(\frac{\nu}{a}Gr^{\frac{1}{2}}u)}{\partial(aGr^{-\frac{1}{4}}y)}\right)_{y=0}$

$$= \frac{\mu\nu Gr^{\frac{1}{2}}}{a^2 Gr^{-\frac{1}{4}}}\left(\frac{\partial u}{\partial y}\right)_{y=0}$$

$$= \frac{\mu\nu}{a^2 Gr^{-\frac{3}{4}}}\left(\frac{\partial u}{\partial y}\right)_{y=0}$$

Putting the above values in equations (2.129) with the boundary conditions (2.128), we have

$$Nu_x = \frac{aGr^{-\frac{1}{4}}}{k\left(T_w - T_\infty\right)} \times -\frac{k(T_w - T_\infty)}{aGr^{-\frac{1}{4}}}\left(\frac{\partial\theta}{\partial y}\right)_{y=0}$$

$$Nu_x = -\left(1 + (4/3)Rd\theta_w^3\right)\frac{\partial\theta(x,0)}{\partial y} \tag{2.130}$$

And $C_{fx} = \dfrac{Gr^{-\frac{3}{4}}a^2}{\mu\nu} \times \dfrac{\mu\nu}{a^2 Gr^{-\frac{3}{4}}}\left(\dfrac{\partial u}{\partial y}\right)_{y=0} = x\left(\dfrac{\partial^2 f}{\partial y^2}\right)_{y=0}$

$$\therefore C_{fx} = x\left(\frac{\partial^2 f}{\partial y^2}\right)_{y=0} \qquad\qquad (2\ 131)$$

Now we will discuss velocity distribution as well as temperature distribution for a selection of parameter sets consisting of heat generation parameter Q, radiation parameter Rd, the surface temperature parameter θ_w, the viscous dissipation parameter N, the pressure work parameter Ge, magnetic parameter M and the Prandlt number Pr.

2.3.1 Method of Solution

The numerical methods used is finite difference method together with Keller box Scheme (1971). To begin with, the partial differential Eqs. (2.123)-(2.124) are first converted into a system of first order differential equations. Then these equations are expressed in finite difference forms by approximating the functions and their derivatives in terms of the center difference. Denoting the mesh points in the (x,η)-plane by x_i and η_j where $i = 1, 2, \ldots, M$ and $j = 1, 2, \ldots, N$, central difference approximations are made, such that those equations involving x explicitly are centered at $(x_{i-1/2}, \eta_{j-1/2})$ and the remainder at $(x_i, \eta_{j-1/2})$, where $\eta_{j-1/2} = \frac{1}{2}(\eta_j + \eta_{j-1})$ etc. The above central difference approximations reduces the system of first order differential equations to a set of non-linear difference equations for the unknown at x_i in terms of their values at x_{i-1}. The resulting set of nonlinear difference equations are solved by using the Newton's quasi-linearization method. The Jacobian matrix has a block-tridiagonal structure and the difference equations are solved using a block-matrix version of the Thomas algorithm; the details of the computational procedure have been discussed further by in the book by Cebeci and Bradshow (1984) and widely used by Hossain *et al.* (1998, 1997).

CONJUGATE EFFECTS OF VISCOUS DISSIPATION AND PRESSURE WORK ON MHD NATURAL CONVECTION FLOW ALONG A VERTICAL FLAT PLATE WITH HEAT CONDUCTION

Natural convection heat transfer has gained considerable attention because of its numerous applications in the areas of energy conservations; cooling of electrical and electronic components, design of solar collectors, heat exchangers and many others. The main difficulty in solving natural convection problems lies in the determination of the velocity field, which greatly influences the heat transfer process. The viscous dissipation effect plays an important role in natural convection in various devices which are subjected to large deceleration or which operate at high rotational speeds and also in strong gravitational field processes on large scales (on large planets) and in geological processes. In order to explain the effect of viscous dissipation, we shall first take a grossly simplified view that the compressibility effect may be neglected and the properties such as viscosity, thermal conductivity and specific heat are constant and there consider the flow between two parallel flat plates one of which is stationary and the other moving in its own plane with a constant velocity U_∞. The rate at which the pressure does work known as pressure work on one side of a flat surface in the fluid is the product of the pressure, the area of the surface and the normal component of velocity. Thus rate of doing work = Force (due to pressure) × velocity. Thus pressure work = $Tu\beta\ \partial P/\partial x$, where T is the temperature, u is the velocity, β is the coefficient of thermal expansion and $\partial P/\partial x$ is the pressure gradient. The discussion and analysis of natural convection flows, pressure and viscous stress work effects are generally ignored but here we have considered the effects of viscous dissipation and pressure work on a MHD natural convection flow along a vertical flat plate with heat conduction. Magnetohydrodynamics is that branch of continuum mechanics, which deals with the flow of electrically conducting fluids in a magnetic field. It is of importance in connection with many engineering problems such as plasma confinement, liquid-metal cooling of nuclear reactors, and electromagnetic casting. Originally, MHD included only the study of strictly incompressible fluid, but today the terminology is applied to the study of partially ionized gases as well. Other names have been suggested, such as magnetofluidmechanics. or magnetoaerodynamics. Magnetohydrodynamic equations

are the ordinary electromagnetic and hydrodynamic equations modified to take account of the interaction between the motion of the fluid and electromagnetic field. In case of natural convection flows, now a days, MHD analysis is playing a vital role. It is also useful in geophysics and astronomy. Geophysicists encounter MHD phenomena in the interactions of conducting fluids and magnetic fields that are present in and around heavenly bodies. Engineers employ MHD principles in the design of heat exchangers, pumps and flowerets, in space vehicle propulsion, control and re-entry and in controlled fusion.

In the present work, we have investigated the viscous dissipation and pressure effect on the skin friction and the surface temperature distribution in the entire region from up stream to down stream of a viscous incompressible and electrically conducting fluid from a vertical flat plate in presence of magnetic field and heat conduction. The transformed non-similar boundary layer equations governing the flow together with the boundary conditions based on conduction and convection were solved numerically using the Keller box (implicit finite difference) method along with Newton's linearization approximation method, which described by Cebeci and Bradshow (1984). The effects is of the Prandtl number Pr, the viscous dissipation parameter N, the magnetic parameter M and pressure work parameter G_e on the velocity and temperature fields as well as on the skin friction and surface temperature have been studied. In the following sections detailed derivations of the governing equations for the flow and heat transfer and the method of solutions along with the results and discussions are presented. All the investigations for the fluid with low Prandtl number appropriates for the liquid metals are carried out.

3.1 Governing equations of the flow

The mathematical statement of the basic conservation laws of mass (2.26), momentum equation (2.27) and energy equation (2.28) ignoring Joule heating and heat generation terms for the steady viscous incompressible and electrically conducting flow after simplifying are given by

Figure 3.1: Physical configuration and coordinate system

$$\frac{\partial U}{\partial X}+\frac{\partial V}{\partial Y}=0 \tag{3.1}$$

$$U\frac{\partial U}{\partial X}+V\frac{\partial U}{\partial Y}=v\frac{\partial^2 U}{\partial Y^2}+g\beta(T-T_\infty)-\frac{\sigma B_0^2 U}{\rho} \tag{3.2}$$

$$U\frac{\partial T}{\partial X}+V\frac{\partial T}{\partial Y}=\frac{\kappa}{\rho c_p}\frac{\partial^2 T}{\partial Y^2}+\frac{v}{c_p}(\frac{\partial U}{\partial Y})^2+\frac{T\beta U}{\rho C_p}\rho g \tag{3.3}$$

Using boundary conditions (2.32)-(2.33) and the transformation equation (2.35) in equations (3.1) to (3.3), we have the following dimensionless equations

$$\frac{\partial u}{\partial x}+\frac{\partial v}{\partial y}=0 \tag{3.4}$$

$$u\frac{\partial u}{\partial x}+v\frac{\partial u}{\partial y}+Mu=\frac{\partial^2 u}{\partial y^2}+\theta \tag{3.5}$$

$$u\frac{\partial \theta}{\partial x}+v\frac{\partial \theta}{\partial y}=\frac{1}{Pr}\frac{\partial^2 \theta}{\partial y^2}+N(\frac{\partial u}{\partial y})^2+G_e\frac{\{T_\infty'+(T_b-T_\infty)\theta\}}{(T_b-T_\infty')} \tag{3.6}$$

Where *M*, *N*, *Ge* and *Pr* are defined earlier. Also their boundary conditions are same *i.e.* (2.39). Substituting (2.40) into equations (3.5) and (3.6) and after simplifying, we get the following transformed non-dimensional equations.

$$f'''+\frac{16+15x}{20(1+x)}ff''-\frac{6+5x}{10(1+x)}f'^2-Mx^{2/5}(1+x)^{1/10}f'+h=x(f'\frac{\partial f'}{\partial x}-f''\frac{\partial f}{\partial x}) \tag{3.7}$$

$$\frac{1}{P_r}h'' + \frac{16+15x}{20(1+x)}fh' - \frac{1}{5(1+x)}f'h + Nxf''^2$$

$$+G_e x\left\{\left(\frac{1+x}{x}\right)^{\frac{1}{5}}\left(\frac{T_\infty}{T_b - T_\infty}\right)\frac{\partial f}{\partial \eta} + h(x,\eta)\frac{\partial f}{\partial \eta}\right\} = x(f'\frac{\partial h}{\partial x} - h'\frac{\partial f}{\partial x}) \tag{3.8}$$

In the above equations the primes denote differentiation with respect to η. The boundary conditions (2.39) then take the following form

$$f(x,0) = f'(x,0) = 0, h'(x,0) = -(1+x)^{1/4} + x^{1/5}(1+x)^{1/20} h(x,0)$$
$$f'(x,\infty) = 0, h'(x,\infty) = 0 \tag{3.9}$$

The skin friction τ and the surface temperature θ at the surface in the boundary layer given by

$$\tau = \mu\{x^{2/5}(1+x)^{-3/20}f''(x, 0)\} \tag{3.10}$$
$$\theta = x^{1/5}(1+x)^{-1/5}h(x, 0)$$

3.2 Results and discussion

Here we have investigated the problem of the steady two dimensional laminar free convection boundary layer flow of a viscous incompressible and electrically conducting fluid with pressure work along a side of a vertical flat plate of thickness 'b' insulated on the edges with temperature T_b maintained on the other side in the presence of a uniformly distributed transverse magnetic field. Solutions are obtained for the fluid having Prandtl number $Pr = 0.01, 0.10, 0.50, 0.72, 1.00$ and for a wide range of the values of the viscous dissipation parameter $N = 0.20, 0.40, 0.60, 0.90$ and the magnetic parameter or Hartmann Number $M = 1.00, 1.30, 1.50, 1.70, 2.00$ and also the pressure work parameter $Ge = 0.20, 0.40, 0.70, 0.90$. If we know the values of the functions $f'(x, \eta)$, $h(x, \eta)$ and their derivatives for different values of the Prandtl number Pr, the magnetic parameter or Hartmann Number M, the viscous dissipation parameter N and the pressure work parameter Ge, we may calculate the numerical values of the surface temperature $\theta(x, 0)$ and the shear stress $f''(x, 0)$ at the surface that are important from the physical point of view.

Figure 3.2(a) and figure 3.2(b) deal with the effect of the viscous dissipation parameter N (=0.20, 0.40, 0.60, 0.90) for different values of the controlling parameters $Pr = 0.72$, $M = 0.80$ and $Ge = 0.50$ on the velocity profiles $f'(x, \eta)$ and the temperature profiles h (x, η). From figure 3.2(a), it is revealed that the velocity profiles $f'(x, \eta)$ increase slightly with the increase of the viscous dissipation parameter N that indicates the

viscous dissipation accelerates the fluid motion slowly. From figure 3 2(b), it is shown that the temperature profiles $h(x, \eta)$ increase for increasing values of N.

From figure 3.3(a) and figure 3.3(b), it is seen that both the velocity profiles $f'(x, \eta)$ and the temperature profiles $h(x, \eta)$ increase with the increasing values of the pressure work parameter $Ge (= 0.20, 0.40, 0.70, 0.90)$ with others controlling parameters $Pr = 0.72$, $M = 0.70$, $N = 0.60$

Figure 3.4(a) and figure 3.4(b) represent the velocity profiles $f'(x, \eta)$ and temperature profiles $h(x, \eta)$ for the different values of magnetic parameter or Hartmann Number $M (= 1 00, 1.30, 1.50, 1.70, 2.00)$ with other controlling parameters $Pr = 0 72$, $N = 0.50$ and $Ge = 0.70$ From figure 3.4(a), it can be seen that the velocity profiles decrease with the increasing values of magnetic parameter. On the other hand from figure 3.4 (b), it is observed that the temperature profiles increase due to the increase of magnetic parameter or Hartmann Number M.

Figure 3.5(a) depicts the velocity profiles for different values of the Prandtl number Pr ($= 0.01, 0.10, 0 50, 0.72, 1.00$) while the other controlling parameters are $M = 1.00$, $N = 0.60$ and $Ge = 0.50$. Corresponding distribution of the temperature profiles $h(x, \eta)$ in the fluids is shown in figure 3.5(b). From figure 3.5(a), it can be seen that if the Prandtl number increases, the velocity distribution decreases. On the other hand, from figure 3.5(b) it can be observed that the temperature profile decreases within the boundary layer due to increase of the Prandtl number Pr.

From figure 3.6(a), it can be observed that increase in the value of the viscous dissipation parameter N leads to increase the value of the skin friction coefficient $f''(x, 0)$. Again figure 3.6(b) shows that the increase the viscous dissipation parameter N leads to increase the surface temperature $\theta(x, 0)$. Similar results hold in the skin friction coefficient $f''(x, 0)$ and the surface temperature distribution $\theta(x, 0)$ shown in figure 3.7(a) and figure 3.7(b) respectively for different values of the parameter such as $Ge (= 0.20, 0.40, 0.70, 0.90)$ and other controlling parameter are fixed ($Pr = 0 72$, $M = 0 70$, $N = 0.60$).

Figure 3.8(a) and figure 3.8(b) represent the results of the skin friction coefficient and the surface temperature distribution respectively for different values of magnetic parameters or Hartmann Number $M (= 1.00, 1.30, 1.50, 1.70, 2.00)$ when the value of the Prandtl numbers $Pr = 0.72$, the viscous dissipation parameter $N = 0.50$ and the

pressure work parameter $Ge = 0.70$. Here it can be observed that the skin friction coefficient $f''(x, 0)$ and the surface temperature distributions $\theta(x, 0)$ both are decreasing with the increasing values of M.

From figure 3.9(a), it is shown that the skin friction coefficient $f''(x, 0)$ decreases monotonically with the increase of the Prandtl number Pr (=0.01, 0.10, 0.50, 0.72, 1.00) and from the figure 3.9(b), the same result is observed on the surface temperature distribution due to increase of the value of the Prandtl number when other values of the controlling parameters are $M = 1.00$, $N = 0.60$ and $Ge = 0.50$.
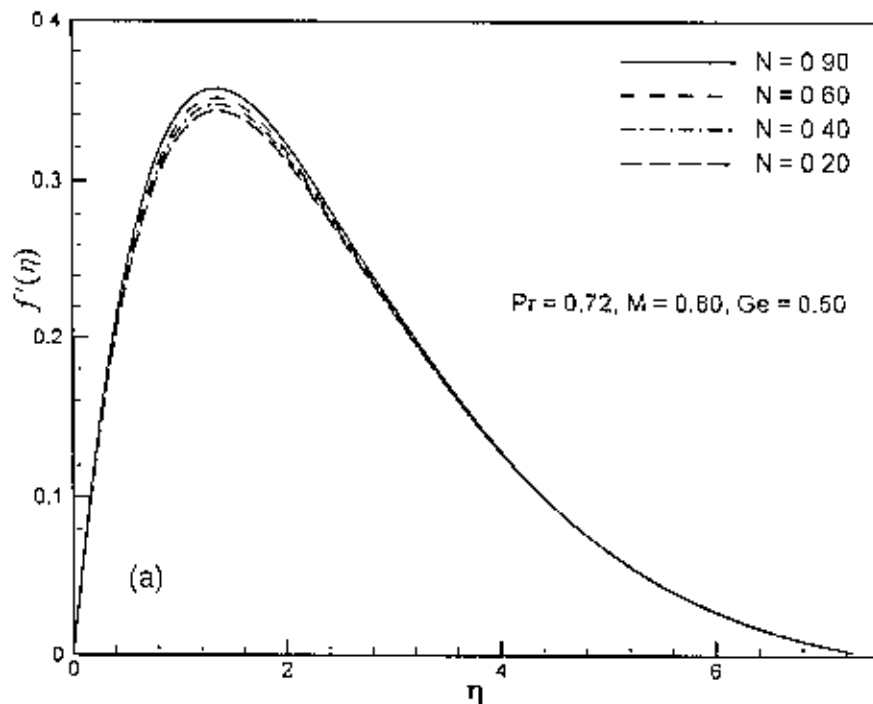
Figure 3.2(a): Variation of dimensionless velocity distribution $f'(x, \eta)$ against dimensionless distance η for different values of viscous dissipation parameter N with $Pr = 0.72$, $M = 0.8$ and $Ge = 0.5$.
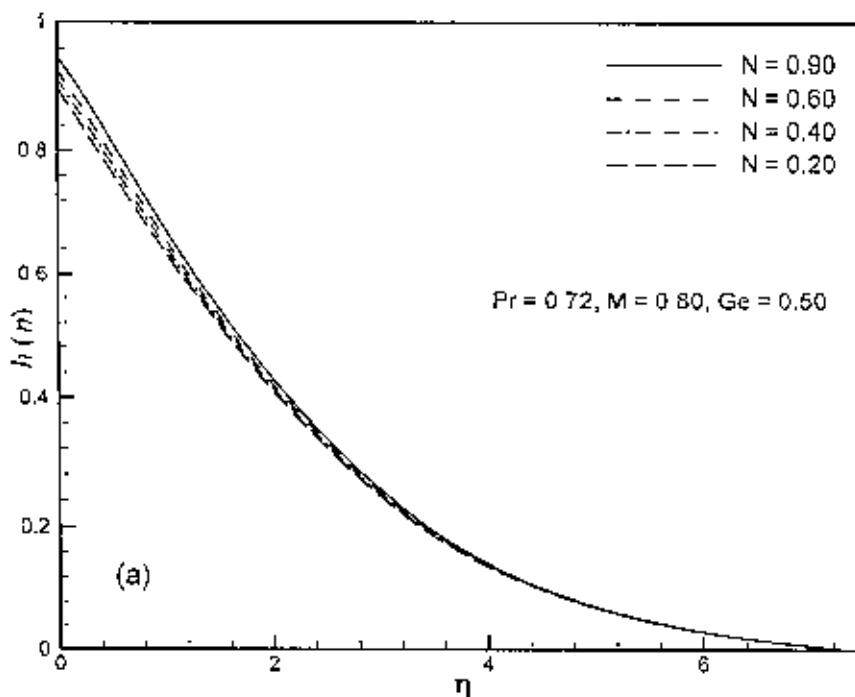
Figure 3.2(b): Variation of dimensionless temperature distribution $h(x, \eta)$ against dimensionless distance η for different values of viscous dissipation parameter N with $Pr = 0.72$, $M = 0.8$ and $Ge = 0.5$.
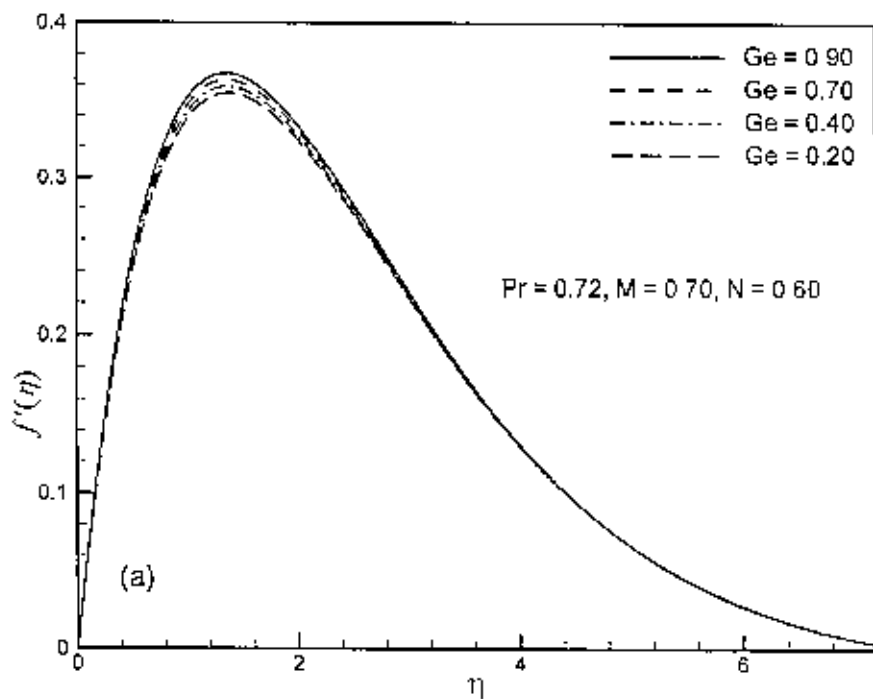
Figure 3.3(a): Variation of dimensionless velocity distribution $f'(x,\eta)$ against dimensionless distance η for different values of pressure work parameter Ge with $Pr = 0.72$, $M = 0.70$ and $N = 0.60$.
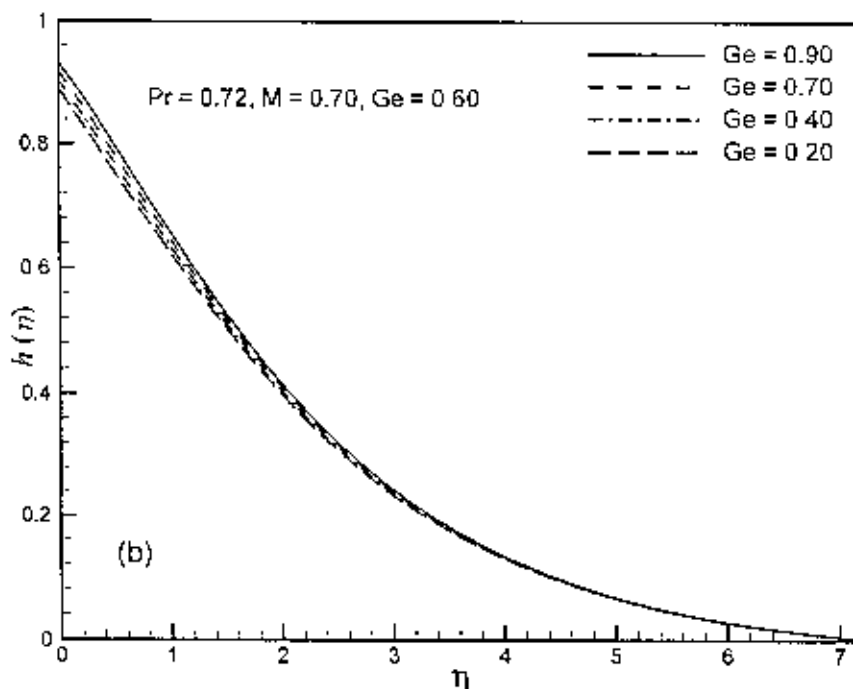
Figure 3.3(b): Variation of dimensionless temperature distribution $h(x,\eta)$ against dimensionless distance η for different values of pressure work parameter Ge with $Pr = 0.72$, $M = 0.70$ and $N = 0.60$.
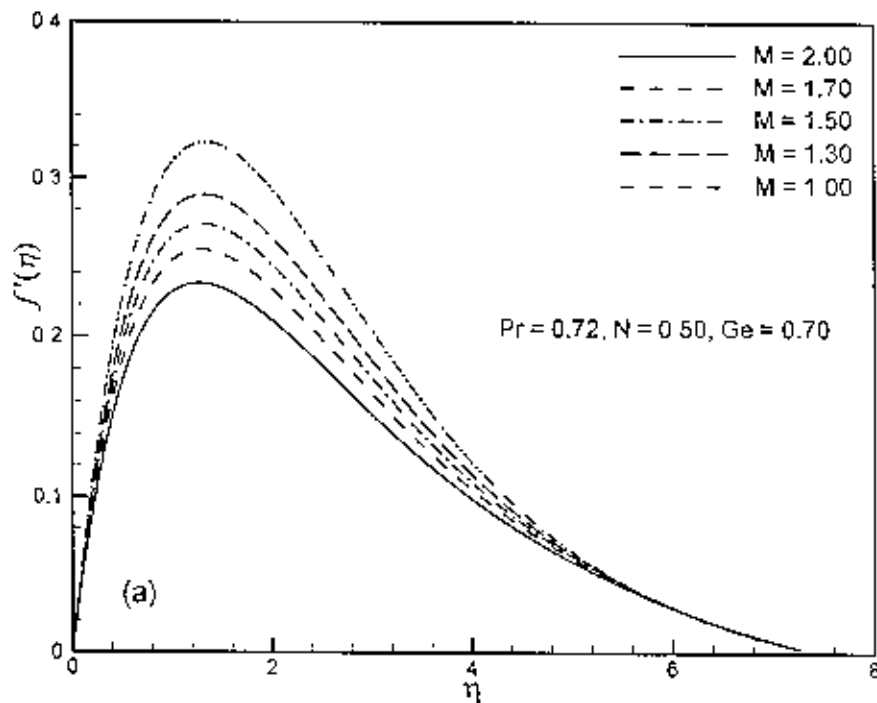
Figure 3.4(a): Variation of dimensionless velocity distribution $f'(x,\eta)$ against dimensionless distance η for different values of magnetic parameter or Hartmann Number M with $Pr = 0.72$, $N = 0.40$ and $Ge = 0.60$.
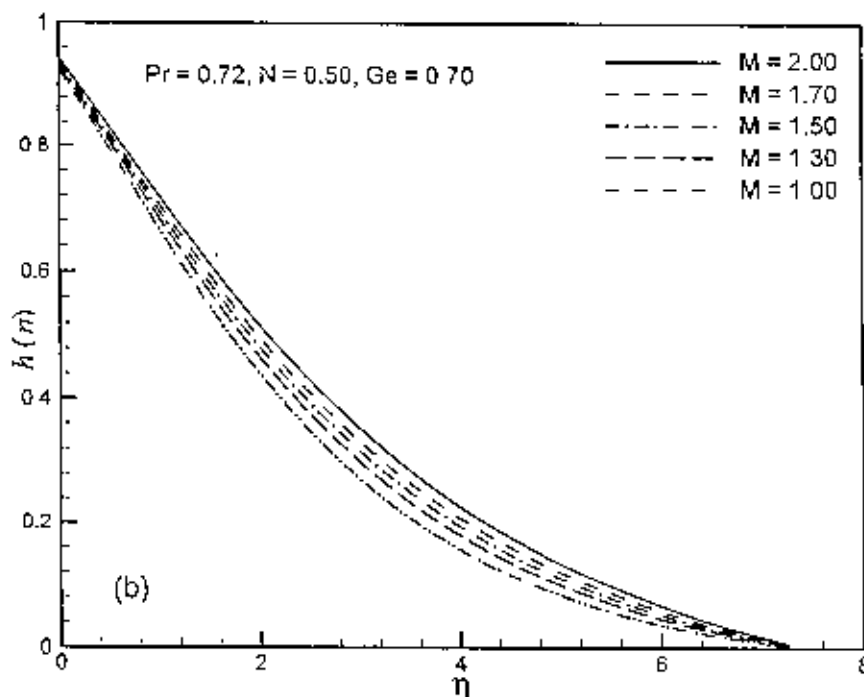
Figure 3.4(b): Variation of dimensionless temperature distribution $h(\eta)$ with dimensionless distance η for different values of magnetic parameter or Hartmann Number M with $Pr = 0.72$, $N = 0.40$ and $Ge = 0.60$.
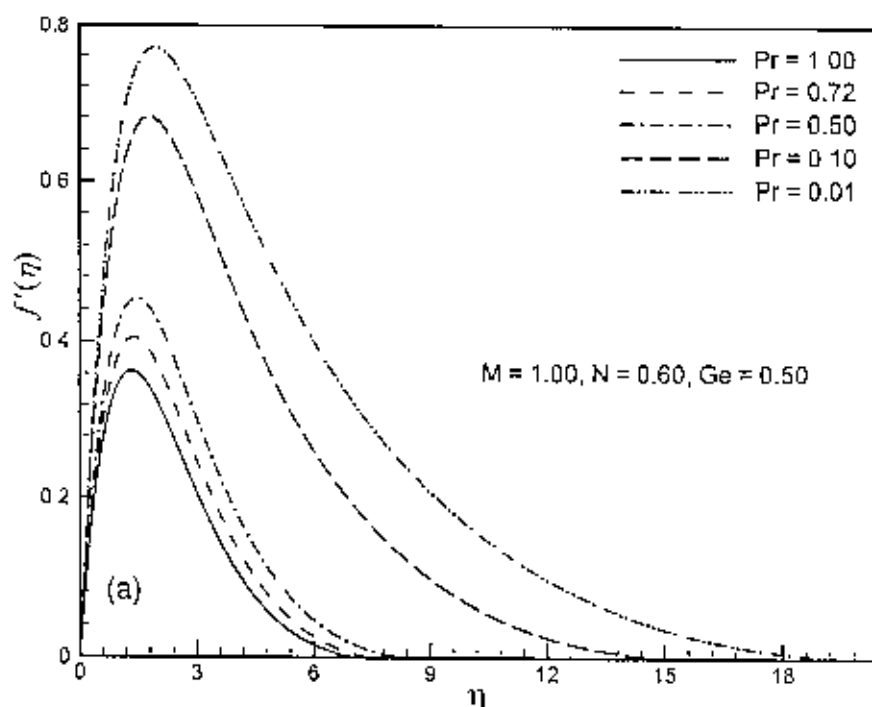
Figure 3.5(a): Variation of dimensionless velocity distribution $f'(x,\eta)$ with dimensionless distance η for different values of Prandtl number Pr with $N = 0.60$, $M = 1.00$ and $Ge = 0.50$.
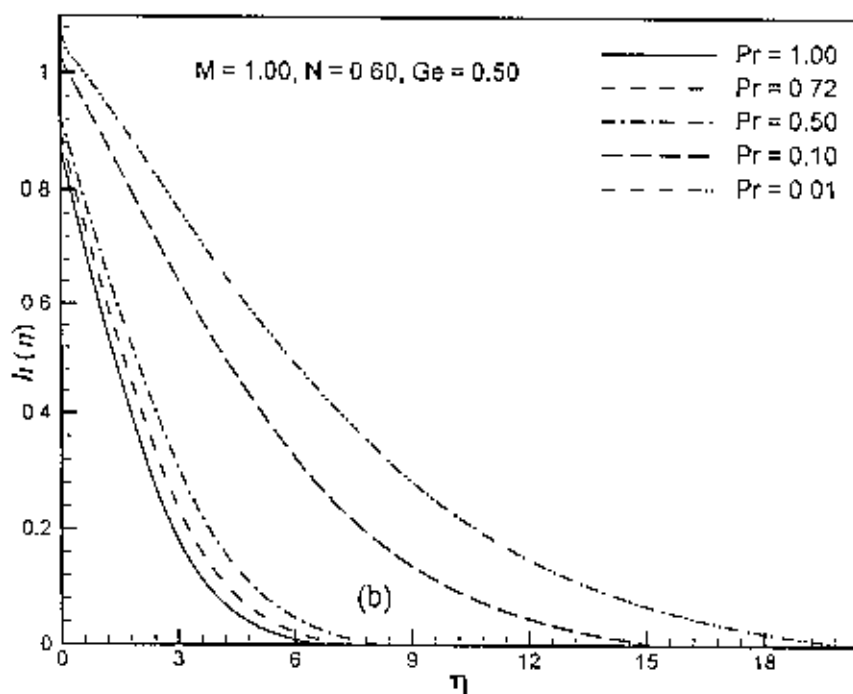
Figure 3.5(b): Variation of dimensionless temperature $h(x,\eta)$ with dimensionless distance η for different values of Prandtl number Pr with $N = 0.60$, $M = 1.00$ and $Ge = 0.50$.
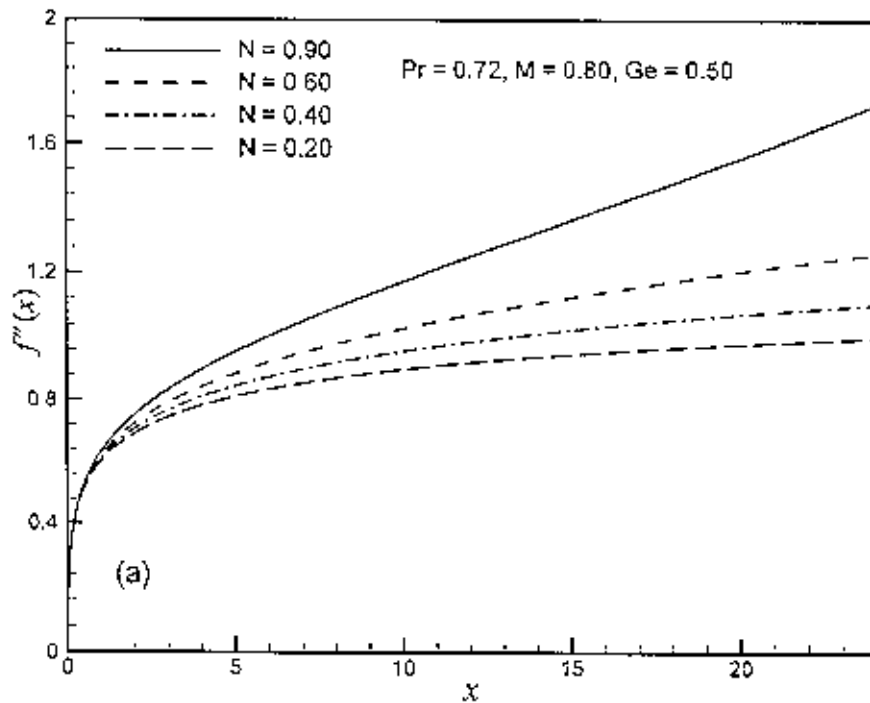
Figure 3.6(a): Variation of skin friction coefficient $f''(x, 0)$ with dimensionless distance x for different values of viscous dissipation parameter N with $Pr = 0.72$, $M = 0.80$ and $Ge = 0.50$
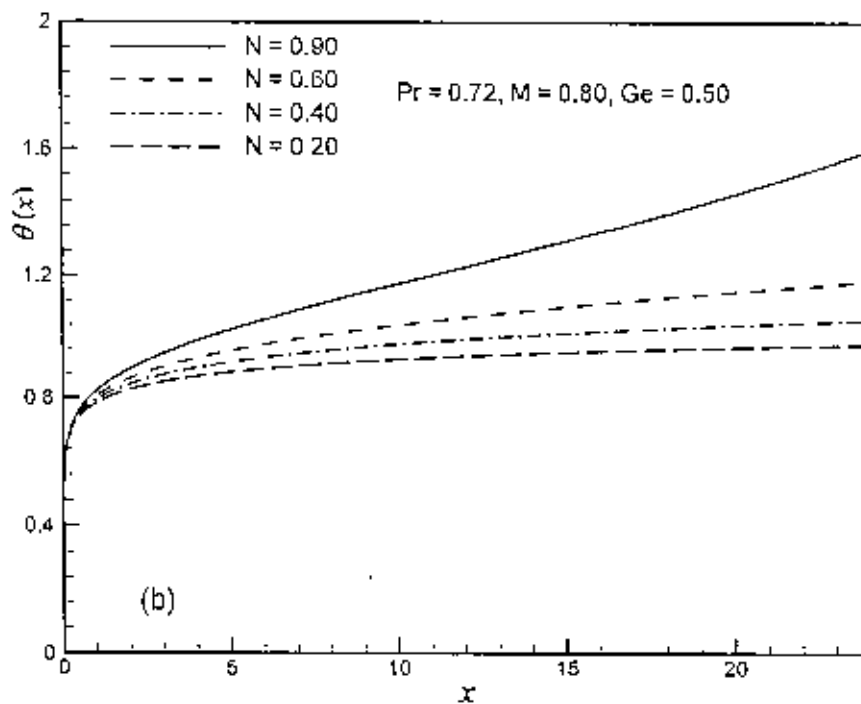
Figure 3.6(b): Variation of surface temperature $\theta(x, 0)$ with dimensionless distance x for different values of viscous dissipation parameter N with $Pr = 0.72$, $M = 0.80$ and $Ge = 0.50$.
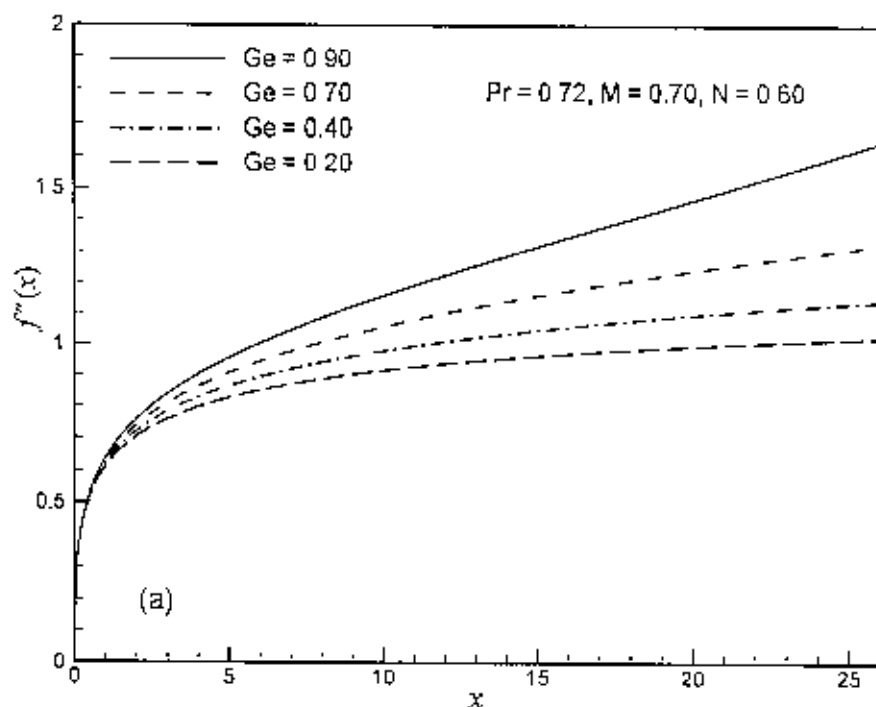
Figure 3.7(a): Variation of skin friction coefficient $f''(x, 0)$ with dimensionless distance x for different values of pressure work parameter Ge with $Pr = 0.72$, $M = 0.70$ and $N = 0.60$.
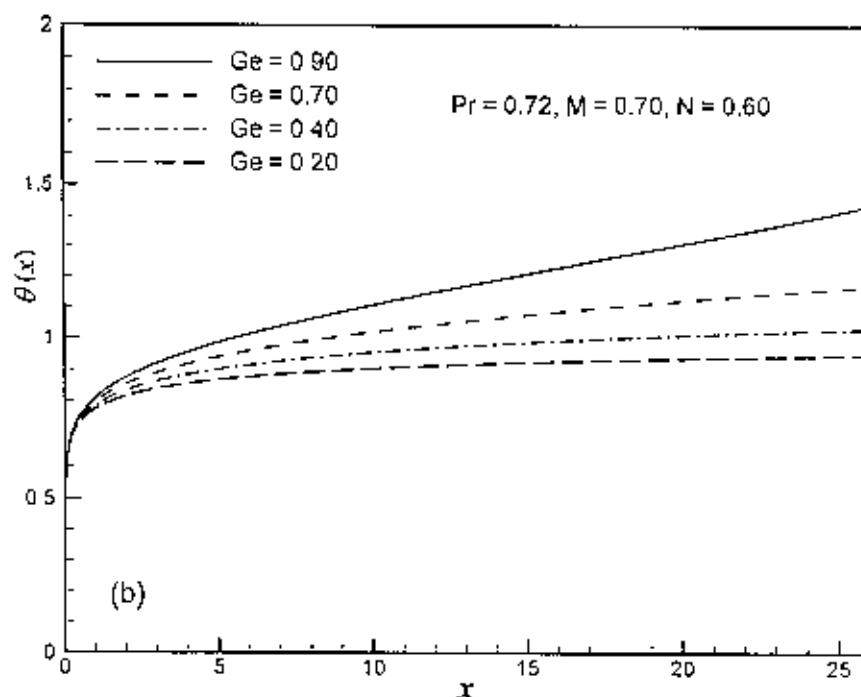
Figure 3.7(b): Variation of surface temperature $\theta(x, 0)$ with dimensionless distance x for different values of pressure work parameter Ge with $Pr = 0.72$, $M = 0.70$ and $N = 0.60$.
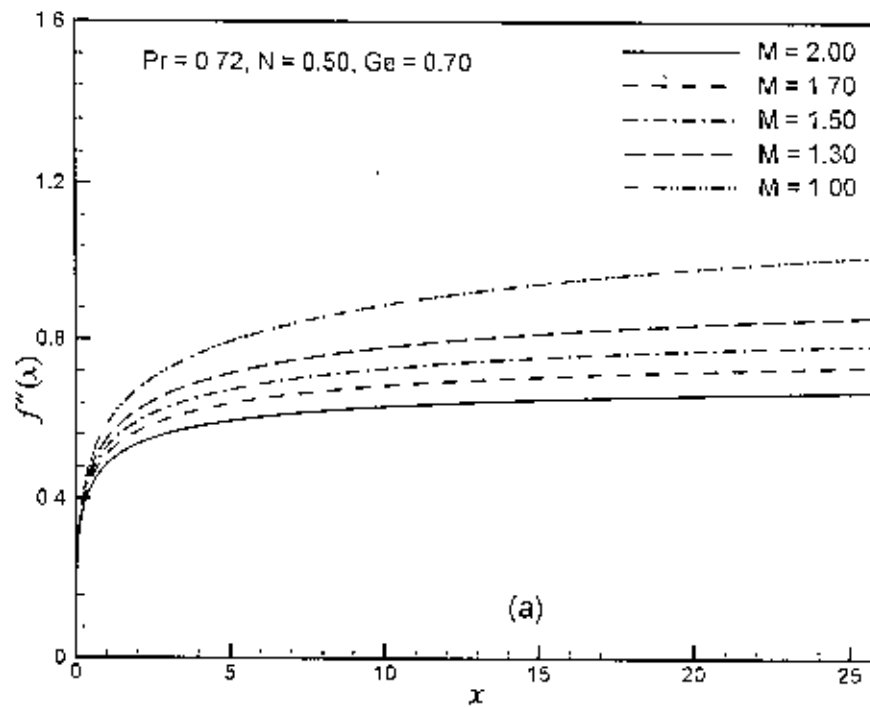
Figure 3.8(a): Variation of skin friction coefficient $f''(x, 0)$ with dimensionless distance x for different values of magnetic parameter or Hartmann Number M with $Pr = 0.72$, $N = 0.50$ and $Ge = 0.70$.
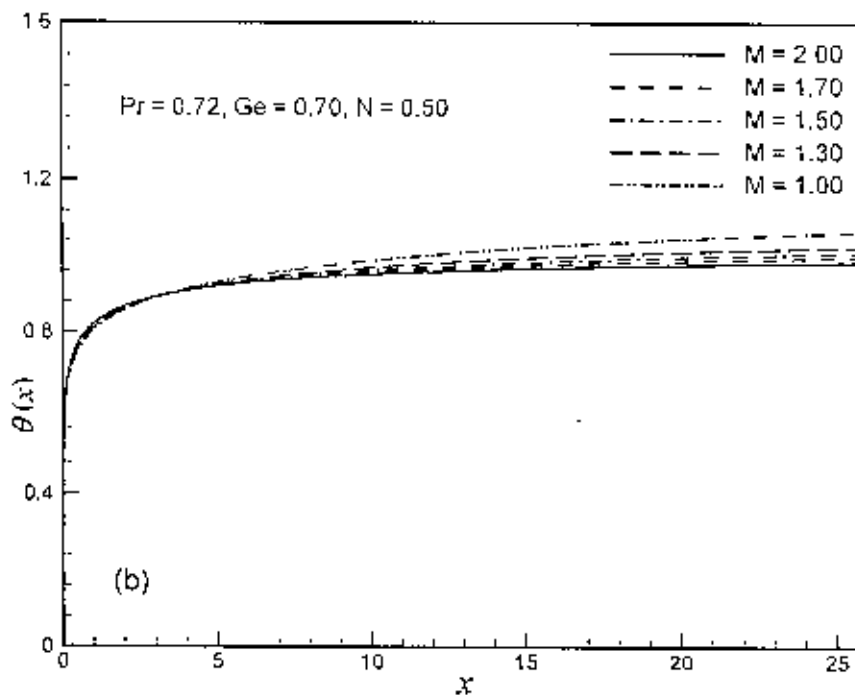
Figure 3.8(b): Variation of surface temperature $\theta(x, 0)$ with dimensionless distance x for different values of magnetic parameter or Hartmann Number M with $Pr = 0.72$, $N = 0.50$ and $Ge = 0.70$.
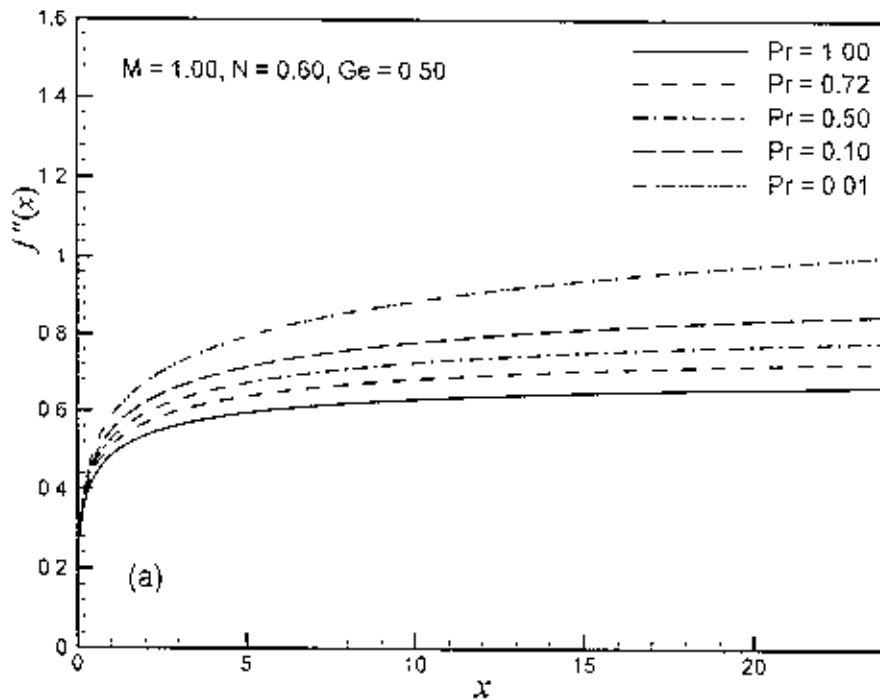
Figure 3.9(a): Variation of skin friction coefficient $f''(x, 0)$ with dimensionless distance x for different values of Prandtl number Pr with $M = 1.00$, $N = 0.60$ and $Ge = 0.50$.
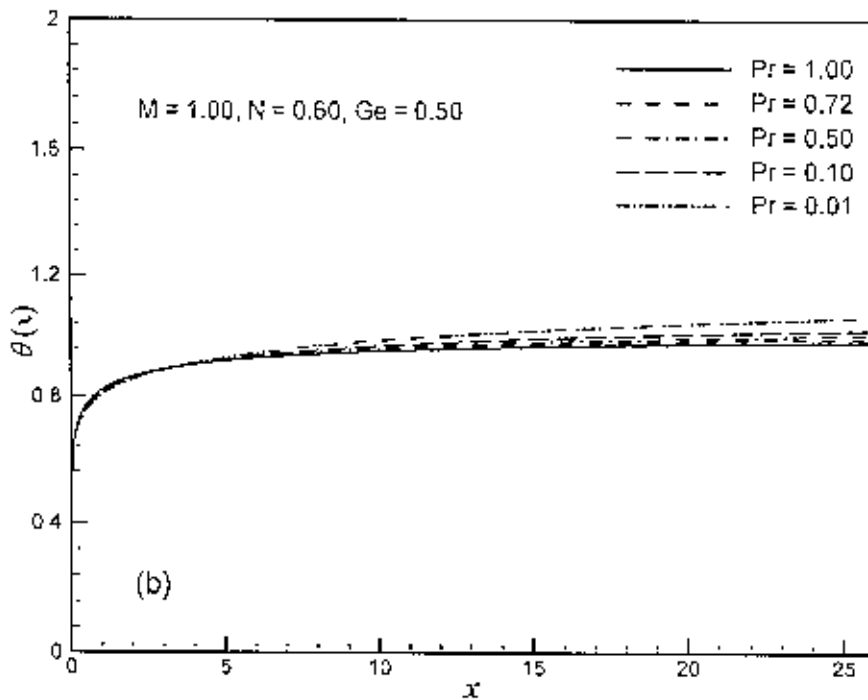
Figure 3.9(b): Variation of surface temperature $\theta(x, 0)$ with dimensionless distance x for different values of Prandtl number Pr with $M = 1.00$, $N = 0.60$ and $Ge = 0.50$.

Table-C_1 represents the values of the skin friction coefficient and surface temperature for different values of magnetic parameter or Hartmann Number M while $Pr = 0.72$, $N = 0.50$ and $Ge = 0.70$ which shown in Appendix C. Here we found that the values of skin friction coefficient decrease at different position of x for magnetic parameter or Hartmann Number $M = 1.00$, 1.50, 1.70, 2.00. The rate of the skin friction coefficient decreases by 19.33% as the magnetic parameter or Hartmann Number M changes from 1.00 to 2.00 and $x = 1.60$. Furthermore, it is seen that the numerical values of the surface temperature distribution decrease for increasing values of magnetic parameter or Hartmann Number M. The rate of decrease of surface temperature distribution is 3.90% at position $x = 1.60$ as the magnetic parameter changes from 1.00 to 2.00

The values of skin friction and the surface temperature have been presented in Table-C_2 for different values of Prandtl number Pr while $M = 1.00$, $N = 0.60$ and $Ge = 0.50$ which shown in Appendix C. Here we observed that the values of skin friction coefficient decrease at different position of x for Prandtl number $Pr = 0.10$, 0.72, 1.00. The rate of the skin friction coefficient decreases by 31.83% as the Prandtl number Pr changes from 0.100 to 1.00 and $x = 1.0409$. Furthermore, it is seen that the numerical values of the surface temperature distribution decrease for increasing values of Prandtl number Pr. The rate of decrease of surface temperature distribution is 10.91% at position $x = 1.0409$ as the Prandtl number changes from 0.10 to 1.00.

The values of the skin friction coefficient and surface temperature for different values of viscous dissipation parameter N while $Pr = 0.72$, $M = 0.80$ and $Ge = 0.50$ are given in the Table-C_3 which showed in Appendix C. Here the values of skin friction coefficient increases at different position of x for viscous dissipation parameter $N = 0.20$, 0.40, 0.60, 0.90. The rate of increase of the skin friction coefficient is 15.01% as the viscous dissipation parameter N changes from 0.20 to 0.90 and $x = 4.0635$. Furthermore, it is seen that the numerical values of the surface temperature distribution increase for increasing values of viscous dissipation parameter N. The rate of increase of surface temperature distribution is 13.50% at position $x = 4.0635$ as the viscous dissipation parameter changes from 0.20 to 0.90.

The values of the skin friction coefficient and surface temperature for different values of pressure work parameter Ge while $Pr = 0.72$, $M = 0.80$ and $N = 0.60$ are entered in Table-C_4 which shown in Appendix C. Here the values of skin friction coefficient

increases at different position of x for pressure work parameter $Ge = 0.20$, 0.40, 0.70, 0.90. The rate of increase of the skin friction coefficient is 9.20% as the pressure work parameter Ge changes from 0.20 to 0.90 and $x = 4.0635$. Furthermore, it is seen that the numerical values of the surface temperature distribution increase for increasing values of pressure work parameter Ge. The rate of increase of surface temperature distribution is 12.94% at position $x = 4.0635$ as the pressure work parameter changes from 0.20 to 0.90.

3.3 Conclusions

The effect of viscous dissipation parameter N, magnetic parameter or Hartmann Number M, the pressure work parameter Ge and the Prandtl number Pr on the magneto-hydrodynamic natural convection boundary layer flow along a vertical flat plate has been studied introducing a new class of transformations. The transformed non-similar boundary layer equations governing the flow together with the boundary conditions based on conduction and convection were solved numerically using the very efficient implicit finite difference method together with Keller box scheme. The coupled effect of natural convection and conduction required the temperature and the heat flux is continuous at the interface. . From the present investigation, the following conclusions may be drawn:

- Both the skin friction coefficient and the velocity distribution increase for increasing values of the viscous dissipation parameter N and the pressure work parameter Ge.

- Increased values of the viscous dissipation parameter N leads to increase the surface temperature distribution as well as the temperature distribution.

- Increased values of the pressure work parameter Ge leads to increase the surface temperature distribution as well as the temperature distribution.

- It has been observed that the skin friction coefficient, the surface temperature distribution, the temperature profiles and the velocity distribution decrease over the whole boundary layer with the increase of the Prandtl number Pr.

- For the effect of magnetic parameter or Hartmann Number M, the skin friction coefficient, the surface temperature distribution and the velocity distribution over the whole boundary layer decreases, but the temperature distribution increases.

VISCOUS DISSIPATION AND PRESSURE WORK EFFECTS ON MAGNETOHYDRODYNAMIC FREE CONVECTION FLOW ALONG A VERTICAL FLAT PLATE WITH JOULE HEATING AND HEAT CONDUCTION

Free convection flow is often encountered in cooling of nuclear reactors or in the study of the structure of stars and planets. The study of temperature and heat transfer is of great importance to the engineers because of its almost universal occurrence in many branches of science and engineering. Heat transfer analysis is most important for the proper sizing of fuel elements in the nuclear reactor cores to prevent burnout. The viscous dissipation effect plays an important role in natural convection in various devices which are subjected to large deceleration or which operate at high rotational speeds and also in strong gravitational field processes on large scales (on large planets) and in geological processes. The discussion and analysis of natural convection flows, pressure and viscous stress work effects are generally ignored but here the effects of viscous dissipation and pressure work on a MHD natural convection flow along a vertical flat plate with Joule heating and heat conduction have been considered. When current flows in an electrical conductor such wire, electrical energy is lost due to the resistance of the electrical conductor, this lost electrical energy is converted into thermal energy called Joule heating. This is because the electrical power loss equals the heat transfer. In electronics, and more broadly in physics, Joule heating or ohmic heating refers to the increase in temperature of a conductor as a result of resistance to an electrical current flowing through it.

In the present chapter, we shall investigate the viscous dissipation and pressure effect on the skin friction and the rate of heat transfer in the entire region from upstream to downstream of a viscous incompressible and electrically conducting fluid from a vertical flat plate in presence of transverse magnetic field. We have studied the effect of the magnetic parameter M, the Prandtl number Pr, the viscous dissipation parameter N and pressure work parameter Ge on the velocity and temperature fields as well as on the skin friction and surface temperature.

4.1 Governing equations of the flow

The mathematical statement of the basic conservation laws of mass (2.26), momentum equation (2.27) and energy equation (2.28) ignoring heat generation terms for the steady viscous incompressible and electrically conducting flow after simplifying are given by
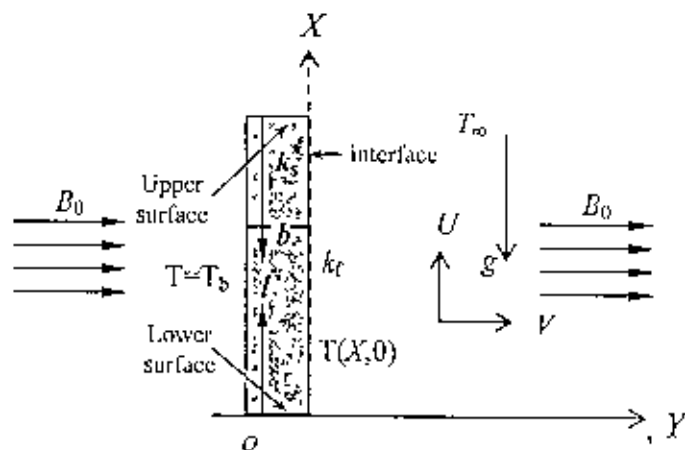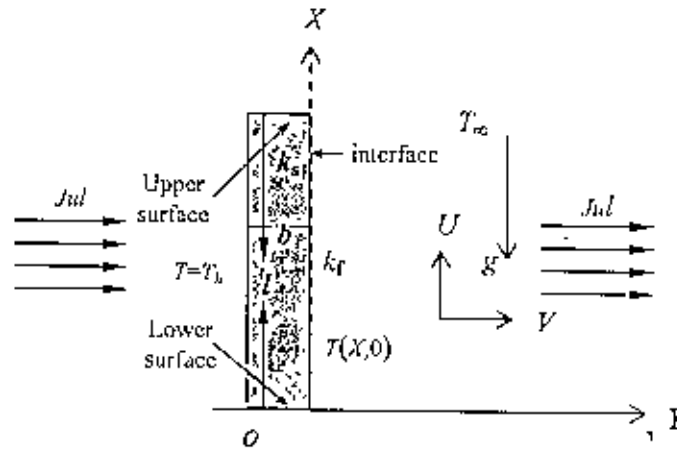

Figure 4.1: Physical configuration and coordinate system

$$\frac{\partial U}{\partial X} + \frac{\partial V}{\partial Y} = 0 \tag{4.1}$$

$$U\frac{\partial U}{\partial X} + V\frac{\partial U}{\partial Y} = \nu\frac{\partial^2 U}{\partial Y^2} + g\beta(T - T_\infty) - \frac{\sigma B_0^2 U}{\rho} \tag{4.2}$$

$$U\frac{\partial T}{\partial X} + V\frac{\partial T}{\partial Y} = \frac{\kappa}{\rho\,C_p}\frac{\partial^2 T}{\partial Y^2} + \frac{\nu}{C_p}(\frac{\partial U}{\partial Y})^2 + \frac{T\beta\,U}{\rho C_p}\rho g + \frac{\sigma B_0^2}{\rho C_p}U^2 \tag{4.3}$$

Using boundary conditions (2.32)-(2.33) and the transformation equation (2.35) in equations (4.1) to (4.3), we have the following dimensionless equations

$$\frac{\partial u}{\partial x} + \frac{\partial v}{\partial y} = 0 \tag{4.4}$$

$$u\frac{\partial u}{\partial x} + v\frac{\partial u}{\partial y} + Mu = \frac{\partial^2 u}{\partial y^2} + \theta \tag{4.5}$$

$$u\frac{\partial\theta}{\partial x} + v\frac{\partial\theta}{\partial y} = \frac{1}{Pr}\frac{\partial^2\theta}{\partial y^2} + N(\frac{\partial u}{\partial y})^2 + Jul(u^2) + G_e\frac{\{T_\infty + (T_b - T_\infty)\theta\}}{(T_b - T_\infty)} \tag{4.6}$$

Where M, N, Ge, Jul and Pr are defined earlier. Also their boundary conditions are same *i.e.* (2.39). Substituting (2.40) into equations (4.5) and (4.6) and after simplifying, we get the following transformed non-dimensional equations.

$$f''' + \frac{16+15x}{20(1+x)} ff'' - \frac{6+5x}{10(1+x)} f'^2 - Mx^{2/5}(1+x)^{1/10} f' + h = x(f' \frac{\partial f'}{\partial x} - f'' \frac{\partial f}{\partial x}) \quad (4.7)$$

$$\frac{1}{P_r} h'' + \frac{16+15x}{20(1+x)} fh' - \frac{1}{5(1+x)} f'h + Nxf''^2 + Jul\, x^{2/5}(1+x)^{1/10} f'^2$$

$$+ G_c x \left\{ \left(\frac{1+x}{x} \right)^{\frac{1}{5}} \left(\frac{T_\infty}{T_b - T_\infty} \right) \frac{\partial f}{\partial \eta} + h(x,\eta) \ \frac{\partial f}{\partial \eta} \right\} = x(f' \frac{\partial h}{\partial x} - h' \frac{\partial f}{\partial x}) \quad (4.8)$$

In the above equations the primes denote differentiation with respect to η.

The boundary conditions (2.39) then take the following form

$$f(x,0) = f'(x,0) = 0, h'(x,0) = -(1+x)^{1/4} + x^{1/5}(1+x)^{1/20} h(x,0)$$
$$f'(x,\infty) = 0, h'(x,\infty) = 0 \quad (4.9)$$

4.2 Results and discussion

The system of non-linear ordinary differential equations (4.7) and (4.8) together with the boundary condition (4.9) have been solved numerically by employing implicit finite difference method together with Keller-box elimination technique. Numerical computation are carried out for Prandtl number Pr = 0.01, 0.10, 0.50, 0.72, 1.00 and for a wide range of the values of the viscous dissipation parameter N = 0.10, 0.30, 0.60, 0.90, the magnetic parameter or Hartmann Number M =0.10, 0.30, 0.50, 0.70, 0.90, the Joule heating parameter Jul = 0.20, 0.40, 0.70, 0.90 and also pressure work parameter is Ge = 0.20, 0.40, 0.60, 0.80. With the above-mentioned flow parameters the results are displayed in figures 4.2 to figures 4.11 for predicting velocity profiles, temperature profiles, skin friction and surface temperature coefficient

Figure 4.2(a) and figure 4.2(b) display results for the velocity and temperature profiles, based on equations (4.17)-(4.18) with boundary conditions (4.19), for different small values of viscous dissipation parameter N (=0.90, 0.60, 0.30, 0.10) plotted against η at Pr = 0.72, M = 0.80, Jul = 0.40 and Ge = 0.70. From figure 4.2(a), it is seen that an increase in the viscous dissipation parameter N is associated with a considerable increase in velocity profiles but near the surface of the plate, the velocity increases and become maximum and then decreases and finally approaches to zero asymptotically. The maximum values of the velocity are 0 3735, 0.3671, 0.3609 and 0.3568 for N = 0.90, 0.60, 0.30, 0 10 respectively which occur at η = 1.3693 for all maximum values. Here we see that the velocity increases by 4.68% as N increases from 0.10 to 0.90. A similar situation is also observed from figure 4.2(b) in the case of temperature field. Here it is seen that the local maximum values of the temperature profiles are 0.9630,

0.9416, 0.9216, 0.9031 for N = 0.90, 0.60, 0.30, 0.10 respectively and each of which occurs at the surface. Thus the temperature profiles increase by 6.63% as N increases from 0.10 to 0.90.

Figure 4.3(a) and figure 4.3(b) represent respectively the velocity and the temperature profiles for different values of the pressure work parameter Ge for particular values of Pr, Jul, N and M. From figure 4.3(a). it is observed that an increase in pressure work parameter Ge, is associated with a considerable increase in velocity profiles but near the surface of the plate the velocity increases and become maximum and then decreases and finally approaches to zero asymptotically. The maximum values of the velocity are 0.4416, 0.4261, 0.4110, 0.3963 for Ge = 0.80, 0.60, 0.40, 0.20 respectively and each of which occurs at η = 1.3693. Here we see that the velocity increases by 11.43% as Ge increases from 0.20 to 0.80. However figure 4.3(b) shows the distribution of the temperature profiles against η for some values of the pressure work parameter Ge (=0.80, 0.60, 0.40, 0.20). Clearly it is seen that the temperature distribution increases owing to increasing values of the pressure work parameter Ge and the maximum is at the adjacent to the plate wall. The local maximum values of the temperature profiles are 0.9630, 0.9416, 0.9216, 0.9031 for (Ge =0.80, 0.60, 0.40, 0.20) respectively and each of which attains at the surface. Thus the temperature profiles increase by 6.63% as Ge increases from 0.20 to 0.80.

Figure 4.4(a) and figure 4.4(b) display results for the velocity and temperature profiles, for different small values of magnetic parameter or Hartmann Number M = 0.10, 0.30, 0.50, 0.70, 0.90 plotted against η at Pr = 0.72, N = 0.40, Jul = 0.50 and Ge = 0.60. It is seen from figure 4.4(a) that the velocity profile is influenced considerably and decreases when the value of magnetic parameter M increases. But near the surface of the plate velocity increases significantly and then decreases slowly and finally approaches to zero. The maximum values of the velocity are 0.3522, 0.3830, 0.4186, 0.4596 and 0.5068 for M = 0.90, 0.70, 0.50, 0.30, 0.10 respectively which occur at η = 1.3025 for the first maximum value and η = 1.3693 for other maximum values. Here we see that the velocity decreases by 30.51% as M increases from 0.10 to 0.90. Also it has been observed that the temperature field increases for increasing values of magnetic parameter or Hartmann Number M in figure 4.4(b). Here it is seen that the local maximum values of the temperature profiles are 0.9409, 0.9316, 0.9268, 0.9217 and 0.9146 for M = 0.10, 0.30, 0.50, 0.70, 0.90 respectively and each of which occurs at the

surface. Thus the temperature profiles increase by 2.88% as M increases from 0 10 to 0.90.

Figure 4 5(a) and figure 4.5(b) deal with the effect of the Joule heating parameter Jul (=0.20, 0.40, 0.70, 0.90) for different values of the controlling parameters $Pr = 0.72$, $M = 0.40$, $N = 0.50$ and $Ge = 0.70$ on the velocity profile $f'(x, \eta)$ and the temperature profile $h(x, \eta)$. From figure 4.5(a), it is revealed that the velocity profile $f'(x, \eta)$ increases slightly with the increase of the Joule heating parameter Jul which indicates that Joule heating parameter accelerates the fluid motion Small increment is shown from figure 4.5(b) on the temperature profile $h(x, \eta)$ for increasing values of Jul.

Figure 4.6 (a) depicts the velocity profiles for different values of the Prandtl number Pr (= 0.01, 0.10, 0.50, 0.72, 1.00) with the others controlling parameters $M = 0.50$, $N = 0.30$, $Jul = 0.40$ and $Ge = 0.60$. Corresponding distribution of the temperature profile $h(x, \eta)$ in the fluids is shown in figure 4.6(b) From figure 4.6(a), it can be seen that if the Prandtl number increases the velocity of the fluid decreases. On the other hand, from figure 4.6(b) it is observed that the temperature profiles decrease within the boundary layer due to increase of the Prandtl number Pr.

Numerical values of the skin friction coefficient $f''(x, 0)$ and the surface temperature $\theta(x, 0)$ are depicted graphically in figure 4.7(a) and figure 4.7(b) respectively against the axial distance x in the interval [0,16] for different values of the viscous dissipation parameter N (=0.10, 0.40, 0.60, 0.90) for the fluid having Prandtl number $Pr = 0.72$. the magnetic parameter $M = 0.80$, the Joule-heating parameter $Jul = 0.40$ and the pressure work parameter $Ge = 0.70$. It is seen from figure 4.7(a) that the skin-friction $f''(x, 0)$ increases when the viscous dissipation parameter, N increases. The same result holds from figure 4 7(b) for surface temperature distribution $\theta(x, 0)$ while N increases.

From figure 4.8(a), it can be observed that increase in the value of the pressure work parameter Ge leads to increase the value of skin friction coefficient $f''(x, 0)$ which is usually expected. Again figure 4.8(b) shows that the increase of the pressure work parameter Ge leads to increase the surface temperature $\theta(x, 0)$.

Figure 4.9(a) and figure 4.9(b) illustrate the variation of skin-friction $f''(x, 0)$ and surface temperature distribution $\theta(x, 0)$ against x for different values of magnetic parameter or Hartmann Number M (= 0.90, 0.70, 0.50, 0.30, 0.10). It is seen from figure 4.9(a) that the skin-friction $f''(x, 0)$ decreases when the magnetic parameter or Hartmann Number

M increases. It is also observed from figure 4.9(b) that the surface temperature distribution $\theta(x, 0)$ increases while M increases.

The effect of Joule heating parameter Jul (=0.90, 0.70, 0.40, 0.20) on the skin-friction coefficient $f''(x, 0)$ and the surface temperature distribution $\theta(x, 0)$ against x for $Pr = 0.72$, $M = 0.40$, $N = 0.50$ and $Ge = 0.70$ is shown in figure 4.10(a) and figure 4.10(b). It is found that the values of the skin-friction coefficient $f''(x, 0)$ and the surface temperature distribution $\theta(x, 0)$ both increase for increasing values of Joule heating parameter Jul. Here it has been observed that the values of the skin-friction coefficient $f''(x, 0)$ increases by 95.73% and the surface temperature distribution $\theta(x, 0)$ increases by 97.26% while Jul increases from 0.20 to 0.90.

In figure 4.11(a), the skin friction coefficient $f''(x, 0)$ and figure 4.11(b), the surface temperature $\theta(x, 0)$ are shown graphically for different values of the Prandtl number Pr (=0.01, 0.10, 0.50, 0.72, 1.00) when other values of the controlling parameters are $M = 0.50$, $N = 0.30$, $Jul = 0.40$ and $Ge = 0.60$.
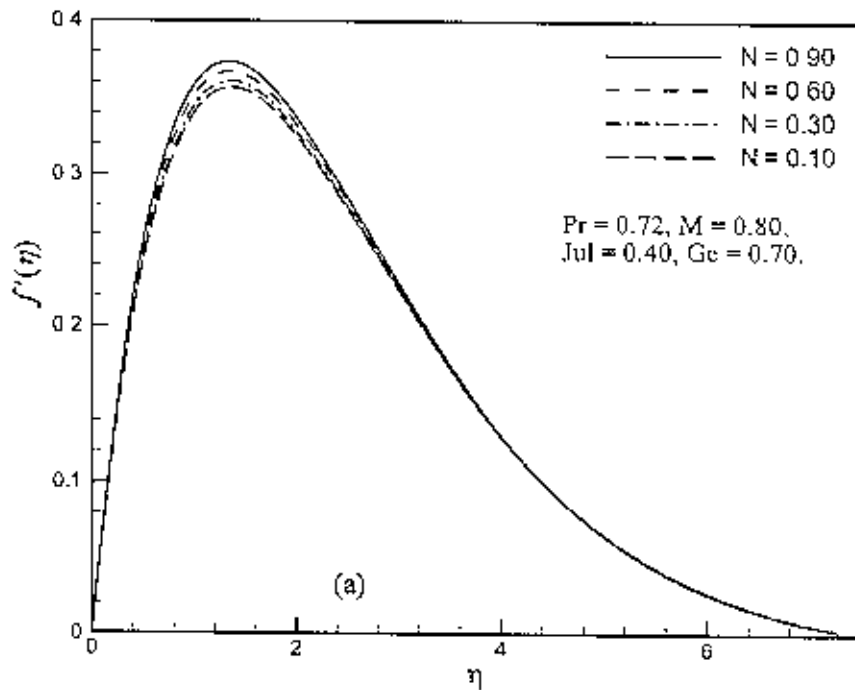
Figure 4.2(a): Variation of dimensionless velocity profiles f' (x,η) against dimensionless distance η for different values of viscous dissipation parameter N with $Pr = 0.72$, $M = 0.80$, $Ge = 0.70$ and $Jul = 0.60$.
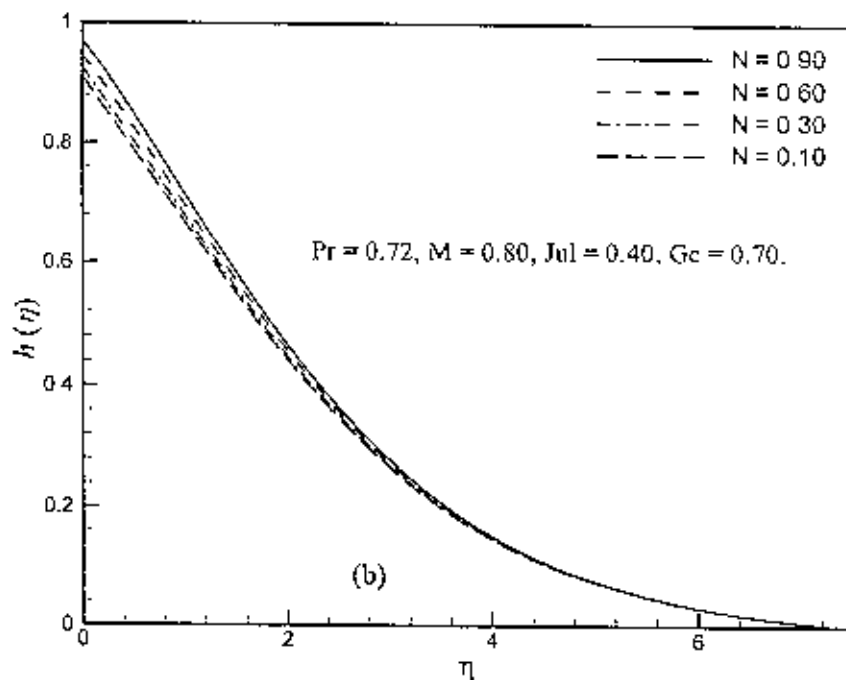
Figure 4.2(b): Variation of dimensionless temperature profiles h (x,η) against dimensionless distance η for different values of viscous dissipation parameter N with $Pr = 0.72$, $M = 0.80$, $Ge = 0.70$ and $Jul = 0.60$.
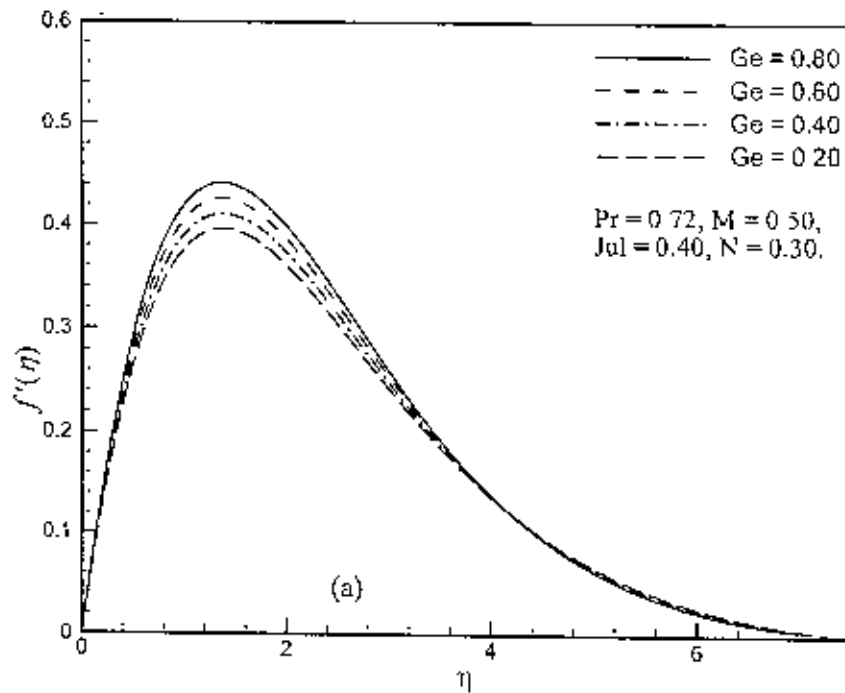
Figure 4.3(a): Variation of dimensionless velocity profiles $f'(x,\eta)$ against dimensionless distance η for different values of pressure work parameter Ge with $Pr = 0.72$, $M = 0.50$, $N = 0.30$ and $Jul = 0.40$.
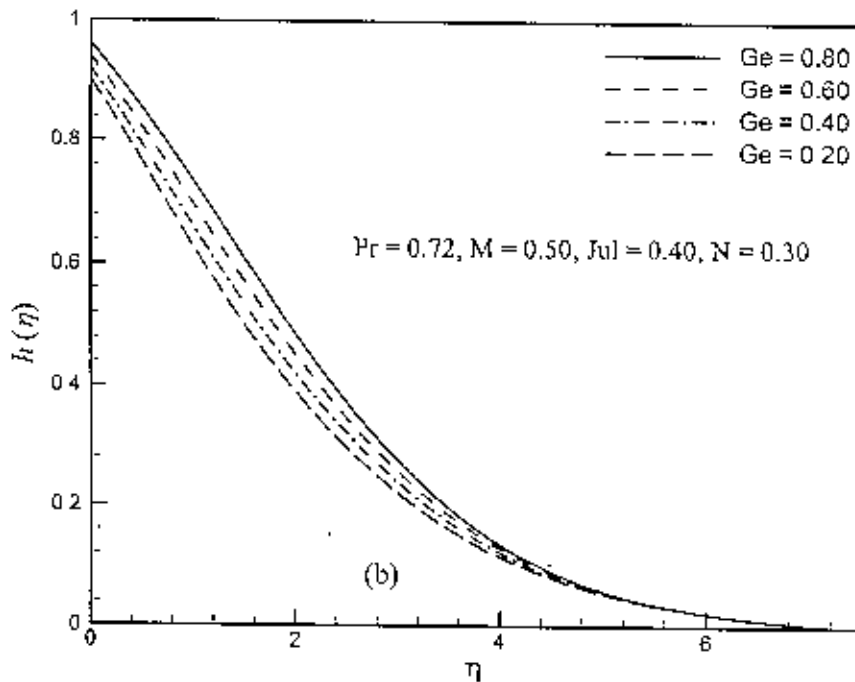
Figure 4.3(b): Variation of dimensionless temperature profiles $h(x,\eta)$ against dimensionless distance η for different values of pressure work parameter Ge with $Pr = 0.72$, $M = 0.50$, $N = 0.30$ and $Jul = 0.40$.
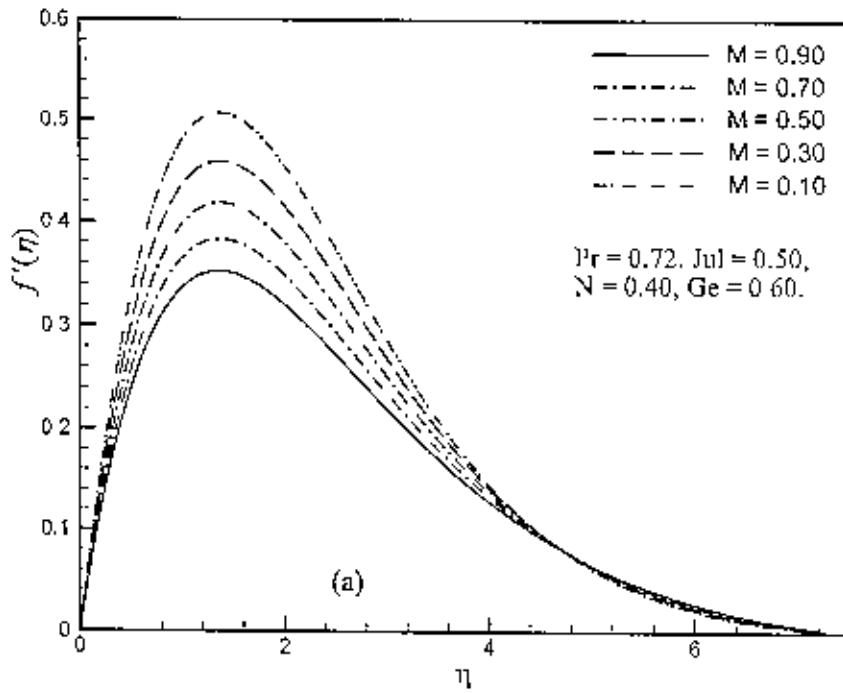
Figure 4.4(a): Variation of dimensionless velocity profiles $f'(x,\eta)$ against dimensionless distance η for different values of magnetic parameter or Hartmann Number M with $Pr = 0.72$, $Ge = 0.50$, $N = 0.60$ and $Jul = 0.50$
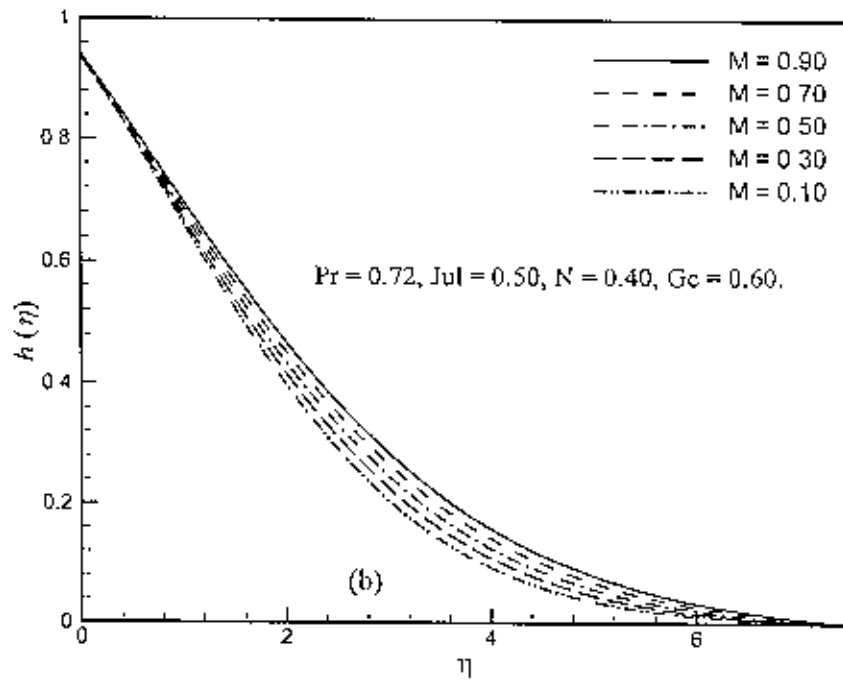
Figure 4.4(b): Variation of dimensionless temperature profiles $h(x,\eta)$ against dimensionless distance η for different values of magnetic parameter or Hartmann Number M with $Pr = 0.72$, $Ge = 0.50$, $N = 0.60$ and $Jul = 0.50$.
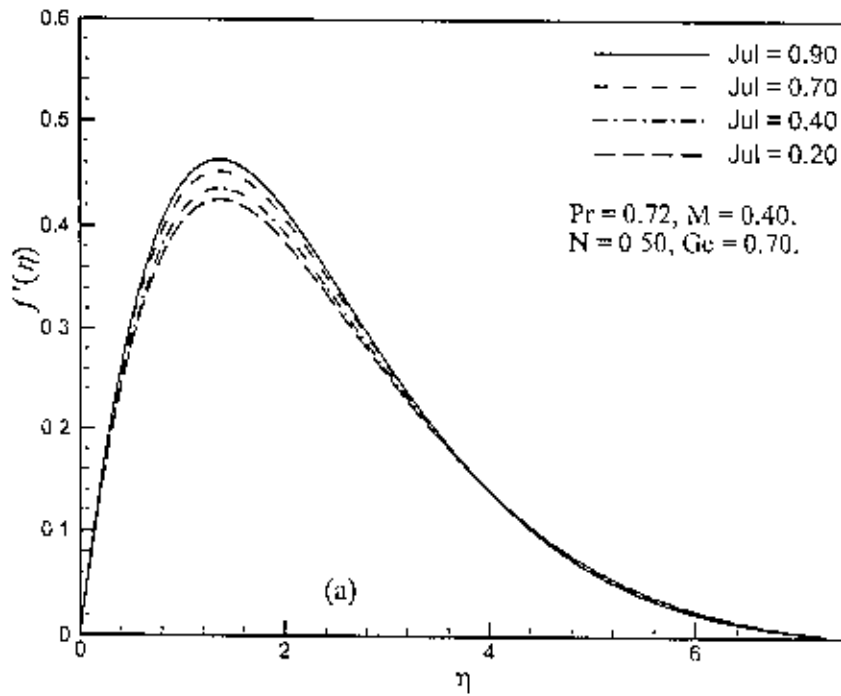
Figure 4.5(a): Variation of dimensionless velocity profiles $f'(x,\eta)$ against dimensionless distance η for different values of Joule heating parameter Jul with $Pr = 0.72$, $Gc = 0.70$, $N = 0.50$ and $M = 0.40$.
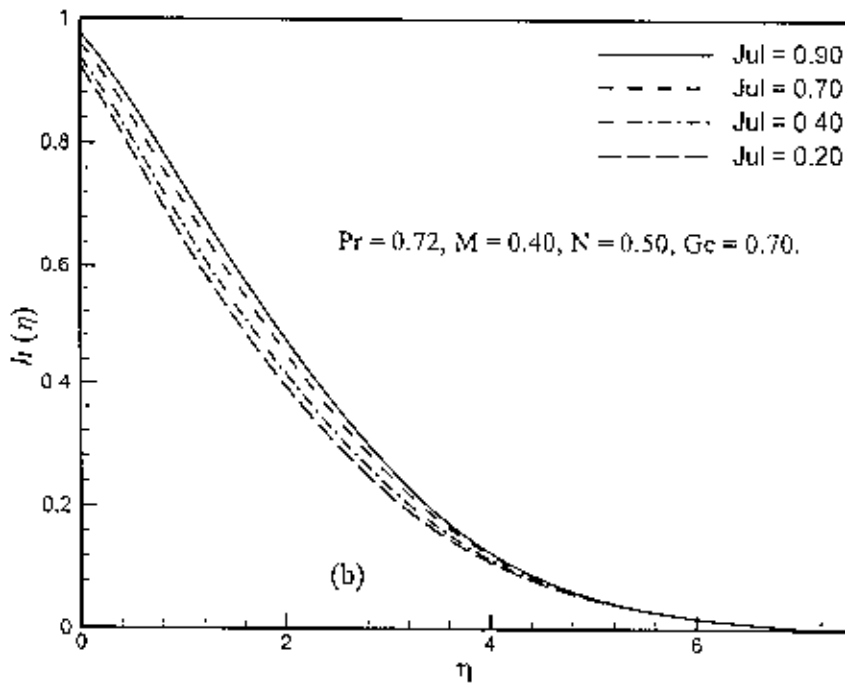
Figure 4.5(b): Variation of dimensionless temperature profiles $h(x,\eta)$ against dimensionless distance η for different values of Joule heating parameter Jul with $Pr = 0.72$, $Gc = 0.70$, $N = 0.50$ and $M = 0.40$.
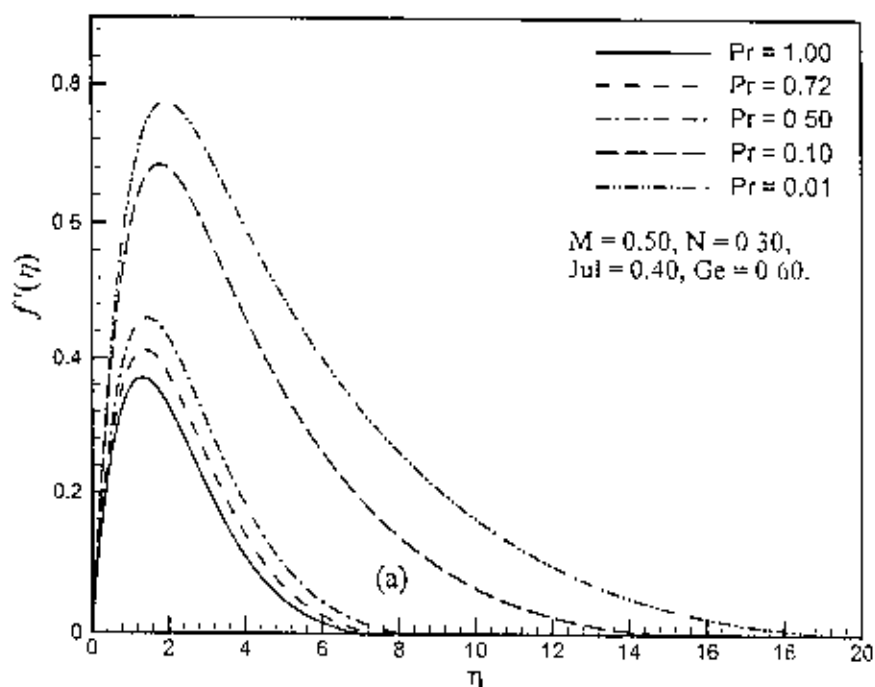
Figure 4.6(a): Variation of dimensionless velocity profiles $f'(x, \eta)$ against dimensionless distance η for different values of Prandtl number Pr with $Jul = 0.40$, $Ge = 0.60$, $N = 0.30$ and $M = 0.50$.
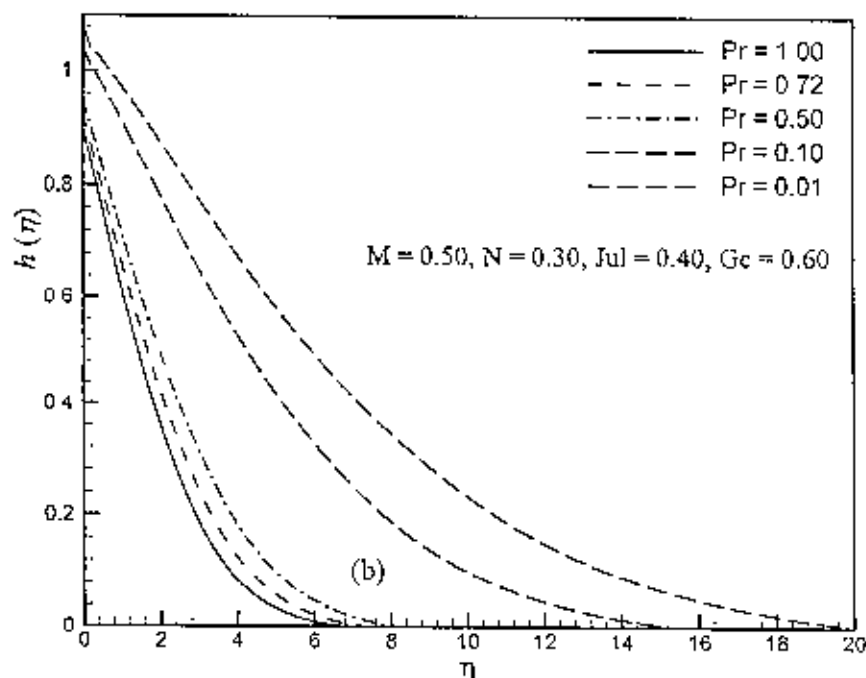
Figure 4.6(b): Variation of dimensionless temperature profiles $h(x, \eta)$ against dimensionless distance η for different values of Prandtl number Pr with $Jul = 0.40$, $Ge = 0.60$, $N = 0.30$ and $M = 0.50$
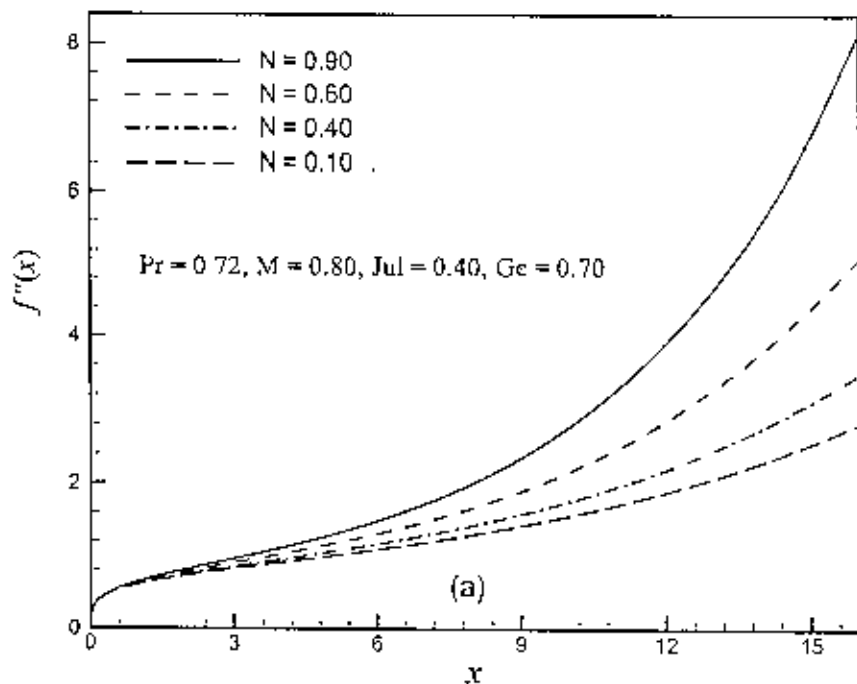
Figure 4.7(a): Variation of skin friction coefficient $f''(x, 0)$ with dimensionless distance x for different values of viscous dissipation parameter N with $Pr = 0.72$, $M = 0.80$, $Jul = 0.40$ and $Ge = 0.70$.
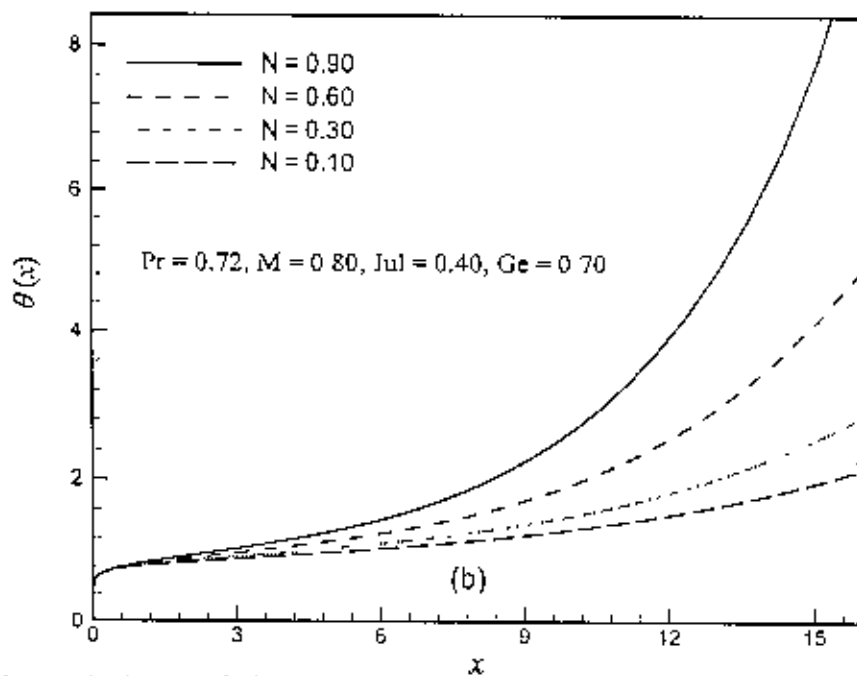
Figure 4.7(b): Variation of surface temperature $\theta(x, 0)$ with dimensionless distance x for different values of viscous dissipation parameter N with $Pr = 0.72$, $M = 0.80$, $Jul = 0.40$ and $Ge = 0.70$.
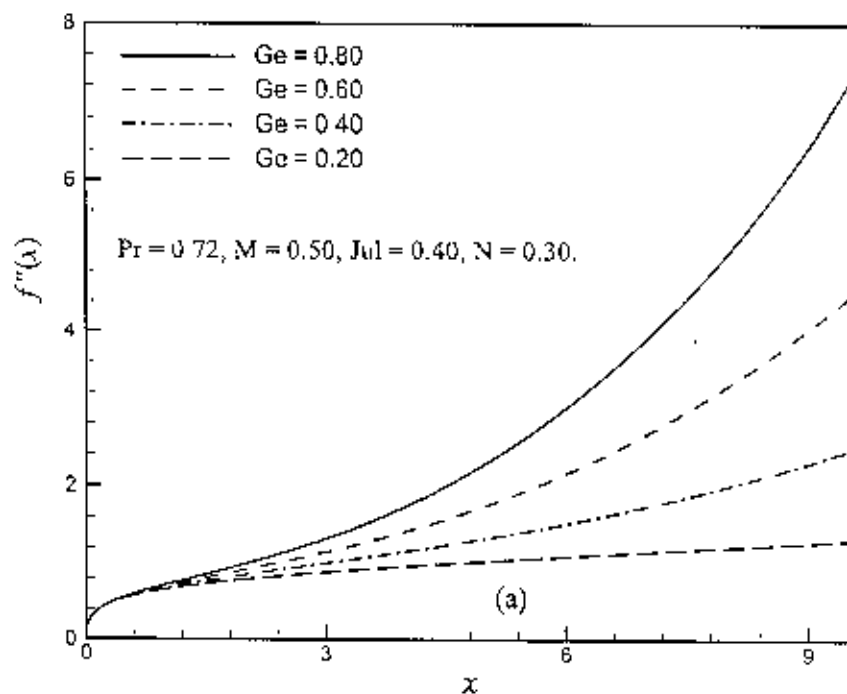
Figure 4.8(a): Variation of skin friction coefficient $f''(x, 0)$ with dimensionless distance x for different values of pressure work parameter Ge with $Pr = 0.72$, $M = 0.50$, $Jul = 0.40$ and $N = 0.30$.
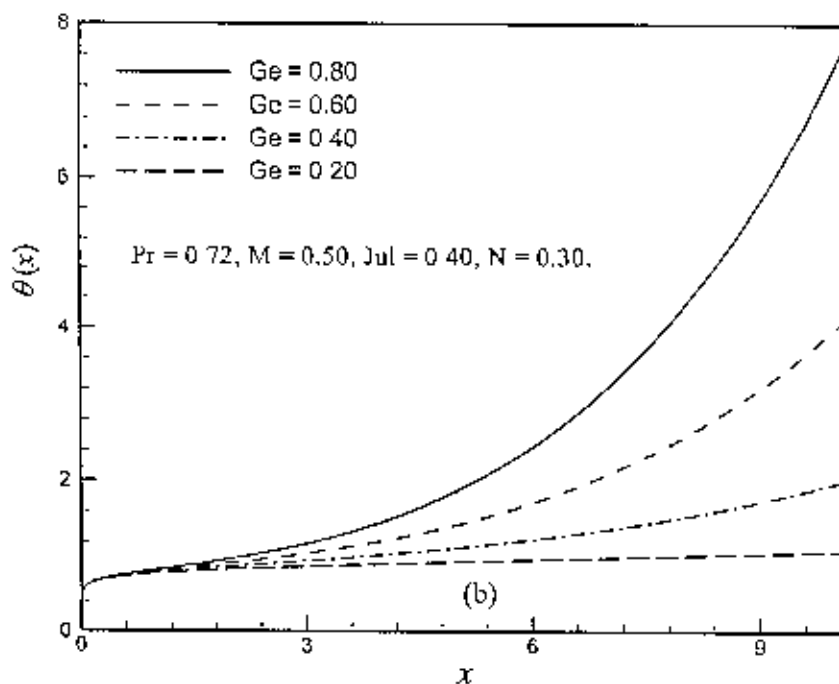
Figure 4.8(b): Variation of surface temperature $\theta(x, 0)$ with dimensionless distance x for different values of pressure work parameter Ge with $Pr = 0.72$, $M = 0.50$, $Jul = 0.40$ and $N = 0.30$.
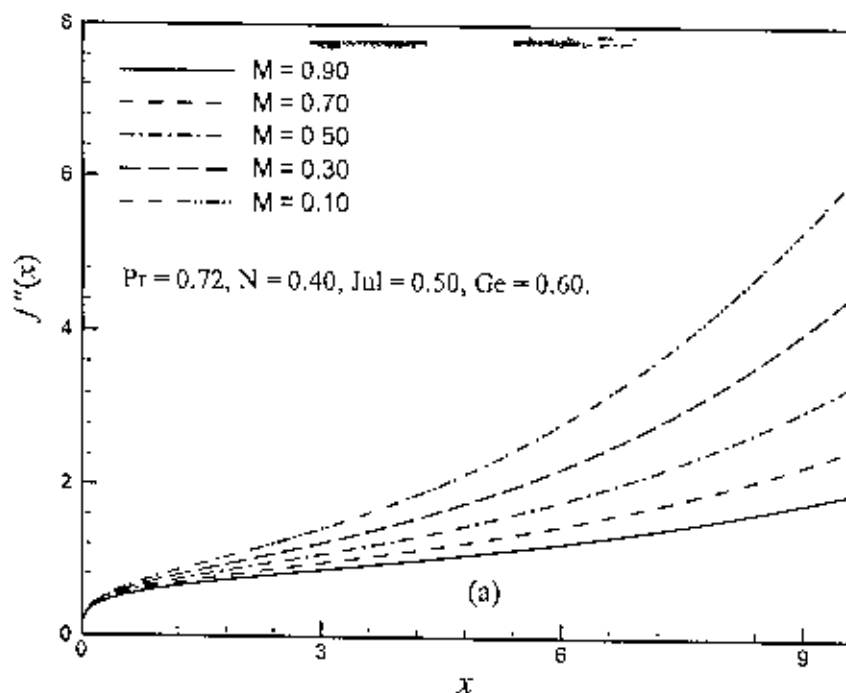
Figure 4.9(a): Variation of skin friction coefficient $f''(x, 0)$ with dimensionless distance x for different values of magnetic parameter or Hartmann Number M with $Pr = 0.72$, $Ge = 0.50$, $Jul = 0.40$ and $N = 0.30$
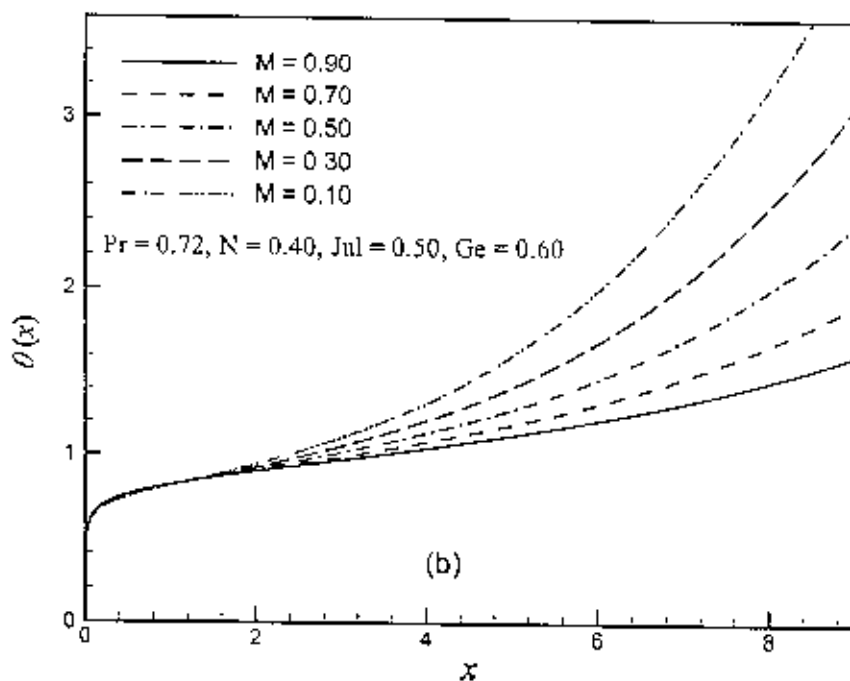
Figure 4.9(b): Variation of surface temperature $\theta(x, 0)$ with dimensionless distance x for different values of magnetic parameter or Hartmann Number M with $Pr = 0.72$, $Ge = 0.50$, $Jul = 0.40$ and $N = 0.30$.
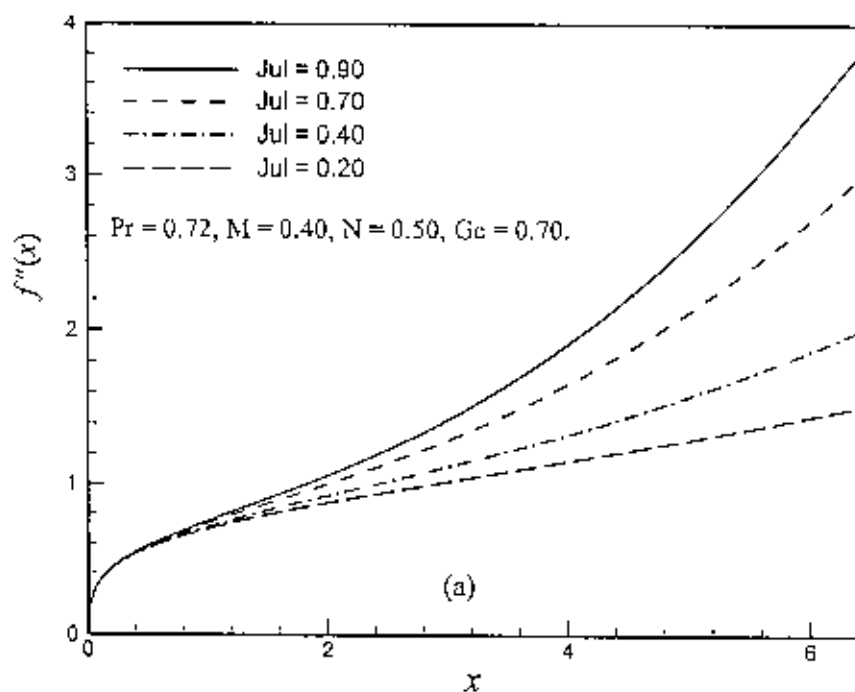
Figure 4.10(a): Variation of skin friction coefficient $f''(x, 0)$ with dimensionless distance x for different values of Joule heating parameter Jul with $Pr = 0.72$, $Ge = 0.70$, $M = 0.40$ and $N = 0.50$.
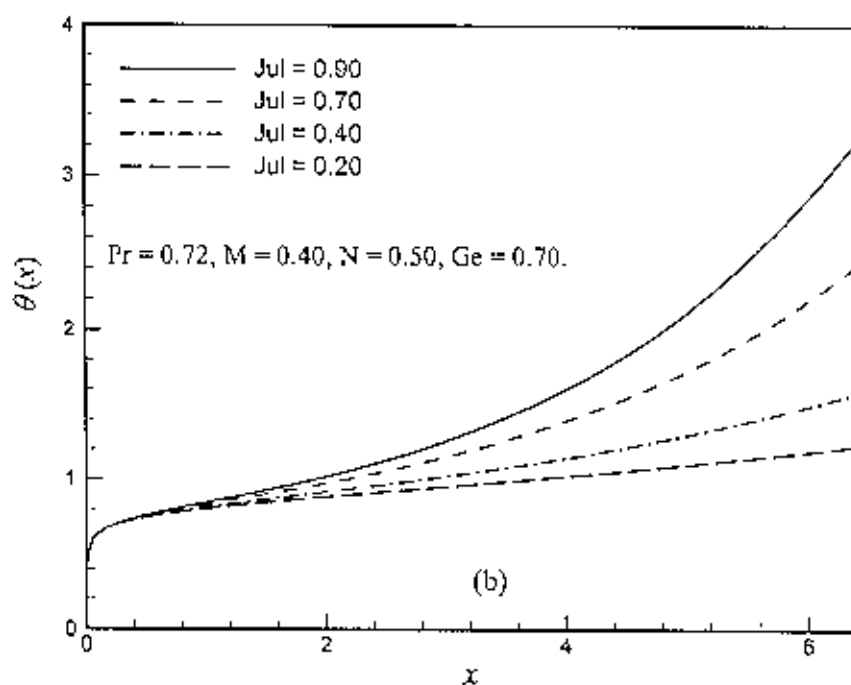
Figure 4.10(b): Variation of surface temperature $\theta(x, 0)$ with dimensionless distance x for different values of Joule heating parameter Jul with $Pr = 0.72$, $Ge = 0.70$, $M = 0.40$ and $N = 0.50$.
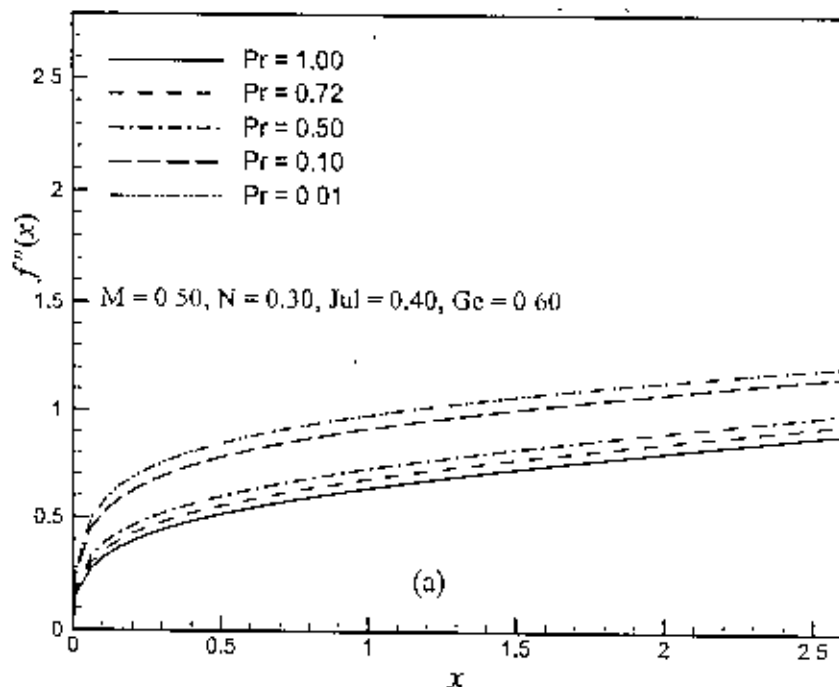
Figure 4.11(a): Variation of skin friction coefficient $f''(x, 0)$ with dimensionless distance x for different values of Prandtl number Pr with $Jul = 0.40$, $Ge = 0.60$, $M = 0.50$ and $N = 0.50$.
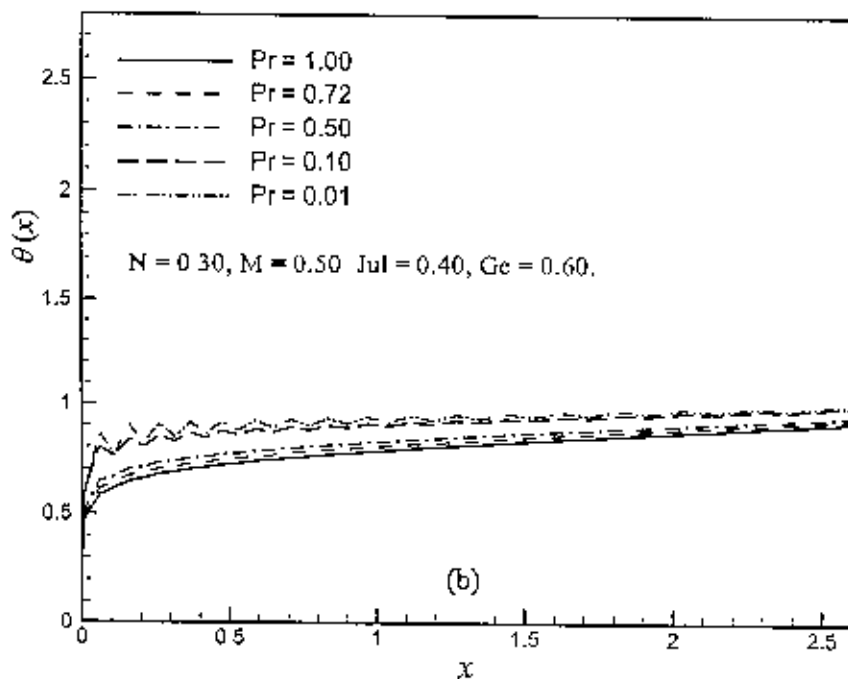
Figure 4.11(b): Variation of surface temperature $\theta(x, 0)$ with dimensionless distance x for different values of Prandtl number Pr with $Jul = 0.40$, $Ge = 0.60$, $M = 0.50$ and $N = 0.50$.

The values of the skin friction coefficient and surface temperature distribution for different values of Prandtl number Pr while $M = 0.5$, $N = 0.4$, $Jul = 0.4$ and $Ge = 0.6$ are entered in Table-C_5 which is showed in Appendix C. Here it is observed that the values of skin friction coefficient decrease at different position of x for Prandtl number Pr $=1.00$, 0.72, 0.50, 0.10. The rate of skin friction coefficient decreases by 16.436% as the Prandtl number Pr changes from 0.10 to 1.00 and $x = 4.0635$. Furthermore, it is seen that the numerical values of the surface temperature distribution decrease for increasing values of Prandtl number Pr. This suggests that the interface of the plate having thickness 'b' remains heated more in the lower Prandtl number fluid than that of the higher Prandtl number fluid and the rate of decrease of surface temperature distribution is 9.633% at position $x = 4.0635$ as the Prandtl number changes from 0.10 to 1.00.

The values of the skin friction coefficient and surface temperature for different values of pressure work parameter Ge while $M = 0.50$, $N = 0.30$, $Jul = 0.40$ and $Pr = 0.72$ are entered in Table-C_6 that is showed in Appendix C. Here it is concluded that the values of skin friction coefficient increase at different position of x for pressure work parameter $Ge =0.20$, 0.40, 0.60, 0.80. The rate of the skin friction coefficient increases by 83.0815% as the pressure work parameter Ge changes from 0.20 to 0.80 and $x = 4.0635$. Furthermore, it is seen that the numerical values of the surface temperature distribution increase for increasing values of pressure work parameter Ge. The rate of increase of surface temperature distribution is 62.2983% at position $x = 4.0635$ as the pressure work parameter Ge changes from 0.20 to 0.80.

The values of the skin friction coefficient and surface temperature for different values of viscous dissipation parameter N while $M = 0.80$, $Ge = 0.70$, $Jul = 0.40$ and $Pr = 0.72$ are depicted in Table-C_7 which is showed in Appendix C. Here we find that the values of skin friction coefficient increase at different position of x for viscous dissipation parameter $N =0.10$, 0.30, 0.60, 0.90. The rate of the skin friction coefficient increases by 22.3172% as the viscous dissipation parameter N changes from 0.10 to 0.90 and $x = 4.0635$. Furthermore, it is seen that the numerical values of the surface temperature distribution increase for increasing values of viscous dissipation parameter N. The rate of increase of surface temperature distribution is 22.5327% at position $x = 4.0635$ as the pressure work parameter changes from 0.10 to 0.90.

The values of the skin friction coefficient and surface temperature for different values of Joule heating parameter Jul while $N = 0.50$, $Ge = 0.70$, $M = 0.40$ and $Pr = 0.72$ illustrate

that the values of skin friction coefficient increase at different position of x for Joule heating parameter Jul =0.20, 0.40, 0.70, 0.90 as seen from Table-C_8 which is shown Appendix in C. The rate of the skin friction coefficient increases by 43.1684% as the Joule heating parameter Jul changes from 0.10 to 0.90 and $x = 3.1340$. Furthermore, it is observed that the numerical values of the surface temperature distribution increase for increasing values of Joule heating parameter Jul. The rate of increase of surface temperature distribution is 34.4605% at position $x = 3.1340$ as the Joule heating parameter changes from 0 10 to 0.90.

4.3 Conclusions

From the present investigation, the following conclusions may be drawn:

- Both the skin friction coefficient and the velocity profile increase for increasing values of the viscous dissipation parameter N, the pressure works parameter Ge and the Joule heating parameter Jul.

- Increased values of the viscous dissipation parameter N leads to increase the surface temperature distribution as well as the temperature distribution.

- Increased values of the pressure work parameter Ge leads to increase the surface temperature distribution as well as the temperature distribution.

- Increased values the Joule heating parameter Jul leads to increase the surface temperature distribution as well as the temperature distribution.

- It has been observed that the skin friction coefficient, the surface temperature distribution, the temperature profile and the velocity profile decrease over the whole boundary layer with the increase of the Prandtl number Pr.

- The effect of magnetic parameter or Hartmann Number M is to decrease the skin friction coefficient, the surface temperature distribution and the velocity distribution over the whole boundary layer decrease, but reverse case happens for temperature distributions.

CONJUGATE EFFECTS OF STRESS WORK AND HEAT GENERATION ON MAGNETOHYDRODYNAMIC FREE CONVECTION FLOW ALONG A VERTICAL FLAT PLATE WITH JOULE HEATING AND HEAT CONDUCTION

The most important application of MHD is in the generation of electrical power with the flow of an electrically conducting fluid through a transverse magnetic field. In case of natural convection flows, now a day, MHD analysis is playing a vital role. It is also useful in geophysics and astronomy. Geophysicists encounter MHD phenomena in the interactions of conducting fluids and magnetic fields that are present in and around heavenly bodies. Engineers employ MHD principles in the design of heat exchangers, pumps and flowerets, in space vehicle propulsion, control and re-entry and in controlled fusion. Heat is generated internally due to Joule heating of electrical conductor or internal heating of solid-state electronic device.

The present investigation is concerned with the effects of heat generation on the skin friction and the surface temperature distribution in the entire region from up stream to down stream of a viscous incompressible and electrically conducting fluid from a vertical flat plate in presence of magnetic field. The transformed non-similar boundary layer equations governing the flow together with the boundary conditions based on conduction and convection were solved numerically using the Keller box (implicit finite difference) method along with Newton's linearization approximation method, which was described by Cebeci and Bradshow (1984). The effect of the magnetic parameter M, the Joule heating parameter Jul, the Prandtl number Pr, the viscous dissipation parameter N, the pressure work parameter Ge and the heat generation parameter Q on the velocity and temperature fields as well as on the skin friction and surface temperature have been studied. In the following sections detailed derivations of the governing equations for the flow are discussed.

5.1 Governing equations of the flow

The steady two dimensional laminar free convection boundary layer flow of a viscous incompressible and electrically conducting fluid along a side of a vertical flat plate of thickness 'b' insulated on the edges with temperature T_b maintained on the other side in

the presence of a uniformly distributed transverse magnetic field has been considered. The configuration of the problem are given below:
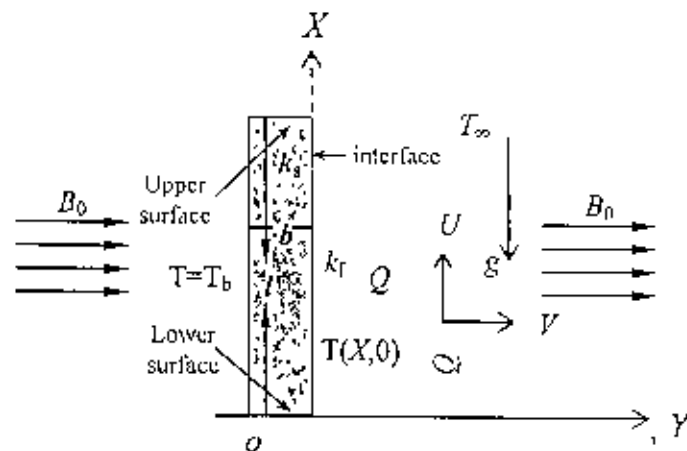
Figure 5.1: Physical configuration and coordinate system

The mathematical statement of the basic conservation laws of mass (2.26), momentum equation (2.27) and energy equation (2.28) with Joule heating and heat generation terms for the steady viscous incompressible and electrically conducting flow after simplifying are given by

$$\frac{\partial U}{\partial X}+\frac{\partial V}{\partial Y}=0 \tag{5.1}$$

$$U\frac{\partial U}{\partial X}+V\frac{\partial U}{\partial Y}=\nu\frac{\partial^2 U}{\partial Y^2}+g\,\beta\left(T-T_\infty\right)-\frac{\sigma\,B_0^2\,U}{\rho} \tag{5.2}$$

$$U\frac{\partial T}{\partial X}+V\frac{\partial T}{\partial Y}=\frac{\kappa}{\rho c_p}\frac{\partial^2 T}{\partial Y^2}+\frac{\nu}{c_p}(\frac{\partial U}{\partial Y})^2+\frac{T\,\beta U}{\rho C_p}\rho g+\frac{\sigma B_0^2}{\rho C_p}U^2+\frac{Q_0}{\rho C_p}\left(T-T_\infty\right) \tag{5.3}$$

Using boundary conditions (2.32)-(2.33) and the transformation equation (2.35) in equations (5.1) to (5.3), we have the following dimensionless equations

$$\frac{\partial u}{\partial x}+\frac{\partial v}{\partial y}=0 \tag{5.4}$$

$$u\frac{\partial u}{\partial x}+v\frac{\partial u}{\partial y}+Mu=\frac{\partial^2 u}{\partial y^2}+0 \tag{5.5}$$

$$u\frac{\partial \theta}{\partial x}+v\frac{\partial \theta}{\partial y}=\frac{1}{Pr}\frac{\partial^2 \theta}{\partial y^2}+N(\frac{\partial u}{\partial y})^2+Jul\left(u^2\right)+G_e\frac{\{T_\infty+(T_b-T_\infty)\theta\}}{(T_b-T_\infty)}+Q\theta \tag{5.6}$$

where M, N, Ge and Pr are defined earlier. Also their boundary conditions are same *i.e.* (2.39) Substituting (2.40) into equations (5.5) and (5.6) and after simplifying, we get the following transformed non-dimensional equations.

$$f''' + \frac{16+15x}{20(1+x)} ff'' - \frac{6+5x}{10(1+x)} f'^2 - Mx^{2/5}(1+x)^{1/10} f' + h = x\left(f' \frac{\partial f'}{\partial x} - f'' \frac{\partial f}{\partial x}\right) \quad (5.7)$$

$$\frac{1}{P_r} h'' + \frac{16+15x}{20(1+x)} fh' - \frac{1}{5(1+x)} f'h + Jul\, x^{2/5}(1+x)^{1/10} f'^2 + Q x^{2/5}(1+x)^{1/10} h(x,\eta)$$

$$+ Nx f'^2 + G_e x \left\{ \left(\frac{1+x}{x}\right)^{\frac{1}{5}} \left(\frac{T_\infty}{T_b - T_\infty}\right) \frac{\partial f}{\partial \eta} + h(x,\eta) \; \frac{\partial f}{\partial \eta} \right\} = x\left(f' \frac{\partial h}{\partial x} - h' \frac{\partial f}{\partial x}\right) \quad (5.8)$$

In the above equations the primes denote differentiation with respect to η.

The boundary conditions (2.39) then take the following form

$$f(x,0) = f'(x,0) = 0, h'(x,0) = -(1+x)^{1/4} + x^{1/5}(1+x)^{1/20} h(x,0)$$
$$f'(x,\infty) = 0, h'(x,\infty) = 0 \quad (5.9)$$

5.2 Results and discussion

Here we have investigated the problem of the steady two dimensional laminar free convection boundary layer flow of a viscous incompressible and electrically conducting fluid with stress work along a side of a vertical flat plate of thickness 'b' insulated on the edges with temperature T_b maintained on the other side in the presence of a uniformly distributed transverse magnetic field and heat generation. Solutions are obtained for the fluid having Prandtl number Pr = 0.10, 0 50, 0.72. 1.00, 1.74 and for a wide range of the values of the viscous dissipation parameter N = 0.20, 0.40, 0.60. 0.80, the pressure work parameter is Ge = 0.10, 0.30, 0.60, 0.90, the Joule heating parameter Jul = 0.30, 0.50, 0.70, 0.90, the magnetic parameter M = 0.10, 0.30, 0.50, 0.70, 1.00 and the heat generation parameter Q = 0.70, 0.50, 0.30, 0.10. We again used another Joule-heating parameter Jul. If we know the values of the functions $f(x, \eta)$, $h(x, \eta)$ and their derivatives for different values of the Prandtl number Pr and the magnetic parameter or Hartmann Number M, we may calculate the numerical values of the surface temperature $\theta(x, 0)$ and the skin friction coefficient $f''(x, 0)$ at the surface that are important from the physical point of view.

Figure 5.2(a) and figure 5.2(b) display results for the velocity and temperature profiles, based on equations (5.16)-(5.17) with boundary conditions (5.18), for different small values of viscous dissipation parameter N (=0.80, 0.60, 0.40, 0.20) plotted against η at Pr = 1.00, M = 0.60, Jul = 0.007, Ge = 0.20 and Q = 0.50. From figure 5.2(a), it is seen that an increase in the viscous dissipation parameter N, is associated with a considerable increase in velocity profiles but near the surface of the plate the velocity increases and become maximum and then decreases and finally approaches to zero asymptotically.

The maximum values of the velocity are 0.6852, 0.6750, 0.6651 and 0.6558 for $N = 0.80$, 0.60, 0.40, 0.20 respectively which occur at $\eta = 1.31752$ for the first and 2nd maximum values and $\eta = 1.2379$ the last two maximum values. Here we see that the velocity increases by 4.48% as N increases from 0.20 to 0.80, which is very negligible From figure 5.2(b), it is also observed that a similar situation arises in the case of temperature. Here it is seen that the local maximum values of the temperature profiles are 1.6658, 1.5922, 1.5235, 1 4593 for $N = 0.80$, 0.60, 0.40, 0.20 respectively and each of which occurs at the surface. Thus the temperature profiles increase by 14.15% as N increases from 0.20 to 0.80.

Figure 5.3(a) and figure 5.3(b) represent, respectively, the velocity and the temperature profiles for different values of the pressure work parameter Ge for particular values of Pr, Jul, N, M and Q. Here it is found from figure 5.3(a), that the velocity distribution increases slightly as the pressure work parameter Ge (=0 90, 0.60, 0.30, 0.10) increases in a region $\eta \in [0, 6.5]$, but near the surface of the plate, velocity increases and become maximum and then decreases and finally approaces to zero The maximum values of the velocity are 1.0268, 0.8947, 0.7680, 0.6854 for $Ge = 0.90$, 0.60, 0 30, 0.10 respectively and each of which occurs at $\eta = 0.9981$ for first maximum value, $\eta = 1.1144$ for second maximum value and $\eta = 1.1752$ for the third and fourth maximum values. Here we found that the velocity increases by 49.81% as Ge increases from 0 10 to 0.90. However figure 5.3(b) shows the distribution of the temperature profiles against η for some values of the pressure work parameter Ge (=0.90, 0.60, 0.30, 0.10) Clearly it is seen that the temperature distribution increases owing to increasing values of the pressure work parameter Ge and maximum is at the adjacent of the plate wall The local maximum values of the temperature profiles are 2.8603, 2.2725, 1.8171, 1.5737 for Ge =0.90, 0.60, 0.30, 0.10 respectively and each of which attains at the surface. Thus the temperature profiles increase by 81.76% as Ge increases from 0.10 to 0.90.

Figure 5.4(a) and figure 5.4(b) represent, respectively, the velocity and the temperature profiles for different values of the Joule heating parameter Jul for particular values of the Prandtl number $Pr =1.00$, the magnetic parameter $M = 0.60$, the dissipation parameter $N = 0.006$, the pressure work parameter $Ge = 0.70$ and the heat generation parameter $Q = 0.20$. From figure 5.4(a), it is observed that an increase in the Joule heating parameter Jul, is associated with a considerable increase in velocity profiles but near the surface of the plate the velocity increases and become maximum and then

decreases and finally approaches to zero asymptotically. The maximum values of the velocity are 0.7909, 0.7620, 0.7337, 0.7060 for Jul = 0.90, 0.70, 0.50, 0.30 respectively and each of which occurs at η = 1.1752. Here it is seen that the velocity increases by 12.03% as Jul increases from 0.30 to 0.90. However figure 5.4(b) shows the distribution of the temperature profiles against η for some values of the Joule heating parameter Jul (=0.90, 0.70, 0.50, 0.30). Clearly it is seen that the temperature distribution increases owing to increasing values of the Joule heating parameter Jul and the maximum is at the adjacent of the plate wall. The local maximum values of the temperature profiles are 1.7662, 1.6886, 1.6164, 1.5496 for Jul = 0.90, 0.70, 0.50, 0.30 respectively and each of which attains at the surface. Thus the temperature profiles increase by 13.98% as Jul increases from 0.30 to 0.90.

Figure 5.5(a) and figure 5.5(b) display results for the velocity and temperature profiles, for different small values of magnetic parameter or Hartmann Number M (=0.10, 0.30, 0.50, 0.70, 1.00) plotted against η at Pr = 1.00, N = 0.60, Jul = 0.20, Ge = 0.30 and Q = 0.40. It is seen from figure 5.5(a) that the velocity profile is influenced considerably and decreases when the value of magnetic parameter or Hartmann Number M increases. But near the surface of the plate velocity increases significantly and then decreases slowly and finally approaches to zero. The maximum values of the velocity are 0.6235, 0.6661, 0.6986, 0.7348 and 0.7750 for M = 1.00, 0.70, 0.50, 0.30, 0.10 respectively which occur at η = 1.1752 for all maximum values. Here it is seen that the velocity decreases by 19.55% as M increases from 0.10 to 1.00. Also, it has been observed that the temperature field increases for increasing values of magnetic parameter or Hartmann Number M in figure 5.5(b). Here it is seen that the local maximum values of the temperature profiles are 1.6278, 1.6101, 1.6009, 1.5942, 1.5906 for M = 1.00, 0.70, 0.50, 0.30, 0.10 respectively and each of which occurs at the surface. Thus the temperature profiles increase by 2.34% as M increases from 0.10 to 1.00.

Figure 5.6(a) to figure 5.6(b) display results for the velocity and temperature profiles, for different small values of heat generation parameter Q (= 0.10, 0.30, 0.50, 0.70) plotted against η at Pr = 1.00, M = 0.50, N = 0.10, Jul = 0.005 and Ge = 0.01. It is seen from figure 5.6(a) that the velocity profile is influenced considerably and increases when the value of heat generation parameter Q increases. But near the surface of the plate, velocity increases significantly and then decreases slowly and finally approaches to zero. The maximum values of the velocity are 0.7343, 0.6661, 0.6193, 0.5172 and

0.4297 for Q = 0.70, 0.50, 0.30, 0.10 respectively which occur at η = 1.3025 for 1$^\eta$ maximum value and η = 1.3693 for all others maximum values. Here it is seen that the velocity increases by 70.89% as Q increases from 0.10 to 0.70. Also figure 5.6(b), it has been observed that when value of heat generation parameter Q increases, the temperature distribution also increases significantly. Here it is observed that the local maximum values of the temperature profiles are 1.4146, 1.2072, 1.0503, 0.9336 while Q = 0.70, 0.50, 0.30, 0.10 respectively and each of which occurs at the surface. Thus the temperature profiles increase by 51.52% as Q increases from 0.10 to 0.70

Numerical values of the velocity gradient $f''(x, 0)$ and the surface temperature $\theta(x, 0)$ are depicted graphically in figure 5.7(a) and figure 5.7(b) respectively against the axial distance x in the interval [0,12] for different values of the viscous dissipation parameter N (=0.20, 0.40, 0.60, 0.80) for the fluid with other controlling parameters. It is seen from figure 5.7(a) that the skin-friction coefficient $f''(x, 0)$ increases when the viscous dissipation parameter, N increases. The same result holds in figure 5.7(b) for surface temperature distribution $\theta(x, 0)$ while N increases.

From figure 5.8(a), it can be observed that increase in the value of the pressure work parameter Ge leads to increase the value of the skin friction coefficient $f''(x, 0)$ which is usually expected. Again figure 5.8(b) shows that the increase of the pressure work parameter Ge leads to increase the surface temperature $\theta(x, 0)$.

Figure 5.9(a) and figure 5.9(b) illustrate the variation of skin-friction coefficient $f''(x, 0)$ and surface temperature $\theta(x, 0)$ distribution against x for different values of Joule heating parameter Jul (= 0.90, 0.70, 0.50, 0.30). It is seen from figure 5.9(a) that the skin-friction coefficient $f''(x, 0)$ increases when the Joule heating parameter, Jul increases. It is also observed in figure 5.9(b) that the surface temperature $\theta(x, 0)$ distribution increases while Jul increases.

The effect of magnetic parameter or Hartmann Number M (=1.00, 0.70, 0.50, 0.30, 0.10) on the skin-friction coefficient $f''(x, 0)$ and the surface temperature distribution $\theta(x, 0)$ against x for Pr = 1.00, N = 0.60, Jul = 0.20, Ge = 0.30 and Q = 0.40 is shown in figures 5.10(a) - 5.10(b). It is found that the values of the skin-friction coefficient $f''(x, 0)$ and the surface temperature distribution $\theta(x, 0)$ both decrease for increasing values of magnetic parameter or Hartmann Number M. Also, it is observed that the values of the skin-friction coefficient $f''(x, 0)$ decrease by 95.73% and the surface

temperature distribution θ (x, 0) decrease by 97.26% while M increases from 0.10 to 1.00.

In figure 5.11(a), the shear stress coefficient $f''(x, 0)$ and figure 5.11(b), the surface temperature $\theta(x, 0)$ are shown graphically for different values of the Prandtl number Pr (=0.10, 0.50, 0.72, 1.00, 1.74) when other values of the controlling parameter ($M = 0.50$, $N = 0.30$, $Jul = 0.005$, $Ge = 0.20$ and $Q = 0.50$). Five values 0.10, 0.50, 0.72, 1.00, 1.74 are taken for Pr, the Prandtl number, 0.72 represents air. 1.00 corresponds to electrolyte solutions such as salt water, 0.10, 0.50 and 1.74 have been used theoretically. Here, it is found that the skin friction and the surface temperature both decrease for increasing values of Prandtls number.

Figure 5.12(a) to figure 5.12(b) illustrate the variation of skin-friction coefficient $f''(x, 0)$ and surface temperature distribution θ (0, x) against x for different values of heat generation parameter Q (=0.70, 0.50, 0.30, 0.10). It is seen from figure 5.12(a) that the skin-friction coefficient $f''(x, 0)$ increases when the heat generation parameter, Q increases. It is also observed in figure 5.12(b) that the surface temperature distribution θ (x, 0) increases while Q increases. Also, it is observed that the values of the skin-friction coefficient $f''(x, 0)$ increase by 52.86% and the surface temperature distribution $\theta(x, 0)$ increase by 45.04% while Q increases from 0.10 to 0.70.
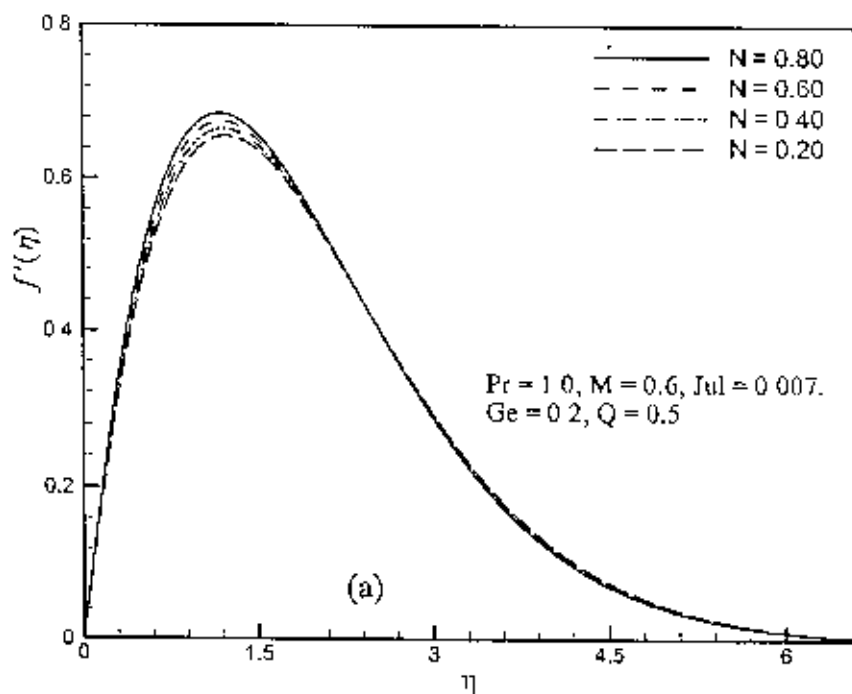
Figure 5.2(a): Variation of dimensionless velocity profiles $f'(x,\eta)$ against dimensionless distance η for different values of viscous dissipation parameter N with $Pr = 1.00$, $M = 0.60$, $Ge = 0.20$, $Jul = 0.60$ and $Q = 0.50$.
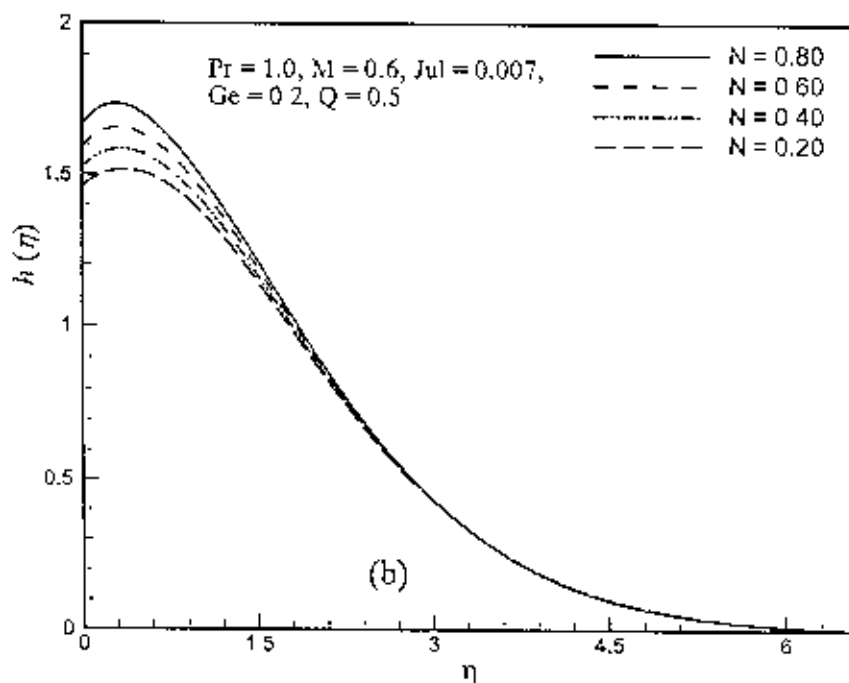
Figure 5.2(b): Variation of dimensionless temperature profiles $h(x,\eta)$ against dimensionless distance η for different values of viscous dissipation parameter N with $Pr = 1.00$, $M = 0.60$, $Ge = 0.20$, $Jul = 0.60$ and $Q = 0.50$.
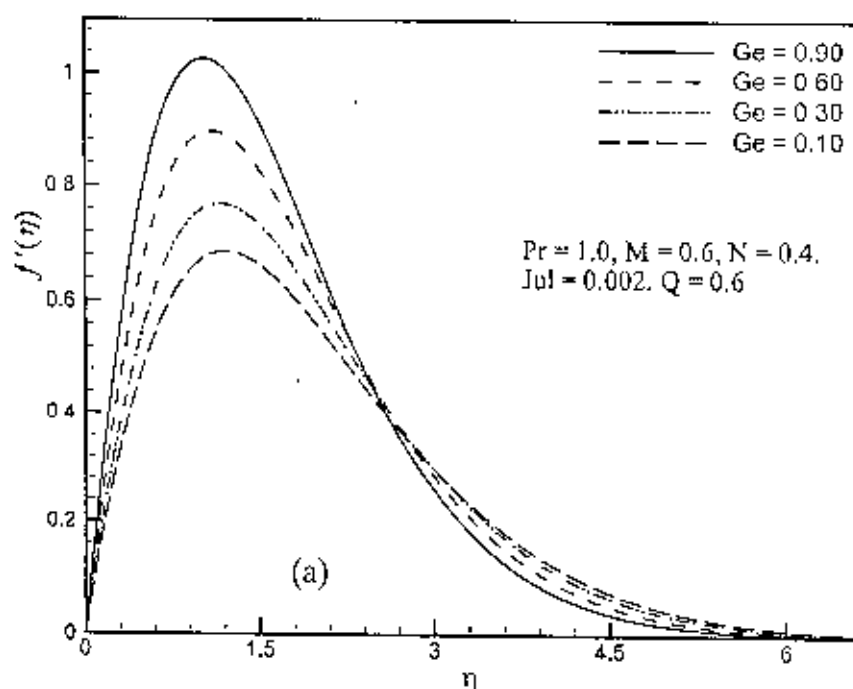
Figure 5.3(a): Variation of dimensionless velocity profiles $f'(x,\eta)$ against dimensionless distance η for different values of pressure work parameter Ge with $Pr = 1.00$, $M = 0.60$, $N = 0.40$, $Jul = 0.002$ and $Q = 0.60$.
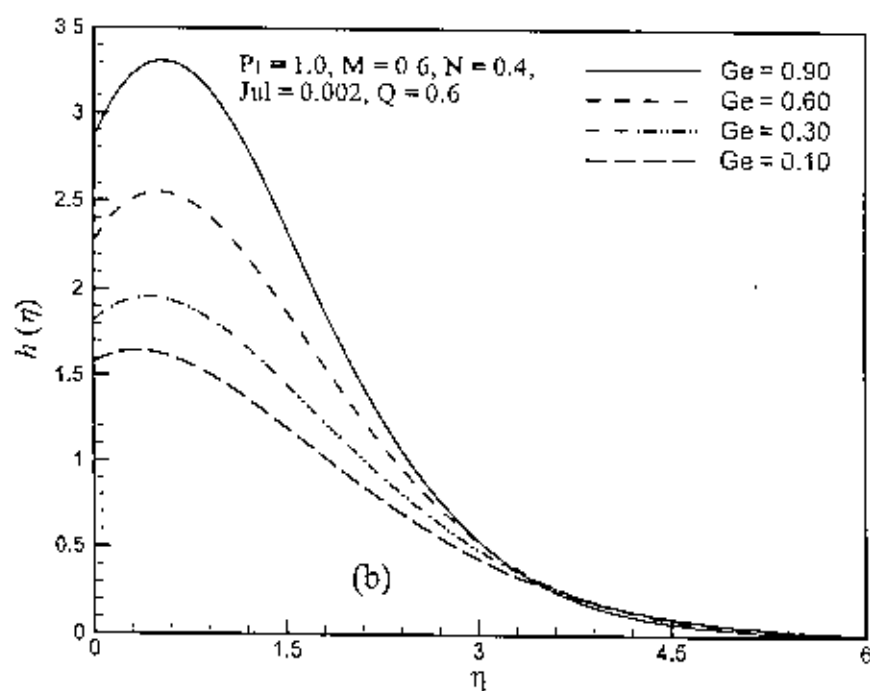
Figure 5.3(b): Variation of dimensionless temperature profiles $h(x,\eta)$ against dimensionless distance η for different values of pressure work parameter Ge with $Pr = 1.00$, $M = 0.60$, $N = 0.40$, $Jul = 0.002$ and $Q = 0.60$.
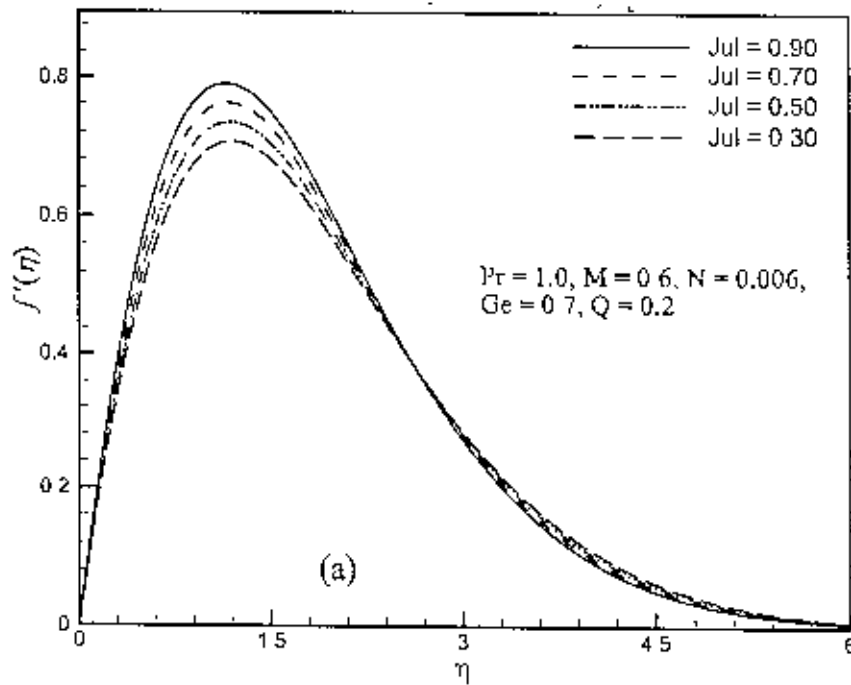
Figure 5.4(a): Variation of dimensionless velocity profiles $f'(x, \eta)$ against dimensionless distance η for different values of Joule heating parameter Jul with $Pr = 1.00$, $M = 0.60$, $N = 0.006$, $Ge = 0.70$ and $Q = 0.20$.
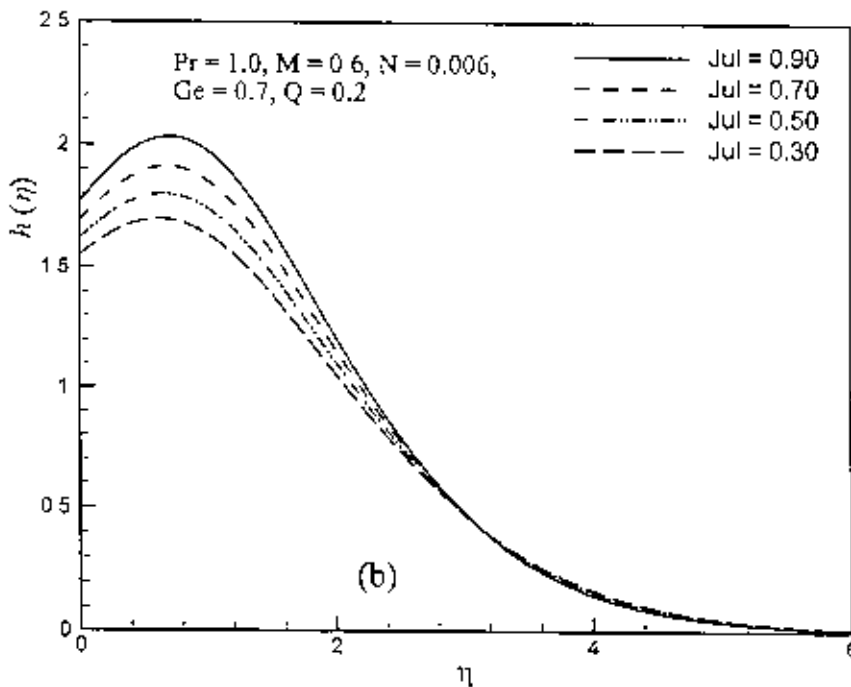
Figure 5.4(b): Variation of dimensionless temperature profiles $h(x, \eta)$ against dimensionless distance η for different values of Joule heating parameter Jul with $Pr = 1.00$, $M = 0.60$, $N = 0.006$, $Ge = 0.70$ and $Q = 0.20$.
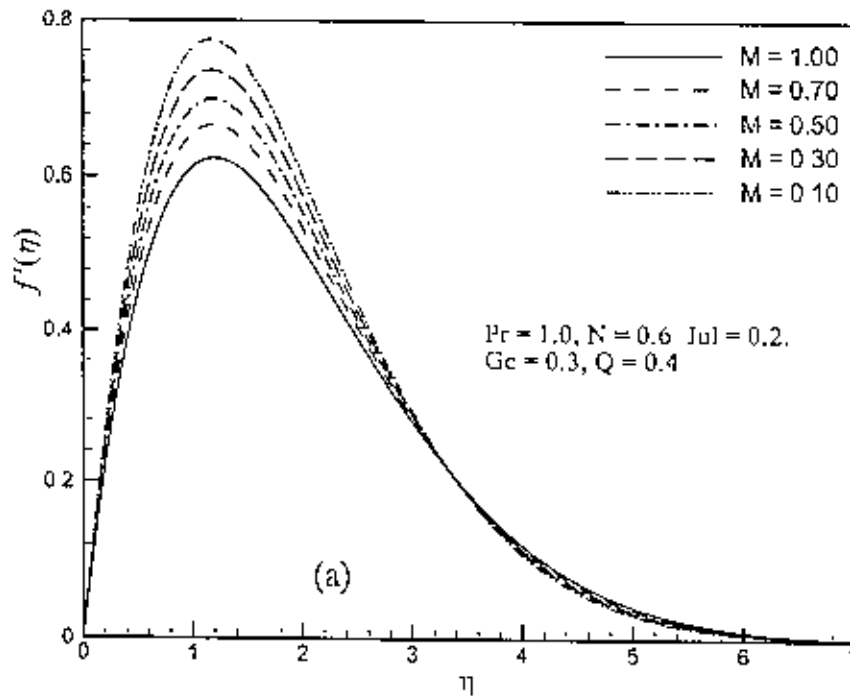
Figure 5.5(a): Variation of dimensionless velocity profiles $f'(x,\eta)$ against dimensionless distance η for different values of magnetic parameter or Hartmann Number M with $Pr = 1.00$, $Jul = 0.20$, $N = 0.60$, $Ge = 0.30$ and $Q = 0.40$.
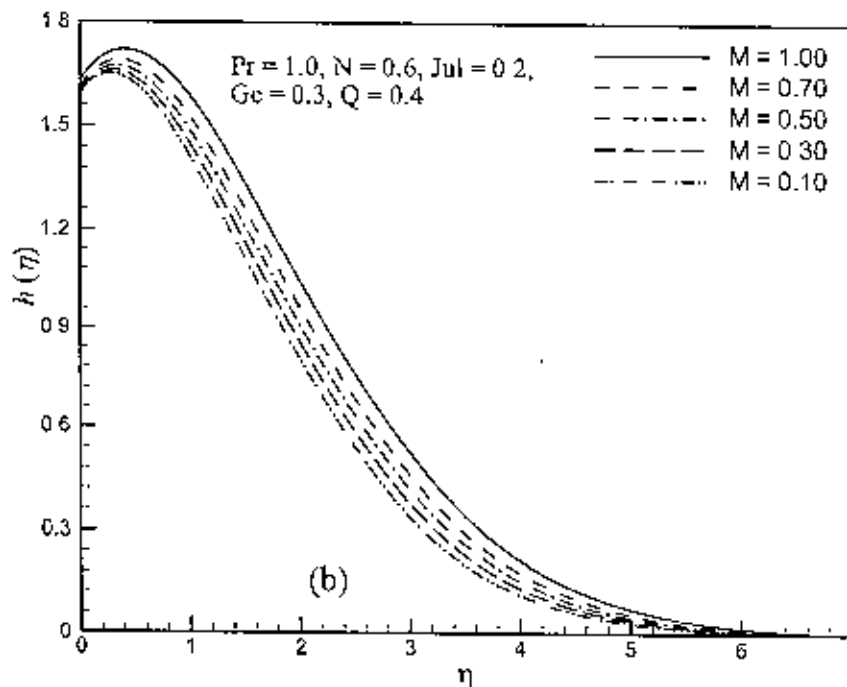
Figure 5.5(b): Variation of dimensionless temperature profiles $h(x,\eta)$ against dimensionless distance η for different values of magnetic parameter or Hartmann Number M with $Pr = 1.00$, $Jul = 0.20$, $N = 0.60$, $Ge = 0.30$ and $Q = 0.40$.
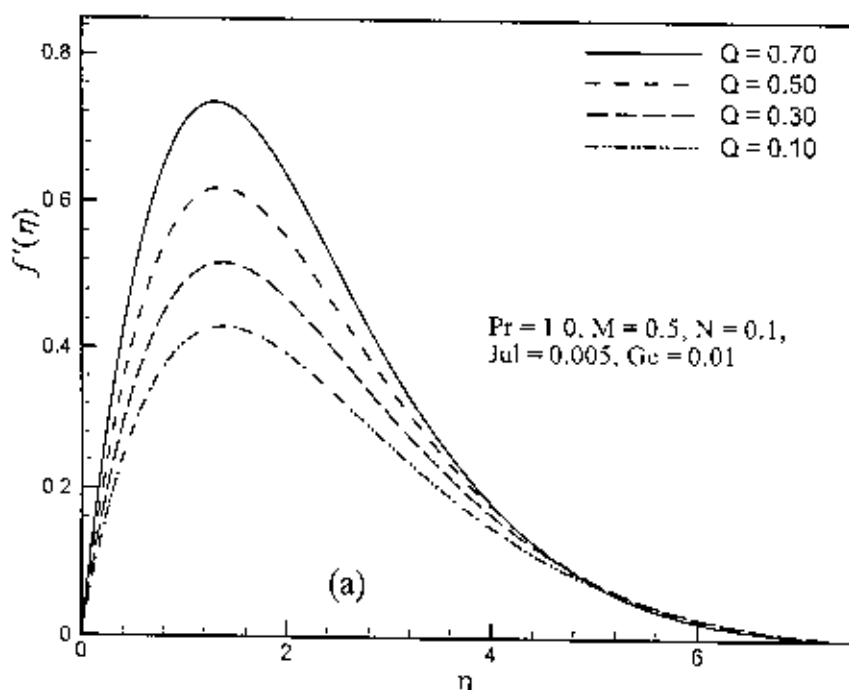
Figure 5.6(a): Variation of dimensionless temperature profiles h (x,η) against dimensionless distance η for different values of heat generation parameter Q with $Pr = 1.00$, $M = 0.50$, $N = 0.10$, $Ge = 0.01$ and $Jul = 0.005$.
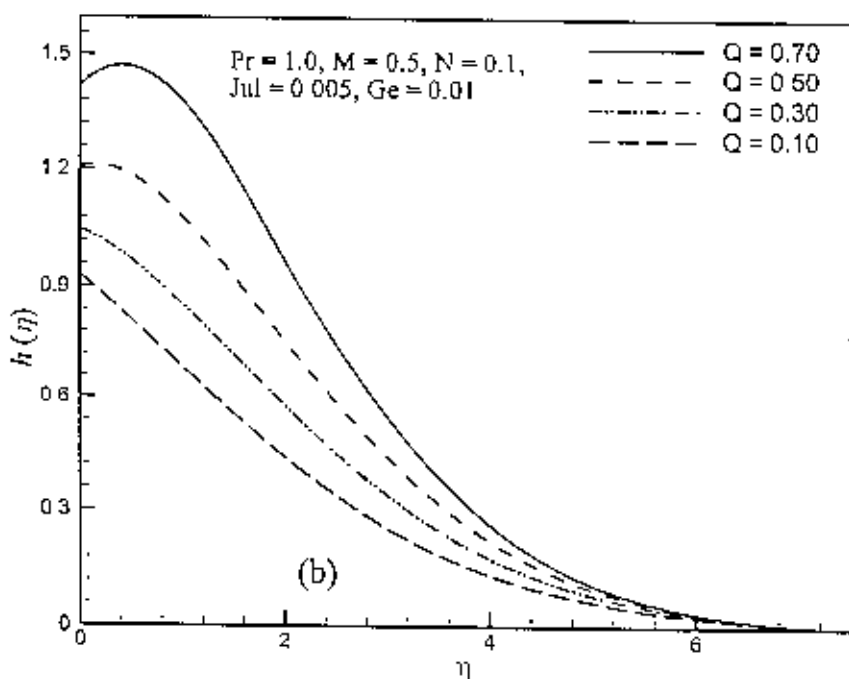
Figure 5.6(b): Variation of dimensionless temperature profiles h (x,η) against dimensionless distance η for different values of heat generation parameter Q with $Pr = 1.00$, $M = 0.50$, $N = 0.10$, $Ge = 0.01$ and $Jul = 0.005$.
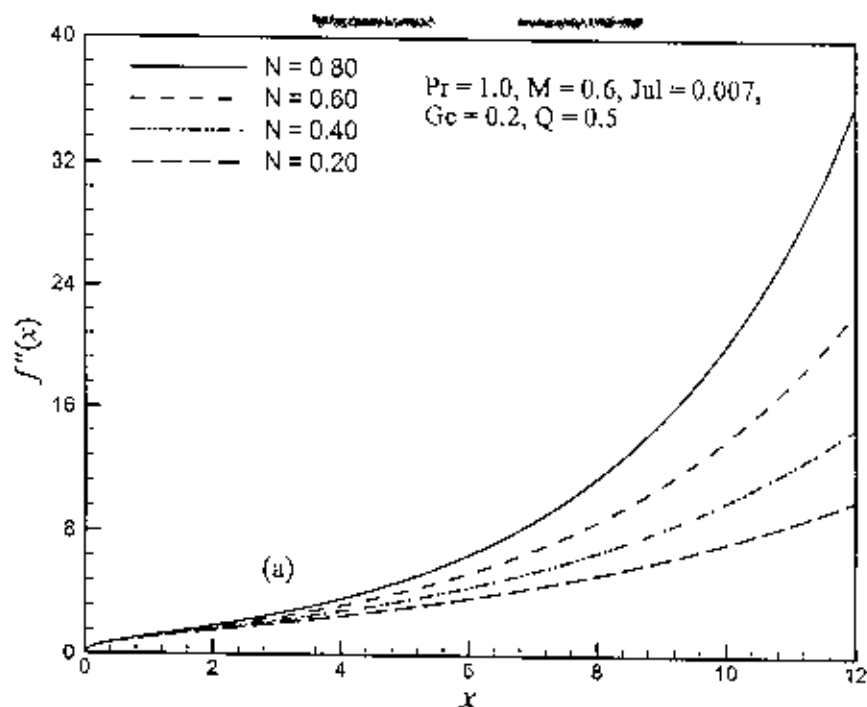
Figure 5.7(a): Variation of skin friction coefficient $f''(x, 0)$ with dimensionless distance x for different values of viscous dissipation parameter N with $Pr = 1.00$, $M = 0.60$, $Jul = 0.007$, $Ge = 0.20$ and $Q = 0.50$.
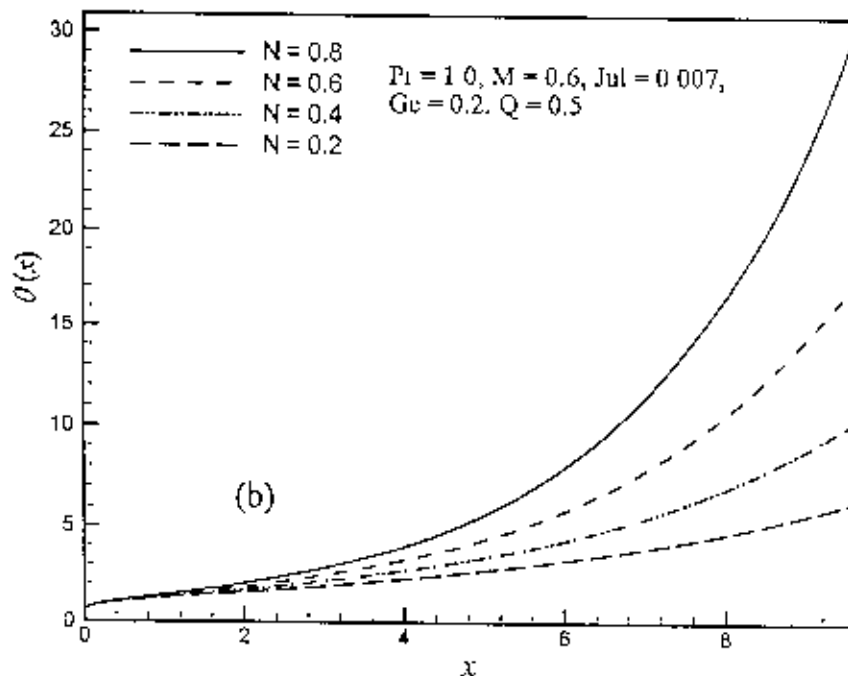
Figure 5.7(b): Variation of surface temperature $\theta(x, 0)$ with dimensionless distance x for different values of viscous dissipation parameter N with $Pr = 1.00$, $M = 0.60$, $Jul = 0.007$, $Ge = 0.20$ and $Q = 0.50$.
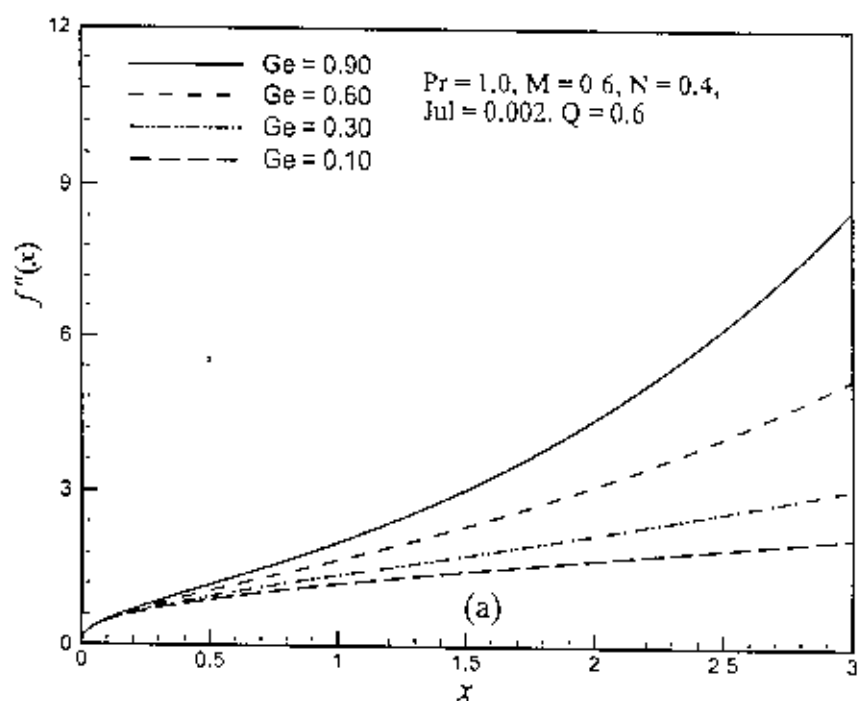
Figure 5.8(a): Variation of skin friction coefficient $f''(x, 0)$ with dimensionless distance x for different values of pressure work parameter Ge with $Pr = 1.00$, $M = 0.60$, $Jul = 0.002$, $N = 0.40$ and $Q = 0.60$.
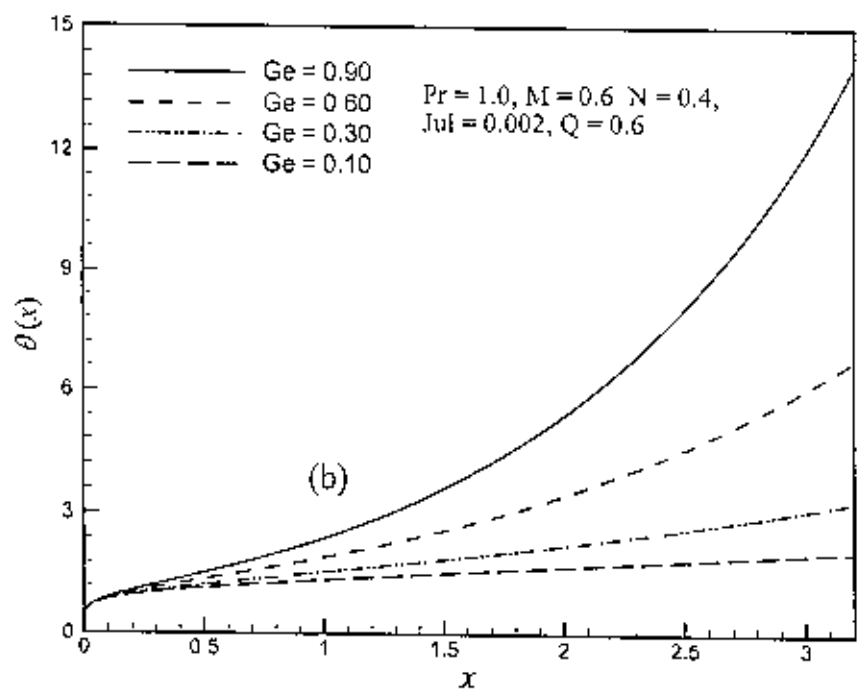
Figure 5.8(b): Variation of surface temperature $\theta(x, 0)$ with dimensionless distance x for different values of pressure work parameter Ge with $Pr = 1.00$, $M = 0.60$, $Jul = 0.002$, $N = 0.40$ and $Q = 0.60$.
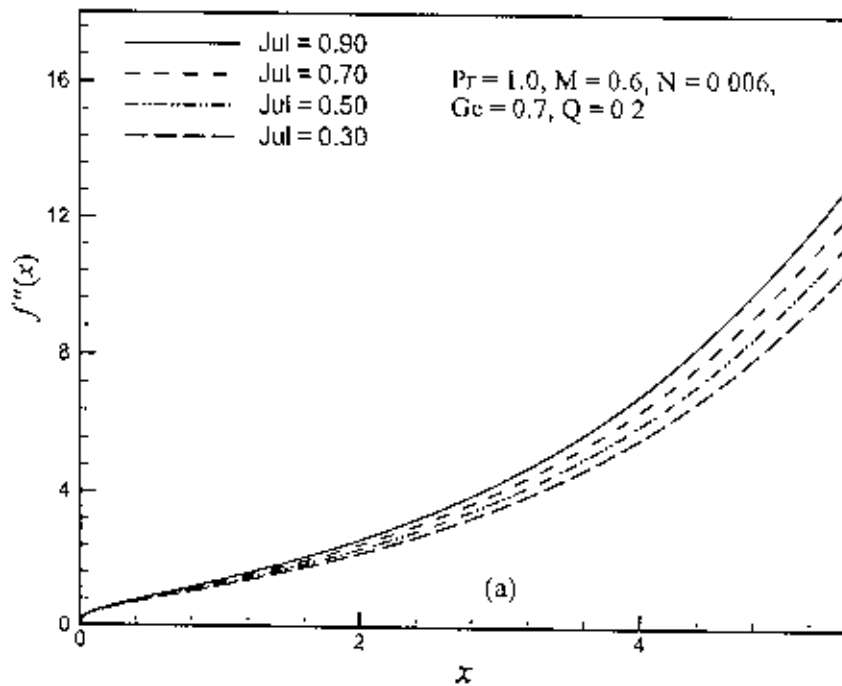
Figure 5.9(a): Variation of skin friction coefficient $f''(x, 0)$ with dimensionless distance x for different values of Joule heating parameter Jul with $Pr = 1.00$. $M = 0.60$, $Ge = 0.70$, $N = 0.006$ and $Q = 0.20$.
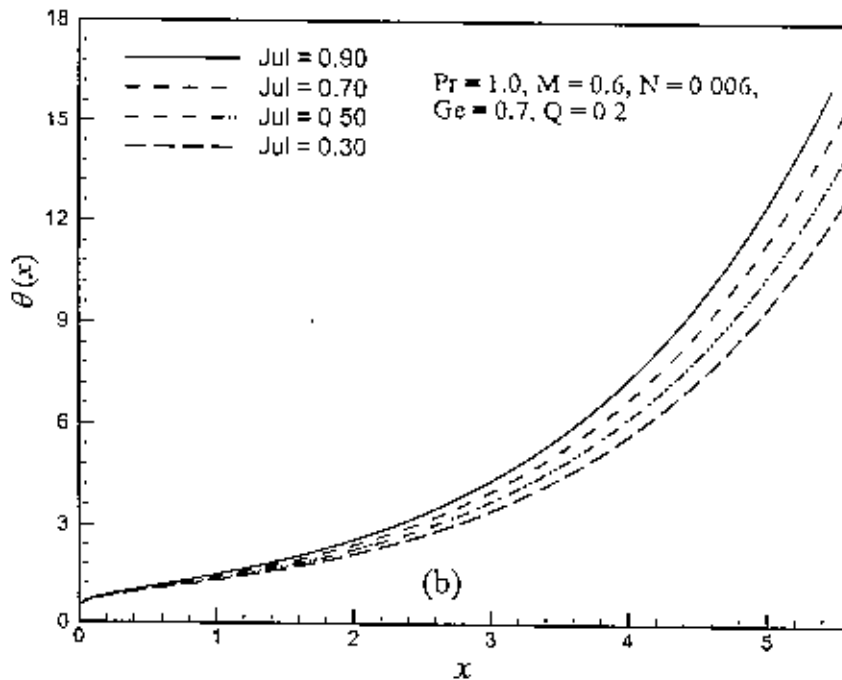
Figure 5.9(b): Variation of surface temperature $\theta(x, 0)$ with dimensionless distance x for different values of Joule heating parameter Jul with $Pr = 1.00$, $M = 0.60$, $Ge = 0.70$, $N = 0.006$ and $Q = 0.20$.
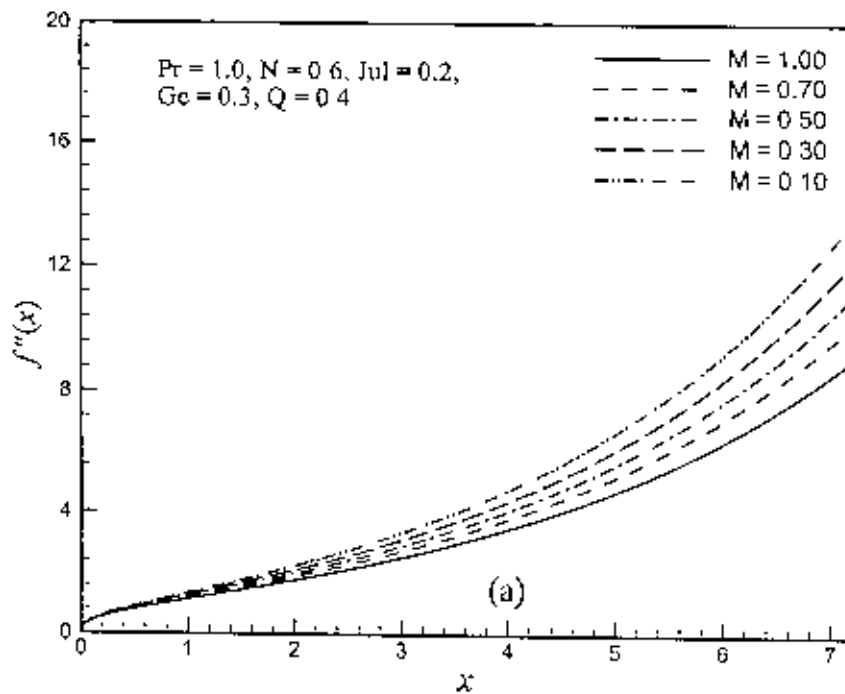
Figure 5.10(a): Variation of skin friction coefficient $f''(x, 0)$ with dimensionless distance x for different values of magnetic parameter or Hartmann Number M with $Pr = 1.00$, $N = 0.60$, $Ge = 0.30$, $Jul = 0.20$ and $Q = 0.40$.
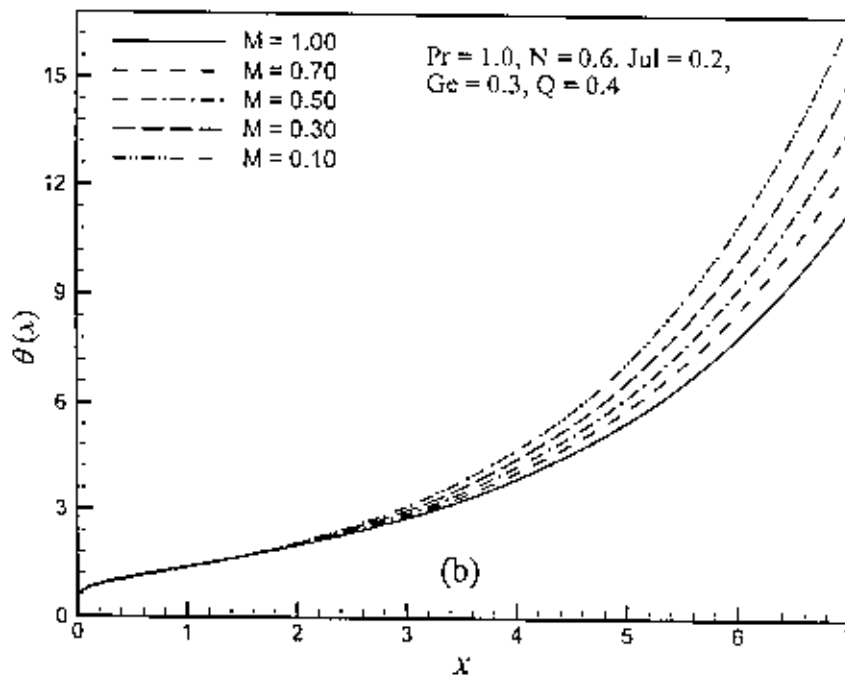
Figure 5.10(b): Variation of surface temperature $\theta(x, 0)$ with dimensionless distance x for different values of magnetic parameter or Hartmann Number M with $Pr = 1.00$, $N = 0.60$, $Ge = 0.30$, $Jul = 0.20$ and $Q = 0.40$.
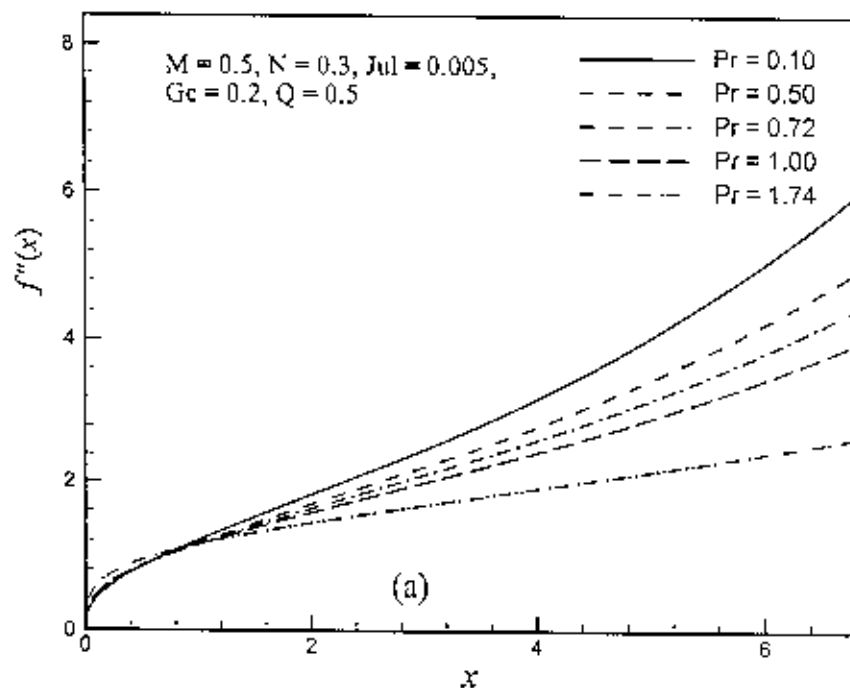
Figure 5.11(a): Variation of skin friction coefficient $f''(x, 0)$ with dimensionless distance x for different values of Prandtl number Pr with $M = 0.50$, $N = 0.30$, Ge = 0.20, $Jul = 0.005$ and $Q = 0.50$.
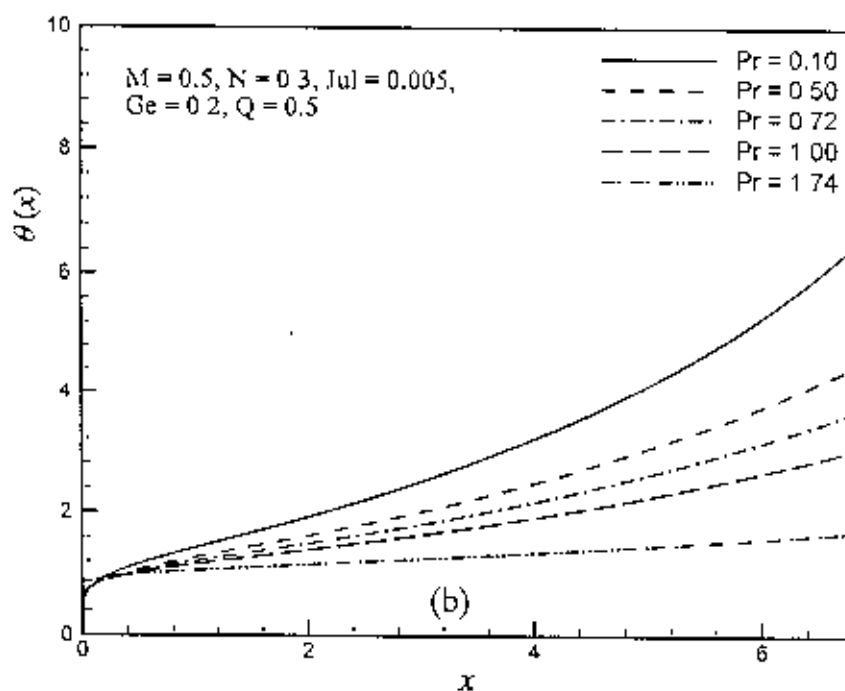
Figure 5.11(b): Variation of surface temperature $\theta(x, 0)$ with dimensionless distance x for different values of Prandtl number Pr with $M = 0.50$, $N = 0.30$, Ge = 0.20, $Jul = 0.005$ and $Q = 0.50$.
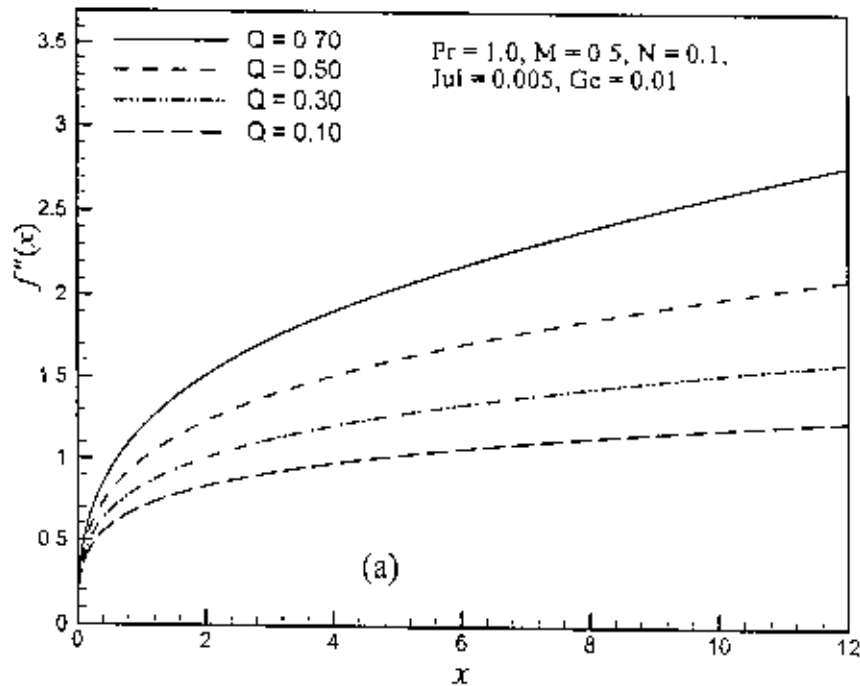
Figure 5.12(a): Variation of skin friction coefficient $f''(x, 0)$ with dimensionless distance x for different values of heat generation parameter Q with $M = 0.50$, $N = 0.10$, $Ge = 0.01$, $Jul = 0.005$ and $Pr = 1.00$.
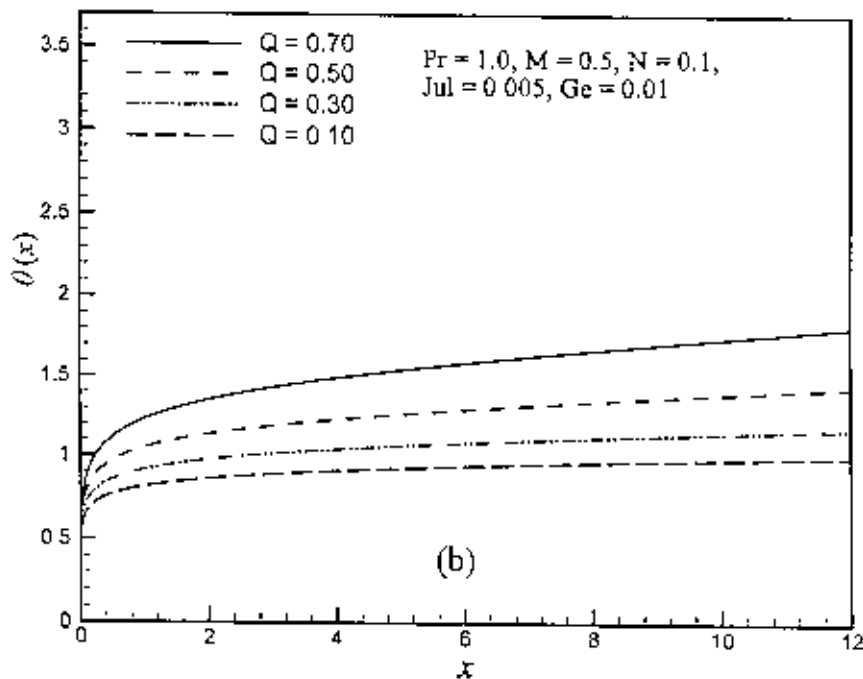
Figure 5.12(b): Variation of surface temperature $\theta(x, 0)$ with dimensionless distance x for different values of heat generation parameter Q with $M = 0.50$, $N = 0.10$, $Ge = 0.01$, $Jul = 0.005$ and $Pr = 1.00$.

The values of the skin friction coefficient and surface temperature distribution for different values of heat generation Q while $M = 0.50$, $N = 0.10$, $Jul = 0.005$, $Ge = 0.01$ and $Pr = 1.00$ are entered in Table-C_9 that is shown in Appendix C. Here it is found that the values of skin friction decrease at different position of x for heat generation parameter $Q = 0.10$, 0.30, 0.50, 0.70. The rate of the skin friction increases by 89.08% as the heat generation parameter Q changes from 0.10 to 0.70 and $x = 3.0049$. Furthermore, it is seen that the numerical values of the surface temperature distribution increase for increasing values of heat generation parameter Q. The rate of increase of surface temperature distribution is 61.07% at position $x = 3.0049$ as the heat generation parameter changes from 0.10 to 0.70.

Table-C_{10} represents the skin friction coefficient and surface temperature for different values of magnetic parameter or Hartmann Number M while $Pr = 1.00$, $N = 0.60$, $Jul = 0.20$ and $Ge = 0.30$, $Q = 0.40$ which is shown Appendix C. Here it is depicted that the values of skin friction coefficient decrease at different position of x for magnetic parameter $M = 0.20$, 0.40, 0.60, 1.00. The rate of the skin friction coefficient decreases by 45.27% as the magnetic parameter or Hartmann Number M changes from 0.20 to 1.00 and $x = 10.0179$. Furthermore, it is seen that the numerical values of the surface temperature distribution decrease for increasing values of magnetic parameter or Hartmann Number M. This suggests that the interface of the plate having thickness 'b' remains heated more in the lower magnetic fluid than that of the higher magnetic fluid and the rate of decrease of surface temperature distribution is 23.77% at position $x = 10.0179$ as the magnetic parameter or Hartmann Number M changes from 0.20 to 1.00.

Table-C_{11} depicts the values of the skin friction coefficient and surface temperature for different values of Joule heating parameter Jul while $Pr = 1.00$, $N = 0.006$, $M = 0.60$ and $Ge = 0.70$, $Q = 0.20$ which is shown in Appendix C. Here it is found that the values of skin friction coefficient increase at different position of x for Joule heating parameter $Jul = 0.30$, 0.50, 0.70, 0.90. The rate of the skin friction coefficient increases by 20.87% as the Joule heating parameter Jul changes from 0.30 to 0.90 and $x = 3.0049$. Furthermore, it is seen that the numerical values of the surface temperature distribution increase for increasing values of Joule heating parameter Jul. The rate of increase of surface temperature distribution is 25.67% at position $x = 3.0049$ as the Joule heating parameter Jul changes from 0.30 to 0.90.

The values of the skin friction coefficient and surface temperature for different values of pressure work parameter Ge while $Pr = 0.72$, $N = 0.001$, $M = 0.50$ and $Jul = 0.005$, $Q = 0.50$ are depicted in Table-C_{12} which is shown in Appendix C. Here it is observed that the values of skin friction coefficient increase at different position of x for pressure work parameter $Ge = 0.10$, 0.30, 0.60, 0.90. The rate of the skin friction coefficient increases by 109.67% as the pressure work parameter Ge changes from 0.10 to 0.90 and $x = 1.5095$. Furthermore, it is seen that the numerical values of the surface temperature distribution increase for increasing values of pressure work parameter Ge. The rate of increase of surface temperature distribution is 136.99% at position $x = 1.5095$ as the pressure work parameter Ge changes from 0.10 to 0.90.

5.3 Conclusions

From the present investigation, the following conclusions may be drawn:

* The skin friction coefficient, the surface temperature, the velocity and the temperature profiles increase for the increasing values of the viscous dissipation parameter N.

* The skin friction coefficient, the surface temperature, the velocity and the temperature profiles increase for the increasing values of the pressure work parameter Ge.

* The skin friction coefficient, the surface temperature, the velocity and the temperature profiles increase for the increasing values of the Joule heating parameter Jul.

* The skin friction coefficient, the surface temperature, the velocity and the temperature profiles increase for the increasing values of the heat generation parameter Q.

* It has been observed that the skin friction coefficient, the surface temperature distribution, the velocity profile decreases over the whole boundary layer with the increase of the Prandtl number Pr. But the temperature profile increases at some distance against η and then it stars to decrease over the whole boundary layer with the increase of the Prandtl number Pr.

* The effect of magnetic parameter or Hartmann Number M is to decrease the skin friction coefficient, the surface temperature distribution and the velocity distribution over the whole boundary layer, but reverse case happens for temperature distributions.

VISCOUS DISSIPATION AND PRESSURE WORK EFFECTS ON MAGNETOHYDRODYNAMIC NATURAL CONVECTION FLOW OVER A SPHERE IN THE PRESENCE OF HEAT GENERATION

A study of the flow of electrically conducting fluid in presence of magnetic field is important from the technical point of view and such types of problems have received much attention by many researches. The specific problem selected for study is the flow and heat transfer in an electrically conducting fluid adjacent to the surface. The surface is maintained at a uniform temperature T_w that may either exceed the ambient temperature T_∞ or may be less then T_∞. When $T_w > T_\infty$ an upward flow is established along the surface due to free convection; while when $T_w < T_\infty$ there is a down flow. In addition a magnetic field of strength B_0 acts normal to the surface. The interaction of the magnetic field and the moving electric charge carried by the flowing fluid induces a force, which tends to oppose the fluid motion so that the velocity is very small. The magnetic force, which is proportional to the magnitude of the longitudinal velocity and acts in the opposite direction is also very small. Consequently, the influence of the magnetic field on the boundary layer is exerted only through induced forces within the boundary layer itself, with no additional effects arising from the free stream pressure gradient.

However, the study of heat generation or absorption in moving fluids is important dealing with chemical reactions and those concerned with dissociating fluids. Possible heat generation effects may alter the temperature distribution. Vajravelu and Hadjinolauo (1993) studied the heat transfer characteristics in the laminar boundary layer of a viscous fluid over a linearly stretching continuous surface with viscous dissipation or frictional heating and internal heat generation. In this study they considered that the volumetric rate of heat generation, q''' [w/m³], should be $q''' = Q_0(T - T_\infty)$, for $T \geq T_\infty$ and equal to zero for $T < T_\infty$. Q_0 is the heat generation / absorption constant. Hossain et $al.$ (2004) also discussed the problem of natural convection flow along a vertical wavy surface with uniform surface temperature in presence of heat generation / absorption. To our best of knowledge, heat generation effect on

magnetohydrodynamics free convection flow from an isothermal sphere has not yet been studied and the present work demonstrates the issue.

The present work considers the natural convection boundary layer flow on a sphere of an electrically conducting and steady viscous in compressible fluid in presence of strong magnetic field, the pressure stress work and heat generation. The governing partial differential equations are reduced to locally non-similar partial differential forms by adopting appropriate transformations. The transformed boundary layer equations are solved numerically using implicit finite difference scheme together with the Keller box technique. Here we have focused our attention on the evolution of the surface shear stress in terms of local skin friction and the rate of heat transfer in terms of local Nusselt number, velocity distribution as well as temperature distribution for a selection of parameter sets consisting of heat generation parameter Q, viscous dissipation parameter N, the pressure work parameter Ge, the magnetic parameter M and the Prandtl number Pr.

6.1 Formulation of the problems

Natural convection boundary layer flow on a sphere of an electrically conducting and steady two-dimensional viscous incompressible fluid in presence of strong magnetic field and heat generation is considered, but radiation effect is neglected. Then the basic equations (2.106) to (2 108) can be written as

$$\frac{\partial}{\partial X}(r\,U) + \frac{\partial}{\partial Y}(r\,V) = 0 \tag{6.1}$$

$$U\frac{\partial U}{\partial X} + V\frac{\partial U}{\partial Y} = v\frac{\partial^2 U}{\partial Y^2} + g\beta(T\text{-}T_\infty)\,\sin\!\left(\frac{X}{a}\right) - \frac{\sigma_0\beta_0^{\,2}}{\rho}U \tag{6.2}$$

$$U\frac{\partial T}{\partial X} + V\frac{\partial T}{\partial Y} = \frac{k}{\rho C_p}\frac{\partial^2 T}{\partial Y^2} + \frac{T\beta}{\rho C_p}U\frac{\partial p}{\partial X} + \frac{v}{\rho C_p}\left(\frac{\partial U}{\partial Y}\right)^2 + \frac{Q_0}{\rho C_p}(T - T_\infty) \tag{6.3}$$

The boundary conditions for the equations (6 2) to (6.3) are

$$U = V = 0, \quad T = T_w \text{ on } Y = 0 \tag{6.4}$$

$$U \to 0, T \to T_\infty \quad at \ Y \to \infty \tag{6 5}$$

$$r(X) = a\ \sin\left(\frac{X}{a}\right), \quad \text{where } r = r(X) \tag{6.6}$$
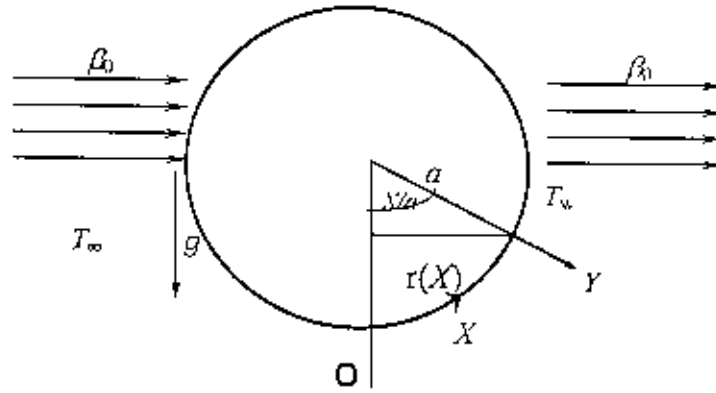
Figure 6.1: Physical model and coordinate system

where, symbols have their usual meanings. To transform the above equations into non-dimensional form the following dimensionless variables (2.112) are introduced:

$$x = \frac{X}{a}\ ,\ y = G_r^{1/4}\frac{Y}{a}\ ,\ u = \frac{a}{v}G_r^{-1/2}U\ ,\ v = \frac{a}{v}G_r^{-1/4}V,\ \theta = \frac{T - T_\infty}{T_w - T_\infty} \tag{6.7}$$

Where Gr and θ are defined in chapter two.

Thus (6.6) becomes $r(x) = a \sin x$

$$\tag{7.8}$$

Using the above values, the equations (6.1) to (6.3) take the following form:

$$\frac{\partial}{\partial x}(ru) + \frac{\partial}{\partial y}(rv) = 0 \tag{6.9}$$

$$u\frac{\partial u}{\partial x} + v\frac{\partial u}{\partial y} = \frac{\partial^2 u}{\partial y^2} + \theta \sin x - \frac{\sigma_0 \beta_0^2 a^2}{\rho v G_r^{1/2}}u \tag{6.10}$$

$$u\frac{\partial\theta}{\partial x}+v\frac{\partial\theta}{\partial y}=\frac{1}{Pr}\frac{\partial^2\theta}{\partial y^2}+\frac{Gr}{a^2 C_P\left(T_w-T_\infty\right)}\left(\frac{\partial u}{\partial y}\right)^2$$

$$-\left(\frac{T_r}{T_w-T_\infty}+\theta\right)\frac{g\beta a}{C_P}u+\frac{Q_a}{\rho C_P}\frac{a^2}{\nu\, Gr^{\frac{1}{2}}}\theta \qquad (6.11)$$

where, M, Q, N and Ge are defined earlier. Therefore momentum and energy equations (6.10) and (6.11) reduces to

$$u\frac{\partial u}{\partial x}+v\frac{\partial u}{\partial y}\;=\;\frac{\partial^2 u}{\partial y^2}+\theta\sin x-Mu \qquad (6.12)$$

$$u\frac{\partial\theta}{\partial x}+v\frac{\partial\theta}{\partial y}=\frac{1}{Pr}\frac{\partial^2\theta}{\partial y^2}+N\left(\frac{\partial u}{\partial y}\right)^2-Ge\left(\frac{T_\infty}{T_w-T_\infty}+\theta\right)u+Q\theta \qquad (6.13)$$

The boundary conditions associated with (6.4) to (6.5) becomes

$$u=v=0,\quad \theta=1 \text{ at } y=0$$
$$u\to 0,\;\; \theta\to 0 \text{ as } y\to\infty \qquad (6.14)$$

Now substituting equations (2.121 and (2.122)) into equations (6.12) and (6.13) subject to the boundary conditions (6.14), after simplifying we have the followings:

$$\frac{\partial^3 f}{\partial y^3}+\left(1+\frac{x}{\sin x}\cos x\right)f\frac{\partial^2 f}{\partial y^2}-\left(\frac{\partial f}{\partial y}\right)^2+\frac{\theta}{x}\sin x-M\frac{\partial f}{\partial y}=x\left(\frac{\partial f}{\partial y}\frac{\partial^2 f}{\partial y\partial x}-\frac{\partial f}{\partial x}\frac{\partial^2 f}{\partial y^2}\right) \qquad (6.15)$$

$$\frac{1}{Pr}\frac{\partial^2\theta}{\partial y^2}+\left(1+\frac{x}{\sin x}\cos x\right)f\frac{\partial\theta}{\partial y}+Q\theta+Nx^2\left(\frac{\partial^2 f}{\partial y^2}\right)^2$$

$$-Ge\left(\frac{T_\infty}{T_w-T_\infty}+\theta\right)\frac{\partial f}{\partial y}=x\left(\frac{\partial f}{\partial y}\frac{\partial\theta}{\partial x}-\frac{\partial f}{\partial x}\frac{\partial\theta}{\partial y}\right) \qquad (6.16)$$

The corresponding boundary conditions are

$$f=\frac{\partial f}{\partial y}=0 \;,\; \theta=1 \text{ at } y=0$$

$$\frac{\partial f}{\partial y}\to 0 \,,\, \theta\to 0 \quad \text{as } y\to\infty \qquad (6.17)$$

The skin friction coefficient and the heat transfer coefficient, which can be written in non-dimensional form as

$$\therefore C_{px} = x\left(\frac{\partial^2 f}{\partial y^2}\right)_{y=0} \tag{6.18}$$

$$Nu_x = -\left(\frac{\partial \theta}{\partial y}\right)_{y=0} \tag{6.19}$$

Now velocity distribution as well as temperature distribution for a selection of parameter sets consisting of heat generation parameter, MHD parameter, and the Prandlt number at different position of x $(= 0, \pi/6, \pi/4, -- ----\pi/2)$ will be studied.

6.2 Results and Discussion

Solutions are obtained for the fluid having Prandtl number Pr $(= 1.00. 1.74, 2.00, 3.00)$, viscous dissipation parameter N $(= 0.10, 0.30, 0.50, 0.70, 1.00)$, pressure work parameter Ge $(= 0.10, 0.40, 0.70, 0.90)$ against y at any position of x and for a wide range of values of magnetic parameter M with the heat generation parameter Q $(= 0.40, 0.50, 0.60)$. Also the results for the skin friction coefficient and the rate of heat transfer have been obtained for fluids having Prandtl number Pr $(= 1.00. 1.74, 2.00, 3.00)$, the heat generation parameter Q $(= 0.60, 0.40, 0.20)$, the magnetic parameter or Hartmann number M $(= 1.00, 0.80, 0.60, 0.40)$ and pressure work parameter Ge $(= 0.10, 0.40, 0.70, 0.90)$ at different position of x for a wide range of values of magnetic parameter M with the heat generation parameter $Q = 0.40, 0.50, 0.60$.

The effects of magnetic parameter or Hartmann number M for $Pr = 0.72$, $Q = 2.00$, $N = 0.90$ and $Ge = 0.50$ on the velocity profiles and temperature profiles are shown in figures 6.2(a) to 6.2(b). Figure 6.2(a) and figure 6.2(b) represent respectively the effects of magnetic parameter M on the velocity and temperature profiles. From these figures, it is seen that the velocity profiles decrease with the increasing values of M and the temperature profiles increase with the increasing values of M.

From figure 6.3(a) it is observed that velocity distribution increases as the values of viscous dissipation parameter N increase in the region $y \in [0, 12]$ but near the surface of the sphere, velocity increases significantly and then decreases slowly and finally approaches to zero. The maximum values of the velocity are recorded to be 0.48450, 0.51282, 0.53527, 0.55384 and 0.56949 for $N = 0.10, 0.30, 0.50, 0.70$ and 1.00 respectively which occur at $y = 1.23788$ for first, second and third maximum values, $y = 1.30254$ for fourth and fifth maximum values. Here it is observed that the velocity increases by 17.54 % as N increases from 0.10 to 1.00. From figure 6.3(b), it is seen that

when the values of viscous dissipation parameter N increases in the region $y \in [0, 12]$, the temperature distribution also increases. It is observed that the maximum temperature has been found at the surface on the sphere.

From figure 6.4(a) it depicts that the velocity distribution increases slightly as the pressure work parameter Ge increases in the region $y \in [0, 9]$ but near the surface of the sphere, velocity increases and becomes maximum and then decreases and at a certain point velocity profiles coincide and finally approaches to zero. The maximum values of the velocity are recorded to be 0.43056, 0.44332, 0.47589 and 0 53463 for $Ge = 0 10$, 0.40, 0 70 and 0.90 respectively which occur at $y = 1 17520$ for first, second and third maximum values and at $y = 1.23788$ for last maximum values. Here we see that the velocity increases by 24 17 % as Ge increases from 0.10 to 0.90. From figure 6.4(b), it is seen that when the values of pressure work parameter Ge increases in the region $y \in [0, 9]$, the temperature distribution also increases. But near the surface of the sphere temperature profiles are maximum and then decreases away from the surface and finally take asymptotic value.

From figure 6.5(a) it is illustrated that velocity distribution increases as the values of heat generation Q increase in the region $y \in [0, 8]$. The changes of velocity profiles in the y direction reveals the typical velocity profile for natural convection boundary layer flow that is the velocity is zero at the boundary surface then the velocity increases to the peak value as y increases and finally the velocity approaches to zero (the asymptotic value). The maximum values of the velocity are 0.47717, 0.52815 and 0.54807 for $Q = 0.20$, 0.50 and 0.60 respectively which occur at $y = 1.17520$ for first maximum value and $y = 1.123788$ for second and third maximum values. Here it is observed that the velocity increase by 14.86 % as Q increases from 0 10 to 0.60. From figure 6.5(b), it is seen that when the values of heat generation parameter Q increases in the region $y \in [0, 8]$, the temperature distribution also increases. But near the surface of the sphere temperature profiles are maximum and then decreases away from the surface and finally take asymptotic value.

Figure 6.6(a) and figure 6.6(b) indicate the effects of the Prandtl number Pr with $M = 0.50$, $Q = 0.60$, $N = 0 40$ and $Ge = 0.30$ on the velocity profiles and the temperature profiles. From figure 6.6(a) it is observed that the increasing values of Prandtl number Pr lead to decrease the velocity profiles. The maximum values of the velocity are

recorded to be 0.52815, 0.42524, 0.38592 and 0.36155 for $Pr = 1.00$, 1.74, 2.00 and 3.00 respectively which occur at $y = 1.23788$ for first maximum value and $y = 0.99806$ for second, third and fourth maximum values. Here it is depicted that the velocity decreases by 31.54 % as Pr increases from 1.00 to 3.00. Again from figure 6.6(b) it is observed that the temperature profiles decrease with the increasing values of Prandtl number Pr. But near the surface of the sphere temperature profiles are maximum and then decreases away from the surface and finally take asymptotic value.

The effects of magnetic parameter or Hartmann number M for $Pr = 0.72$, $Q = 2.00$, $N = 0.90$ and $Ge = 0.50$ on the local skin friction coefficient C_{fx} and local heat transfer coefficient Nu_x are shown in figure 6.7(a) to figure 6.7(b). From figure 6.7(a) and figure 6.7(b) it is evident that the increasing values of magnetic parameter M leads to decrease both the skin friction co-efficient C_{fx} and the local heat transfer co-efficient Nu_x.

Figure 6.8(a) and figure 6.8(b), represent the effects for different values of pressure work parameter Ge for the magnetic parameter $M = 1.00$, heat generation parameter $Q = 0.40$, viscous dissipation parameter $N = 0.50$ and Prandtl number $Pr = 0.72$ on the reduced local skin friction coefficient C_{fx} and local rate of heat transfer Nu_x. The skin friction coefficient C_{fx} and heat transfer coefficient Nu_x increase with the increasing values of pressure work parameter Ge

Figure 6.9(a) and figure 6.9(b) show that both skin friction coefficient C_{fx} and heat transfer coefficient Nu_x decrease for increasing values of Prandtl number Pr while heat generation parameter $Q = 0.60$, magnetic parameter $M = 0.50$, pressure work parameter $Ge = 0.30$ and viscous dissipation parameter $N = 0.40$. The values of skin friction coefficient C_{fx} and Nusselt number Nu_x are recorded to be 0.33987, 0.33486, 0.32018, 0.31108 and 0.27366, 0.25235, 0.15165, 0.02378 for $Pr = 1.00$, 1.74, 2.00, 3.00 respectively which occur at the same point $x = 0.38397$. Here, it is observed that at $x = 0.38397$, the skin friction coefficient decreases by 8.47% and Nusselt number Nu_x decreases by 91.31% as the Prandtl number Pr changes from 1.00 to 3.00

From figure 6.10(a) and figure 6.10(b), it is seen that for different values of heat generation parameter Q while the magnetic parameter $M = 1.00$, pressure work parameter $Ge = 0.10$, viscous dissipation parameter $N = 0.40$ and Prandtl number $Pr = 0.72$ on the reduced local skin friction coefficient C_{fx} and local rate of heat transfer Nu_x. The skin friction coefficient C_{fx} increases and the heat transfer coefficient Nu_x decreases with the increasing values of heat generation parameter Q.
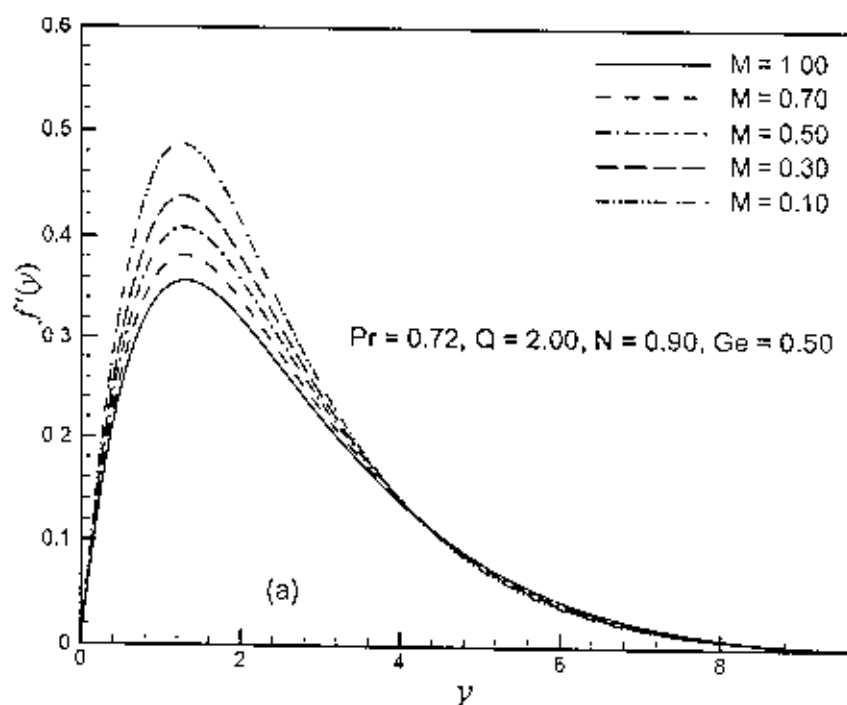
Figure 6.2(a): Variation of dimensionless velocity profiles $f'(x, v)$ against dimensionless distance y for different values of magnetic parameter or Hartmann number M with $Pr = 0.72$, $N = 0.90$, $Ge = 0.50$ and $Q = 2.00$.
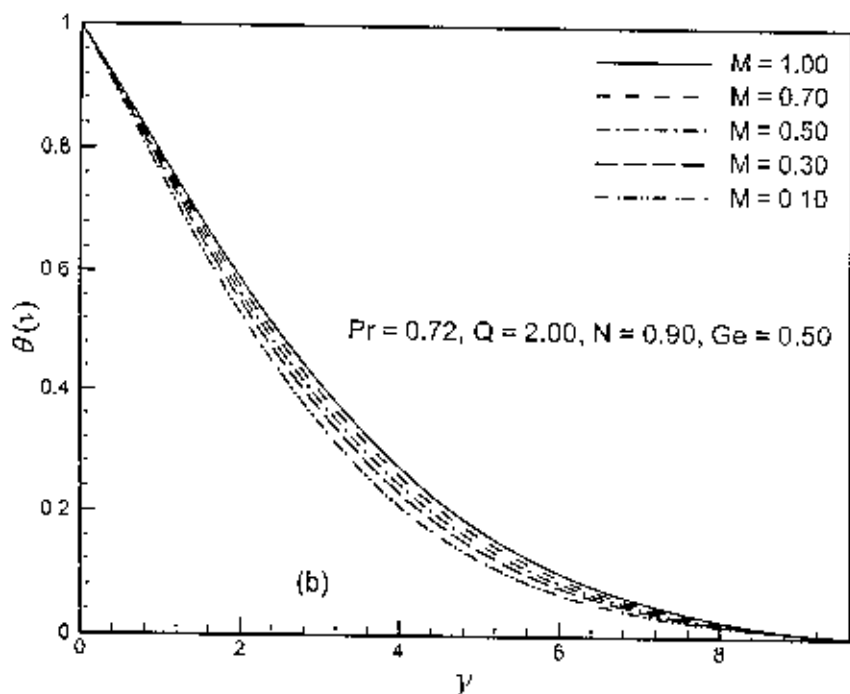
Figure 6.2(b): Variation of dimensionless temperature profiles $\theta(x, y)$ against dimensionless distance y for different values of magnetic parameter or Hartmann number M with $Pr = 0.72$, $N = 0.90$, $Ge = 0.50$ and $Q = 2.00$.
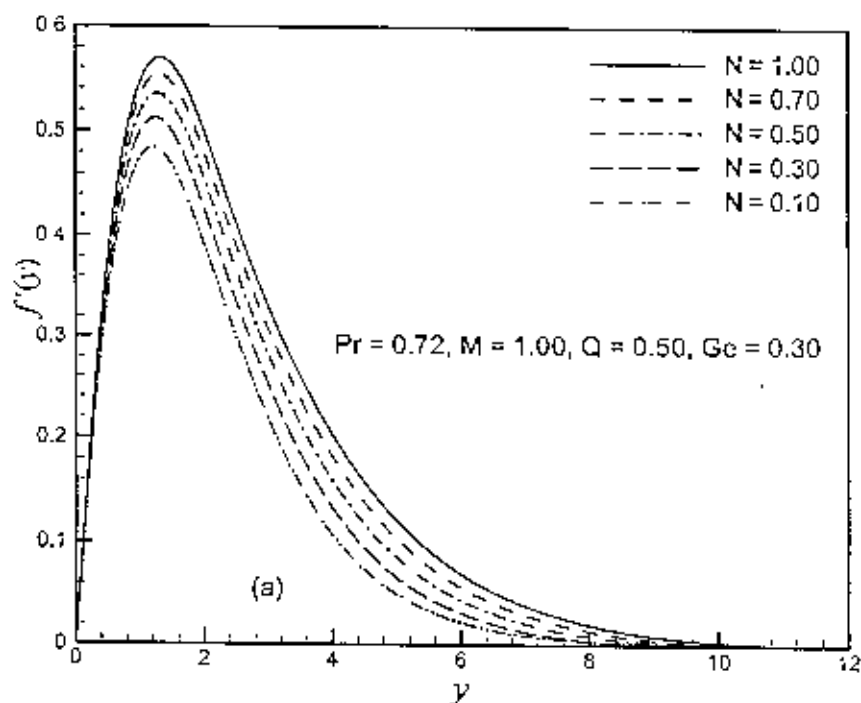
Figure 6.3(a): Variation of dimensionless velocity profiles $f'(x, y)$ against dimensionless distance y for different values of viscous dissipation parameter N with $Pr = 0.72$, $M = 1.00$, $Ge = 0.30$ and $Q = 0.50$.
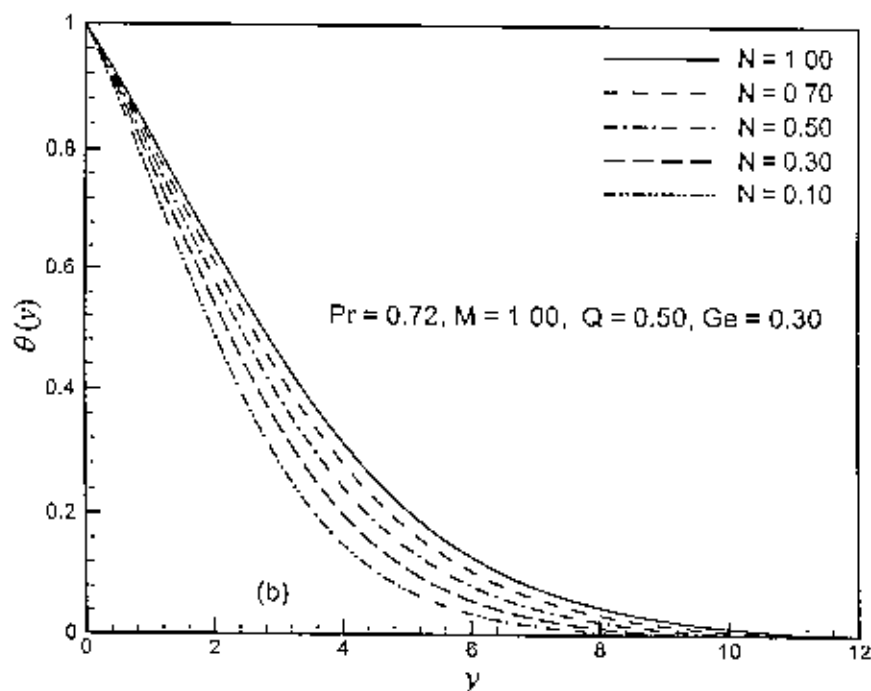
Figure 6.3(b): Variation of dimensionless temperature profiles $\theta(x, y)$ against dimensionless distance y for different values of viscous dissipation parameter N with $Pr = 0.72$, $M = 1.00$, $Ge = 0.30$ and $Q = 0.50$.
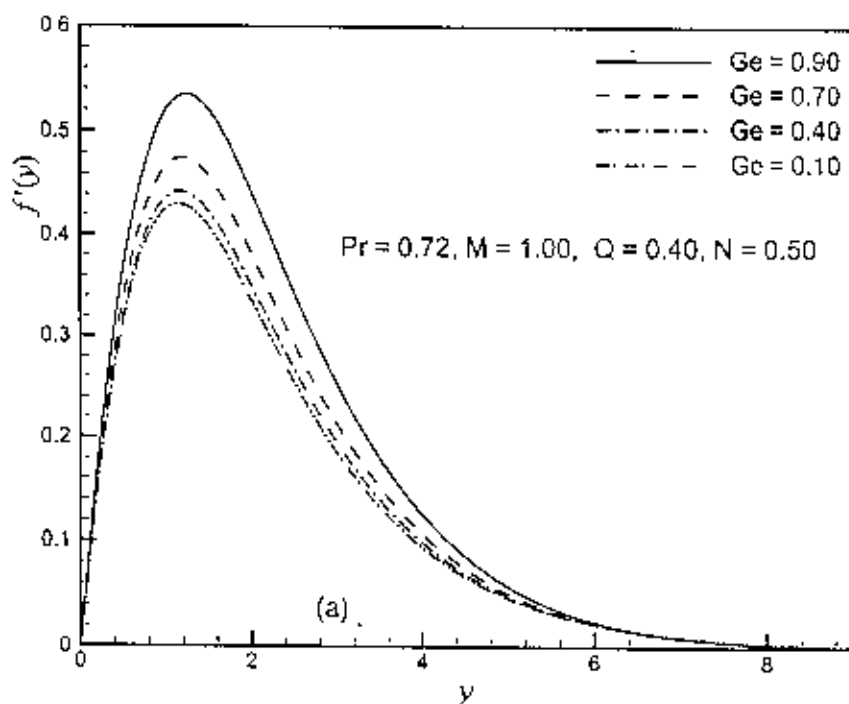
Figure 6.4(a): Variation of dimensionless velocity profiles $f'(x, y)$ against dimensionless distance y for different values of pressure work parameter Ge with $Pr = 0.72$, $M = 1.00$, $N = 0.50$ and $Q = 0.40$.
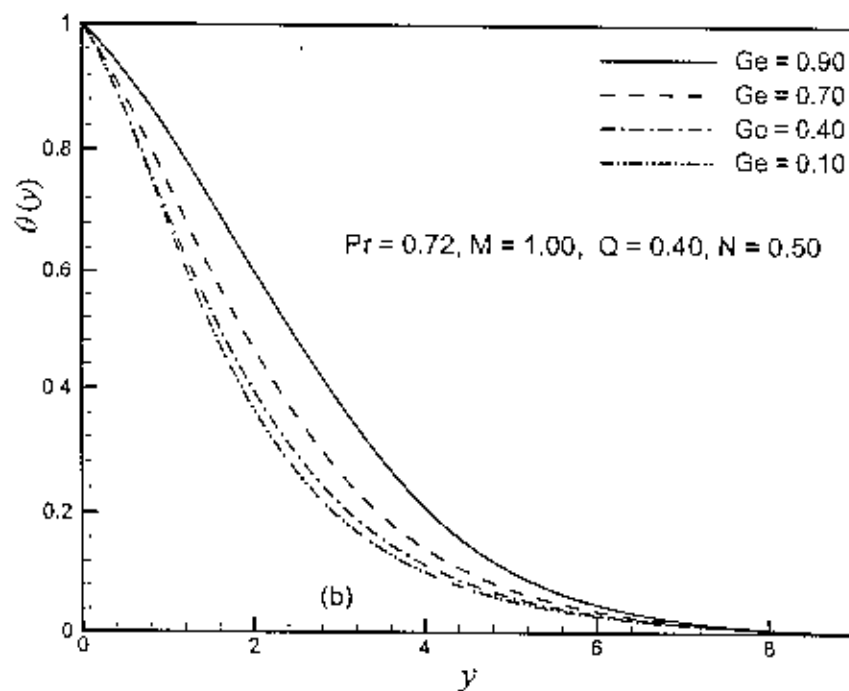
Figure 6.4(b): Variation of dimensionless temperature profiles $\theta(x, y)$ against dimensionless distance y for different values of pressure work parameter Ge with $Pr = 0.72$, $M = 1.00$, $N = 0.50$ and $Q = 0.40$.
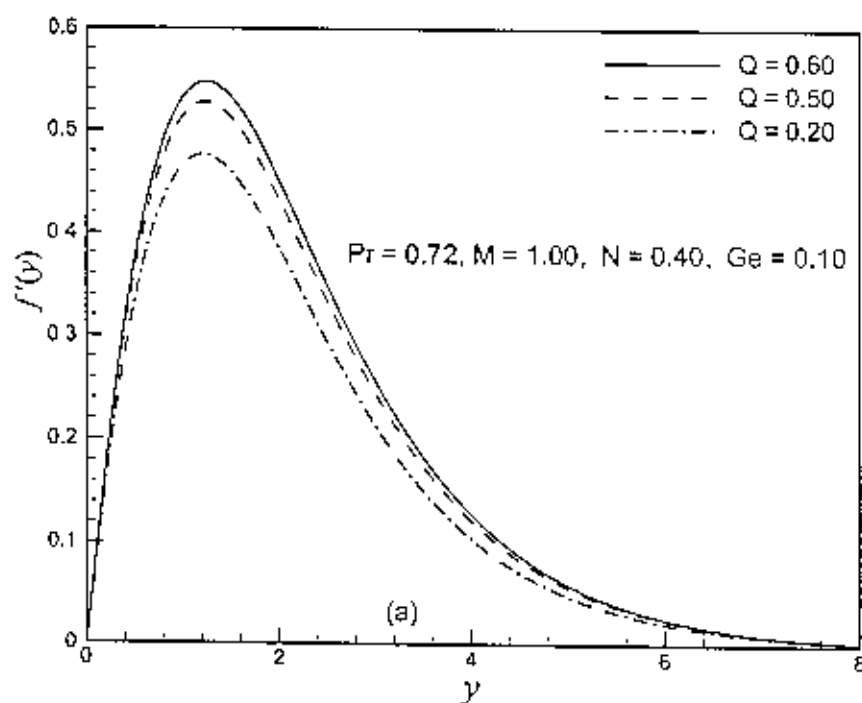
Figure 6.5(a): Variation of dimensionless velocity profiles $f'(x, y)$ against dimensionless distance y for different values of heat generation parameter Q with $Pr = 0.72$, $M = 1.00$, $N = 0.40$ and $Ge = 0.10$.
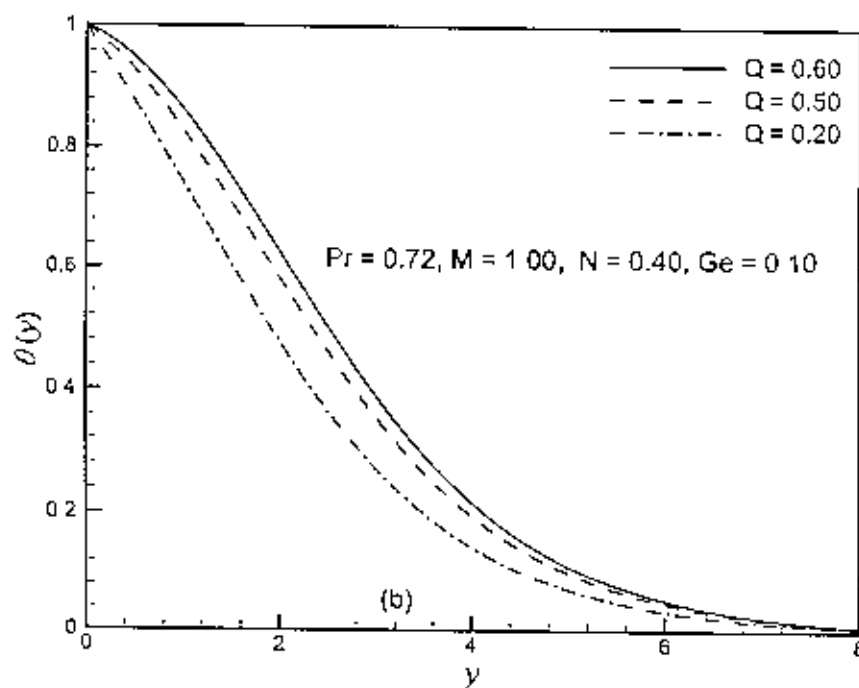
Figure 6.5(b): Variation of dimensionless temperature profiles $\theta(x, y)$ against dimensionless distance y for different values of heat generation parameter Q with $Pr = 0.72$, $M = 1.00$, $N = 0.40$ and $Ge = 0.10$.
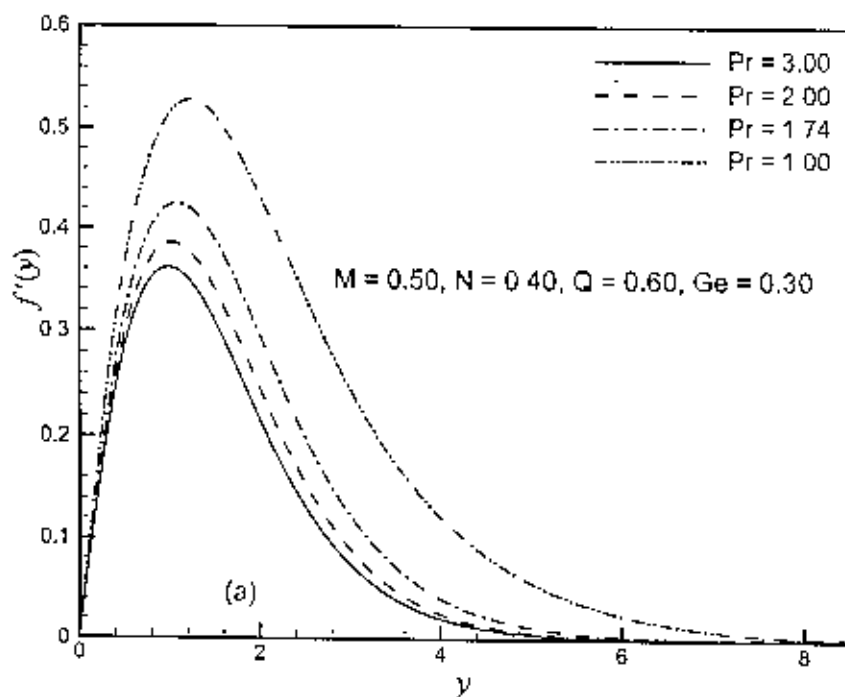
Figure 6.6(a): Variation of dimensionless velocity profiles $f'(x, y)$ against dimensionless distance y for different values of Prandtl number Pr with $Q = 0.60$, $M = 0.50$, $N = 0.40$ and $Ge = 0.30$.
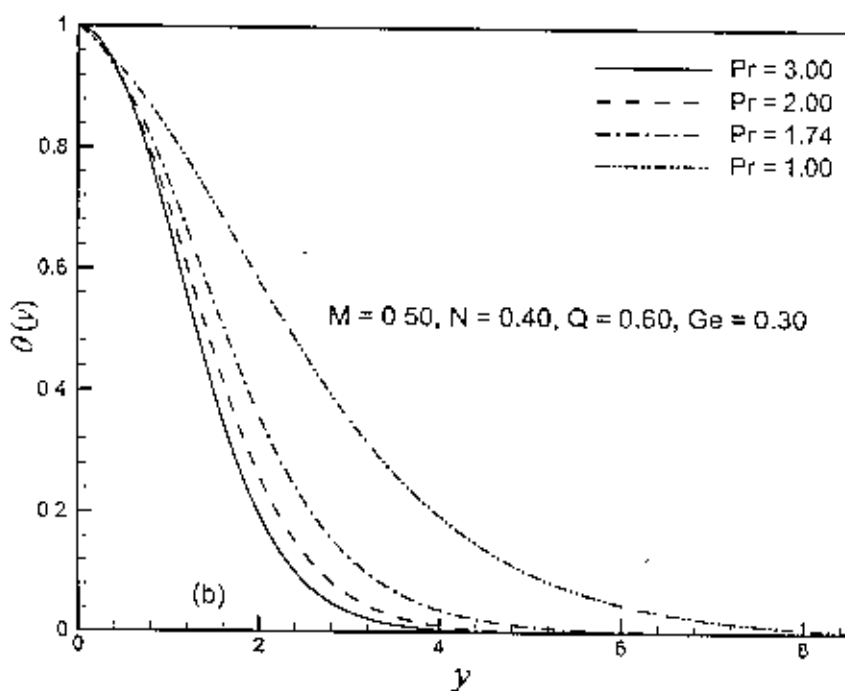
Figure 6.6(b): Variation of dimensionless temperature profiles $\theta(x, y)$ against dimensionless distance y for different values of Prandtl number Pr with $Q = 0.60$, $M = 0.50$, $N = 0.40$ and $Ge = 0.30$.
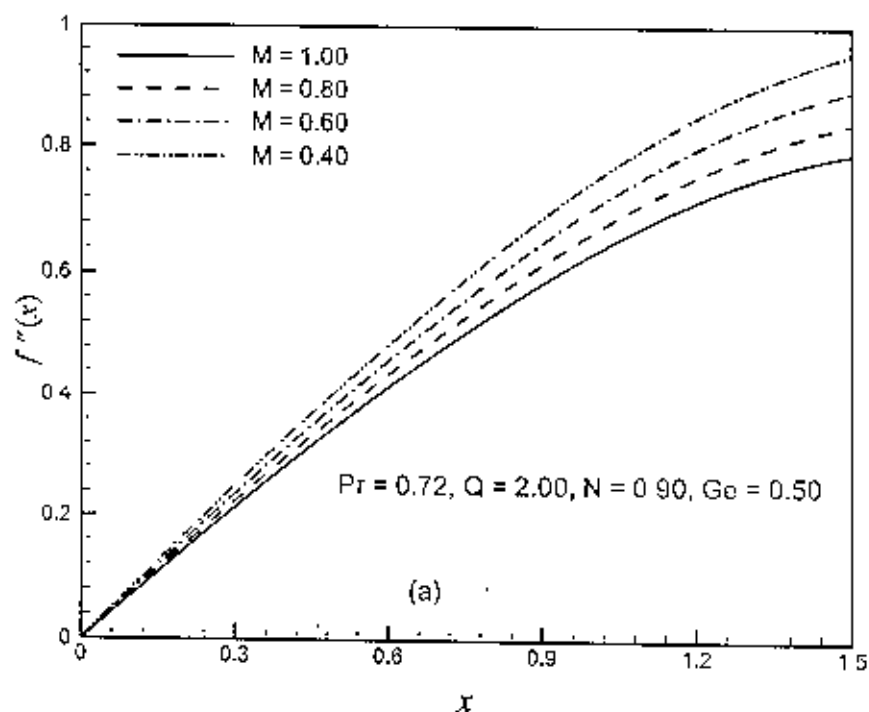
Figure 6.7(a): Variation of skin friction coefficient, C_{fx} with dimensionless distance x for different values of magnetic parameter or Hartmann number M with $Q = 2.00$, $N = 0.90$, $Ge = 0.50$ and $Pr = 0.72$.
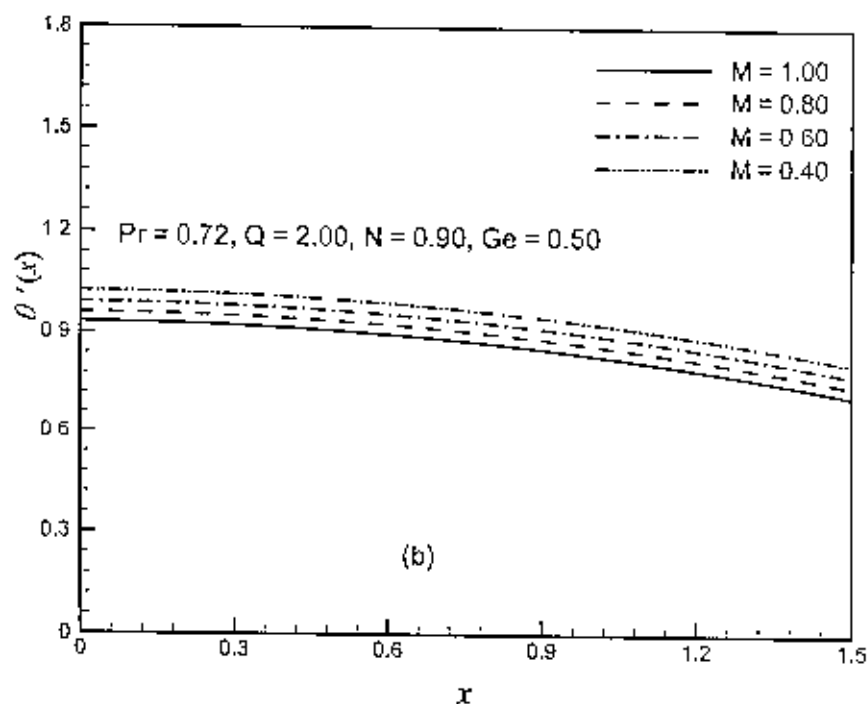
Figure 6.7(b): Variation of local heat transfer coefficient, Nu_x with dimensionless distance x for different values of magnetic parameter or Hartmann number M with $Q = 2.00$, $N = 0.90$, $Ge = 0.50$ and $Pr = 0.72$.
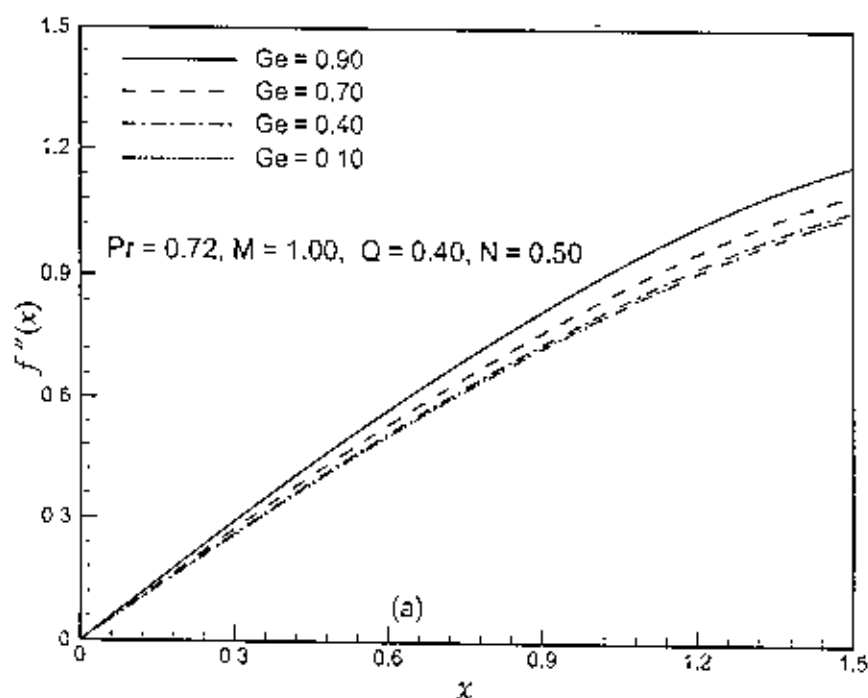
Figure 6.8(a): Variation of skin friction coefficient, C_{fx} with dimensionless distance x for different values of pressure work parameter Ge with $Q = 0.40$, $N = 0.50$, $M = 1.00$ and $Pr = 0.72$.
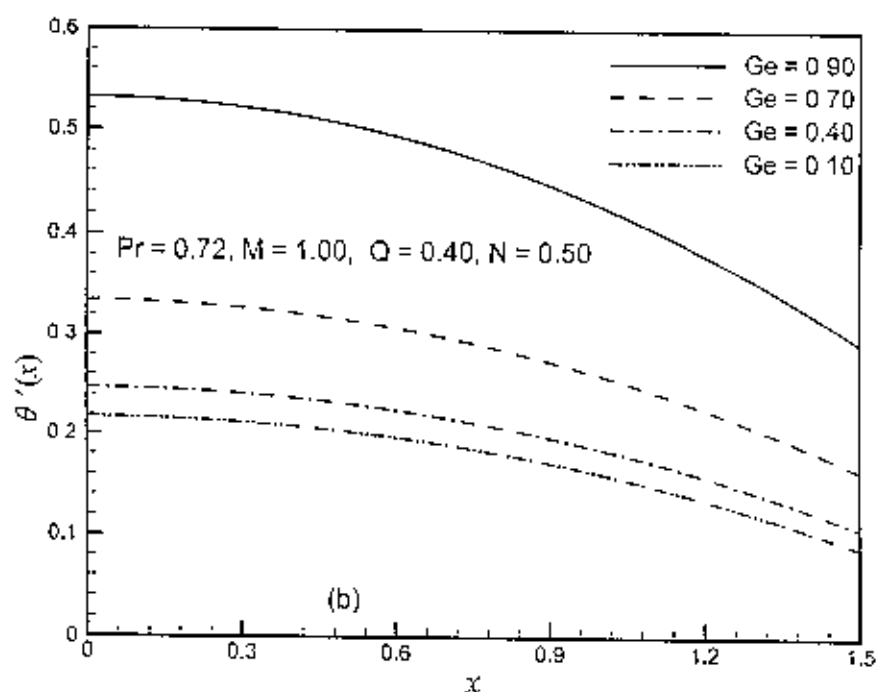
Figure 6.8(b): Variation of local Nusselt number, Nu_x with dimensionless distance x for different values of pressure work parameter Ge with $Q = 0.40$, $N = 0.50$, $M = 1.00$ and $Pr = 0.72$.
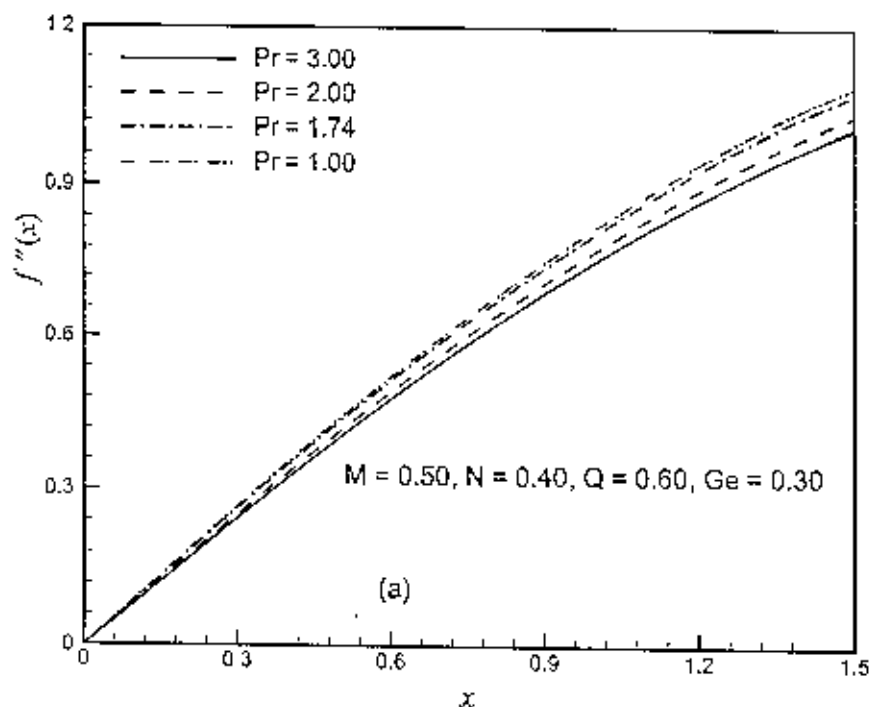
Figure 6.9(a): Variation of skin friction coefficient, C_{fx} with dimensionless distance x for different values of Prandtl number Pr with $M = 0.50$, $N = 0.40$, $Ge = 0.30$ and $Q = 0.60$.
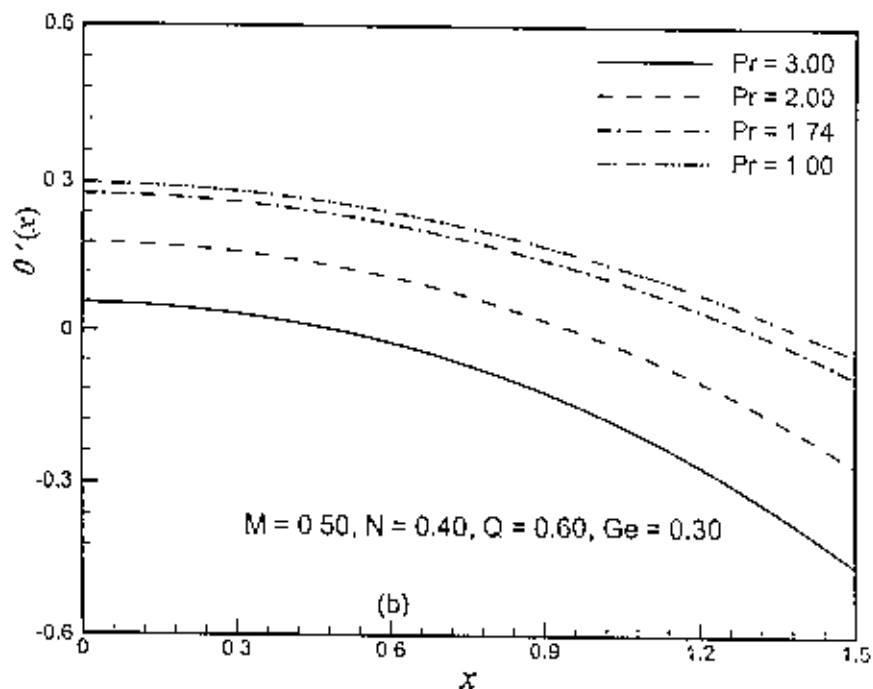
Figure 6.9(b): Variation of local Nusselt number, Nu_x with dimensionless distance x for different values of Prandtl number Pr with $M = 0.50$, $N = 0.40$. $Ge = 0.30$ and $Q = 0.60$.
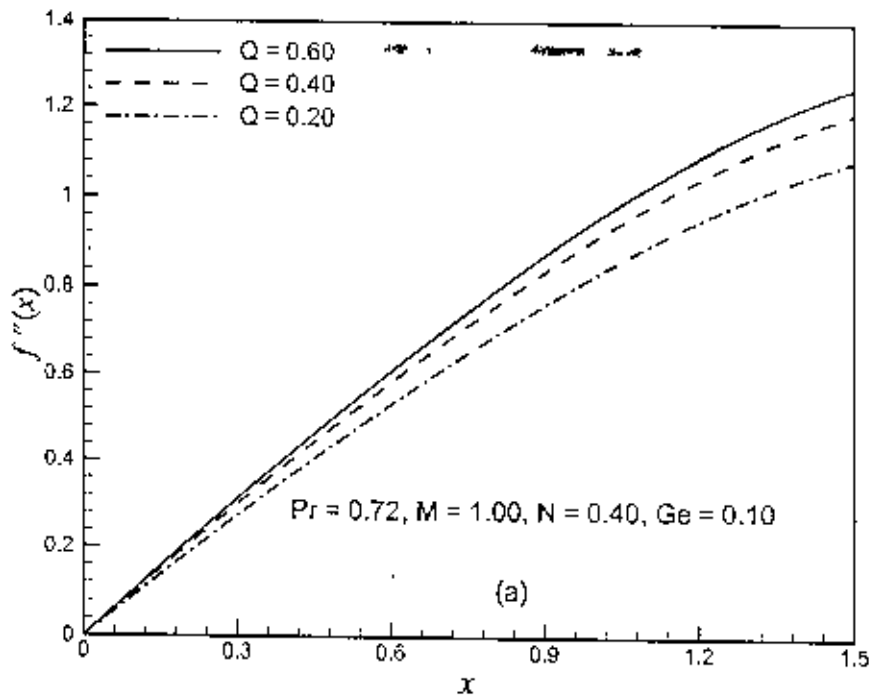
Figure 6.10(a): Variation of skin friction coefficient, C_{fx} with dimensionless distance x for different values of heat generation parameter Q with $M = 1.00$, $N = 0.40$, $Ge = 0.10$ and $Pr = 0.72$
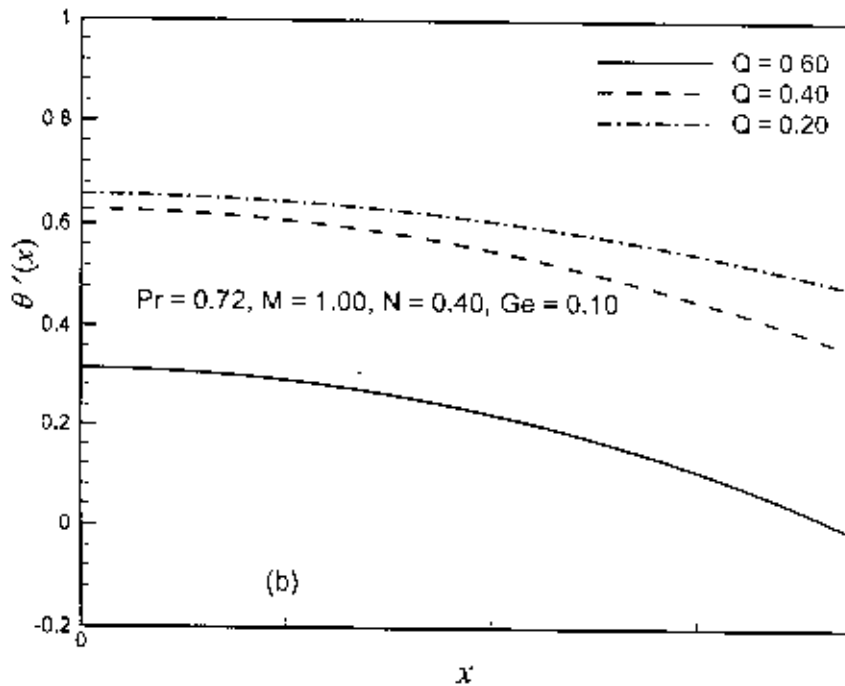
Figure 6.10(b): Variation of local Nusselt number, Nu_x with dimensionless distance x for different values of heat generation parameter Q with $M = 1.00$, $N = 0.40$, $Ge = 0.10$ and $Pr = 0.72$.

The values of the local skin friction coefficient C_{fx} and local Nusselt number Nu_x for different values of magnetic parameter or Hartmann number M while $Pr = 0.72$, $Q = 2.00$, $N = 0.90$ and $Ge = 0.50$ are given in Table-C_{13} which is shown in Appendix C. Here we see that the values of local skin friction coefficient C_{fx} decrease at different position of x for magnetic parameter $M = 0.40, 0.60, 0.80, 1.00$. The rate of the local skin friction coefficient C_{fx} decreases by 14.72% as the magnetic parameter M changes from 0.400 to 1.00 and $x = 0.80285$. Furthermore, it is seen that the numerical values of the local Nusselt number Nu_x decrease as magnetic parameter or Hartmann number M increase. The rate of decrease of the local Nusselt number Nu_x is 9.64% at position $x = 0.80285$ as the magnetic parameter M changes from 0.40 to 1.00

The values of the local skin friction coefficient C_{fx} and local Nusselt number Nu_x for different values of viscous dissipation parameter N while $Pr = 0.72$, $M = 0.90$. $Ge = 0.50$ and $Q = 2.00$ are recorded in Table-C_{14} which is shown in Appendix C. Here it is seen that the values of local skin friction coefficient C_{fx} increase at different position of x for viscous dissipation parameter $N = 0.10, 0.50, 0.70, 1.00$. The rate of the local skin friction coefficient C_{fx} increases by 8.57% as the viscous dissipation parameter N changes from 0.10 to 1.00 and $x = 1.04720$. Furthermore, it is seen that the numerical values of the local Nusselt number Nu_x increase for increasing values of viscous dissipation parameter N. The rate of increase of the local Nusselt number Nu_x is 69.08% at position $x = 1.04720$ as the viscous dissipation parameter N changes from 0.10 to 1.00.

The values of the local skin friction coefficient C_{fx} and local Nusselt number Nu_x for different values of pressure work parameter Ge while $Pr = 0.72$, $M = 1.00$, $N = 0.50$ and $Q = 0.40$ are recorded in Table-C_{15} which is shown in Appendix C. Here it is found that the values of local skin friction coefficient C_{fx} increase at different position of x for pressure work parameter $Ge = 0.10, 0.40, 0.70, 0.90$. The rate of the local skin friction coefficient C_{fx} increases by 11.74% as the pressure work parameter Ge changes from 0.10 to 0.90 and $x = 1.30900$. Furthermore, it is seen that the numerical values of the local Nusselt number Nu_x increase for increasing values of pressure work parameter Ge. The rate of increase of the local Nusselt number Nu_x is 194.02% at position $x = 1.30900$ as the pressure work parameter Ge changes from 0.10 to 0.90.

Numerical values of local heat transfer rate, Nu_X are calculated from equation (6.18) for the surface of the sphere from lower stagnation point to upper stagnation point. In order to verify the accuracy of the present work, the values of non dimensional heat transfer parameter Nu_X for $N = Ge = M = Q = 0.00$ having Prandtl number $Pr = 0.70$, 7.00 at different position of x (in degree) are compared with those reported by Nazar *et al.* (2002) and Molla *et al* (2004) as presented in Table-C_{16} which is shown in Appendix C. The results are found to be in excellent agreement.

6.3 Conclusions

From the present problem the following conclusions may be drawn:

- Significant effects of heat generation parameter Q and magnetic parameter M on velocity and temperature profiles as well as on skin friction coefficient C_{fx} and the rate of heat transfer Nu_X have been found in this investigation but the effects of heat generation parameter Q and magnetic parameter or Hartmann number M on rate of heat transfer is more significant

- An increase in the values of magnetic parameter or Hartmann number M lead to decrease both the local skin friction coefficient C_{fx} and the local rate of heat transfer Nu_X The velocity profiles also decrease but the temperature profiles increase.

- All the velocity profiles, temperature profiles, the local skin friction coefficient C_{fx} and the local rate of heat transfer Nu_X increase significantly when the values of pressure work parameter Ge increase while $Q=0.40$, $Pr = 0.72$, $M = 1.00$ and $N =0.50$.

- As viscous dissipation parameter N increases, both the velocity and the temperature profiles also increase significantly.

- Increasing values of Prandtl number Pr lead to decrease the velocity profiles, the temperature profiles, the local skin friction coefficient C_{fx} and also the local rate of heat transfer Nu_X.

- An increase in the values of heat generation parameter Q leads to increase both the velocity profiles and the temperature profiles, also the local skin friction coefficient C_{fx} increases and the local rate of heat transfer Nu_X decreases with the increasing values of heat generation parameter.

CONJUGATE EFFECTS OF STRESS WORK AND MAGNETOHYDRODYNAMIC NATURAL CONVECTION FLOW OVER A SPHERE IN THE PRESENCE OF HEAT GENERATION AND RADIATION

Radiation is transformed in the form of electromagnetic waves that directly transport energy through space and this is the only process which brings light and heat to our planet and earth from the sun which is millions of miles away from us. Convection is the transfer of heat by the actual movement of the warmed matter. It cannot occur in solids due to the particles not being able to flow freely. The most common cause of internal movement is a variation in density due to transfer of heat. Free convection is the convection in which motion of the fluid arises solely due to the density gradients that can be maintained in the fluid, for example hot air rising off the surface of a radiator.

The effects of radiation on free convection flow are important in the context of space technology and very little is known about the effects of radiation on the boundary layer flow of a radiating fluid past a body. The inclusion of a radiation effects in the energy equation, however, leads to a highly non-linear partial differential equation. The problem of free convection boundary layer over or on various shapes such as vertical flat plate, cylinder, sphere etc have been studied by many investigators and it has been a very popular research topic for many years. It is readily recognized that a wealth of information is now available on convective heat and mass transfer for viscous (Newtonian) fluids

The governing partial differential equations are to deal with in the case of incompressible viscous fluid such as continuity equation, momentum equation and energy equation. The radiation energy emitted by a body is transmitted in the space in the form of electromagnetic waves according to Maxwell's classic electromagnetic wave theory or in the form of discrete photons according to Planck's hypothesis. Both concepts have been utilized in the investigation of radiative-heat transfer. The emission or absorption of radiation energy by a body is a bulk process; that is, radiation originating from the interior of the body is emitted through the surface.

Vajravelu and Hadjinolaou (1993) studied the heat transfer characteristics in the laminar boundary layer of a viscous fluid over a linearly stretching continuous surface with viscous dissipation or frictional heating and internal heat generation. In this study they considered that the volumetric rate of heat generation q''' [w/m^{-3}]. should he $q''' = Q_0 (T-T_\infty)$, for $T \geq T_\infty$ and equal to zero for $T < T_\infty$, Q_0 is the heat generation / absorption constant.

The present work considers the natural convection boundary layer flow on a sphere of an electrically conducting and steady viscous incompressible fluid in presence of strong magnetic field, effect of radiation, the pressure stress work and heat generation. Here we have focused our attention on the evolution of the surface shear stress in terms of local skin friction and the rate of heat transfer in terms of local Nusselt number, velocity distribution as well as temperature distribution for a selection of parameters set consisting of heat generation parameter Q, the dissipation parameter N, the pressure work parameter Ge, the magnetic parameter or Hartmann number M, the radiation parameter Rd, the surface temperature θ_w and the Prandtl number Pr.

7.1 Formulation of the problem

The governing equations of the flow under the usual Boussinesq and boundary layer approximations are,

$$\frac{\partial}{\partial X}(r U) + \frac{\partial}{\partial Y}(r V) = 0 \tag{7.1}$$

$$U \frac{\partial U}{\partial X} + V \frac{\partial U}{\partial Y} = v \frac{\partial^2 U}{\partial Y^2} + g\beta (T - T_\infty) \sin\left(\frac{X}{a}\right) - \frac{\sigma_0 \beta_0^2}{\rho} U \tag{7.2}$$

$$U \frac{\partial T}{\partial X} + V \frac{\partial T}{\partial Y} = \frac{k}{\rho c_p}\left(\frac{\partial^2 T}{\partial Y^2} - \frac{1}{k}\frac{\partial q_r}{\partial Y}\right) + \frac{v}{\rho C_p}\left(\frac{\partial U}{\partial Y}\right)^2$$

$$+ \frac{Q_0}{\rho C_p}(T - T_\infty) + \frac{T\beta}{\rho C_p} U \frac{\partial p}{\partial X} \tag{7.3}$$

The boundary conditions for the equations (7.2) to (7.3) are

$$U = V = 0, \quad T = T_w \quad \text{on } Y = 0$$

$$U \to 0, \quad T \to T_\infty \quad \text{at } Y \to \infty \tag{7.4}$$

$$r(X) = a \, \sin \left(\frac{X}{a} \right), \text{ where } r = r(X).$$ (7.5)
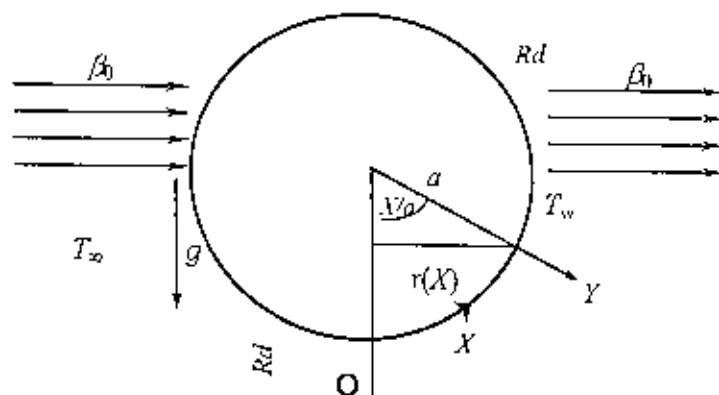
Figure 7.1: Physical model and coordinate system

where, all symbols represent their usual meanings. To transform the above equations into non-dimensional form, the following dimensionless variables [(2.112), (2.113)] are introduced.

Thus (7.5) becomes $r(x) = a \sin x$ (7 6)

Substituting equations (2.112) and (2.113) into the equations (7.1) to (7.3) and after simplifying we have the following equations

$$\frac{\partial}{\partial x}(ru) + \frac{\partial}{\partial y}(rv) = 0$$ (7.7)

$$u \frac{\partial u}{\partial x} + v \frac{\partial u}{\partial y} = \frac{\partial^2 u}{\partial y^2} + \theta \sin x - \frac{\sigma_0 \beta_0^2 a^2}{\rho v Gr^{1/2}} u$$ (7.8)

$$u \frac{\partial \theta}{\partial x} + v \frac{\partial \theta}{\partial y} = \frac{1}{Pr} \frac{\partial}{\partial y} \left[\left\{ 1 + \frac{4}{3} Rd \left(1 + (\theta_w - 1)\theta \right)^3 \right\} \frac{\partial \theta}{\partial y} \right]$$

$$+ \frac{Gr}{a^2 C_p (T_w - T_\infty)} \left(\frac{\partial u}{\partial y} \right)^2 - \left(\frac{T_\infty}{T_w - T_\infty} + \theta \right) \frac{g\beta a}{C_p} u + \frac{Q_0}{\rho C_p} \frac{a^2}{v Gr^{1/2}} \theta$$ (7.9)

where, M, Q, N, Gc, θ_w and Rd are defined earlier. Therefore momentum and energy equations (7.8) and (7.9) can be written as

$$u\frac{\partial u}{\partial x} + v\frac{\partial u}{\partial y} + Mu - \theta\sin x = \frac{\partial^2 u}{\partial y^2} \tag{7.10}$$

$$u\frac{\partial \theta}{\partial x} + v\frac{\partial \theta}{\partial y} = \frac{1}{Pr}\frac{\partial}{\partial y}\left[\left\{1+\frac{4}{3}Rd(1+(\theta_w-1)\theta)^3\right\}\frac{\partial\theta}{\partial y}\right]$$

$$+Q\theta + N\left(\frac{\partial u}{\partial y}\right)^2 - Ge\left(\frac{T_\infty}{T_w-T_\infty}+\theta\right)u \tag{7.11}$$

The boundary conditions associated with equations (7.4) become

$$u=v=0,\ \theta=1\ \text{at}\ y=0$$
$$u\rightarrow 0,\ \theta\rightarrow 0\ \text{as}\ y\rightarrow\infty \tag{7.12}$$

Now substituting equations (2.121 and (2.123)) into equations (7.10) and (7.11) subject to the boundary conditions (7.12), after simplifying then we have the followings

$$\frac{\partial^3 f}{\partial y^3}+\left(1+\frac{x}{\sin x}\cos x\right)f\frac{\partial^2 f}{\partial y^2}-\left(\frac{\partial f}{\partial y}\right)^2+\frac{\theta}{x}\sin x - M\frac{\partial f}{\partial y}=x\left(\frac{\partial f}{\partial y}\frac{\partial^2 f}{\partial y\partial x}-\frac{\partial f}{\partial x}\frac{\partial^2 f}{\partial y^2}\right) \tag{7.13}$$

$$\frac{1}{Pr}\frac{\partial}{\partial y}\left\{\left(1+\frac{4}{3}Rd(1+(\theta_w-1)\theta)^3\right)\frac{\partial\theta}{\partial y}\right\}+\left(1+\frac{x}{\sin x}\cos x\right)f\frac{\partial\theta}{\partial y}+Q\theta$$

$$+Nx^2\left(\frac{\partial^2 f}{\partial y^2}\right)^2-Ge\left(\frac{T_\infty}{T_w-T_\infty}+\theta\right)\frac{\partial f}{\partial y}=x\left(\frac{\partial f}{\partial y}\frac{\partial\theta}{\partial x}-\frac{\partial\theta}{\partial y}\frac{\partial f}{\partial x}\right) \tag{7.14}$$

The corresponding boundary conditions are

$$f=\frac{\partial f}{\partial y}=0,\ \theta=1\ \text{at}\ y=0$$
$$\frac{\partial f}{\partial y}\rightarrow 0,\ \theta\rightarrow 0\quad\text{as}\ y\rightarrow\infty \tag{7.15}$$

In practical application, the physical quantities of principal interest are the heat transfer and the skin- friction coefficient, which can be written in non- dimensional form as

$$Nu_x=\frac{aGr^{-\frac{1}{4}}}{k\left(T_w-T_\infty\right)}\times-\frac{k(T_w-T_\infty)}{aGr^{-\frac{1}{4}}}\left(\frac{\partial\theta}{\partial y}\right)_{y=0}$$

$$\therefore Nu_x=-\left(1+(4/3)Rd\theta_w^3\right)\frac{\partial\theta(x,0)}{\partial y} \tag{7.16}$$

$$\therefore C_{fx} = x \left(\frac{\partial^2 f}{\partial y^2} \right)_{y=0}$$

(7.17)

Now we will discuss velocity distribution as well as temperature distribution for a selection of parameter sets consisting of heat generation parameter Q, radiation parameter Rd, the surface temperature parameter θ_w, the viscous dissipation parameter N, the pressure work parameter Ge, magnetic parameter M and the Prandlt number Pr.

7.2: Results and Discussion

The effect of stress work and magnetohydrodynamic natural convection flow on a sphere in presence of heat generation parameter and radiation parameter has been investigated. The problem considered here involves a number of parameters on the basis of which a wide range of numerical results have been derived. Of these results, a small section is presented here for brevity. The numerical results of velocity and temperature profiles and also for local skin frictions as well as local heat transfer coefficient are shown in figures 7.2 to figures 7.13 for various values of parameters entering into the problem.

Figure 7.2(a) and figure 7.2(b) display the effects of the velocity and temperature profiles, based on equations (7.13) and (7.14) with boundary conditions (7.15), for different small values of pressure work parameter Ge (= -0 10, 0.10, 0.30, 0 50) plotted against y at $x = \pi/6$ having $Pr = 0.72$, $Rd = 1.00$, $\theta_w = 1.10$, $M = 0.50$, $N = 0.10$ and $Q = 0.40$.

From figure 7.2(a), it is seen that the velocity profile is influenced considerably when the value of pressure work parameter Ge increases. But near the surface of the sphere velocity increases significantly and decreases slowly and finally approaches to zero. The maximum values of the velocity are 0.36546, 0.39176, 0.42331 and 0.46132 for Ge (= -0.10, 0.10, 0.30, 0.50) respectively which occur at $y = 1.17520$ for first maximum value, $y = 1.23788$ for second and third maximum values and at $y = 1.30254$ for last maximum value. Here it is observed that the velocity increase by 26 23% as Ge increases from -0.10 to 0.50. Also from figure 7 2(b), it has been observed that when the value of pressure work parameter Ge increases, the temperature profiles also increases significantly. The temperatures are 0.68229, 0.73077, 0.78949 and 0.86191 for Ge = -0.10, 0.10, 0.30, 0.50 at $y = 1.05539$ which indicates that the temperature increase by 26.33% at that point.

Figure 7 3 (a) and figure 7.3(b) deal with the effect of the magnetic parameters or Hartmann number M (=0.1, 0.4, 0.6, 0.8, 1.0) with other controlling parameters $Pr = 0.72$, $Rd = 2.00$, $\theta_w = 1.10$, $Q = 0.03$, $N = 0\ 30$ and $G_e = 0.50$ on the velocity and temperature profiles. From figure 7.3(a), it is revealed that the velocity profile retards with the increase of the magnetic parameter M that indicates that magnetic parameter decreases the fluid motion. But it is observed that the temperature profiles increase with the increase of magnetic parameter M that is evident from figure 7.3 (b).

Figure 7.4(a) depicts the velocity profile for different values of the Prandtl number Pr (= 0.50, 0.72, 1 00, 1.74) with parameters $Rd = 2.00$, $\theta_w = 1,10$, $M = 0.50$, $Q = 0.30$. $N = 0.20$ and $G_e = 0.40$. Corresponding distribution of the temperature profile is shown in figure 7.4 (b). From figure 7.4(a), it can be seen that if the Prandtl number increases, the velocity of the fluid decreases. On the other hand, from figure 7.4(b) we observe that the temperature profile decreases within the boundary layer due to increase of the Prandtl number Pr.

Figure 7.5 (a) and figure 7.5(b) illustrate the effect of the heat generation parameter Q (= 0.00, 0.20, 0.40, 0.50) with parameters $Pr = 0\ 72$, $Rd = 1.00$, $\theta_w = 1.1$, $M = 0.50$, $N = 0.10$ and $Ge = 0.50$ on the velocity profile and the temperature profile. From figure 7.5(a), it is revealed that the velocity profile increases with the increase of the heat generation parameter Q that indicates that heat generation parameter accelerates the fluid motion. Small increment is shown from figure 7.5(b) on the temperature profile for increasing values of Q.

From figure 7.6(a), it may be concluded that the radiation heat increases the velocity field in the region $y \in [0, 12]$. The changes of velocity profiles in the y direction reveals the typical velocity profile for natural convection boundary layer flow i.e. the velocity is zero at the boundary of wall then it increases and reaches to the peak value as y increases and finally the velocity approaches to zero (the asymptotic value). The maximum values of the velocity are 0.40934, 0.44132, 0.47876, 0.50425, 0.52296 for $Rd = 0.00$, 1.00, 2.00, 3.00, 4.00 respectively and which occurs at $y = 1.23788$ for first and second maximum values, at $y = 1.36929$ for third and fourth maximum values and $y = 1.43822$ for last maximum value. Here we see that the velocity increases by 27.76% as Rd increases from 0.00 to 4 00. In figure 7.6(b) it is clearly seen that the temperature distribution increases owing to increase of the values of the radiation parameter Rd and maximum is at the wall.

Figure 7.7(a) shows the effects of the velocity profile for different values of the surface temperature parameter θ_w = 0.00, 0.40, 0.60, 0.80, 1.00, 1.20 while the other controlling parameters Rd = 1.00, Pr = 0.72, Q = 0.30, M = 0.50, N = 0.20 and Ge = 0.50. Corresponding distribution of the temperature profile is shown in figure 7.7(b). From figure 7.7(a), it is seen that if the surface temperature parameter increases, the velocity of the fluid also increases. On the other hand, it is observed that the temperature profile increases within the boundary layer due to increase of the surface temperature parameter θ_w which is evident from figure 7.7(b).

Numerical values of the local skin friction coefficient C_{fx} and the local rate of heat transfer coefficient Nu_x are depicted graphically in figure 7.8(a) and figure 7.8(b) respectively against the axial distance y for different values of the pressure work parameter Ge (= -0.10, 0.10, 0.30, 0.50) for the fluid having Prandtl number Pr = 0.72 and other fixed parameters. From figure 7.8(a) and figure 7.8(b), it is seen that an increase in the value of the pressure work parameter Ge leads to increase the local skin friction coefficient C_{fx} and the local rate of heat transfer coefficient Nu_x.

The variation of the reduced local skin friction coefficient C_{fx} and local rate of heat transfer Nu_x for different values of magnetic parameter M (= 0.10 0.40, 0 60, 0.80, 1.00) with x are illustrated in figure 7.9(a) and figure 7.9(b) both for Pr = 0.72, Rd = 2.00, Q = 0.03, θ_4 = 1.10, N = 0.30 and Ge = 0.50. From figure 7.9(a) and figure 7.9(b), it is observed that both local skin friction coefficient C_{fx} and local rate of heat transfer coefficient Nu_x decrease slightly as the values of magnetic parameter or Hartmann number M increases at different position of x (in radian). Thus we can say that the magnetic field is limited to retardation though in presence of heat generation parameter Q.

Variations of the local skin friction coefficient C_{fx} and local rate of heat transfer Nu_x for different values of Prandtl number Pr (=0.50, 0 72, 1.00, 1.74) with other fixed values of controlling parameters are shown in the figure 7.10(a) and figure 7.10(b). From figure 7.10(a) and figure 7.10(b) it is seen that as the Prandtl number Pr increases, the local skin friction coefficient decreases and heat transfer coefficient increases but the rate of increase in the heat transfer coefficient is higher than that of the skin friction coefficient. So, the effect of Prandtl number Pr on heat transfer coefficient is more than the effect of Pr on local skin friction coefficient.

Figure 7.11(a) and figure 7.11(b) illustrate the variation of local skin friction coefficient C_{fx} and the rate of local heat transfer Nu_x against x for different values of heat generation parameter Q (= 0.00, 0.20, 0.40, 0.50) as obtained by solving numerically equations (7.13) and (7.14) where $Pr = 0.72$, $\theta_w = 1.1$, $M = 0.50$, $Rd = 1.00$, $N = 0.10$ and $Ge = 0.50$. It is seen from figure 7.11(a) that the skin friction coefficient C_{fx} is influenced considerably and increases when the values of heat generation parameter Q increase at different position of x (in radian) with other controlling parameters. Figure 7.11(b) indicates that the rate of local of heat transfer Nu_x decreases owing to increase in values of heat generation parameter Q with other fixed parameters

The effect for different values of radiation parameter Rd (= 0.00, 1.00, 2.00, 3.00, 4.00), the local skin friction coefficient C_{fx} and local rate heat of transfer coefficient Nu_x are shown in the figure 7.12(a) and figure 7.12(b) while Prandtl number $Pr = 0.72$, magnetic parameter $M = 0.50$, heat generation parameter $Q = 0.40$, dissipation parameter $N = 0.40$, pressure work parameter $Ge = 0.60$ and surface temperature parameter $\theta_w = 1.1$. Here, it is seen that as the radiation parameter Rd increases both the local skin friction coefficient and local rate of heat transfer coefficient increase

From figure 7.13(a) and figure 7.13(b), it can also easily be seen that an increase in the surface temperature parameter θ_w leads to increase the local skin friction coefficient C_{fx} and the local rate of heat transfer coefficient Nu_x slightly while Prandtl number $Pr = 0.72$, heat generation parameter $Q = 0.30$, magnetic parameter $M = 0.50$, viscous dissipation parameter $N = 0.20$, pressure work parameter $Ge = 0.50$ and radiation-conduction parameter $Rd = 1.00$. Also it is observed that at any position of x, the local skin friction coefficient C_{fx} and the local Nusselt number Nu_x increase as θ_w increases from 0.00 to 1.2. This phenomenon can easily be understood from the fact that when the surface temperature parameter θ_w increases, the temperature of the fluid rises and the thickness of the velocity boundary layer grows i.e. the thermal boundary layer becomes thinner than the velocity boundary layer. Therefore the skin friction coefficient C_{fx} and the local Nusselt number Nu_x are increased.
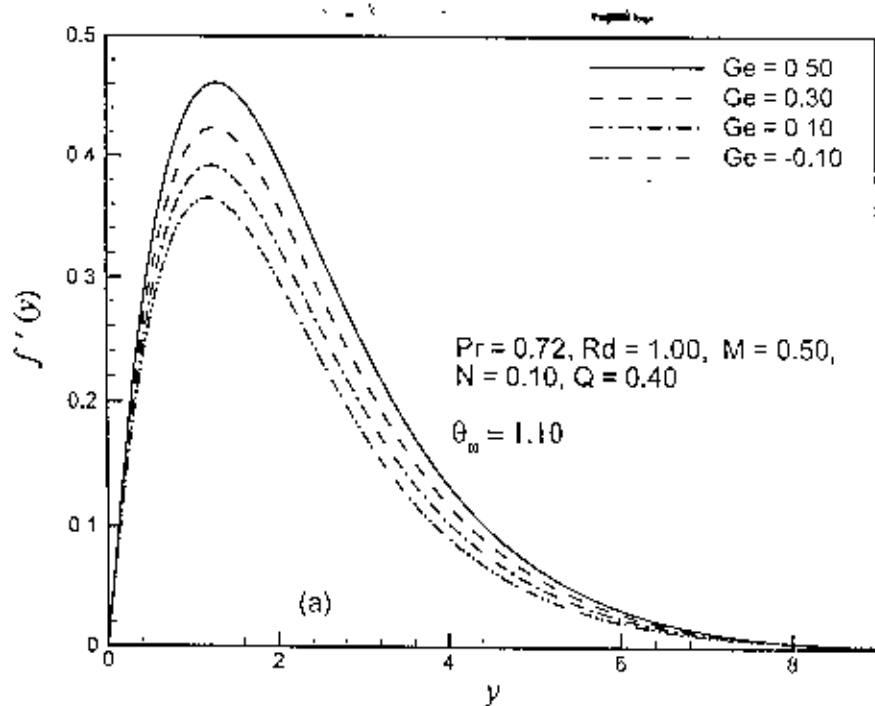
Figure 7.2(a): Variation of dimensionless velocity profiles $f'(x, y)$ against dimensionless distance y for different values of pressure work parameter Ge with $Pr = 0.72$, $M = 0.50$, $N = 0.10$, $Rd = 1.00$, $\theta_w = 1.10$ and $Q = 0.40$.
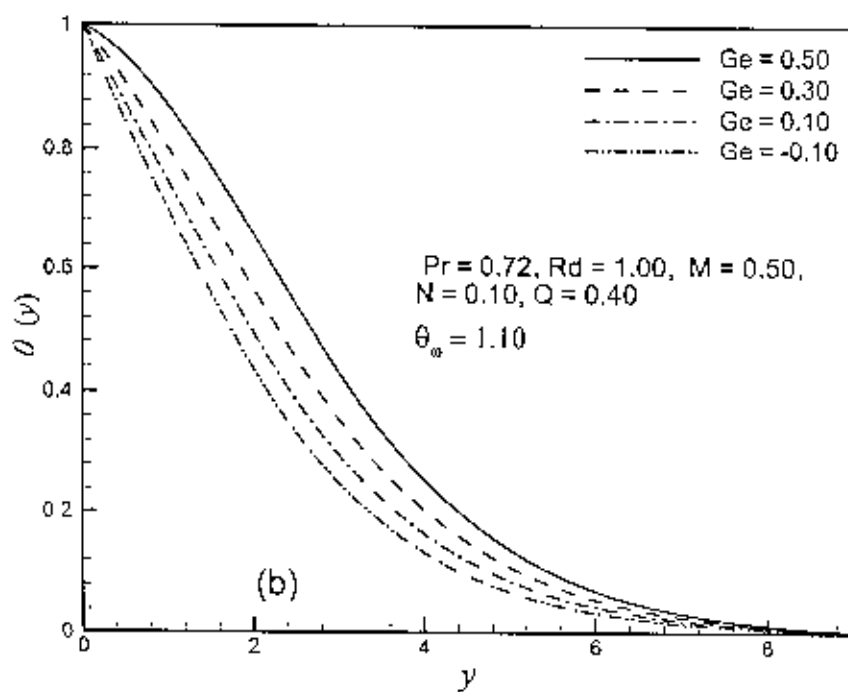
Figure 7.2(b): Variation of dimensionless temperature profiles $\theta(x, y)$ against dimensionless distance y for different values of pressure work parameter Ge with $Pr = 0.72$, $M = 0.50$, $N = 0.10$, $Rd = 1.00$, $\theta_w = 1.10$ and $Q = 0.40$.
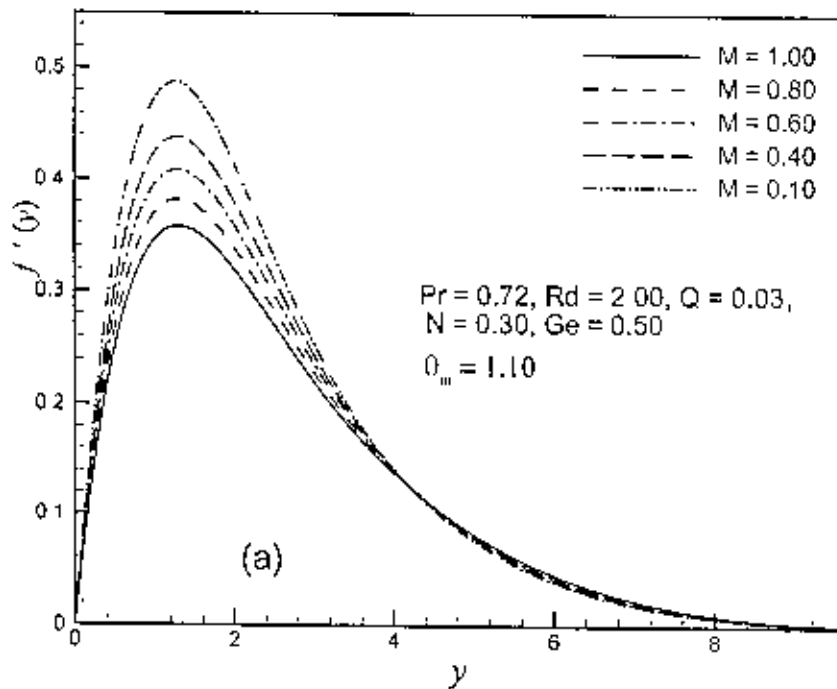
Figure 7.3(a): Variation of dimensionless velocity profiles $f'(x, y)$ against dimensionless distance y for different values of magnetic parameter or Hartmann number M with $Pr = 0.72$, $N = 0.30$, $Ge = 0.50$, $Rd = 2.00$, $\theta_w = 1.10$ and $Q = 0.03$
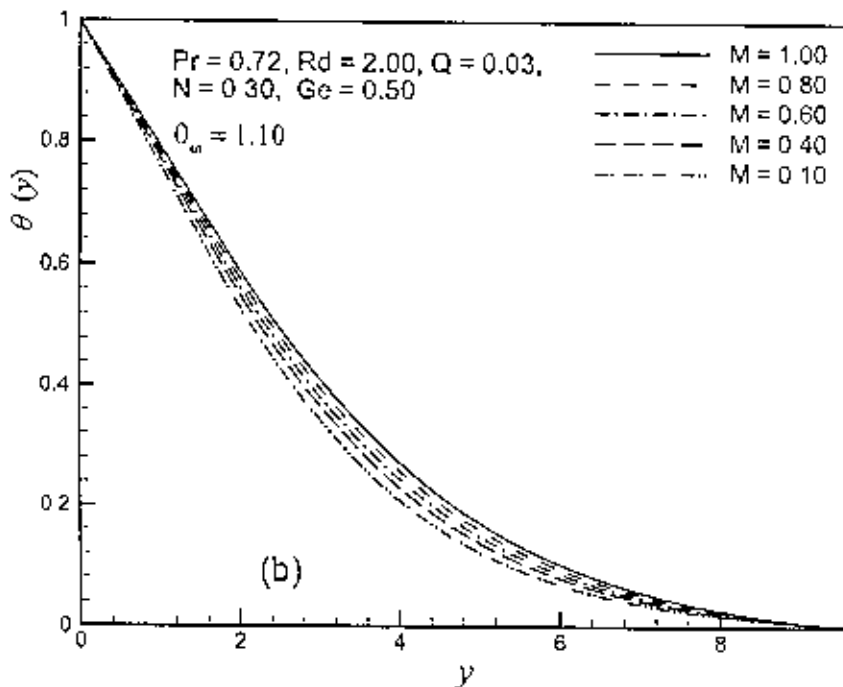
Figure 7.3(b): Variation of dimensionless temperature profiles $\theta(x, y)$ against dimensionless distance y for different values of magnetic parameter or Hartmann number M with $Pr = 0.72$, $N = 0.30$, $Ge = 0.50$, $Rd = 2.00$, $\theta_w = 1.10$ and $Q = 0.03$.
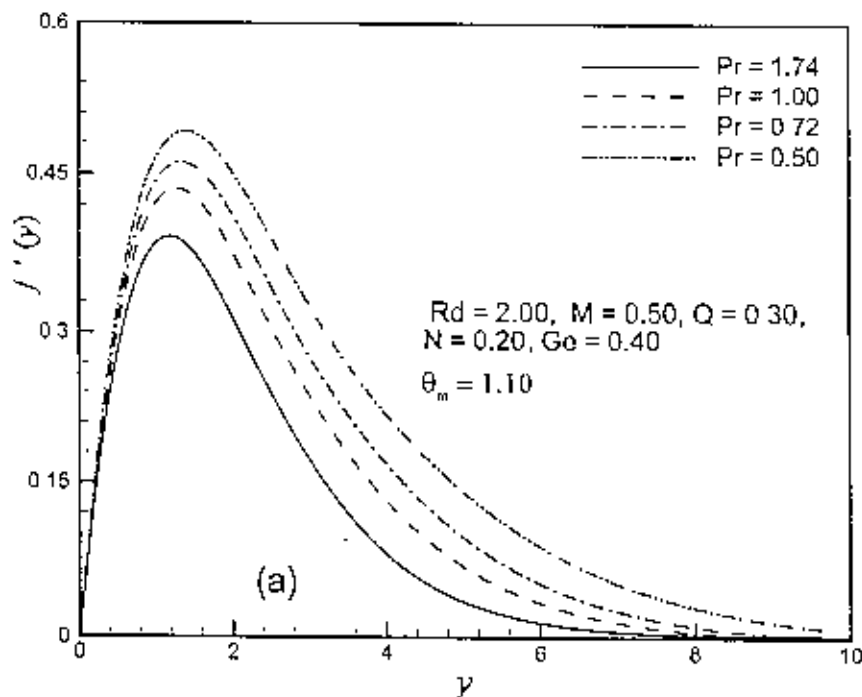
Figure 7.4(a): Variation of dimensionless velocity profiles $f'(x, y)$ against dimensionless distance y for different values of Prandtl number Pr with $M = 0.50$, $N = 0.20$, $Ge = 0.40$, $Rd = 2.00$, $\theta_w = 1.10$ and $Q = 0.30$.
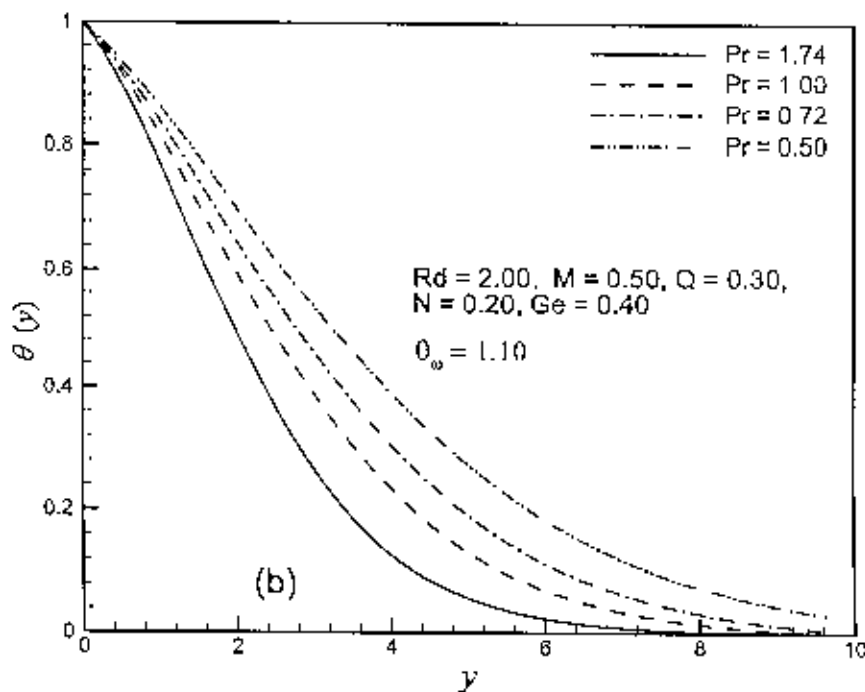
Figure 7.4(b): Variation of dimensionless temperature profiles $\theta(x, y)$ against dimensionless distance y for different values of Prandtl number Pr with $M = 0.50$, $N = 0.20$, $Ge = 0.40$, $Rd = 2.00$, $\theta_w = 1.10$ and $Q = 0.30$.
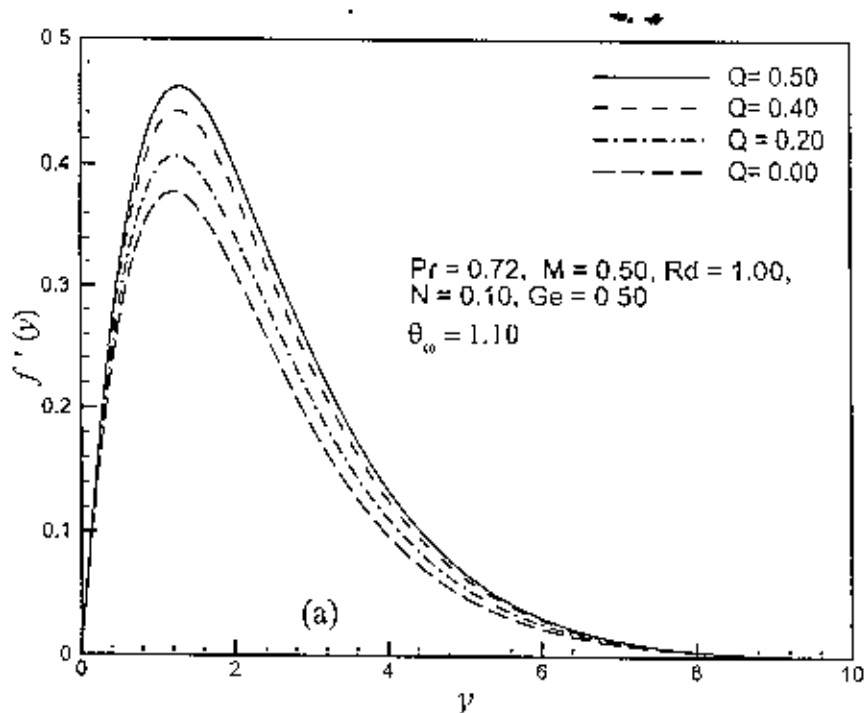
Figure 7.5(a): Variation of dimensionless velocity profiles $f'(x, y)$ against dimensionless distance y for different values of heat generation parameter Q with $M = 0.50$, $N = 0.10$, $Ge = 0.50$, $Rd = 1.00$, $\theta_w = 1.10$ and $Pr = 0.72$.
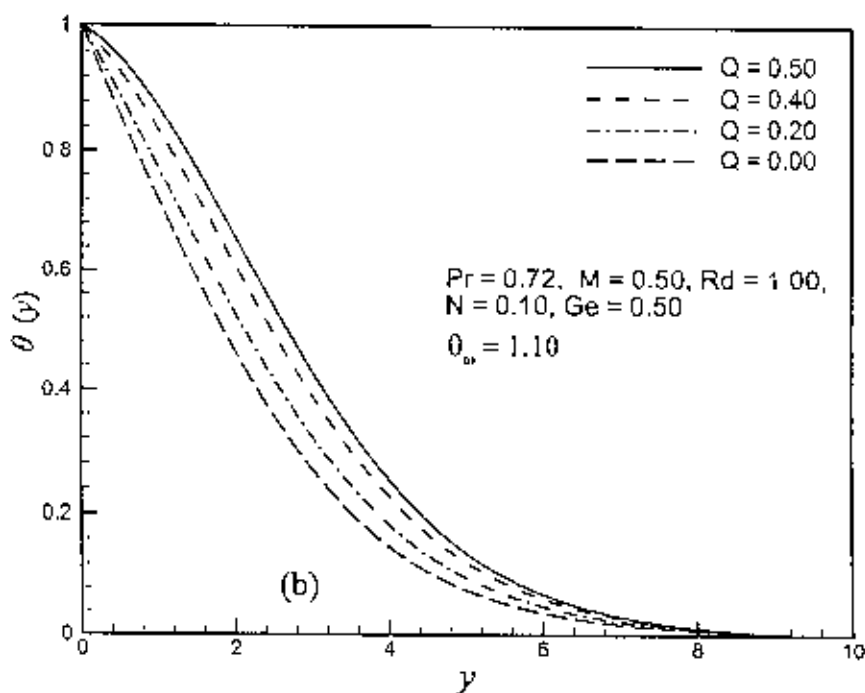
Figure 7.5(b): Variation of dimensionless temperature profiles $\theta(x, y)$ against dimensionless distance y for different values of heat generation parameter Q with $M = 0.50$, $N = 0.10$, $Ge = 0.50$, $Rd = 1.00$, $\theta_w = 1.10$ and $Pr = 0.72$.
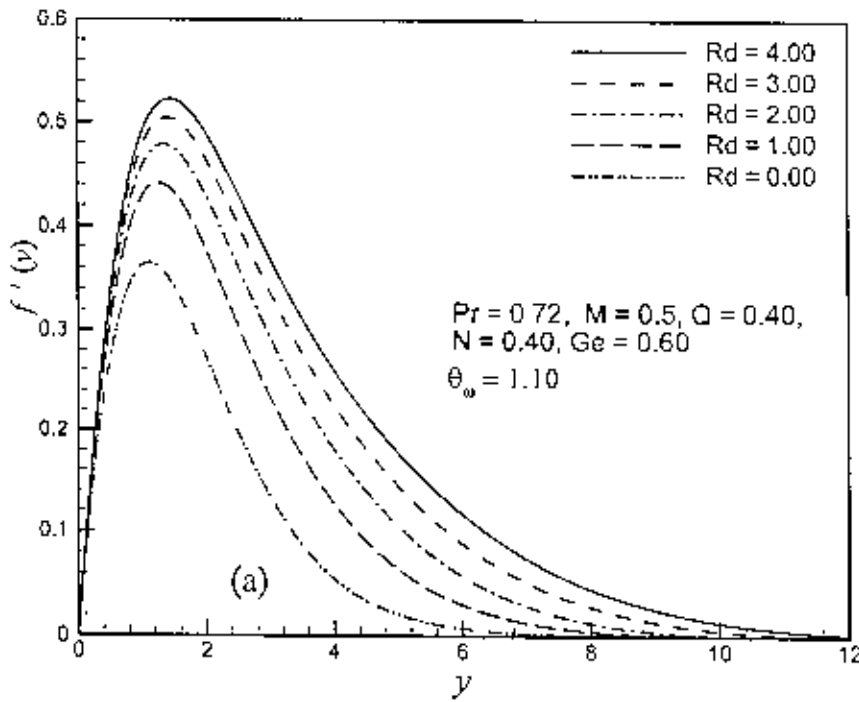
Figure 7.6(a): Variation of dimensionless velocity profiles $f'(x, y)$ against dimensionless distance y for different values of radiation parameter Rd with $M = 0.60$, $N = 0.40$, $Ge = 0.60$, $Q = 0.40$, $\theta_v = 1.10$ and $Pr = 0.72$.
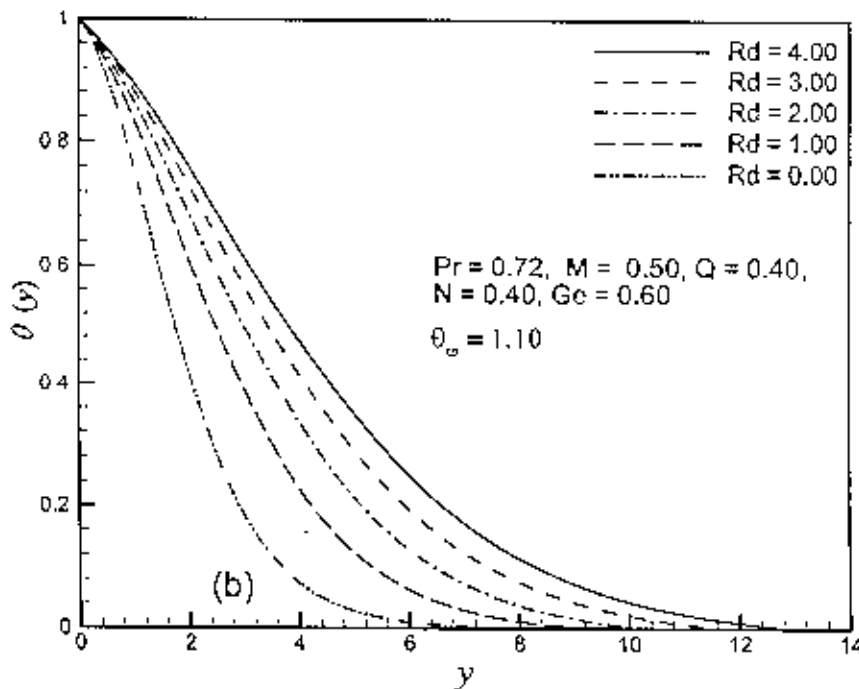
Figure 7.6(b): Variation of dimensionless temperature profiles $\theta(x, y)$ against dimensionless distance y for different values of radiation parameter Rd with $M = 0.60$, $N = 0.40$, $Ge = 0.60$, $Q = 0.40$, $\theta_e = 1.10$ and $Pr = 0.72$.
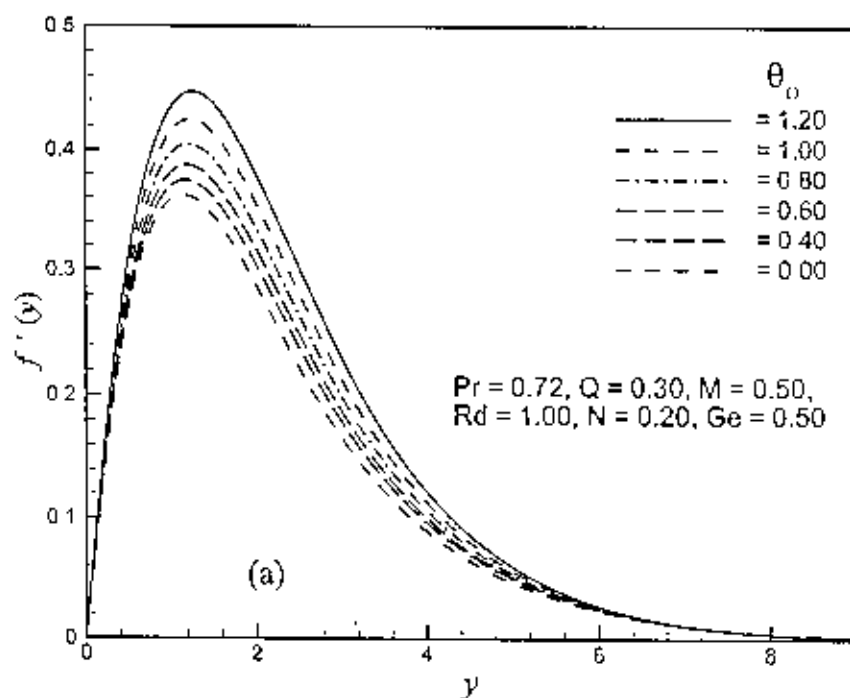
Figure 7.7(a): Variation of dimensionless velocity profiles $f'(x, y)$ against dimensionless distance y for different values of surface temperature parameter θ_w with $M = 0.50$, $N = 0.20$, $Ge = 0.50$, $Q = 0.30$, $Rd = 1.00$ and $Pr = 0.72$.
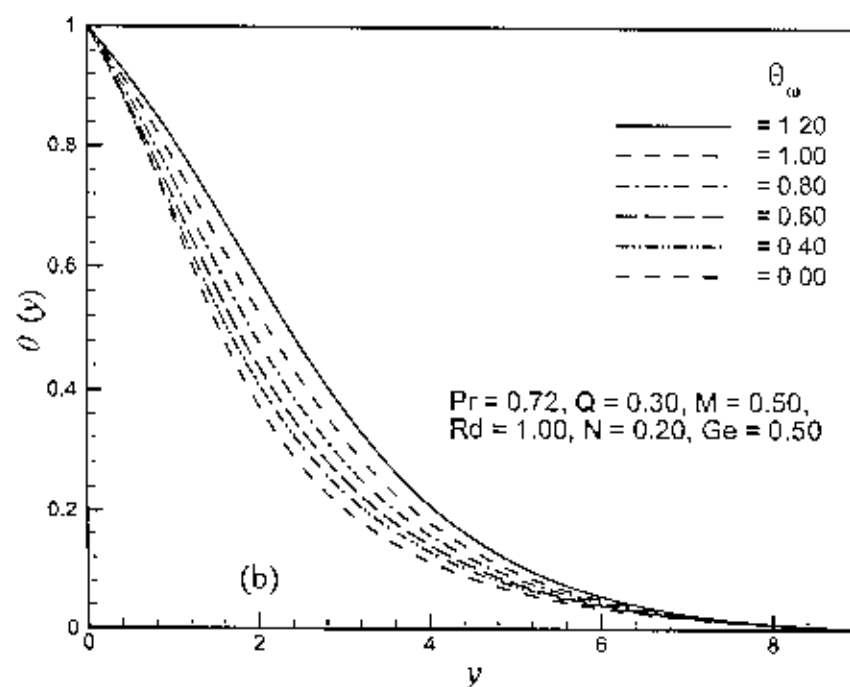
Figure 7.7(b): Variation of dimensionless temperature profiles $\theta(x, y)$ against dimensionless distance y for different values of surface temperature parameter θ_w with $M = 0.50$, $N = 0.20$, $Ge = 0.50$, $Q = 0.30$, $Rd = 1.00$ and $Pr = 0.72$.
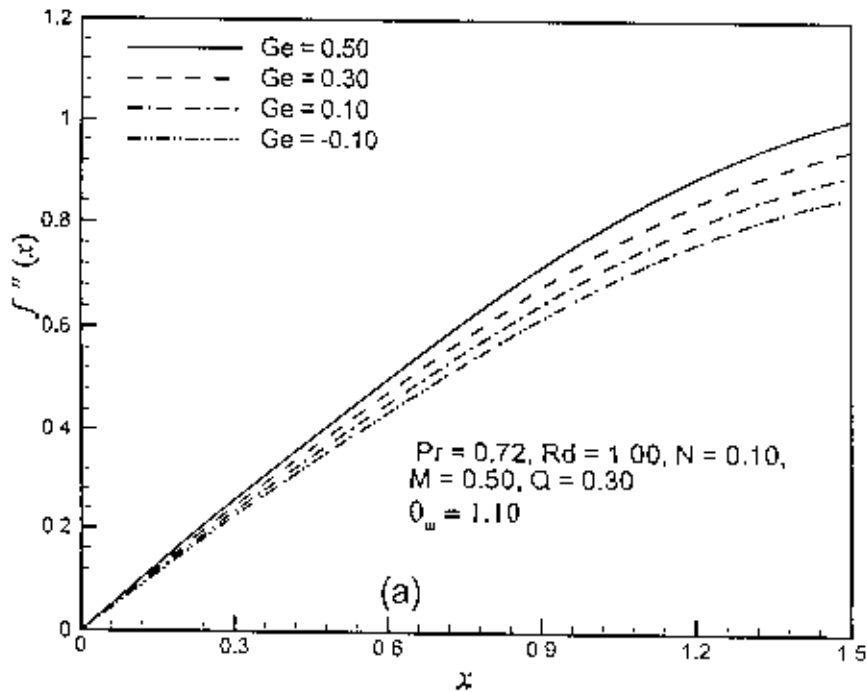
Figure 7.8(a): Variation of skin friction coefficient, C_{fx} with dimensionless distance x for different values of pressure work parameter Ge with $Q = 0.40$, $N = 0.10$, $M = 0.50$ Rd = 1.00, $\theta_w = 1.10$ and $Pr = 0.72$.
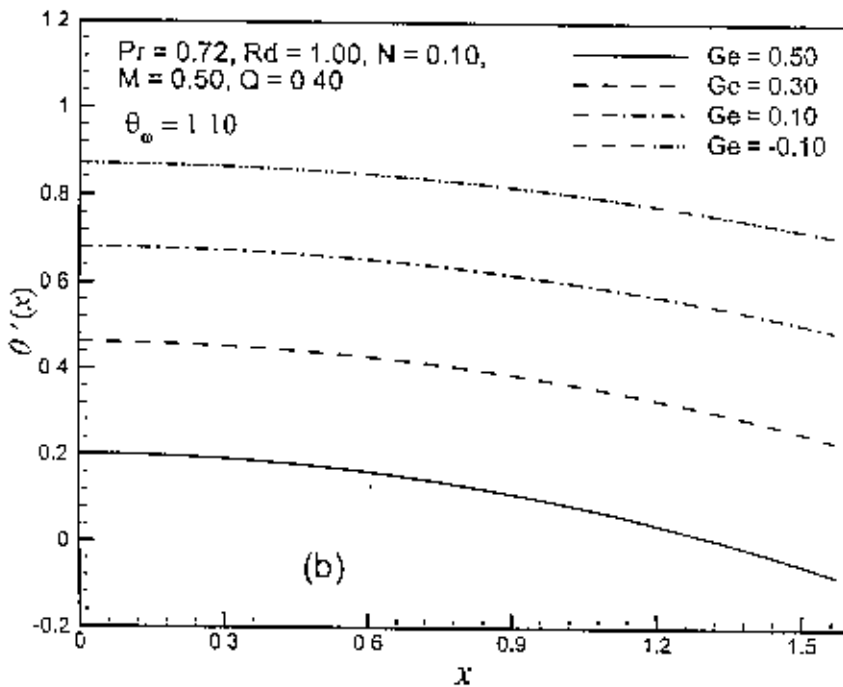
Figure 7.8(b): Variation of local Nusselt number, Nu_x with dimensionless distance x for different values of pressure work parameter Ge with $Q = 0.40$, $N = 0.10$, $M = 0.50$ Rd = 1.00, $\theta_w = 1.10$ and $Pr = 0.72$.
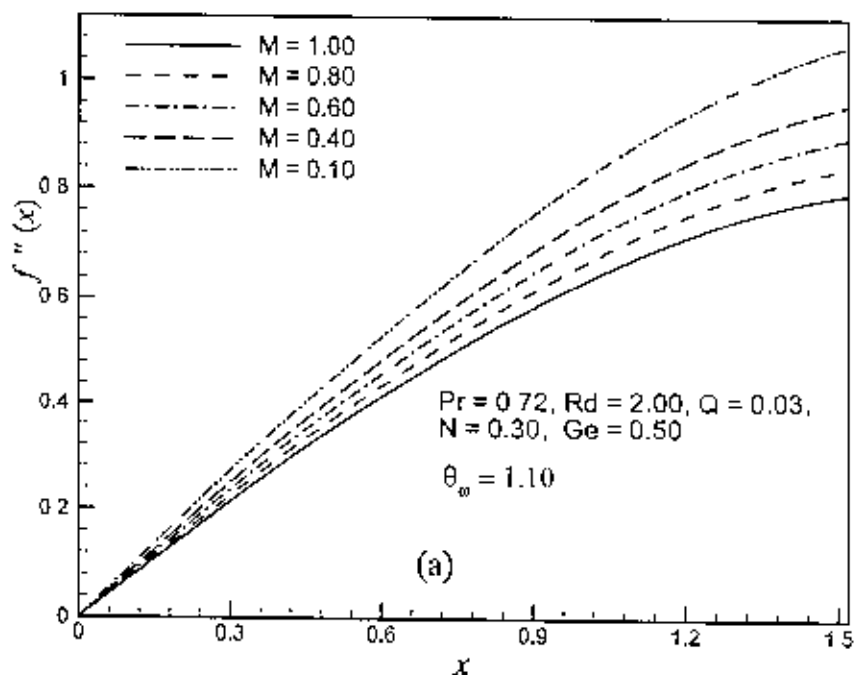
Figure 7.9(a): Variation of skin friction coefficient, C_{fx} with dimensionless distance x for different values of magnetic parameter or Hartmann Number M with $Q = 0.03$, $N = 0.30$, $Ge = 0.50$, $Rd = 2.00$, $\theta_w = 1.10$ and $Pr = 0.72$.
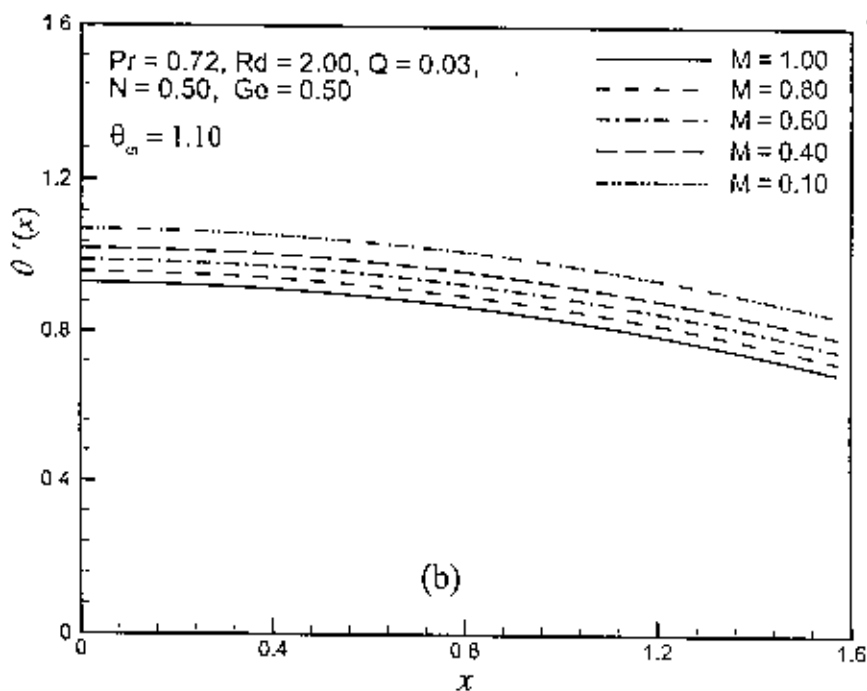
Figure 7.9(b): Variation of local Nusselt number, Nu_x with dimensionless distance x for different values of magnetic parameter or Hartmann Number M with $Q = 0.03$, $N = 0.30$, $Ge = 0.50$, $Rd = 2.00$, $\theta_w = 1.10$ and $Pr = 0.72$.
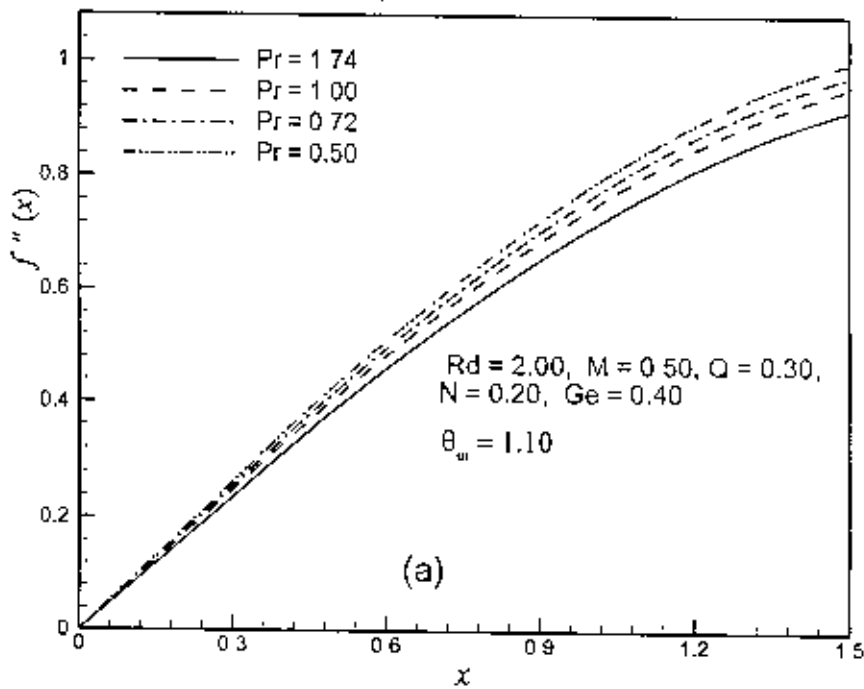
Figure 7.10(a): Variation of skin friction coefficient, C_{fx} with dimensionless distance x for different values of Prandtl number Pr with $Q = 0.30$, $N = 0.20$, $Ge = 0.40$, $Rd = 2.00$, $\theta_w = 1.10$ and $M = 0.50$.
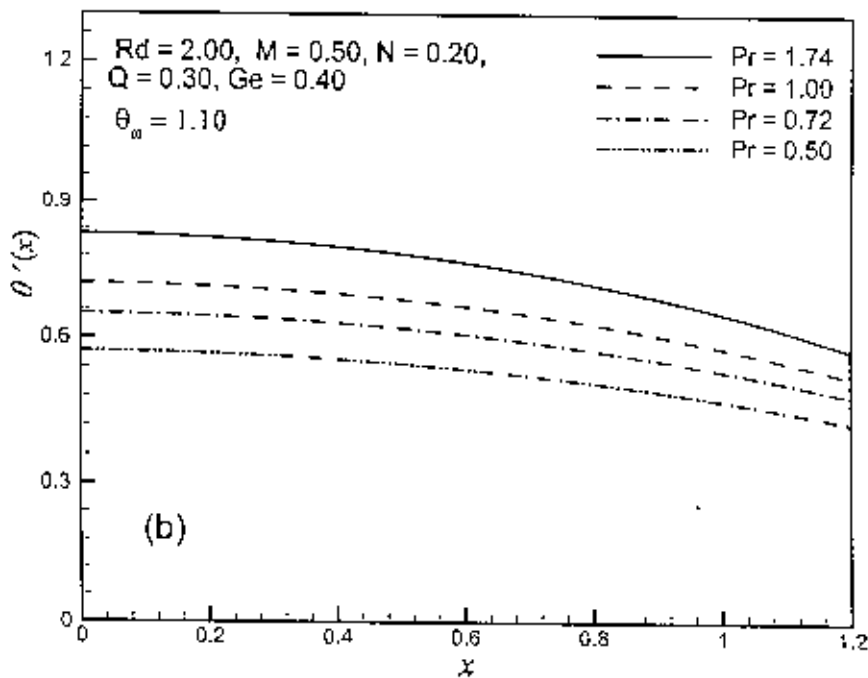
Figure 7.10(b): Variation of local Nusselt number, Nu_x with dimensionless distance x for different values of Prandtl number Pr with $Q = 0.30$, $N = 0.20$, $Ge = 0.40$, $Rd = 2.00$, $\theta_w = 1.10$ and $M = 0.50$.
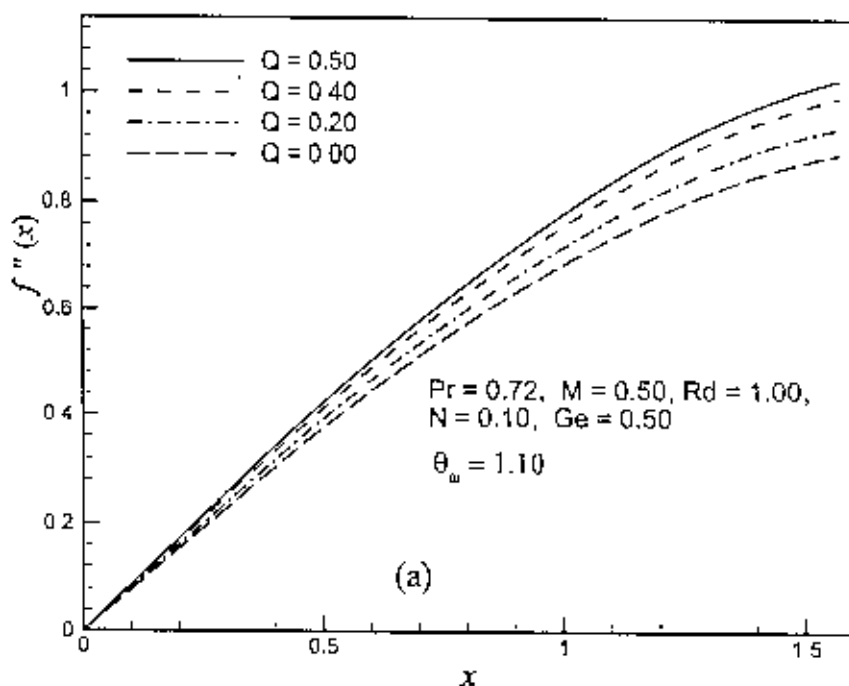
Figure 7.11(a): Variation of skin friction coefficient, C_{fx} with dimensionless distance x for different values of heat generation parameter Q with $Pr = 0.72$, $N = 0.10$, $Ge = 0.50$, $Rd = 1.00$, $\theta_w = 1.10$ and $M = 0.50$.
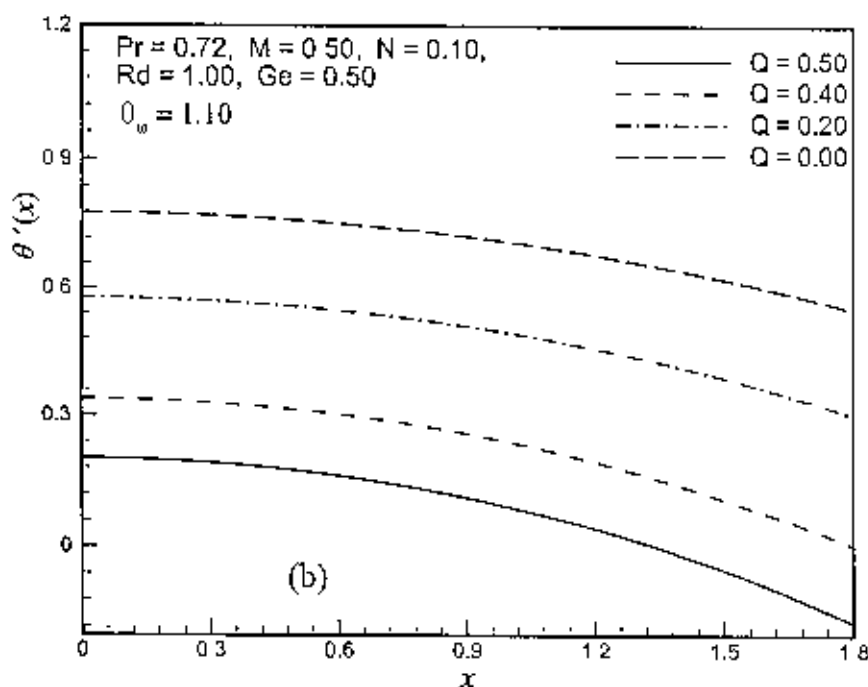
Figure 7.11(b): Variation of local Nusselt number, Nu_x with dimensionless distance x for different values of heat generation parameter Q with $Pr = 0.72$, $N = 0.10$, $Ge = 0.50$, $Rd = 1.00$, $\theta_w = 1.10$ and $M = 0.50$.
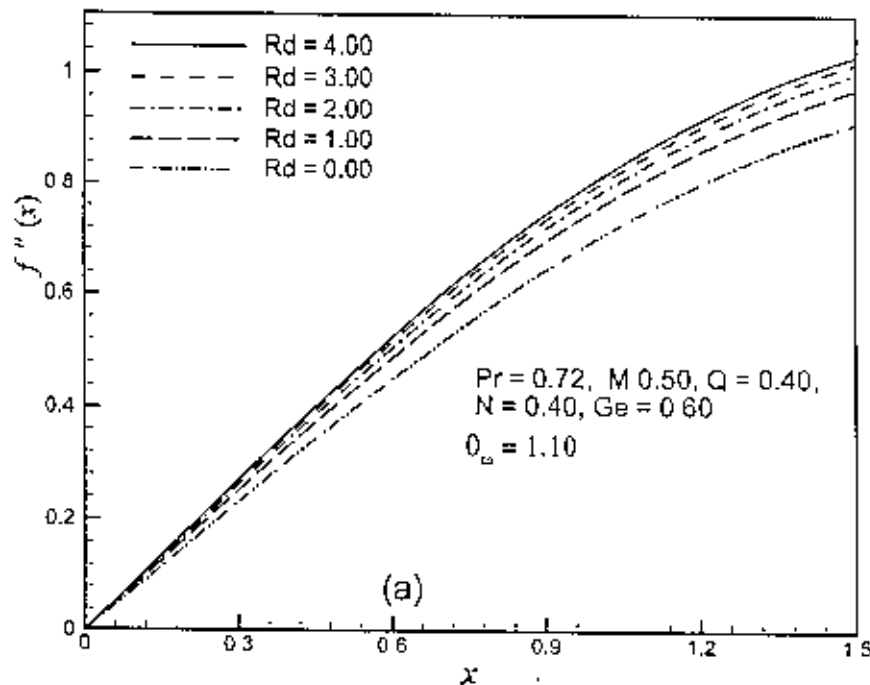
Figure 7.12(a): Variation of skin friction coefficient, C_{fx} with dimensionless distance x for different values of radiation parameter Rd with $Pr = 0.72$, $N = 0.40$, $Ge = 0.60$, $Q = 0.40$, $\theta_w = 1.10$ and $M = 0.50$.
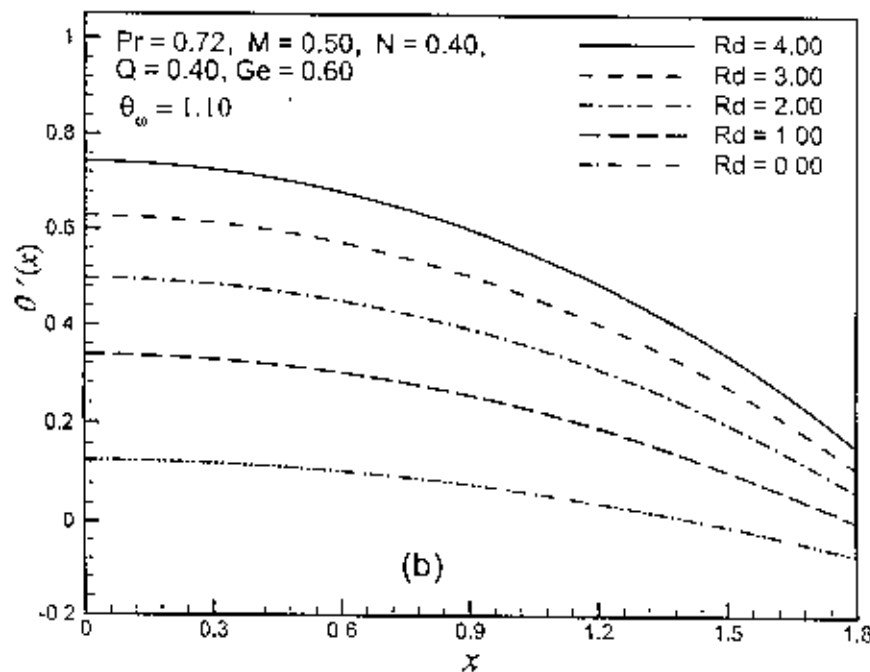
Figure 7.12(b): Variation of local Nusselt number, Nu_x with dimensionless distance x for different values of radiation parameter Rd with $Pr = 0.72$, $N = 0.40$, $Ge = 0.60$, $Q = 0.40$, $\theta_w = 1.10$ and $M = 0.50$.
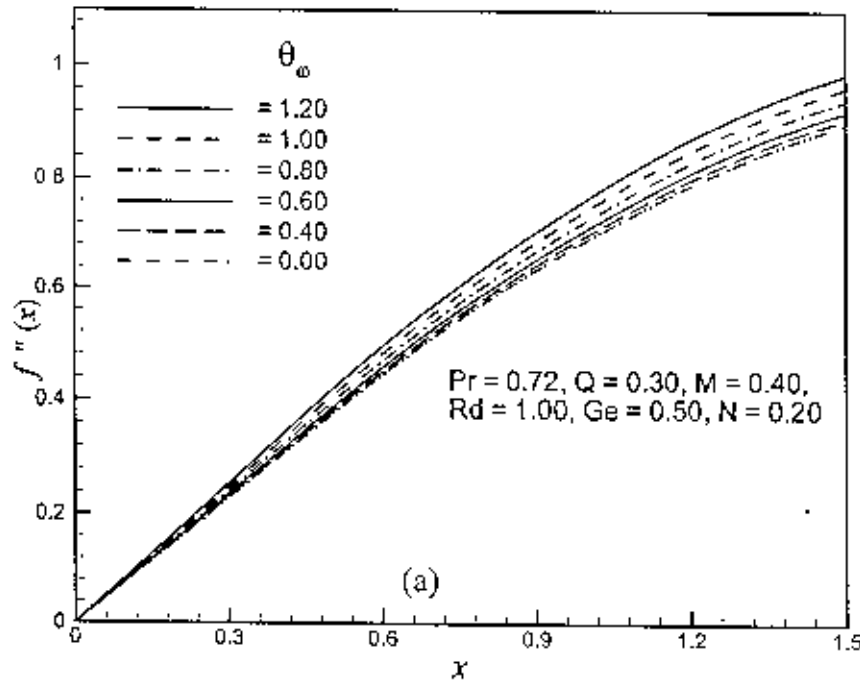
Figure 7.13(a): Variation of skin friction coefficient, C_{fx} with dimensionless distance x for different values of surface temperature parameter θ_w with $Pr = 0.72$, $N = 0.40$, $Ge = 0.50$, $Q = 0.30$, $Rd = 1.00$ and $M = 0.50$.
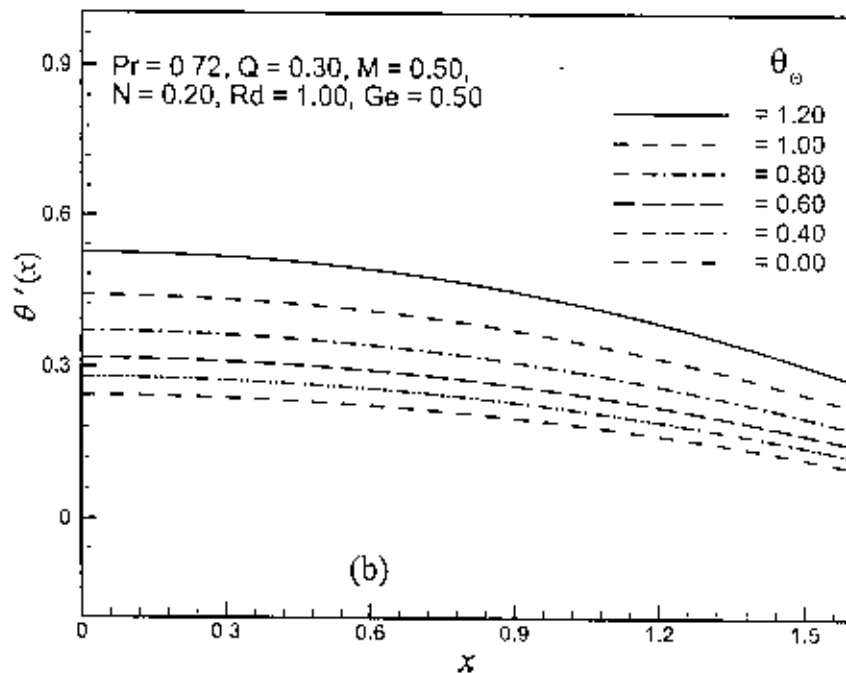
Figure 7.13(b): Variation of local Nusselt number, Nu_x with dimensionless distance x for different values of surface temperature parameter θ_w with $Pr = 0.72$, $N = 0.40$, $Ge = 0.50$, $Q = 0.30$, $Rd = 1.00$ and $M = 0.50$.

The values of the local skin friction coefficient C_{fx} and local Nusselt number Nu_x for different values of radiation parameter Rd while $Pr = 0.72$, $\theta_w = 1.1$, $M = 0.5$, $Q = 0.40$, $N = 0.40$ and $Ge = 0.60$ are presented in Table-C_{17} which is showed in Appendix C. Here we see that the values of local skin friction coefficient C_{fx} increase at different position of x for radiation parameter $Rd = 1.00$, 2.00, 3.00, 4.00. The rate of the local skin friction coefficient C_{fx} increases by 6.76% as the radiation parameter Rd changes from 1.00 to 4.00 and $x = 0.8028$. Furthermore, it is seen that the numerical values of the local Nusselt number Nu_x increase for increasing values of radiation parameter Rd. The rate of increase of the local Nusselt number Nu_x is 56.49% at position $x = 0.8028$ as the radiation parameter Rd changes from 1.00 to 4.00.

The values of the skin friction coefficient and local Nusselt number for different values of heat generation parameter Q while $Pr = 0.72$, $\theta_w = 1.1$, $Rd = 1.0$, $M = 0.5$, $N = 0.20$ and $Ge = 0.50$ are entered in Table-C_{18} which is shown in Appendix C. Here we observe that the values of skin friction coefficient C_{fx} decrease at different position of x for heat generation parameter $Q = 0.00$, 0.20, 0.40. The rate of the skin friction coefficient increases by 9.98% as the heat generation parameter Q changes from 0.10 to 1.00 and $x = 0.80285$. Furthermore, it is seen that the numerical values of the local Nusselt number Nu_x decrease for increasing values of heat generation parameter Q. The rate of decrease of local Nusselt number is 62.66% at position $x = 0.80285$ as the heat generation parameter Q changes from 0.00 to 0.40.

The values of the local skin friction coefficient and local Nusselt number for different values of surface temperature parameter θ_w while $Pr = 0.72$, $Q = 0.30$, $Rd = 1.00$, $M = 0.40$, $N = 0.20$ and $Ge = 0.50$ are recorded in Table-C_{19} which is showed in Appendix C. Here it is depicted that the values of skin friction coefficient C_{fx} increase at different position of x for of surface temperature parameter $\theta_w = 0.40$, 0.80, 1.00, 1.20. The rate of the skin friction coefficient increases by 8.94% as surface temperature parameter θ_w changes from 0.40 to 1.20 and $x = 1.30900$. Furthermore, it is seen that the numerical values of the local Nusselt number Nu_x increase for increasing values of surface temperature parameter θ_w. The rate of increase of local Nusselt number is 103.86% at position $x = 1.30900$ as the surface temperature parameter θ_w changes from 0.40 to 1.20. In Table-C_{20}, the values of the skin friction coefficient and local Nusselt number for different values of pressure work parameter Ge while $Pr = 0.72$, $Q = 0.40$, $Rd = 1.00$, $\theta_w = 1.10$, $M = 0.50$ and $N = 0.50$ are depicted which is shown in Appendix C. It is

concluded that the values of skin friction coefficient increase at different position of x for the pressure work parameter Ge = - 0.10, 0.10, 0.30, 0 50. The rate of the skin friction coefficient increases by 16.93% as pressure work parameter Ge changes from - 0.10 to 0.50 and x = 1 30900. Furthermore, it is seen that the numerical values of the local Nusselt number Nu_x decrease for increasing values of pressure work parameter Ge The rate of decrease of local Nusselt number is 98.62% at position x = 1.30900 as the pressure work parameter Ge changes from - 0.10 to 0.50.

Numerical values of local heat transfer rate, Nu_x are calculated from equation (10.19) for the surface of the sphere from lower stagnation point to upper stagnation point. Numerical values of Nu_x are entered in Table-C_{21} that is showed in Appendix C. In order to verify the accuracy of the present work, the values of non dimensional heat transfer parameter Nu_x for $N = Ge = M = Q = Rd = \theta_w = 0.00$ having Prandtl number Pr =0.70, 7.00 at different position of x (in degree) are compared with those reported by Nazar *et al.* (2002) and Molla *et al.* (2004) as presented in Table-C_{21}. The results are found to be in excellent agreement.

7.3 Conclusions

From the present investigation, the following conclusions may be drawn.

- Increase in the values of pressure work parameter Ge leads to increase the velocity profile, the temperature profile, the local skin friction coefficient C_{fx} but the local rate of heat transfer Nu_x decreases with the increase of pressure work parameter Ge while Q=0.40, θ_w = 1.1, M = 0.50, Rd = 1 00 and Pr = 0 72

- The velocity profile, the skin friction coefficient C_{fx} and local rate of heat transfer Nu_x, all are decreasing for increasing values of magnetic parameter or Hartmann number M, but the temperature profile increase with the increase of magnetic parameter M.

- Significant effects of heat generation parameter Q on velocity and temperature profiles as well as on local skin friction coefficient and the rate of heat transfer have been found in this investigation but the effect of heat generation parameter Q on rate of heat transfer is more significant. An increase in the values of heat generation parameter Q leads to both the velocity and the temperature profiles increase. The local skin friction coefficient C_{fx} increases at different position of v,

but the local rate of heat transfer Nu_X decreases at different position of x for Pr =0.72, θ_w = 1.1, M = 0.50, Rd = 1.00, Ge = 0 50.

- The increased values of radiation parameter Rd leads to increase the velocity profile, the temperature profile, the local skin friction coefficient C_{fx} and the local rate of heat transfer Nu_X while Q=0.40, θ_w = 1.1, M = 0.50, Ge = 0.60 and Pr = 0.72.

- All the velocity profiles, temperature profiles, the local skin friction coefficient C_{fx} and the local rate of heat transfer Nu_X increase significantly when the values of surface temperature parameterθ_w = 1.1, increases while Q = 0 30, M = 0.50, Rd = 1.00, Ge = 0.50 and Pr =0.72.

- Increasing values of Prandtl number Pr leads to decrease the velocity profiles. The temperature profiles, the local skin friction coefficient C_{fx} but the local rate of heat transfer Nu_X increases with the increase of Prandtl number Pr while Q=0 30, θ_w = 1.1, Rd = 2.00, M = 0.50, Ge = 0.40 and Pr =0.72.

Conclusions

The problems of free convection boundary layer flow over or on bodies of various shapes have been discussed by many mathematicians, versed engineers and researchers. Many natural phenomena and engineering problems are susceptible to MHD analysis. Natural convection heat transfer gained considerable attention because of its numerous applications in the areas of energy conservations cooling of electrical and electronic components, design of solar collectors, heat exchangers, pumps and flow meters and many others. Magnetohydrodynamics is that branch of continuum mechanics that deals with the flow of electrically conducting fluids in electric and magnetic fields. Probably the largest advance towards such phenomena comes from the field of astrophysics. It has long been suspected that most of the matter in the universe is in the plasma or highly ionized gaseous state, and much of the basic knowledge in the area of electromagnetic fluid dynamics evolved from these studies. The most important application of MHD is in the generation of electrical power with the flow of an electrically conducting fluid through a transverse magnetic field.

In the present dissertation, the solutions of two dimensional steady MHD convective flow of viscous incompressible fluid due to a vertical flat plate with heat conduction, over a sphere and on a circular cone with the effects of magnetic field, heat generation, Joule heating, radiation, surface temperature, viscous dissipation and pressure work have been examined separately. The flow problem with all these phenomena together, infect results in a very complicated structure physically as well as mathematically. We have, however, taken into account relatively simpler structural forms of the above-mentioned flows In view of this, the effects of viscous dissipation and pressure stress work on magneto hydrodynamics free convection flow along a vertical flat plate with heat conduction taken into account in chapter 3, we have considered the stress work effect on magneto-hydrodynamic (MHD) free convection flow from the vertical flat plate with Joule-heating and heat conduction in chapter 4. Conjugate effect of stress work and heat generation on MHD free convection flow along a vertical flat plate with Joule heating and heat conduction is considered in chapter 5. We described the pressure work and viscous dissipation effects with magnetohydrodynamic natural convection flow over a sphere in the presence of heat generation in chapter 6. The conjugate stress

work and magnetohydrodynamic effects on natural convection flow over a sphere in the presence of heat generation and radiation are studied in chapter 7

We applied the implicit finite difference method together with Keller-box scheme in chapter 3, chapter 4, chapter 5, chapter 6 and chapter 7.

The results obtained for each of the models have been discussed and analyzed in the respective sections. However, an overall discussion on the works are presented below in brief:

There is significant effect of the pressure work parameter Ge on the velocity profiles and temperature profiles as seen in chapter 3, chapter 4, chapter 5, chapter 6 and chapter 7. In most of the cases, it's found that the increase of the magnitude of Ge is proportional to the increase of the velocity and temperature profiles. Also, the pressure work parameter Ge leads to increase the skin friction coefficient as well as the surface temperature observed in chapters 3-5. In chapter 6, the local skin friction coefficient C_{fx} increases and the rate of heat transfer Nu_x decreases significantly when the values of pressure work parameter Ge increases while $Q=0.40$, $Pr = 0.72$, $M = 1.00$ and $N =0.50$. Again in chapter 7, as the pressure work parameter Ge increases, the local skin friction coefficient also increases but the local rate of heat transfer coefficient decreases which means that the radiation parameter dominates the Nusselts number

The effect of viscous dissipation parameter N on the velocity profiles and temperature profiles are displayed in chapter 3, chapter 4, chapter 5 and chapter 6. In these chapters, it is clearly observed that for increased values of viscous dissipation parameter N lead to increase the velocity profiles as well as temperature profiles. Also in chapter 3, chapter 4 and chapter 5, it is seen that the skin friction and surface temperature distribution increase for increasing values of viscous dissipation parameter N.

For the effect of magnetic parameter M in chapter 3, chapter 4 and chapter 5, it is depicted that the skin friction coefficient, the surface temperature distribution and the velocity distribution over the whole boundary layer decrease, but the temperature distribution increases. Again in chapter 6 and chapter 7, it is seen that the velocity profiles, the skin friction coefficient C_{fx} and local rate of heat transfer Nu_x all are decreasing for increasing values of magnetic parameter M but the temperature profiles increase with the increase of magnetic parameter M.

In chapter 5, it is seen that the skin friction coefficient, the surface temperature, the velocity and the temperature profiles all are increasing for the increasing values of the heat generation parameter Q. Further, significant effects of heat generation parameter Q

on velocity and temperature profiles as well as on local skin friction coefficient and the rate of heat transfer have been found in chapter 6 and chapter 8 but the effect of heat generation parameter Q on rate of heat transfer is more significant. An increase in the values of heat generation parameter Q leads to both the velocity and the temperature profiles to increase, the local skin friction coefficient C_{fx} increases, but the local rate of heat transfer Nu_x decreases at different position of x for $Pr = 0.72$, $\theta_w = 1.1$, $M = 0.50$, $Rd = 1.00$, $Ge = 0.50$.

The skin friction coefficient, the surface temperature, the velocity and the temperature profiles all are increasing for the increasing values of the Joule heating parameter Jd described in chapter 4 and chapter 5

The effect of radiation parameter Rd leads to increase the velocity profiles, the temperature profiles, the local skin friction coefficient C_{fx} and the local rate of heat transfer Nu_x while $Q = 0.40$, $\theta_w = 1.1$, $M = 0.50$, $Ge = 0.60$ and $Pr = 0.72$ as displayed in chapter 7.

In chapter 7, all the velocity profiles, temperature profiles, the local skin friction coefficient C_{fx} and the local rate of heat transfer Nu_x increase significantly when the values of surface temperature parameter $\theta_w = 1.1$, increases while $Q = 0.30$, $M = 0.50$, $Rd = 1.00$, $Ge = 0.50$ and $Pr = 0.72$.

There is marked effect of the Prandtls number Pr on the velocity profiles, temperature profiles, the skin friction and the surface temperature as seen in chapter 3, chapter 4 and chapter 5. In most of the cases, it has been observed that the skin friction coefficient, the surface temperature distribution, the temperature profiles and the velocity profiles decrease over the whole boundary layer with the increase of the Prandtl number Pr. Increasing values of Prandtls number Pr lead to decrease the velocity profiles, the temperature profiles, the skin friction coefficient and the rate of heat transfer coefficient as illustrated in chapters 6-7

Since we could not obtain experimental results of the models we considered, comparison of our results could not be made with experimental results. However, we have made some comparisons of our results with theoretical results of Nazar and Chen (2002), Molla _et al._ (2004) in chapter 6 which is shown in Appendix C (Table-C_{16}), by Nazar and Chen (2002), Molla _et al._ (2004) in chapter 7 which is shown in Appendix C

(Table-C_{21}). These comparisons show good agreements between our results and of those mentioned above and hence an encouragement for our works.

It is evident from Table-C_{22} that the skin friction coefficient and the surface temperature for different values of viscous dissipation parameter N obtained from Table-C_3 and Table-C_7 are in excellent agreement which is shown in appendix C.

Similarly from chapter 5, it is concluded that the heat generation parameter dominates the pressure work parameter, viscous dissipation parameter, Joule heating parameter and also Prandtls number. For the same values of pressure work parameter $Ge = 0.60$, the skin friction and the surface temperature in Table-C_6 and Table-C_{12} against $x = 0.7090$ are 0.6251 and 0.7810, 1.3160 and 1.5961 respectively. The variation of the skin friction coefficient and surface temperature at $x = 0.7090$ in chapter 4 and chapter 5 occurred only for heat generation parameter. Therefore, it is clearly illustrated that the heat generation parameter dominates the pressure work parameter. Also, all other cases such as viscous dissipation parameter, Joule heating parameter and Prandtls number analysis can be shown in a similar way.

Possible Future Works

❖ The effects of stress work on magnetohydrodynamics(MHD) free convection flow along a vertical flat plate with temperature-dependent viscosity.

❖ Conjugate effects of pressure work and viscous dissipation on magneto-hydrodynamics(MHD) free convection flow along a vertical flat plate with heat conduction and temperature-dependent viscosity.

❖ Conjugate effects of pressure work and viscous dissipation on magneto-hydrodynamics(MHD) free convection flow along a vertical flat plate with heat conduction and temperature-dependent thermal conductivity.

❖ The stress work effects on the magnetohydrodynamic (MHD) free convection flow along a vertical flat plate with Joule-heating and heat conduction in the presence of temperature-dependent thermal conductivity.

❖ Conjugate effects of stress work and Joule-heating on the magnetohydrodynamic (MHD) free convection flow along a vertical flat plate with heat generation and heat conduction in the presence of temperature-dependent thermal conductivity.

❖ Conjugate effects of stress work and heat generation on the magnetohydrodynamic (MHD) free convection flow along a vertical flat plate with Joule-heating and heat conduction in the presence of temperature-dependent viscosity.

❖ The pressure work and viscous dissipation effects on magnetohydrodynamic natural convection flow over a sphere in the presence of heat generation and temperature-dependent viscosity.

❖ The pressure work and viscous dissipation effects on magnetohydrodynamic natural convection flow over a sphere in the presence of heat generation and temperature-dependent thermal conductivity.

❖ The conjugate effects of stress work and magnetohydrodynamic natural convection flow over a sphere in the presence of heat generation and radiation with temperature-dependent thermal conductivity.

❖ The conjugate effects of stress work and magnetohydrodynamic natural convection flow over a sphere in the presence of heat generation and radiation with temperature-dependent viscosity.

❖ The stress work effects of laminar free convection from a vertical permeable circular cone maintained at non-uniform surface temperature.

❖ The stress work effects of laminar free convection from a vertical permeable circular cone maintained at uniform surface temperature.

References

Ackroyd, J.A.D., (1974): "Stress work effects in laminar flat-plate natural convection", *J. Fluid Mech.*, Vol. 62, pp.677-695.

Alam M. M., (1995): "Heat and mass transfer flow with thermal diffusion." *Ph.D Thesis*, Department of Mathematics, University of Dhaka.

Alam, Md. M., Alim, M. A., and Chowdhury, Md. M. K., (2007): "Free convection from a vertical permeable circular cone with pressure work and non-uniform surface temperature", *Nonlinear Analysis, Modelling and Control*, Vol.12, No.1, pp.21-32.

Alam, Md. M., Alim, M. A., and Chowdhury, Md. M. K., (2006): "Effect of pressure stress work and viscous dissipation in natural convection flow along a vertical flat plate with heat conduction", *Journal of Naval Architecture and Marine Engineering*, Vol.3. No.2, pp. 69-76.

Alam, Md. M., Alim, M. A., and Chowdhury, Md. M. K., (2006): "Viscous Dissipation Effects on MHD Natural Convection Flow Along a Sphere", *Journal of Mechanical Engineering*, Vol ME 36, No.2, pp. 44-48.

Alam, Md. M., Alim, M. A., and Chowdhury, Md. M. K., (2007): "Viscous Dissipation Effects on MHD Natural Convection Flow Over a Sphere in the Presence of Heat Generation", *Nonlinear Analysis; Modelling and Control* (inpress).

Alim, M. A. Alam, Md. M., and Chowdhury, Md. M. K., (2006): "Pressure work effect on natural convection flow from a vertical circular cone with suction and non-uniform surface temperature", *Journal of Mechanical Engineering*, Vol.ME 36, No.2, pp. 44-48

Alim, M. A. Alam, Md. M., and Abdullah-Al-Mamun,(2007): "Joule heating effect on the coupling of conduction with magnetohydrodynamic free convection flow from a vertical flat plate", *Nonlinear Analysis: Modelling and Control*, Vol. 12, No.3 pp.307-316.

Alim, M. A., Alam, Md. M, Abdullah-Al-Mamun and Belal Hossain, Md .(2007): "Combined effect of viscous dissipation and Joule heating on the coupling of conduction and free convection along a vertical flat plate", *International communication of heat and mass transfer*, (inpress)

Alamgir, M., (1979): "Over all heat transfer from vertical cones in laminar free Convection, an approximate method", *ASME J. heat transfer*, Vol.101, No.(1-4), pp.174-176.

Alam, Md. Mahmud, and Sattar Md. Abdus, (2001): " Analytical solution of the free convection and mass transfer flow with thermal diffusion", *Dhaka University Journal of Science*, Vol.49, No 1, pp 95-104.

Al-Khawaja, M.J, Agarwal, R.K & Gardner, R.A , (1999). "Numerical study of magneto-fluid mechanics combined free and forced convection heat transfer", *Int. J. Heat and Mass Transfer*, Vol.42, pp.467-475.

Bejan, A. and Khair, K.R., (1985): " Heat and mass transfer by natural convection in a porous medium," *Int. J. Heat and Mass Transfer*, Vol.28, pp.909-918.

Braun, W. H., Ostrach, S.,& Heighway, J. E., (1961): "Free convection similarity flows about two-dimensional and axisymmetric with closed lower ends", *Int. J. Heat Mass Transfer*, Vol.2, No.(1-2), pp.121-135.

Cebeci, T & Bradshow. P, (1977): "Momentum Transfer in Boundary Layers", *McGraw-Hill Book Company.*

Cebeci, T., & Bradshow, P, (1984): "Physical and Computational Aspects of Convective Heat Transfer", Spring, New York

Chen, T. S. and Mucoglu, A., (1977): "Analysis of mixed forced and free convection about a sphere", *Int. J. Heat Mass Transfer*, Vol.20, pp. 867-875.

Chen, T.S., Sparrow, E.M., and Mueoglu, A., (1977): " Mixed convection in boundary layer flow on a horizontal plate," *ASME J. Heat Transfer*, Vol 99, pp.66-71.

Cheng, P., (1982): "Mixed convection about a horizontal cylinder and a sphere in a fluid-saturated porous medium", *Int. J. Heat & Mass Transfer*, Vol.25, No.1, pp 1245-1247.

Chiam, T. C., (1998): "A numerical solution for laminar boundary layer flow with an exponentially decreasing velocity distribution," *Proc. Acta Mechanica* Vol.192, pp.255-261.

Chida, K. and Katto, Y., (1976): "Steady on conjugate heat transfer by vectorial dimensional analysis," *Int. J. Heat Mass Transfer*, Vol.90, pp. 453-460.

Chowdhury, Md. M.K. and Islam, M.N., (2000): "MHD free convection flow of visco-elastic fluid past an infinite porous plate", *Heat and Mass Transfer*, Vol.36, pp 439-447.

Curle, N., (1981): "Development and separation of a laminar boundary layer flow with an exponentially increasing pressure gradient", *Q. J Mech. Appl. Math*, Vol.34, pp.383-395.

Cramer, K R., (1963). "Several magnetohydrodynamic free convection solutions", *ASME Journal of Heat Transfer*, Vol. 85, pp.35-40.

Cramer K. R.& Pai, S. I., (1974). "Magnetofluid Dynamics for Engineering and Applied Physicists", *McGraw-Hill, New York*, pp.164-172.

Chao,P., and Ozoe, H., (1983): "Laminar natural convection in an inclined rectangular box with lower surface half-heated and half insulated", *ASME, J. Heat Transfer*, Vol.105, pp.425-432.

Clarke J. F., (1973): " Transpiration and natural convection the vertical flat plate problem", *J. Fluid Mechanics*, Vol.57, pp.45-61.

Cohen, C.B., and Reshotko, E., (1956). "Similar solutions the compressible boundary layer with heat transfer and arbitrary pressure gradient", *NACA*, Rept. Pp 1294.

El-Amin, M. F., (2003). "Combined effect of viscous dissipation and Joule heating on MHD forced convection over a non isothermal horizontal cylinder embedded in a fluid saturated porous medium", *Journal of Magnetism and Magnetic Materials*, Vol 263, pp.337-343.

El-Amin M. F., and Mohammadein, A. A., (2005): "Effects of viscous dissipation and Joule heating on magnetohydrodynamic hiemenz flow of micropolar fluid", Heat Transfer Engineering, Vol. 26, pp 75-81.

Elbashbeshy, E. M. A., (2000). "Free convection flow with variable viscosity and thermal diffusivity along a vertical plate in the presence of magnetic field", *Int. J. Engineering Science*, Vol.38, pp. 207-213.

Gansan, P. & Palani, G., (2004): "Finite difference analysis of unsteady natural convection MHD flow past an inclined plate with variable surface heat and mass flux", *Int. J. Heat and Mass Transfer*, Vol 47, pp. 4449-4457.

Ganzarolli, M. M. and Milanez, L. F., (1995): " Natural convection in rectangular enclosures heated from below and symmetrically cooled from the sides", *Int. J Heat Mass Transfer*, Vol.38, pp.1063-1073.

Gebhart, B., (1962): "Effects of viscous dissipation in natural convection". *J. Fluid Mech.* Vol.14, pp. 225-232.

Gebhart,B., and Mollendorf, J., (1969): "Viscous dissipation in external natural convection flows", *J. Fluid Mech*, Vol. 38, pp.97-107.

Gupta, A.S., (1961): "Steady and transient free convection of an electrically conducting fluid from a vertical plate in the presence of magnetic field", *Appl. Sci Res.*, Vol.9A, pp 319-333.

Hansen,A. G., (1964): "Similarity analysis of boundary value problems in Prentic-Engineering", *Hall, Inc. Englewood Cliffs*, New Jersey.

Hartmann, J., (1937): "Hg-Dynamics I, Theory of laminar flow of an electrically conduction liquid in a homogeneous magnetic field", *Kgl. Danske Videnskabernes Selskab, Math-fys, Meddeleser XV*, 6, Copenhagen.

Hassan, A. L. A., and Hazem Ali Attia (1997) "Flow due to a rotating disk with Hall effect" *Physics Letters*, Vol.A 228, pp. 246-290.

Hering, R. G., (1965): "Laminar free convection from a non-isotermal cone at low Prandtl numbers", *Int. J Heat Mass Transfer*, Vol. 8, No 10, pp.1333-1337.

Hering, R. G., & Grosh, R. J., (1962). "Laminar free convection from a non-isothermal cone", *Int. J. Heat Mass Transfer*, Vol. 5, No.11, pp.1059-1068.

Hossain, M. A. and Rashid, R. I. M. A., (1987). "Hall effects on hydromagnetic free convection flow along a porous flat plate with mass transfer", Journ. Physical Society of Japan, vol. 56, pp. 97-104.

Hossain, M. A. and Mohammad, K., (1988): "Effect of Hall current on hydromagnetic free convection flow near an accelerated porous plate", Japanese J. Applied Physics, vol. 27, pp. 1531-1535.

Hossain, M. A., & Ahmed, M, (1990): "MHD Forced and free convection Boundary layer flow near the leading edge", *Int. J. Heat Mass Transfer*, Vol.33, pp. 571-575.

Hossain, M. A., (1992): "Viscous and Joule heating effects on MHD free convection flow with variable plate temperature", *Int. J. Heat and Mass Transfer*, Vol.35, pp.3485-3487.

Hossain, M.A., Banu, N., Nakayama, A., (1994): "Non-Darcy forced convection boundary layer flow over a flat plate embedded ina saturated porous media," *Num. Heat Transfer*, Vol.20, pp.399-414. .

Hossain M. A. and Takhar H. S, (1996): "Radiation effect on mixed convection along a vertical plate with uniform surface temperature", *Heat and Mass Transfer*, Vol 31, pp. 243-248.

Hossain, M. A. and Alim M. A., (1997a): "Natural convection-radiation interaction on boundary layer flow along a Thin cylinder", *J. Heat and Mass Transfer*, Vol.32, pp 515-520.

Hossain, M.A., Alam, K.C.A. and Rees, D.A.S., (1997b): "MHD forced and free convection boundary layer flow along a vertical porous plate", *Applied Mechanics and Engineering*. Vol. 2, No.1, pp.33-51.

Hossain, M. A., Alim, M. A., & Rees, D. A. S.. (1998a): "Effects of thermal radiation on natural convection over cylinders of elliptic cross section", *Acta Mechanica*, Vol.129, pp.177-186.

Hossain, M. A., Das, S. K. and Pop, I., (1998b): "Heat transfer response of MHD free convection flow along a vertical plate to surface temperature oscillation", *Int. J. Non-Linear Mechanics*, Vol.33, No.3, pp 541-553.

Hossain, M. A., Alim, M. A and Rees, D. A. S., (1999): "The effect of radiation on free convection from a porous vertical plate", *Int. J. Heat Mass Transfer*, Vol.42. pp.181-191.

Hossain, M. A., Munir, M. S. and Takhar, H. S., (2000): "Natural convection flow of a viscous fluid about a truncated cone with temperature dependent viscosity and thermal conductivity", *Acta* Mechanica , Vol.140, No.(3-4), pp.171-181.

Hossain, M. A, and Paul, S.C., (2001a): "Free convection from a vertical permeable circular cone with non-uniform surface temperature", *ACTA MECHANICA*, Vol.151, pp.103-114.

Hossain, M.A. and Paul, S.C., (2001b): "Free convection from a vertical permeable circular cone with non-uniform surface heat flux", *Heat and Mass Transfer*, Vol.37, pp.167-173.

Hossain, M. A., Molla, M. M., and Gorla, R. S. R., (2004): "Conjugate effect of heat and mass transfer in natural convection flow from on isothermal sphere with chemicial reaction", *Int. J Fluid Mech. Research*, Vol.31, pp. 104-117.

Hossian, M. A., & Wilson, M., (1998): "Unsteady flow and heat transfer of a viscous fluid with variable viscosity due to a rotating disc", *Proc Mini workshop on applied Math*, SUST, Sylhet, Bangladesh, 1-3 September, 85.

Hossain, M. A. and Rees, D. A. S., (2003). "Natural convection flow of a viscous incompressible fluid in a rectangular porous medium cavity heated from below", Heat Mass Transfer, vol. Vol.39, pp. 657-663.

Hughes, W. F. and Young, F. J.,(1966): "The Electromagnetodynamics of Fluids", John Wiley and Sons,. Inc., New York, London, pp. 530-581.

Huang, M. J. and Chen, C. K., (1987): "Laminar free convection from a sphere with blowing and suction", *J. Heat Transfer*, Vol.109, pp. 529-532.

Ingham, D. B., Merkin, J. H. and Pop, I., (1985): " Natural convection from a semi infinite plate inclined at a small angle at the horizontal in saturated porous medium," *Acta Mechanica*, Vol.57, pp 183-202.

Jha, B.K., (1991): "MHD unsteady mixed convection flow through a porous medium", *Astrophys. Space sci*, Vol.175, pp.79-101.

Jin, Y.Y., & Chen, C.F., (1996): "Natural convection of high Prandlt number fluids with variable viscosity in a vertical slot", *Int. J. Heat Mass Transfer*, Vol. 39, pp.2663-,.

Joshi and Gebhart., (1981): " The effect of pressure stress work and viscous dissipation in some natural convection flows", *Int. J. Heat Mass Transfer*, Vol.24, No.10, pp. 1377-1388.

Kafoussius N.G., and Williams E.W., (1995): " The effect of temperature dependent viscosity on the free convective laminar boundary layer past a vertical isothermal flat plate," *Acta Mechanica*, Vol 110, pp.123-137.

Kafoussius N.G., and Rees D A.S., (1998). "Numerical study of the combined free and convective laminar boundary layer flow past a vertical isothermal flat plate with temperature dependent viscosity", *Acta Mechanica*, Vol.127, pp 39-50.

Keller H.B., (1978): " Numerical methods in boundary layer theory". *Annual Rev. Fluid Mech.*, Vol.10, pp.417-443.

Keller H.B. and Cebeci T., (1971): "Accurate numerical methods for boundary layer flows I. Twodimensional laminar flows", in: *Proceedings of the Second Int. Conference on numerical Methods in fluid dynamics*, Springer, New York, pp. 92–100.

Keller H.B. and Cebeci T., (1972): "Accurate numerical methods for boundary layer flows, part II, Two dimensional turbulent flow", *AIAAJ*, Vol.10, pp.1193–1199

Khan. Z I.,(2002): "Conjugate effect of conduction and convection with natural convection flow from a vertical flat plate and in an inclined square cavity", M. Phil thesis, BUET.

Kuiken, H. K., (1968). "Axisystemmetric free convection boundary layer flow past slender bodies", *Int. J. Heat Mass Transfer*, Vol 11, No.7, pp.1141-1153

Kuiken, H. K., (1970): "Magneto-hydrodynamic free convection in strong cross flow field", *J. Fluid Mech.*, Vol.40, pp.21-38.

Kumari, M., Pop, I., & Nath, G., (1990). " Natural convection in porous media above a near horizontal uniform heat flux surface", *Warme and Stoffubertrang*, Vol.25, pp.155-159.

Lin, F. N., (1976): "Laminar free convection from a vertical cone with uniform surface heat flux", *Letters in Heat and Mass Transfer*, 3(1), pp.49-58.

Lin II. T., and Yu W.S., (1988): " Free convection on a horizontal plate with blowing and suction", *J. Heat Transfer*, ASME, Vol.110, pp.793-796.

Lock, G. S. H. and Gunn, J. C., (1968): "Laminar free convection from a downward projecting fin", *J. Heat Transfer*, Vol 90, pp. 63-70.

Loyd, J. R & Sparrow, E. M., (1970): "Combined forced and free convection flow on vertical surface", *Int. J. Heat Mass Transfer*, Vol.13, pp. 434-438.

Lykoudis, P. S., (1962): "Natural convection of an electrically conducting fluid in the presence of a magnetic field", *Int. J. heat and Mass Transfer*, Vol.5, pp.23-34.

Na, T. Y. & Chiou, J. P., (1979). "Laminar natural convection over a frustum of a cone", *Appl. Sci. Res.*, Vol.35, pp.409-,.

Na, T. Y. & Chiou, J. P., (1979): "Laminar natural convection over a slender vertical frustum of a cone", *Warme and Stoffubertragung*, Vol.12, pp.83-87.

Nachhtsheim, P.R. and Swigert, P., (1965): "Satisfaction of Asymptotic Boundary Conditions in Numerical Solutions of Systems of Non-linear Equations of Boundary-layer Type", *NASA* TND3004.

Nicolas, J.D. and Nansteel, M.W., (1993): " Natural convection in a rectangular enclosure with partial heating on the lower surface; experimental results", *Int. J Heat Mass Transfer*, Vol.36, pp. 4067-4071.

November,M. and Nansteel, M.W, (1987): " Natural convection in a rectangular enclosure heated from below and cooled along one surface", *Int. J. Heat Mass Transfer*, Vol.30, pp. 2433-2440.

Maleque, K.A.,(1996): "Similarity solutions of combined forced and free convection laminar boundary layer flows in curvilinear co-ordinates". *M. Phil. Thesis.*, BUET.

Mendez, F., Trevino, C., (2000): "The conjugate conduction-natural convection heat transfer along a thin vertical plate with non-uniform internal heat generation", *Int. J. Heat and Mass Transfer*, Vol.43, pp. 2739-2748.

Merk, E J.,& Prins, J. A.,(1954): "Thermal convection in laminar boundary", *Appl. Sci Res*, 4A, pp.11-24.

Merkin, J.H., (1972): " Free convection with blowing and suction", *Int. J. Heat Mass Transfer*, Vol.15, pp.989-999.

Merkin, J.H.,(1975): " The effects of blowing and suction on free convection boundary layers", *Int. J. Heat Mass Transfer*, Vol.18, pp.237-244

Miyamoto. M., Sumikawa.J., Akiyoshi.T & Nakamura. T., (1980): "Effect of axial heat conduction in a vertical flat plate on free convection heat transfer", *Int. J. Heat Mass Transfer*, Vol.23, pp.1545-1533.

Moalem, Devid, (1976): " Steady state heat transfer within porous medium with temperature-dependent heat generation", *J. Heat Mass Transfer*, 19, pp.529-534.

Molla, M.M., Hossain, M.A. and Yao, L.S., (2004): "Natural convection flow along a vertical wavy surface with uniform surface temperature in presence of heat generation / absorption", *Int. J. Thermal Science*, Vol.43, pp. 157-163.

Molla, M. M., Glasgow, Hossain, M. A. and Taher, M. A., (2006) "Magnetohydrodynamic natural convection flow on a sphere with uniform heat flux in presence of heat generation", Vol.186, pp.75-86.

Na, T. Y.,& Chiou, J. P., (1979a): "Laminar natural convection over a slender vertical frustum of a cone", *Warme and Stoffubertragung*, Vol.12, No.2, pp.83-87.

Na, T. Y. and Chiou, J. P., (1979b): "Laminar natural convection over a frustum of a cone", *Appl. Sc. Res.*, Vol.35, pp.409-421.

Nanda,R. S. & Mohanty, H. K., (1970): "Hydromagnetic free convection for high and low Prandtl numbers", *J.Phys. Soc. Japan.*, Vol. 29, No. 6, pp.1608-1618

Nazar, R., Amin, N., Grosan, T. and Pop, I., (2002a): "Free convection boundary layer on an isothermal sphere in a micropolar fluid", *Int. Comm.Heat Mass Transfer*. Vol 29, No.3, pp. 377-386.

Nazar, R., Amin, N. and Pop, I., (2002b): "Free convection boundary layer on an isothermal horizontal circular cylinder in a micropolar fluid. *Heat Transfer*", *Proceeding of the Twelfth International Heat Transfer Conference.*

Oosthuizen, P. H.,& Donaldson, E., (1972): "Free convection heat transfer from vertical cone", *J. Heat Transfer, C*, Vol.94, No.3, pp.330-331.

Pai, S. I., (1962): "Magnetogasdynamics and Plasma Dynamics", Springer-Verlag, Vienna. Ray Wylie, C., 1975, Advanced Engineering Mathematics, fourth edition.

Poots, G , (1961): "Laminar natural convection flow in magnetohydrodynamics", *Int.J. Heat and Mass Transfer*, Vol. 3, No.1, pp.1-25.

Pop, I., (1971): "Effect of Hall current on the unsteady MHD fluid past an accelerated flat plate", *J. Math. Phys. Sci.*, Vol.5, pp.375-386.

Pop, I. & Merkin, J. H., (1995): "Conjugate free convection on a vertical surface in a saturated porous medium", *Fluid Dynamics Res.*, Vol.16, pp.71-86.

Pozzi, A and Lupo, M., (1988): "The coupling of conduction with laminar natural convection along a flat plate", *Int. J. Heat Mass Transfer*, Vol.31, No.9, pp 1807-1814.

Ramadan Hasan M., and Chamkha Ali J., (2003): "Hydromagnetic free convection of a particulate suspension from a permeable inclined plate with heat absorption for non-uniform particle-phase density", *Heat and Mass transfer*, Vol.39, pp 367-374.

Rapits, A , & Kafoussias, N., (1982): "Magnetohydrodynamic free convection flow and mass transfer through porous medium bounded by an infinite vertical porous plate with constant heat flux", *Canadian Journal of Physics*, Vol.60, No 12, pp.1725-1729.

Roy, S., (1974): "Free convection over a slender vertical cone at high Prandtl numbers", *ASME, J. Heat Transfer*, Vol.101, pp.174-176.

Sattar, Md. Abdus, (1994): "Unsteady hydromagnetic free convection flow with Hall current mass transfer and variable suction through a porous medium near an infinite vertical porous plate with constant heat flux". *Int. J. of Energy Research*, Vol.18. pp.771-775.

Sattar, Md. Abdus and Kalim, Md. Hamid, (1996): "Unsteady free convection interaction with thermal radiation in a boundary layer flow past a vertical porous plate", *Journal of Mathematical and Physical Science*, Vol. 30, No. 1, pp. 25-37.

Sattar, Md. A., and Maleque, Kh. A., (2000): "Numerical solution of MHD free convection and mass transfer flow with Hall current, viscous dissipation and Joule heating", *Journal of Energy Heat and Mass Transfer*, IIT, Madras, Vol. 22, pp. 237-244.

Shariful M. A., (2004): "Thermal-Diffusion and diffusion thermo effects on magneto hydrodynamics heat and mass transfer", *M. Phil Thesis*, Department of Mathematics, BUET.

Shercliff, J A., (1965): "A Textbook of Magnetohydrodynamics", Oxford, *Pergamon Press, UK*.

Sing, K. R. & Cowling, T G., (1963). "Thermal convection in magneto-hydrodynamics", *J. Mech. Appl. Math* , Vol.16, pp.1-5.

Shiralkar, G. and Tien,C., (1982): "A numerical study of the effect of a vertical temperature difference imposed on a horizontal enclosure", *Numerical Heat Transfer*, Vol.5, pp.185-197.

Soundalgekar, V. M. and Ganesan, P., (1981): "Finite difference analysis of transient free-convection on an isotherm flat plate," *Regional J Energy Heat Mass Transfer*, Vol.3, pp 219-224.

Sparrow, E. M., (1956): "Free convection with variable properties and variable wall temperature", *Ph.D. thesis*, Harvard University.

Sparrow, E. M. and Cess, R. D., (1961a): "The effect of a magnetic field on free convection heat transfer", *Int. J. Heat Mass Transfer*, Vol.3, pp.267-274.

Sparrow, E. M., & Cess, R. D., (1961b): "Free convection with blowing or suction", *J. Heat Transfer*, Vol.81c, pp.387-389.

Sparrow, E.M. and Gregg, J. L., (1956): "Laminar free convection from a vertical flat plate with Uniform Surface Heat Flux", *Tran. ASME*, Vol 78, pp. 435-440.

Sparrow, E.M. and Gregg, J. L., (1958): " The variable fluid property problem in free convection", *Trans Am. Mech. Engrs*, Vol.80, PP. 879-886.

Sparrow, E.M. and Guinle, L.D.F., (1968): "Daviation from classical free convection boundary layer theory at low Prandtl numbers", *Int. J. Heat Mass Transfer*, Vol.11. pp.1403-1415.

Takhar, H.S and Soundalgekar, V.M., (1980a): "On the diffusion of a chemically reactive species in a laminar boundary layer flow past a porous media", *Applied Scientific Research*, Vol. 28, pp.525-526.

Takhar, H.S. and Soundalgekar, V.M., (1980b): "Dissipation effects on MHD free convection flow past a semi-infinite vertical plate", *Applied Scientific Research*, Vol.36, pp.163-171.

Umavathi, J. C. & Malashetty, M. S., (2005): "Magnetohydrodynamic mixed convection in a vertical channel", *Int. J NON-LINEAR MECHANICS*, Vol. 40, pp. 91-101.

Van Driest, E. R., (1951): "Turbulent boundary layers in compressible fluids", *J. Aero. Sci.*, Vol.18, pp.145-160.

Vafai, K. and Tien, C.L., (1981): " Boundary and inertia effects on flow and heat transfer in porous media", *Int. J. Heat Mass Transfer*, Vol.24, pp.195-203.

Vajravelu, K. and Hadjinicolaou, A., (1993): "Heat transfer in a viscous fluid over a stretching sheet with viscous dissipation and internal heat generation", *Int.Comm Heat Mass Transfer*, Vol. 20, pp.417-430.

Vedhanayagam M., Altenkirch R. A. and Eichhorn R., (1980): " A transformation of the boundary layer equations for free convection past a vertical flat plate with arbitrary blowing and wall temperature variations", *Int. J Heat Mass Transfer*, Vol 23, pp.1286-1288.

Velusamy, K., Sundarajan, T. and Seetharamm, K.N., (1998): " Laminar natural convection in an enclosure formed by non-isotherm walls", *Proc. of 11th Int. Conf. Heat Transfer*, Korea, 3, pp. 459-464.

Wilks. G., (1976): "Magneto-hydrodynamic free convection about a semi-infinite vertical plate in a strong cross field", *J Appl. Math. Phys.*, Vol.27, pp.621 – 631

Zakerullah, Md., (1972): "Viscous dissipation and pressure work effects in axisymmetric natural convection flows", *J. Bangladesh Math. Soc. (Ganit)*, Vol. 2, No.1, pp.43-51.

Zakerullah,M., & Ackroyd, J. A. D., (1979): "Laminar natural convection boundary layers on horizontal circular discs", *Journal of applied Mathematics and Physics*, Vol.30, pp.427-435.

Zakerullah, M., & Maleque, Kh.A., (1996): "Laminar combined convection flow about a vertical inclined surface", *J. of Bangladesh Academy of Science*, Vol. 20, No.2, pp.99-110.

Appendix A

Numerical Method

The momentum equation can be written by applying central average finite difference values

$$\frac{1}{2}\left(\frac{v_j^n \div v_{j-1}^n}{h_j} + \frac{v_j^{n-1} + v_{j-1}^{n-1}}{h_j}\right) + (fv)_{j-1/2}^{n-1/2} - \left(M^2 u\right)_{j-1/2}^{n-1/2} - \left(u^2\right)_{j-1/2}^{n-1/2} + g_{j-1/2}^{n-1/2}$$

$$= \xi_{j-1/2}^{n-1/2}\left(u_{j-1/2}^{n-1/2}\frac{u_{j-1/2}^n - u_{j-1/2}^{n-1}}{k_n} - v_{j-1/2}^{n-1/2}\frac{f_{j-1/2}^n - f_{j-1/2}^{n-1}}{k_n}\right) \qquad (2.60)$$

$$\frac{1}{2}\left(\frac{v_j^n - v_{j-1}^n}{h_j} + \frac{v_j^{n-1} - v_{j-1}^{n-1}}{h_j}\right)$$

$$+ \frac{1}{2}\left\{(fv)_{j-1/2}^n \div (fv)_{j-1/2}^{n-1}\right\} - \frac{1}{2}\left\{\left(M^2 u\right)_{j-1/2}^n + \left(M^2 u\right)_{j-1/2}^{n-1}\right\}$$

$$- \frac{1}{2}\left\{\left(u^2\right)_{j-1/2}^n + \left(u^2\right)_{j-1/2}^{n-1}\right\} + \frac{1}{2}\left(g_{j-1/2}^n + g_{j-1/2}^{n-1}\right)$$

$$= \frac{1}{2k_n}\xi_{j-1/2}^{n-1/2}\left(u_{j-1/2}^n + u_{j-1/2}^{n-1}\right)\left(u_{j-1/2}^n - u_{j-1/2}^{n-1}\right)$$

$$- \frac{1}{2k_n}\xi_{j-1/2}^{n-1/2}\left(v_{j-1/2}^n + v_{j-1/2}^{n-1}\right)\left(f_{j-1/2}^n - f_{j-1/2}^{n-1}\right)$$

$$\Rightarrow \left(\frac{v_j^n - v_{j-1}^n}{h_j}\right) \div \left(\frac{v_j^{n-1} - v_{j-1}^{n-1}}{h_j}\right) + (f v)_{j-1/2}^n + (f v)_{j-1/2}^{n-1} - M^2 (u)_{j-1/2}^n$$

$$- M^2 (u)_{j-1/2}^{n-1} - \left(u^2\right)_{j-1/2}^n + \left(u^2\right)_{j-1/2}^{n-1} + g_{j-1/2}^n + g_{j-1/2}^{n-1}$$

$$= \alpha_n\left\{\left(u^2\right)_{j-1/2}^n - \left(u_{j-1/2}^n\right)\left(u_{j-1/2}^{n-1}\right) + \left(u_{j-1/2}^{n-1}\right)\left(u_{j-1/2}^n\right) - \left(u^2\right)_{j-1/2}^{n-1}\right\}$$

$$- \alpha_n\left\{(f v)_{j-1/2}^n + v_{j-1/2}^{n-1} f_{j-1/2}^n - v_{j-1/2}^n f_{j-1/2}^{n-1} - (fv)_{j-1/2}^{n-1}\right\} \qquad (2.62)$$

Where $\alpha_n = \dfrac{1}{k_n}\xi_{j-1/2}^{n-1/2}$

$$\Rightarrow \left(\frac{v_j^n - v_{j-1}^n}{h_j}\right) + (1 \div \alpha_n)(f v)_{j-1}^n - (1 \div \alpha_n)(u^2)_{j-1/2}^n - M^2 (u)_{j-1/2}^n + (g)_{j-1/2}^n$$

$$+ \alpha_n\left\{v_{j-1/2}^{n-1} f_{j-1/2}^n - v_{j-1/2}^n f_{j-1/2}^{n-1}\right\} = \alpha_n\left\{-\left(u^2\right)_{j-1/2}^{n-1} + v_{j-1/2}^n f_{j-1/2}^{n-1}\right.$$

$$\left. - v_{j-1/2}^{n-1} f_{j-1/2}^n + (f v)_{j-1/2}^{n-1}\right\} - (fv)_{j-1/2}^{n-1} \div M^2 (u)_{j-1/2}^{n-1}$$

$$- \left(u^2\right)_{j-1/2}^{n-1} - g_{j-1/2}^{n-1} - \left(\frac{v_j^{n-1} - v_{j-1}^{n-1}}{h_j}\right)$$

$$\frac{1}{2\ \mathrm{Pr}}\left(\frac{P_j^n + P_{j-1}^n}{h_j} + \frac{P_j^{n-1} + P_{j-1}^{n-1}}{h_j}\right) + (fP)_{j-1/2}^{n-1/2} - (ug)_{j-1/2}^{n-1/2} - \left((\gamma\varepsilon(X))u\right)_{j-1/2}^{n-1/2}$$

$$+ \left(\varepsilon(X)(gu)\right)_{j-1/2}^{n-1/2} = \xi_{j-1/2}^{n-1/2}\left(u_{j-1/2}^{n-1/2}\frac{g_{j-1/2}^n - g_{j-1/2}^{n-1}}{k_n}\right. \tag{2.61}$$

$$\frac{f_{j-1/2}^n - f_{j-1/2}^{n-1}}{k_n} - \left(M^2(u^2)\right)_{j-1/2}^{n-1/2} \ \left(v^2\right)_{j-1/2}^{n-1/2} \ - \ P_{j-1/2}^{n-1/2}\ \Big)$$

Also using the same process, we get

$$\frac{1}{2\mathrm{Pr}}\left(\frac{P_j^n - P_{j-1}^n}{h_j} + \frac{P_j^{n-1} - P_{j-1}^{n-1}}{h_j}\right) + \frac{1}{2}\left\{(fP)_{j-1/2}^n + (fP)_{j-1/2}^{n-1}\right\}$$

$$-\frac{1}{2}\left\{(ug)_{j-1/2}^n + (ug)_{j-1/2}^{n-1}\right\} - \frac{1}{2}\left\{\gamma(\varepsilon(X))_{j-1/2}^n(u)_{j-1/2}^n + \gamma(\varepsilon(X))_{j-1/2}^{n-1}(u)_{j-1/2}^{n-1}\right\}$$

$$+\frac{1}{2}\left\{\varepsilon(X)_{j-1/2}^n(gu)_{j-1/2}^n + \varepsilon(X)_{j-1/2}^{n-1}(gu)_{j-1/2}^{n-1}\right\}$$

$$=\frac{\xi_{j-1/2}^{n-1/2}}{2k_n}\left\{\left(u_{j-1/2}^n + u_{j-1/2}^{n-1}\right)\left(g_{j-1/2}^n - g_{j-1/2}^{n-1}\right)\right.$$

$$-\left(P_{j-1/2}^n + P_{j-1/2}^{n-1}\right)\left(f_{j-1/2}^n - f_{j-1/2}^{n-1}\right)\right\} - \frac{1}{2}\left\{M^2(u^2)_{j-1/2}^n\right.$$

$$+ M^2(u^2)_{j-1/2}^{n-1}\right\} - \frac{1}{2}\left\{(v^2)_{j-1/2}^n + (v^2)_{j-1/2}^{n-1}\right\}$$

$$\Rightarrow \frac{1}{\mathrm{Pr}}\left(\frac{P_j^n - P_{j-1}^n}{h_j} + \frac{P_j^{n-1} - P_{j-1}^{n-1}}{h_j}\right) + \left\{(fP)_{j-1/2}^n + (fP)_{j-1/2}^{n-1}\right\}$$

$$-\left\{(ug)_{j-1/2}^n + (ug)_{j-1/2}^{n-1}\right\} - \left\{\gamma(\varepsilon(X))_{j-1/2}^n(u)_{j-1/2}^n + \gamma(\varepsilon(X))_{j-1/2}^{n-1}(U)_{j-1/2}^{n-1}\right\}$$

$$+\left\{\varepsilon(X)_{j-1/2}^n(gu)_{j-1/2}^n + \varepsilon(X)_{j-1/2}^{n-1}(gu)_{j-1/2}^{n-1}\right\}$$

$$= \alpha_n\left\{\left(u_{j-1/2}^n + u_{j-1/2}^{n-1}\right)\left(g_{j-1/2}^n - g_{j-1/2}^{n-1}\right)\right.$$

$$-\left(P_{j-1/2}^n - P_{j-1/2}^{n-1}\right)\left(f_{j-1/2}^n - f_{j-1/2}^{n-1}\right)\right\} - \left\{M^2(u^2)_{j-1/2}^n\right.$$

$$+ M^2(u^2)_{j-1/2}^{n-1}\right\} - \left\{(v^2)_{j-1/2}^n + (v^2)_{j-1/2}^{n-1}\right\}$$

$$\Rightarrow \frac{1}{\mathrm{Pr}}\left(\frac{P_j^n - P_{j-1}^n}{h_j}\right) + (fP)_{j-1/2}^n - (ug)_{j-1/2}^n - \gamma(\varepsilon(X))_{j-1/2}^n(u)_{j-1/2}^n$$

$$-\varepsilon(X)_{j-1/2}^n(gu)_{j-1/2}^n + (fP)_{j-1/2}^{n-1} - (ug)_{j-1/2}^{n-1} - \gamma(\varepsilon(X))_{j-1/2}^{n-1}(u)_{j-1/2}^{n-1}$$

$$-\varepsilon(X)_{j-1/2}^{n-1}(gu)_{j-1/2}^{n-1} = \alpha_n\left\{\left((ug)_{j-1/2}^n + u_{j-1/2}^{n-1}g_{j-1/2}^n - u_{j-1/2}^n g_{j-1/2}^{n-1} - (ug)_{j-1/2}^{n-1}\right.\right.$$

$$-\left(\left(fP\right)^{n}_{j-1/2}+P^{n-1}_{j-1/2}f^{n}_{j-1/2}-P^{n}_{j-1/2}f^{n-1}_{j-1/2}-\left(fP\right)^{n-1}_{j-1/2}\right)\right\}-\left\{M^{2}\left(u^{2}\right)^{n}_{j-1/2}\right.$$

$$+M^{2}\left(u^{2}\right)^{n-1}_{j-1/2}\right\}-\left\{\left(v^{2}\right)^{n}_{j-1/2}+\left(v^{2}\right)^{n-1}_{j-1/2}\right\}$$

$$\Rightarrow\frac{1}{\mathrm{Pr}}\left(\frac{P^{n}_{j}-P^{n}_{j-1}}{h_{j}}\right)+\left(1+\alpha_{n}\right)\left(fP\right)^{n}_{j-1/2}-\left(1+\alpha_{n}+\varepsilon\left(X\right)^{n}_{j-1/2}\right)\left(ug\right)^{n}_{j-1/2}$$

$$-\gamma\left(\varepsilon\left(X\right)\right)^{n}_{j-1/2}\left(u\right)^{n}_{j-1/2}+M^{2}\left(u^{2}\right)^{n}_{j-1/2}+\left(v^{2}\right)^{n}_{j-1/2}$$

$$+\alpha_{n}\left(P^{n}_{j-1/2}f^{n-1}_{j-1/2}-P^{n-1}_{j-1/2}f^{n}_{j-1/2}+u^{n}_{j-1/2}g^{n-1}_{j-1/2}-u^{n-1}_{j-1/2}g^{n}_{j-1/2}\right)$$

$$=\alpha_{n}\left\{\left(fP\right)^{n-1}_{j-1/2}-\left(ug\right)^{n-1}_{j-1/2}\right\}-\frac{1}{\mathrm{Pr}}\left(\frac{P^{n-1}_{j}-P^{n-1}_{j-1}}{h_{j}}\right)-\left\{\left(fP\right)^{n-1}_{j-1/2}-\left(ug\right)^{n-1}_{j-1/2}\right.$$

$$-\gamma\left(\varepsilon\left(X\right)\right)^{n-1}_{j-1/2}\left(u\right)^{n-1}_{j-1/2}-\varepsilon\left(X\right)^{n-1}_{j-1/2}\left(gu\right)^{n-1}_{j-1/2}+M^{2}\left(u^{2}\right)^{n-1}_{j-1/2}\right\}-\left(v^{2}\right)^{n-1}_{j-1/2}$$

Here we applying the Newton's law for first order, then insert the right side of the above equations in place of f'_j, u'_j, v'_j and g'_j dropping the terms that are quadratic in $\delta f'_j$, $\delta u'_j$, $\delta v'_j$ and $\delta P'_j$ we get the equations (2.71), (2.72), (2.73) and (2.74) in the following form:

$$\frac{f_j^{(i)}-f_{j-1}^{(i)}}{h_j}+\frac{\delta f_j^{(i)}-\delta f_{j-1}^{(i)}}{h_j}$$

$$=u^{(i)}_{j-\frac{1}{2}}+\delta u^{(i)}_{j-\frac{1}{2}}=\frac{1}{2}\left[u_j^{(i)}+u_{j-1}^{(i)}+\delta u_j^{(i)}+\delta u_{j-1}^{(i)}\right]$$

$$\Rightarrow f_j^{(i)}+\delta f_j^{(i)}-f_{j-1}^{(i)}-\delta f_{j-1}^{(i)}=\frac{h_j}{2}\left\{u_j^{(i)}+\delta u_j^{(i)}+u_{j-1}^{(i)}+\delta u_{j-1}^{(i)}\right\} \qquad (2.76)$$

$$\delta f_j^{(i)}-\delta f_{j-1}^{(i)}-\frac{h_j}{2}(\delta u_j^{(i)}+\delta u_{j-1}^{(i)})=f_{j-1}^{(i)}-f_j^{(i)}-\frac{h_j}{2}(u_j^{(i)}+u_{j-1}^{(i)}) \qquad (2.77)$$

$$=f_{j-1}^{(i)}-f_j^{(i)}-h_j u^{(i)}_{j-\frac{1}{2}}=(r_1)_j$$

Similarly we have,

$$\delta u_j^{(i)}-\delta u_{j-1}^{(i)}-\frac{h_j}{2}(\delta v_j^{(i)}+\delta v_{j-1}^{(i)})=u_{j-1}^{(i)}-u_j^{(i)}-\frac{h_j}{2}(v_j^{(i)}+v_{j-1}^{(i)}) \qquad (2.78)$$

$$=u_{j-1}^{(i)}-u_j^{(i)}-h_j v^{(i)}_{j-\frac{1}{2}}=(r_4)_j$$

$$\delta g_j^{(i)}-\delta g_{j-1}^{(i)}-\frac{h_j}{2}(\delta P_j^{(i)}+\delta P_{j-1}^{(i)})=g_{j-1}^{(i)}-g_j^{(i)}-\frac{h_j}{2}(P_j^{(i)}+P_{j-1}^{(i)}) \qquad (2.79)$$

$$=g_{j-1}^{(i)}-g_j^{(i)}-h_j P^{(i)}_{j-\frac{1}{2}}=(r_5)_j$$

Appendix B

Table-B$_1$

T °C	ρ kg/m³	C_P kJ/(kg)	ν m²/s	κ W/(m)	α m²/s	Pr	β, K^{-1} 1/K
Mercury							
0	13,628.22	0.1403	0.124×10⁻⁶	8.20	42.99	0.0288	
20	13,579 04	0.1394	0.114	8.69	46.06	0.0249	1.82×10⁻⁴
50	13,505.84	0.1386	0.104	9.40	50.22	0.0207	
100	13384.58	0.1373	0.0928	10.51	57.16	0.0162	
150	13,264.28	0.1365	0.0853	11.49	63.54	0.0134	
200	13,144.94	0.1360	0.0802	12.34	69.08	0 0116	
250	13,025 60	0.1357	0.0765	13.07	74.06	0 0103	
315.5	12,847 00	0.1340	0.0673	14.02	8.15	0 0083	

Table-B$_2$

T °C	ρ kg/m³	C_P kJ/(kg.)	ν m²/s	κ W/(m)	α m²/s	Pr	β, K^{-1} 1/K
Water							
0	1,002.28	4.2178	1.788×10⁻⁶	0.552	1.308	13.6	
20	1,000.52	4.1818	1.006	0.597	1 430	7.02	0 18×10⁻³
40	994.59	4.1784	0.658	0.628	1.512	4.34	
60	985.46	4.1843	0.478	0.651	1.554	3.02	
80	974.08	4.1964	0.364	0.668	1.636	2.22	
100	960.63	4 2161	0 294	0.680	1.680	1.74	
120	945.25	4.250	0.247	0.685	1.708	1.446	
140	928.27	4.283	0.214	0.684	1.724	1.241	
160	909.69	4.342	0 190	0.680	1.729	1.099	
180	889.03	4.417	0.173	0.675	1.724	1.004	
200	866.76	4.505	0.160	0.665	1.706	0.937	
220	842.41	4.610	0.150	0.652	1.680	0.891	
240	815.66	4.756	0.143	0.635	1.639	0.871	
280.6	752.55	5 208	0.135	0.580	1.481	0 910	
300	714.26	5.728	0 135	0 540	1 324	1 019	

Table-B$_3$

T °K	ρ kg/m³	C_P kJ/(kg.)	μ kg/(ms)	ν m²/s	κ W/(m)	α m²/s	Pr
Steam							
380	0.5863	2.060	12.71×10⁻⁶	21.6	0.0246	0.2036	1.060
400	0.5544	2.014	13.44	24.2	0.0261	0.2338	1 040
450	0 4902	1.980	15.25	31.1	0.0299	0.307	1 010
500	0 4450	1.985	17.04	38.6	0.0339	0.387	0 996
550	0 4005	1.997	18.84	47.0	0.0379	0.475	0 991
600	0.3652	2.026	20.67	56.6	0.0422	0.573	0.986
650	0 3380	2.056	22.47	64.4	0.0464	0.666	0 995
700	0.3140	2.058	24.26	77.2	0.0505	0.772	1.000
750	0 2931	2.119	26.04	88.8	0.0549	0.883	1.005
800	0.2739	2.152	27.86	102.0	0.0592	1.001	1 010

Table-B₄

$T\,^{\circ}K$	ρ kg/m³	C_p kJ/(kg.)	μ kg/(ms)	ν m²/s	κ W/(m)	α m²/s	Pr
Air							
100	3.6010	1.0266	0.6924×10^{-5}	1.9230	0.009246	0.02501	0.770
150	2.3675	1.0099	1.0283	4.3430	0.013735	0.05745	0.753
200	1.7684	1.0061	1.3289	7.4900	0.018090	0.10165	0.739
250	1.4128	1.0053	1.4880	9.4900	0.022270	0.13161	0.722
300	1.1774	1.0057	1.9830	15.6800	0.026240	0.22160	0.708
350	0.9980	1.0090	2.0750	20.7600	0.030030	0.29830	0.697
400	0.8826	1.0140	2.2860	25.9000	0.033650	0.37600	0.689
450	0.7833	1.0207	2.4840	28.8600	0.037070	0.42220	0.683
500	0.7048	1.0295	2.6710	37.9000	0.040380	0.55640	0.680
550	0.6423	1.0392	2.8480	44.3400	0.043600	0.65320	0.680
600	0.5879	1.0551	3.0180	51.3400	0.046590	0.75120	0.680
650	0.5430	1.0635	3.1770	58.5100	0.049530	0.85780	0.682
700	0.5030	1.0752	3.3320	66.2500	0.052300	0.96720	0.684
750	0.4709	1.0856	3.4810	73.9100	0.055090	1.07740	0.686
800	0.4405	1.0978	3.6250	82.2900	0.057790	1.19510	0.689
850	0.4149	1.1095	3.7650	90.7500	0.060280	1.30970	0.692
900	0.3925	1.1212	3.8990	99.3000	0.062790	1.42710	0.696
950	0.3716	1.1321	4.0230	108.200	0.065250	1.55100	0.699
1000	0.3524	1.1417	4.1520	117.800	0.067520	1.67790	0.702
1100	0.3204	1.1600	4.4400	138.600	0.073200	1.96900	0.704
1200	0.2947	1.1790	4.6900	159.100	0.078200	2.25100	0.707
1300	0.2707	1.1970	4.9300	182.100	0.083700	2.58300	0.705
1400	0.2515	1.2140	5.1700	205.500	0.089100	2.92000	0.705
1500	0.2355	1.2300	5.40000	229.100	0.094600	3.26200	0.705
1600	0.2211	1.2480	5.6300	254.500	0.100000	3.60900	0.705
1700	0.2082	1.2670	5.8500	280.500	0.105000	3.97700	0.705
1800	0.1970	1.2870	6.0700	308.10	0.111000	4.37900	0.704
1900	0.1858	1.3090	6.2900	338.50	0.117000	4.81100	0.704
2000	0.1762	1.3380	6.5000	369.00	0.124000	5.26000	0.702
2100	0.1682	1.3720	6.7200	399.60	0.131000	5.71500	0.700
2200	0.1602	1.4190	6.9300	432.60	0.139000	6.12000	0.070
2300	0.1538	1.4820	7.1400	464.00	0.149000	6.54000	0.710
2400	0.1458	1.5740	7.3500	504.00	0.161000	7.02000	0.718
2500	0.1394	1.6880	7.5700	543.50	0.175000	7.44100	0.730

Table-B₅

Magnetic Parameter	Author's name	Journal name & Volume No.	Page numbers	Year
M = 0.0, 0 5, 1.0	EL-Amin, M. F.	Journal of magnetism and magnetic materials (Vol. 263)	337-343	2003
M = 1.0, 2.0, 3.0, 4.0	Gansan, P. & Palani, G.	International Journal of Heat and Mass Transfer (Vol. 47)	4449-4457	2004
M = 0.0, 0.2, 1.0, 3.0	Md. Abdul Maleque and Md. Shariful Alam	JNAME	18-25	2004
M = 2.0	Umavathi, J. C. & Malashetty, M. S.	Int. J. NON-LINEAR MECHANICS (Vol. 40)	91-101	2005
M = 0.0, 0.4, 1.0, 3 0	EL-Amin, M. F. & Mohammadein, A. A	Heat transfer Engineering (Vol 26)	75-81	2005
M = 0.0, 0.2, 0.5, 0.8, 1.0	Molla et al.	Nonlinear Analysis; Modelling and Control (Vol. 10) No. 4	349-363	2005
M = 0.0, 0.2, 0.5, 0 8 1 0	Molla et al.	ACATA MECHANICA (Vol. 186)	75-86	2006
M = 1.4, 0.9, 0 5, 0.1	Alim et al.	Nonlinear Analysis: Modeling and Control (Vol. 12) No. 3	307-316	2007

Table-B₆

Surface temperature Parameter	Author's name	Journal name & Volume No.	Page numbers	Year
θ_w = 1.1, 2.0, 3.0	Hossain et al.	MECHANICA (Vol 129)	177-186	1998
θ_w = 1.1, 1.5, 2.0, 3 0, 4.0	Hossain, M. A. & Takhar, H. S.	Heat and Mass Transfer (Vol. 35)	321-326	1999
θ_w = 1.1, 1.5, 2.0, 2.5	Hossain et al.	Int. J. Heat and Mass transfer (Vol. 42)	181-191	1999
θ_w = 1.5	Hossain et al.	Int. J. Therm. Sci. (Vol. 40)	115-124	2001

Table-B$_7$

Radiation parameter	Author's name	Journal name & Volume No.	Page numbers	Year
Rd = 0.1, 0 0, 0.2.0	Md. Abdus Sattar and Md. Hamid Kalim	Journal of Mathematical and Physical Science (Vol. 30), No. 1	25-37	1996
Rd = 1.0, 2 0, 10.0	Hossain et al.	Int. J. Heat and Mass transfer (Vol 42)	181-191	1999
Rd = 1.0, 10.0, 40 0	Hossain, M A. & Takhar, H S.	Heat and Mass Transfer (Vol. 35)	321-326	1999
Rd = 1.0	Hossain et al.	Int. J. Therm Sci. (Vol. 40)	115-124	2001

Table-B$_8$

Viscous dissipation parameter	Author's name	Journal name & Volume No.	Page numbers	Year
N = -0.5, 0.0, 3.0	EL-Amin, M. F.	Journal of magnetism and magnetic materials (Vol. 263)	337-343	2003
N = 0.9, 0.5, 0.3, 0.1	Alam et al.	Journal of Naval Architecture and Marine Engineering	69-76	2006
N = 1.0, 0.7, 0.5, 0.3, 0.1	Alam et al.	Journal of Mechanical Engineering (Vol. ME36)	44-48	2006
N = 1.0, 0.7, 0.4, 0.1	Alim et al.	International Communications in Heat and Mass Transfer	in press	2007

Table-B$_9$

Heat generation parameter	Author's name	Journal name & Volume No.	Page numbers	Year
Q = 0.0, 0.5, 1.0, 2.0	Molla et al.	Nonlinear Analysis; Modelling and Control (Vol. 10) No. 4	349-363	2005
Q = 0.0, 0.2. 0 5, 0.8. 1.0	Molla et al	ACATA MECHANICA (Vol 186)	75-86	2006

Table-B_{10}

Joule heating parameter	Author's name	Journal name & Volume No.	Page numbers	Year
$J = 0.9, 0.7, 0.4,$ 0.2	Alim et al.	Nonlinear Analysis: Modeling and Control (Vol. 12.) No. 3	307-316	2007
$J = 1.0, 0.8, 0.5,$ 0.2	Alim et al.	International Communications in Heat and Mass Transfer	in press	2007

Table-B_{11}

Pressure work parameter	Author's name	Journal name & Volume No.	Page numbers	Year
$Ge = -0.1, 0.3,$ 0.9	Alim et al.	Journal of Mechanical Engineering (Vol. ME36)	6-11	2006
$Ge = 0.9, 0.7,$ 0.4, 0.1	Alam et al.	Journal of Naval Architecture and Marine Engineering	69-76	2006
$Ge = 0.9, 0.6,$ 3.0, -0.1, -0.6	Alam et al.	Nonlinear Analysis. Modeling and Control (Vol. 12,) No. 1	21-32	2007

Table-B_{12}

Water	Magnetic field strength, B_o	Electrical Conductivity, $\sigma(S/m^2)$	Magnetic parameter, M	Joule heating parameter, Jul
$20^{\circ}C$	3205	0.05	1.00	2×10^{-1}
$20^{\circ}C$	4533	0.05	2.00	4×10^{-1}

Appendix C
List of Tables

Table-C₁: Skin friction coefficient and surface temperature for different values of magnetic parameter M against x with other controlling parameters $Pr = 0.72$, $N = 0.50$ and $Ge = 0.70$.

	$M = 1.0$		$M = 1.5$		$M = 1.7$		$M = 2.0$	
x	$f''(x, 0)$	$\theta(x, 0)$	$f''(x, 0)$	$\theta(x, 0)$	$f''(x, 0)$	$\theta(x, 0)$	$f''(x, 0)$	$\theta(x, 0)$
0.00	0.0154	0.2044	0.0154	0.2044	0.0154	0.2044	0.0154	0.2044
0.10	0.3291	0.6634	0.3137	0.6504	0.3198	0.6504	0.3103	0.6449
0.20	0.3967	0.7092	0.3768	0.6907	0.3621	0.6907	0.3597	0.6874
0.30	0.4421	0.7287	0.4134	0.7273	0.3989	0.7273	0.3865	0.7168
0.40	0.4757	0.7516	0.4413	0.7459	0.4271	0.7459	0.4045	0.7386
0.50	0.5017	0.7659	0.4614	0.7669	0.4488	0.7669	0.4224	0.7542
0.70	0.5397	0.7983	0.4901	0.7880	0.4779	0.7880	0.4568	0.7789
0.90	0.5702	0.8128	0.5160	0.8072	0.4987	0.8072	0.4753	0.7950
1.00	0.5837	0.8213	0.5265	0.8182	0.5115	0.8182	0.4857	0.8039
1.20	0.6068	0.8312	0.5489	0.8287	0.5238	0.8287	0.4967	0.8165
1.40	0.6262	0.8456	0.5595	0.8465	0.5304	0.8465	0.5110	0.8208
1.60	0.6437	0.8629	0.5685	0.8488	0.5485	0.8488	0.5193	0.8293
1.80	0.6585	0.8697	0.5803	0.8554	0.5579	0.8554	0.5283	0.8383
2.00	0.6722	0.8775	0.5912	0.8648	0.5684	0.8648	0.5362	0.8469

Table-C₂: Skin friction and surface temperature for different values of Prandtl number Pr against x with other controlling parameters $M = 1.00$, $N = 0.60$ and $Ge = 0.50$.

	$Pr = 0.10$		$Pr = 0.72$		$Pr = 1.00$	
x	$f''(x, 0)$	$\theta(x, 0)$	$f''(x, 0)$	$\theta(x, 0)$	$f''(x, 0)$	$\theta(x, 0)$
0.0000	0.0313	0.3796	0.0154	0.2044	0.0137	0.1873
0.1102	0.5707	0.7505	0.3795	0.6300	0.3505	0.6074
0.3150	0.7801	0.8163	0.5356	0.7006	0.4974	0.6793
0.7090	0.9946	0.8797	0.7067	0.7685	0.6601	0.7495
1.0409	1.1186	0.8874	0.8131	0.8063	0.7626	0.7906
2.0369	1.3927	0.9477	1.0725	0.9105	1.0167	0.9037
3.1340	1.6297	0.9958	1.3332	1.0271	1.2786	1.0345

Table-C₃: Skin friction coefficient and surface temperature distribution for different values of viscous dissipation parameter N against x with other controlling parameters M = 0.80, Ge = 0 50, Pr = 0.72.

x	$N = 0.20$		$N = 0.40$		$N = 0.60$		$N = 0.90$	
	$f''(x, 0)$	$\theta(x,0)$	$f''(x, 0)$	$\theta(x,0)$	$f''(x, 0)$	$\theta(x,0)$	$f''(x, 0)$	$\theta(x,0)$
0.0000	0.0154	0.2044	0.0154	0.2044	0.0154	0.2044	0.0154	0.2044
0.3150	0.4572	0.7086	0.4598	0.7128	0.4624	0.7172	0.4664	0.7239
0.7090	0.5557	0.7630	0.5617	0.7711	0.5678	0.7795	0.5773	0 7927
1.0409	0.6048	0.7854	0.6135	0.7964	0.6225	0.8078	0.6367	0.8259
2.0369	0.6930	0.8294	0.7092	0.8472	0.7264	0.8663	0.7544	0.8980
3.1340	0.7500	0.8566	0.7735	0.8804	0.7991	0.9069	0.8423	0.9525
4.0635	0.7841	0.8720	0.8132	0.9003	0.8456	0.9325	0.9018	0.9897
4.9876	0.8108	0.8848	0.8450	0.9171	0.8839	0 9546	0.9532	1.0232
6.1118	0.8369	0.8973	0.8770	0.9340	0.9236	0.9776	1.0090	1.0604
7.1132	0.8562	0.9072	0.9012	0.9475	0.9544	0 9963	1.0546	1.0918
9.1512	0.8876	0.9216	0.9418	0.9687	1.0080	1.0277	1.1399	1.1503
10.1191	0.8999	0.9275	0.9582	0.9775	1.0304	1.0412	1.1781	1.1773

Table-C₄: Skin friction coefficient and surface temperature distribution for different values of pressure work parameter Ge against x with other controlling parameters M = 0 80, N = 0.60 and Pr = 0.72.

x	$Ge = 0 20$		$Ge = 0.40$		$Ge = 0 70$		$Ge = 0.90$	
	$f''(x, 0)$	$\theta(x,0)$	$f''(x, 0)$	$\theta(x,0)$	$f''(x, 0)$	$\theta(x,0)$	$f''(x, 0)$	$\theta(x,0)$
0.0000	0.0154	0 2044	0.0154	0.2044	0.0154	0.2044	0 0154	0.2044
0.3150	0 4603	0 7111	0.4612	0.7135	0.4651	0.7201	0.4692	0.7269
0.7090	0.5680	0.7720	0 5679	0.7750	0.5774	0.7881	0 5872	0.8018
1.0409	0 6276	0 8014	0.6255	0.8040	0 6397	0.8220	0.6547	0.8414
2.0369	0.7574	0.8709	0.7446	0.8691	0.7738	0.9020	0.8061	0.9391
3.1340	0.8756	0.9343	0.8430	0.9229	0.8911	0.9733	0.9464	1.0334
4.0635	0.9743	0.9879	0.9179	0.9640	0.9845	1.0315	1.0639	1.1157
4.9876	1.0781	1.0464	0.9906	1.0054	1.0786	1.0928	1.1874	1.2065
6.1118	1.2181	1.1273	1.0808	1.0580	1.2001	1.1744	1.3538	1.3343
7.1132	1.3602	1.2121	1.1656	1.1090	1.3186	1.2572	1.5233	1.4710
9.1512	1.7166	1.4313	1.3592	1.2273	1.6036	1.4643	1.9567	1.8432
10.1191	1.9251	1.5647	1.4646	1.2941	1.7661	1.5884	2.2181	2.0834

Table-C₅: Skin friction coefficient and surface temperature distribution for different values of Prandtl number Pr against x with other controlling parameters $Ju\ell = 0.4, M = 0.5, N = 0.3. Ge = 0.6$.

x	$Pr = 0.10$		$Pr = 0.50$		$Pr = 0.72$		$Pr = 1.00$	
	$f''(x, 0)$	$\theta(x, 0)$	$f''(x, 0)$	$\theta(x, 0)$	$f''(x, 0)$	$\theta(x, 0)$	$f''(x, 0)$	$\theta(x,0)$
0.0000	0.0313	0.3796	0.0177	0.2280	0.0155	0.2052	0.0137	0.1873
0.1102	0.5324	0.7562	0.3907	0.6640	0.3587	0.6380	0.3308	0.6143
0.2115	0.6310	0.7997	0.4712	0.7066	0.4344	0.6811	0.4022	0.6578
0.3150	0.6967	0.8240	0.5269	0.7332	0.4872	0.7084	0.4523	0.6856
0.7090	0.8461	0.8906	0.6602	0.7957	0.6151	0.7721	0.5748	0.7504
0.9015	0.8945	0.8886	0.7065	0.8123	0.6601	0.7908	0.6183	0.7707
1.0409	0.9252	0.8983	0.7364	0.8253	0.6893	0.8044	0.6467	0.7848
1.1907	0.9550	0.9078	0.7661	0.8382	0.7184	0.8180	0.6751	0.7990
1.4382	0.9996	0.9327	0.8114	0.8600	0.7629	0.8402	0.7187	0.8217
1.7182	1.0442	0.9371	0.8586	0.8789	0.8096	0.8611	0.7647	0.8440
2.0369	1.0909	0.9615	0.9093	0.9033	0.8600	0.8864	0.8145	0.8702
2.4015	1.1402	0.9704	0.9648	0.9273	0.9156	0.9126	0.8697	0.8982
2.5346	1.1578	0.9843	0.9848	0.9380	0.9357	0.9235	0.8897	0.9093
3.1340	1.2334	1.0715	1.0742	0.9802	1.0259	0.9689	0.9800	0.9576
4.0635	1.3476	1.1491	1.2163	1.0492	1.1708	1.0442	1.1261	1.0384

Table-C₆: Skin friction coefficient and surface temperature distribution for different values of pressure work parameter Ge against x with other controlling parameters $Ju\ell = 0.40, M = 0.50, N = 0.30, Pr = 0.72$

x	$Ge = 0.20$		$Ge = 0.40$		$Ge = 0.60$		$Ge = 0.80$	
	$f''(x, 0)$	$\theta(x, 0)$	$f''(x, 0)$	$\theta(x, 0)$	$f''(x, 0)$	$\theta(x, 0)$	$f''(x, 0)$	$\theta(x, 0)$
0.0000	0.0154	0.2044	0.0154	0.2044	0.0154	0.2044	0.0154	0.2044
0.1102	0.3570	0.6363	0.3575	0.6371	0.3581	0.6378	0.3586	0.6386
0.3150	0.4827	0.7044	0.4858	0.7075	0.4889	0.7107	0.4920	0.7139
0.7090	0.6021	0.7618	0.6134	0.7712	0.6251	0.7810	0.6370	0.7912
1.0409	0.6666	0.7877	0.6875	0.8036	0.7095	0.8208	0.7326	0.8391
2.0369	0.7963	0.8442	0.8582	0.8858	0.9283	0.9352	1.0065	0.9933
3.1340	0.8962	0.8871	1.0242	0.9686	1.1817	1.0775	1.3693	1.2179
4.0635	0.9664	0.9172	1.1692	1.0441	1.4368	1.2310	1.7693	1.4886
4.9876	1.0296	0.9455	1.3265	1.1307	1.7438	1.4290	2.2798	1.8638
6.1118	1.1015	0.9783	1.5440	1.2563	2.2089	1.7506	3.0877	2.5114
7.1132	1.1633	1.0078	1.7689	1.3931	2.7258	2.1347	4.0127	3.3196
9.1512	1.2877	1.0669	2.3431	1.7668	4.1475	3.3045	6.6253	5.8998
10.1191	1.3479	1.0965	2.6826	2.0034	5.0298	4.1014	8.2718	7.7097

Table-C$_7$: Skin friction coefficient and surface temperature distribution for different values of viscous dissipation parameter N against x with other controlling parameters $Jul = 0.40$, $M = 0.80$, $Ge = 0.70$, $Pr = 0.72$.

	$N = 0.10$		$N = 0.30$		$N = 0.60$		$N = 0.90$	
x	$f''(x,0)$	$\theta(x,0)$	$f''(x,0)$	$\theta(x,0)$	$f''(x,0)$	$\theta(x,0)$	$f''(x,0)$	$\theta(x,0)$
0.0000	0.0154	0.2044	0.0154	0.2044	0.0154	0.2044	0.0154	0.2044
0.3150	0.4594	0.7102	0.4621	0.7145	0.4661	0.7211	0.4701	0.7279
0.7090	0.5649	0.7694	0.5711	0.7778	0.5807	0.7910	0.5906	0.8049
1.0409	0.6220	0.7969	0.6312	0.8085	0.6457	0.8270	0.6609	0.8469
2.0369	0.7417	0.8598	0.7605	0.8807	0.7911	0.9153	0.8249	0.9544
3.1340	0.8438	0.9130	0.8748	0.9449	0.9269	1.0002	0.9868	1.0661
4.0635	0.9244	0.9550	0.9674	0.9978	1.0419	1.0745	1.1307	1.1703
4.9876	1.0051	0.9987	1.0624	1.0542	1.1640	1.1572	1.2897	1.2919
6.1118	1.1088	1.0559	1.1871	1.1304	1.3305	1.2745	1.5156	1.4740
7.1132	1.2094	1.1131	1.3107	1.2087	1.5016	1.4006	1.7572	1.6802
9.1512	1.4489	1.2514	1.6136	1.4068	1.9417	1.7441	2.4153	2.2900
10.1191	1.5835	1.3317	1.7883	1.5262	2.2067	1.9645	2.8329	2.7106

Table-C$_8$: Skin friction coefficient and surface temperature distribution for different values of Joule heating parameter Jul against x with other controlling parameters $N = 0.50$, $M = 0.40$, $Ge = 0.70$, $Pr = 0.72$.

	$Jul = 0.20$		$Jul = 0.40$		$Jul = 0.70$		$Jul = 0.90$	
x	$f''(x,0)$	$\theta(x,0)$	$f''(x,0)$	$\theta(x,0)$	$f''(x,0)$	$\theta(x,0)$	$f''(x,0)$	$\theta(x,0)$
0.0000	0.0154	0.2044	0.0154	0.2044	0.0154	0.2044	0.0154	0.2044
0.3150	0.4955	0.7080	0.4977	0.7102	0.5009	0.7136	0.5031	0.7158
0.7090	0.6296	0.7729	0.6378	0.7799	0.6505	0.7906	0.6591	0.7981
1.0409	0.7069	0.8059	0.7226	0.8181	0.7470	0.8374	0.7639	0.8511
2.0369	0.8798	0.8871	0.9294	0.9218	1.0112	0.9820	1.0708	1.0277
3.1340	1.0371	0.9640	1.1463	1.0386	1.3383	1.1802	1.4848	1.2962
4.0635	1.1657	1.0298	1.3472	1.1547	1.6823	1.4095	1.9462	1.6295
6.1118	1.4685	1.1990	1.9027	1.5133	2.7734	2.2499	3.4900	2.9416
7.1132	1.6364	1.3001	2.2536	1.7633	3.5287	2.9104	4.5915	4.0196
9.1512	2.0394	1.5586	3.1890	2.4995	5.6719	5.0504	7.7768	7.6283
10.1191	2.2671	1.7148	3.7618	2.9945	7.0403	6.5874	9.8359	10.2765

Table-C₉: Skin friction coefficient and surface temperature distribution for different values of heat generation parameter Q against x with other controlling parameters $Pr = 0.72$, $Jul = 0.005$, $M = 0.50$, $N = 0.40$, $Ge = 0.01$.

x	$Q = 0.10$		$Q = 0.30$		$Q = 0.50$		$Q = 0.70$	
	$f''(x, 0)$	$\theta(x, 0)$	$f''(x, 0)$	$\theta(x, 0)$	$f''(x, 0)$	$\theta(x, 0)$	$f''(x, 0)$	$\theta(x, 0)$
0.0000	0.0155	0.2052	0.0155	0.2052	0.0155	0.2052	0.0155	0.2052
0.3045	0.5083	0.7352	0.5801	0.8126	0.6663	0.9106	0.7686	1.0338
0.7090	0.6416	0.7907	0.7502	0.8847	0.8851	1.0087	1.0490	1.1701
1.0265	0.7067	0.8152	0.8356	0.9168	0.9982	1.0531	1.1981	1.2332
2.0369	0.8372	0.8614	1.0113	0.9773	1.2373	1.1381	1.5208	1.3559
3.0049	0.9169	0.8885	1.1213	1.0131	1.3913	1.1893	1.7337	1.4311
4.0219	0.9794	0.9095	1.2093	1.0414	1.5169	1.2304	1.9101	1.4924
5.0387	1.0296	0.9263	1.2811	1.0645	1.6211	1.2648	2.0583	1.5443
6.0502	1.0717	0.9405	1.3423	1.0844	1.7111	1.2949	2.1877	1.5903
7.1132	1.1100	0.9534	1.3989	1.1031	1.7955	1.3237	2.3103	1.6348
8.0285	1.1395	0.9635	1.4430	1.1178	1.8621	1.3468	2.4078	1.6710
9.0596	1.1698	0.9738	1.4888	1.1333	1.9320	1.3714	2.5109	1.7100
10.0179	1.1956	0.9826	1.5284	1.1468	1.9930	1.3933	2.6016	1.7451

Table-C₁₀: Skin friction coefficient and surface temperature distribution for different values of magnetic parameter M against x with other controlling parameters $Jul = 0.40$, $Q = 0.50$, $N = 0.30$, $Ge = 0.60$.

x	$M = 0.20$		$M = 0.40$		$M = 0.60$		$M = 1.0$	
	$f''(x, 0)$	$\theta(x, 0)$	$f''(x, 0)$	$\theta(x, 0)$	$f''(x, 0)$	$\theta(x, 0)$	$f''(x, 0)$	$\theta(x, 0)$
0.0000	0.0155	0.2052	0.0155	0.2052	0.0155	0.2052	0.0155	0.2052
0.3045	0.6125	0.8131	0.5950	0.8212	0.5791	0.8294	0.5512	0.8455
0.7090	0.8190	0.8991	0.7849	0.9089	0.7550	0.9190	0.7054	0.9397
1.0265	0.9324	0.9440	0.8862	0.9534	0.8466	0.9636	0.7829	0.9854
2.0369	1.1981	1.0512	1.1144	1.0543	1.0462	1.0608	0.9440	1.0798
3.0049	1.3982	1.1380	1.2772	1.1299	1.1824	1.1292	1.0471	1.1412
4.0219	1.5862	1.2257	1.4232	1.2014	1.2998	1.1906	1.1313	1.1923
5.0387	1.7644	1.3147	1.5557	1.2697	1.4027	1.2464	1.2013	1.2357
6.0502	1.9386	1.4069	1.6803	1.3368	1.4960	1.2987	1.2619	1.2739
8.0285	2.2841	1.6043	1.9144	1.4702	1.6635	1.3965	1.3637	1.3397
9.0596	2.4716	1.7188	2.0353	1.5426	1.7461	1.4466	1.4108	1.3707
10.0179	2.6528	1.8340	2.1484	1.6124	1.8212	1.4931	1.4519	1.3981

Table-C$_{11}$: Skin friction coefficient and surface temperature distribution for different values of Joule heating parameter Jul against x with other controlling parameters $Pr =$ 1.00, $Q = 0.20$, $M = 0.60$, $N = 0.006$, $Ge = 0.70$.

x	$Jul = 0.30$		$Jul = 0.50$		$Jul = 0.70$		$Jul = 0.90$	
	$f''(x, 0)$	$\theta(x,0)$	$f''(x, 0)$	$\theta(x,0)$	$f''(x, 0)$	$\theta(x,0)$	$f''(x, 0)$	$\theta(x,0)$
0.0000	0.0137	0.1873	0.0137	0.1873	0.0137	0.1873	0.0137	0.1873
0.3045	0.6184	0.8871	0.6356	0.9064	0.6535	0.9270	0.6721	0.9488
0.7090	0.9614	1.1362	0.9990	1.1752	1.0387	1.2170	1.0805	1.2618
1.0265	1.2262	1.3369	1.2819	1.3937	1.3407	1.4549	1.4027	1.5208
2.0369	2.2289	2.1726	2.3586	2.3106	2.4962	2.4605	2.6417	2.6228
3.0049	3.5850	3.4674	3.8199	3.7397	4.0692	4.0360	4.3332	4.3575
4.0219	5.6664	5.7475	6.0662	6.2645	6.4906	6.8279	6.9402	7.4402
5.0387	8.7656	9.6629	9.4141	10.6098	10.1026	11.6428	10.8319	12.7665

Table-C$_{12}$: Skin friction coefficient and surface temperature distribution for different values of Pressure work parameter Ge against x with other controlling parameters $Pr =$ 0.72, $Q = 0.50$, $M = 0.50$, $N = 0.001$, $Jul = 0.005$.

x	$Ge = 0.10$		$Ge = 0.30$		$Ge = 0.60$		$Ge = 0.90$	
	$f''(x, 0)$	$\theta(x,0)$	$f''(x, 0)$	$\theta(x,0)$	$f''(x, 0)$	$\theta(x,0)$	$f''(x, 0)$	$\theta(x,0)$
0.0000	0.0137	0.1873	0.0137	0.1873	0.0137	0.1873	0.0137	0.1873
0.3045	0.7268	1.0423	0.7612	1.0892	0.8148	1.1646	0.8710	1.2465
0.7090	1.0346	1.2462	1.1412	1.3736	1.3160	1.5961	1.5102	1.8618
1.0265	1.2197	1.3671	1.3988	1.5723	1.7046	1.9542	2.0607	2.4439
1.5095	1.4641	1.5301	1.7794	1.8812	2.3520	2.5992	3.0697	3.6262
2.0369	1.7075	1.6990	2.2090	2.2533	3.1848	3.5105	4.5136	5.5389
3.0049	2.1349	2.0143	3.0943	3.0931	5.2230	6.0620	8.6175	12.0634
3.2005	2.2212	2.0810	3.2940	3.2948	5.7397	6.7711	9.7696	14.1307

Table-C$_{13}$: Skin friction coefficient and rate of heat transfer against x for different values of magnetic parameter M with other controlling parameters $Pr = 0.72$, $Q = 2.00$, $N = 0.90$ and $Ge = 0.50$.

x	$M = 0.40$		$M = 0.60$		$M = 0.80$		$M = 1.00$	
	C_{fx}	Nu_x	C_{fx}	Nu_x	C_{fx}	Nu_x	C_{fx}	Nu_x
0.00000	0.00000	1.02248	0.00000	0.99028	0.00000	0.96003	0.00000	0.93160
0.10472	0.08795	1.02141	0.08340	0.98919	0.07933	0.95893	0.07569	0.93045
0.20944	0.17522	1.01838	0.16613	0.98612	0.15800	0.95582	0.15073	0.92731
0.40143	0.33132	1.00768	0.31395	0.97528	0.29842	0.94485	0.28455	0.91625
0.50615	0.41318	0.99902	0.39132	0.96651	0.37181	0.93597	0.35437	0.90730
0.80285	0.62615	0.96344	0.59178	0.93047	0.56121	0.89952	0.53401	0.87053
1.01229	0.75407	0.92818	0.71112	0.89478	0.67310	0.86343	0.63938	0.83415
1.20428	0.85072	0.88812	0.80021	0.85425	0.75569	0.82249	0.71638	0.79291
1.30900	0.89399	0.86301	0.83950	0.82887	0.79161	0.79685	0.74945	0.76711
1.50098	0.95406	0.81068	0.89264	0.77603	0.83900	0.74355	0.79206	0.71350
1.57080	0.96930	0.78954	0.90550	0.75471	0.84993	0.72206	0.80142	0.69192

Table-C$_{14}$: Skin friction coefficient and rate of heat transfer against x for different values of viscous dissipation parameter N with other controlling parameters $Pr = 0.72$, $Q = 2.00$, $M = 0.90$ and $Ge = 0.50$.

x	$N = 0.10$		$N = 0.50$		$N = 0.70$		$N = 1.00$	
	C_{fx}	Nu_x	C_{fx}	Nu_x	C_{fx}	Nu_x	C_{fx}	Nu_x
0.00000	0.00000	0.84401	0.00000	1.12528	0.00000	1.24688	0.00000	1.35948
0.17453	0.16143	0.62483	0.17022	0.85247	0.17328	0.95091	0.17583	1.04193
0.34907	0.31993	0.61026	0.33730	0.83433	0.34335	0.93127	0.34839	1.02090
0.52360	0.47266	0.59539	0.49819	0.81517	0.50708	0.91027	0.51449	0.99819
0.69813	0.61686	0.57701	0.64992	0.79122	0.66143	0.88390	0.67101	0.96959
0.87266	0.74982	0.55426	0.78959	0.76142	0.80343	0.85106	0.81496	0.93391
1.04720	0.86897	0.52667	0.91444	0.72523	0.93026	0.81114	0.94344	0.89051
1.22173	0.97186	0.49388	1.02182	0.68213	1.03921	0.76364	1.05369	0.83887
1.39626	1.05612	0.45551	1.10922	0.63180	1.12769	0.70806	1.14308	0.77844
1.57080	1.11947	0.41114	1.17419	0.57358	1.19322	0.64382	1.20908	0.70860

Table-C$_{15}$: Skin friction coefficient and rate of heat transfer against x for different values of pressure work parameter Ge with other controlling parameters $Pr = 0.72$, $Q = 0.40$, $M = 1.00$ and $N = 0.50$

x	$Ge = 0.10$		$Ge = 0.40$		$Ge = 0.70$		$Ge = 0.90$	
	C_{fx}	Nu_x	C_{fx}	Nu_x	C_{fx}	Nu_x	C_{fx}	Nu_x
0.00000	0.00000	0.21716	0.00000	0.24647	0.00000	0.33411	0.00000	0.53155
0.10472	0.09115	0.21652	0.09236	0.24576	0.09626	0.33326	0.10311	0.53036
0.20944	0.18174	0.21467	0.18415	0.24377	0.19192	0.33083	0.20554	0.52698
0.50615	0.43071	0.20291	0.43635	0.23104	0.45454	0.31535	0.48644	0.50540
0.80285	0.65895	0.18123	0.66737	0.20761	0.69455	0.28682	0.74224	0.46557
1.01229	0.80133	0.15969	0.81133	0.18434	0.84355	0.25846	0.90015	0.42591
1.20428	0.91447	0.13516	0.92555	0.15785	0.96121	0.22615	1.02391	0.38063
1.30900	0.96812	0.11977	0.97963	0.14123	1.01661	0.20586	1.08169	0.35215
1.50098	1.04983	0.08765	1.06178	0.10659	1.10009	0.16353	1.16761	0.29257
1.57080	1.07375	0.07467	1.08575	0.09260	1.12416	0.14643	1.19190	0.26843

Table-C₁₆: Comparisons of the present numerical results of Nu_x for the Prandtl numbers $Pr = 0.7, 7.0$ without effect of the viscous dissipation parameter, magnetic parameter and heat generation parameter with those obtained by Molla et al. (2004) and Nazar et al. (2002)

x in degree	Pr = 0.7			Pr = 7.0		
	Nazar et al (2002)	Molla et al. (2004)	Present	Nazar et al (2002)	Molla et al. (2004)	Present
0	0.4576	0.4576	0.4529	0.9595	0 9582	0 9437
10	0.4565	0.4564	0.4516	0.9572	0.9558	0 9416
20	0.4533	0 4532	0 4485	0.9506	0.9492	0.9354
30	0.4480	0.4479	0.4444	0.9397	0.9383	0.9248
40	0.4405	0.4404	0.4367	0.9239	0.9231	0.9100
50	0.4308	0 4307	0.4282	0.9045	0 9034	0.8909
60	0 .4189	0 4188	0 4134	0.8801	0 8791	0.8673
70	0.4046	0.4045	0.4012	0.8510	0 8501	0.8390
80	0.3879	0 3877	0 3836	0.8168	0.8161	0.8059
90	0.3684	0.3683	0.3641	0.7774	0 7768	0.7675

Table-C₁₇: Local skin friction coefficient and local Nusselt number coefficient for different values of radiation parameter Rd against x with other controlling parameters $Pr = 0.72$, $\theta_w = 1.1$, $M = 0.50$, $Q = 0.40$, $N = 0.40$, $Ge = 0.60$.

x	Rd = 1.00		Rd = 2.00		Rd = 3.00		Rd = 4.00	
	C_{fx}	Nu_x	C_{fx}	Nu_x	C_{fx}	Nu_x	C_{fx}	Nu_x
0.0000	0.00000	0.33781	0.00000	0.49783	0.00000	0.62810	0.00000	0.74233
0.1047	0.08857	0.33664	0.09181	0.49630	0.09391	0.62629	0.09539	0 74027
0.2094	0.17649	0.33341	0.18293	0.49212	0.18711	0.62130	0.19005	0 73456
0.3141	0.26316	0 32807	0.27270	0.48522	0.27891	0.61307	0.28327	0.72516
0.4014	0.33398	0.32200	0.34601	0.47737	0.35384	0.60371	0.35935	0 71449
0.5061	0.41674	0.31277	0.43161	0.46543	0.44130	0.58947	0.44812	0 69822
0.6108	0.49652	0.30136	0.51403	0.45068	0.52545	0.57189	0.53348	0 67815
0.7155	0 57273	0.28774	0.59264	0.43309	0.60563	0.55092	0.61478	0 65421
0.8028	0.63310	0.27467	0.65479	0.41621	0.66897	0.53080	0.67895	0 63125
0.9075	0.70129	0.25688	0 72483	0.39324	0.74026	0.50344	0.75111	0.60001
1.0122	0.76432	0.23674	0.78938	0.36725	0 80584	0.47247	0.81741	0 56467
1.1170	0.82165	0.21416	0.84787	0.33814	0.86512	0.43781	0.87726	0 52513
1.2042	0.86472	0.19344	0 89159	0.31144	0.90932	0.40603	0.92180	0.48888
1.3090	0.91030	0.16623	0.93757	0.27639	0.95565	0.36433	0.96837	0.44132
1 5009	0.97505	0.10940	1.00193	0 20329	1.01993	0.27741	1.03260	0.34224

Table-C_{18}: Local skin friction coefficient and local Nusselt number coefficient for different values of heat generation parameter Q against x with other controlling parameters $Pr = 0.72$, $\theta_w = 1.1$, $Rd = 1.0$, $M = 0.5$, $N = 0.20$ and $Ge = 0.5$

	$Q = 0.00$		$Q = 0.20$		$Q = 0.40$	
x	C_{fx}	Nu_x	C_{fx}	Nu_x	C_{fx}	Nu_x
0.00000	0.00000	0.77946	0.00000	0.57605	0.00000	0.33781
0.10472	0.08092	0.77866	0.08441	0 57510	0.08857	0 33664
0.20944	0.16121	0 77641	0.16819	0.57244	0.17649	0 33341
0.40143	0.30478	0 76848	0.31812	0.56303	0.33398	0.32200
0.50615	0.38004	0 76206	0.39680	0.55541	0.41674	0.31277
0.80285	0 57563	0.73568	0.60185	0.52406	0.63310	0.27467
1.01229	0.69287	0.70955	0.72542	0.49291	0.76432	0.23674
1.20428	0.78121	0.67988	0.81922	0.45745	0.86472	0.19344
1.30900	0 82062	0.66128	0.86141	0.43519	0.91030	0.16623
1 50098	0.87502	0.62256	0 92047	0.38876	0.97505	0.10940

Table-C_{19}: Skin friction coefficient and rate of heat transfer against x for different values of surface temperature parameter θ_w with other controlling parameters.

	$\theta_w = 0.40$		$\theta_w = 0.80$		$\theta_w = 1.00$		$\theta_w = 1.20$	
x	C_{fx}	Nu_x	C_{fx}	Nu_x	C_{fx}	Nu_x	C_{fx}	Nu_x
0.00000	0.00000	0.27949	0.00000	0.36957	0.00000	0.43920	0.00000	0.52463
0.10472	0.08146	0.27880	0 08492	0.36872	0 08726	0.43823	0.08971	0.52353
0.20944	0.16236	0.27685	0.16923	0.36634	0.17390	0.43553	0.17877	0.52044
0.50615	0 38378	0.26446	0 39981	0.35121	0.41071	0.41833	0.42206	0.50071
0.80285	0 58427	0.24163	0.60804	0.32334	0.62422	0.38662	0.64106	0.46432
1.01229	0.70694	0.21897	0.73490	0.29564	0.75395	0.35509	0.77378	0.42812
1 20428	0.80197	0.19319	0.83261	0.26411	0.85352	0.31917	0.87527	0 38684
1.30900	0.84575	0.17703	0.87733	0.24432	0.89889	0.29660	0.92132	0 36090
1.50098	0.90951	0.14338	0.94174	0.20306	0.96378	0.24952	0.98671	0.30671
1.57080	0.92699	0.12980	0.95909	0.18641	0.98106	0.23049	1.00392	0 28479

Table-C$_{20}$: Skin friction coefficient and rate of heat transfer against x for different values of pressure work parameter Ge with other controlling parameters $Pr = 0.72$, $Q = 0.40$, $M = 0.50$, $Rd = 1.00$, $\theta_w = 1.10$ and $N = 0.50$.

x	$Ge = -0.10$		$Ge = 0.10$		$Ge = 0.30$		$Ge = 0.50$	
	C_{fx}	Nu_x	C_{fx}	Nu_x	C_{fx}	Nu_x	C_{fx}	Nu_x
0.00000	0.00000	0.87109	0.00000	0.68184	0.00000	0.46222	0.00000	0.20136
0.10472	0.07937	0.87035	0.08258	0.68098	0.10074	0.46081	0.09096	0.20006
0.20944	0.15811	0.86827	0.16453	0.67853	0.17214	0.45824	0.18128	0.19647
0.50615	0.37262	0.85499	0.38799	0.66294	0.40628	0.43954	0.42825	0.17355
0.80285	0.56405	0.83060	0.58807	0.63426	0.61670	0.40508	0.65116	0.13122
1.01229	0.67850	0.80648	0.70832	0.60581	0.74390	0.37080	0.78680	0.08902
1.20428	0.76447	0.77912	0.79924	0.57345	0.84083	0.33172	0.89104	0.04081
1.30900	0.80267	0.76200	0.83997	0.55315	0.88462	0.30717	0.93860	0.01049
1.50098	0.85507	0.72638	0.89658	0.51085	0.94638	0.25592	1.00666	-.05284
1.57080	0.86809	0.71201	0.91096	0.49376	0.96244	0.23521	1.02479	-.07844

Table-C$_{21}$: Comparisons of the present numerical results of Nu_x for the Prandtl numbers $Pr = 0.7$, 7.0 without effect of the viscous dissipation parameter, magnetic parameter and heat generation parameter with those obtained by Molla et al. (2004) and Nazar et al. (2002)

x in degree	$Pr = 0.7$			$Pr = 7.0$		
	Naza et al (2002)	Molla et al. (2004)	Present	Naza et al (2002)	Molla et al. (2004)	Present
0	0.4576	0.4576	0.4495	0.9595	0.9582	0.9527
10	0.4565	0.4564	0.4489	0.9572	0.9558	0.9487
20	0.4533	0.4532	0.4470	0.9506	0.9492	0.9413
30	0.4480	0.4479	0.4402	0.9397	0.9383	0.9283
40	0.4405	0.4404	0.4345	0.9239	0.9231	0.9145
50	0.4308	0.4307	0.4264	0.9045	0.9034	0.8949
60	0.4189	0.4188	0.4107	0.8801	0.8791	0.8616
70	0.4046	0.4045	0.4002	0.8510	0.8501	0.8401
80	0.3879	0.3877	0.3789	0.8168	0.8161	0.8139
90	0.3684	0.3683	0.3613	0.7774	0.7768	0.7711

Table-C$_{23}$: Skin friction coefficient and surface temperature distribution for different values of viscous dissipation parameter N against x in chapter-3 (Table-C$_7$) and chapter-4 (Table-C$_{12}$) with other controlling parameters.

	Chapter-3				Chapter-4			
	$N = 0.60$		$N = 0.90$		$N = 0.60$		$N = 0.90$	
x	$f''(x, 0)$	$\theta(x, 0)$	$f''(x, 0)$	$\theta(x, 0)$	$f''(x, 0)$	$\theta(x, 0)$	$f''(x, 0)$	$\theta(x, 0)$
0.0000	0.0154	0.2044	0.0154	0.2044	0.0154	0.2044	0.0154	0.2044
0.3150	0.4624	0.7172	0.4664	0.7239	0.4661	0.7211	0.4701	0.7279
0.7090	0.5678	0.7795	0.5773	0.7927	0.5807	0.7910	0.5906	0.8049
1.0409	0.6225	0.8078	0.6367	0.8259	0.6457	0.8270	0.6609	0.8469
2.0369	0.7264	0.8663	0.7544	0.8980	0.7911	0.9153	0.8249	0.9544
3.1340	0.7991	0.9069	0.8423	0.9525	0.9269	1.0002	0.9868	1.0661
4.0635	0.8456	0.9325	0.9018	0.9897	1.0419	1.0745	1.1307	1.1703
4.9876	0.8839	0.9546	0.9532	1.0232	1.1640	1.1572	1.2897	1.2919
6.1118	0.9236	0.9776	1.0090	1.0604	1.3305	1.2745	1.5156	1.4740
7.1132	0.9544	0.9963	1.0546	1.0918	1.5016	1.4006	1.7572	1.6802
9.1512	1.0080	1.0277	1.1399	1.1503	1.9417	1.7441	2.4153	2.2900
10.1191	1.0304	1.0412	1.1781	1.1773	2.2067	1.9645	2.8329	2.7106